Dynamical Systems in General Relativity and Modified Gravity Theories

Vitor Emanuel Moreira Bessa
Doutoramento em Matemática Aplicada
Departamento de Matemática, Faculdade de Ciências, Universidade do Porto
2022

Orientadores
Artur Alho, Investigador, Centro de Análise Matemática, Geometria e Sistemas Dinâmicos, Instituto Superior Técnico, Universidade de Lisboa
Filipe Mena, Professor Associado com Agregação, Departamento de Matemática, Instituto Superior Técnico, Universidade de Lisboa
Jorge Carvalho, Professor Associado, Departamento de Matemática, Faculdade de Ciências, Universidade do Porto

Todas as correções determinadas pelo júri, e só essas, foram efetuadas.

O Presidente do Júri,

Porto, ______/______/________

UNIVERSITY OF PORTO

DOCTORAL THESIS

Dynamical Systems in General Relativity and Modified Gravity Theories

Author:
Vitor Bessa

Supervisor:
Artur Alho
Filipe Mena
Jorge Carvalho

A thesis submitted in fulfilment of the requirements for the degree of Doctor of Philosophy

at the

Faculdade de Ciências, Universidade do Porto

September 2022

"If you wait on luck to turn up, life becomes very boring."

Mikhail Tal, 1960-61 Chess World Champion

"Not only is the Universe stranger than we think, it is stranger than we can think"

Werner Heisenberg, 1932 Nobel Prize Winner

"Compromise where you can. Where you can't, don't. Even if everyone is telling you that something wrong is something right. Even if the whole world is telling you to move, it is your duty to plant yourself like a tree, look them in the eye, and say 'No, you move'"

Steve Rogers - Captain America

"Try not to become a man of success. Rather become a man of value."

Albert Einstein, 1921 Nobel Prize Winner

"A lot of people say they want to be great, but they're not willing to make the sacrifices necessary to achieve greatness. They have other concerns, whether important or not, and they spread themselves out. That's totally fine. After all, greatness is not for everybody."

Kobe Bryant

Acknowledgements

Throughout my PhD, several people helped me reach my goals. Therefore, I would like to thank them, starting with my advisors, Filipe Mena, Artur Alho and Jorge Carvalho for all the help given and for the opportunity to work with them. I want to thank also Fundação para a Ciência e Tecnologia for the research grant PD/BD/142891/2018 and CMAT for the travel expenses during these years.

My deepest appreciation to Marta Branco, for all the love and support provided; for always believing in me even when I doubted myself and for being there whenever I needed the most. Without her, this adventure could still be successful, but it certainly would not be so pleasant. Also a special thanks to her parents Dores and Luis Branco.

I'm grateful to my family, in particular, my mother Virginia, my sister Maria, my aunt Conceição, my uncle Justino and my two cousins Helder and João alongside his wife Claudia and the newborn Tomás.; my godparents, Pedro and Raquel, alongside her husband Marcelo and their daughters, Lara and my goddaughter Carolina and of course my aunt Filomena for never denying me a place to stay when I needed it most. Also, a special homage to my father that passed away during my PhD. I have no doubt that he would be proud of all that I have achieved so far and what I will accomplish in the future.

Friends and colleagues have supported me throughout this adventure and for that I am thankful. Special recognition to Filipe Barros for being there for me since 7th grade; my friends João Ferreira and Hugo Mota for all the good evenings and for all the quizzes that make Mondays special days and Lara Martins for always being available for a friendly word. I also would like to thank: Vitor Vicente for being a good friend even if we are not together so often; Sara Pinto, Carlos Nunes and Nelson Gomes for all the quizzes and good laughs over the years; Francisco Oliveira because even though he does not like to leave the house, I know he is there whenever I need him; João Mariz and Paula Ribeiro for all the dinners that always helped me to decompress; Nuno Vale, for never having denied a good conversation accompanied by a good beer and João Morais and José Vilela, for always promoting good conversation and good MTG games. I wish to give a special appreciation to José Sá for always helping me out and for being always available to chat about all kinds of subjects and be a true friend when I needed the most. Lastly, I want to refer to my special partners when working on this thesis: Cuca, Molly, Guppy and Tica.

UNIVERSITY OF PORTO

Abstract

Faculdade de Ciências, Universidade do Porto

Doctor of Philosophy

Dynamical Systems in General Relativity and Modified Gravity Theories

by Vitor Bessa

The scope of this thesis is the analysis of cosmological models arising from Einstein's theory of General Relativity. Motivated by cosmological models of the early universe we focus on matter models such as nonlinear scalar and vector fields in co-evolution with perfect-fluids with linear equations of state in spatially homogeneous spacetimes. We consider three different scenarios: Massless and massive Yang-Mills fields with perfect-fluids in flat Robertson-Walker spacetimes; Monomial scalar-field potentials interacting with perfect fluids in flat Robertson-Walker spacetimes with a friction-like interaction term; Monomial scalar field potentials in Bianchi type I spacetimes. The analysis rely on the introduction of new regular dynamical systems formulation of the Einstein field equations on compact (or future invariant) state spaces, and the use of dynamical systems tools such as monotone functions, quasi-homogeneous blow-ups, and averaging methods involving a time-dependent perturbation parameter. This allow us to give proofs concerning the global dynamics of the models, and their past and future asymptotics. In particular we discuss the issues of asymptotic self-similarity and self-similarity breaking as well as asymptotic source dominance, i.e., if the model is scalar/vector field dominated or fluid dominated towards the asymptotic regimes.

UNIVERSITY OF PORTO

Resumo

Faculdade de Ciências, Universidade do Porto

Doctor of Philosophy

Dynamical Systems in General Relativity and in Modified Gravity Theories

por Vitor Bessa

O âmbito desta tese é a análise de modelos cosmológicos decorrentes da teoria da Relatividade Geral de Einstein. Motivados por modelos cosmológicos do universo primordial, concentramo-nos em modelos de matéria tais como campos escalares não lineares e vectoriais em co-evolução com fluidos perfeitos com equações de estado lineares num espaço-tempo homogéneo. Consideramos três cenários diferentes: Campos Yang-Mills massivos e sem massa com fluidos perfeitos num espaço-tempo plano de Robertson-Walker; Potenciais de campos escalares monomiais interagindo com fluidos perfeitos num espaço-tempo plano de Robertson-Walker com um termo de interacção do tipo fricção; Potenciais de campos escalares monomiais em espaços-tempo de Bianchi tipo I. A análise baseia-se na introdução de uma nova formulação regular de sistemas dinâmicos das equações de campo de Einstein em espaços de estado compactos (ou invariantes futuros), e na utilização de ferramentas de sistemas dinâmicos tais como funções monótonas, blow-ups quase-homogéneos e de averaging envolvendo um parâmetro de perturbação dependente do tempo. Isto permite-nos dar provas rigorosas relativamente à dinâmica global dos modelos, e ao seu passado e futuro assimptóticos. Em particular, discutimos as questões da auto-semelhança assimptótica bem como da dominância assimptótica da fonte, ou seja, se o modelo é dominado por um campo escalar/vectorial ou por fluido nos regimes assimptóticos.

Contents

List of Figures

List of Tables

Abbreviations

GR	**G**eneral **R**elativity
H-G	**H**artman **-** **G**robman
EFE	**E**instein **F**ield **E**quations
BH	**B**lack **H**oles
RW	**R**obertson -**W**alker
FLRW	**F**riedman - **L**emaître - **R**obertson - **W**alker
EoS	**E**quation **o**f **S**tate
CMB	**C**osmic **M**icrowave **B**ackground
YM	**Y**ang **M**ills
ODE	**O**rdinary **D**ifferential **E**quation

Dedicated to the ones that passed away during this journey

Chapter 1

General Relativity and Standard Cosmology

Cosmology concerns the study of the universe as a whole, in particular of large structures and their dynamics which is ruled by the laws of gravity. The most used theory to describe the physics of such large scales is *General Relativity* (GR). In this chapter we review some aspects about GR and cosmology that will be useful in the thesis, with a special focus on cosmological inflation (for more details see [2–4]). We end the chapter revising applications of dynamical systems theory to cosmology.

1.1 General Relativity

The success presented in a variety of experimental tests made GR the principal theory to study gravity and cosmological models [2–7]. GR is a geometric theory where the main features of gravity are encoded in a four-dimensional metric tensor $g_{\mu\nu}$ on a Lorentzian manifold that models spacetime.

An important aspect in GR is spacetime curvature which is encoded in the *Riemann tensor* defined as

$$R^{\lambda}_{\sigma\mu\nu} = \partial_\mu \Gamma^{\lambda}_{\nu\sigma} - \partial_\nu \Gamma^{\lambda}_{\mu\sigma} + \Gamma^{\lambda}_{\mu\rho}\Gamma^{\rho}_{\nu\sigma} - \Gamma^{\lambda}_{\nu\rho}\Gamma^{\rho}_{\mu\sigma}, \tag{1.1}$$

where $\Gamma^{\alpha}_{\beta\gamma}$ are the *Christofel symbols* that can be derived from the metric and are given by

$$\Gamma^{\mu}_{\alpha\beta} = \frac{1}{2} g^{\mu\sigma} \left(\partial_\alpha g_{\beta\sigma} + \partial_\beta g_{\alpha\sigma} - \partial_\sigma g_{\alpha\beta} \right). \tag{1.2}$$

From this equation we can define the *Ricci tensor*

$$Ric = R_{\mu\nu} = R^{\lambda}_{\mu\lambda\nu} \tag{1.3}$$

and the *Ricci scalar*

$$R = g^{\mu\nu}R_{\mu\nu}. \tag{1.4}$$

The action of General Relativity reads

$$S = S_{\mathrm{EH}} + S_{\mathrm{m}} = \int d^4x\sqrt{-g}R + \int d^4x\sqrt{-g}\mathcal{L}_{\mathrm{m}}, \tag{1.5}$$

where g is the determinant of the metric and $\mathcal{L}_{\mathrm{m}}$ is the Lagrangian of the matter. This action combines the *Einstein-Hilbert action* and the matter action that is minimally-coupled with gravity. In this thesis we use geometrized units with $c = 8\pi G = 1$ following the convention of [8].

Taking the variation of (1.5) we get the *Einstein field equations* (EFE)

$$R_{\mu\nu} - \frac{1}{2}g_{\mu\nu}R = T_{\mu\nu} \tag{1.6}$$

where the stress-energy tensor, $T_{\mu\nu}$, is defined as

$$T_{\mu\nu} = -\frac{2}{\sqrt{-g}}\frac{\delta\sqrt{-g}\mathcal{L}_{\mathrm{m}}}{\delta g^{\mu\nu}} = g_{\mu\nu}\mathcal{L}_{\mathrm{m}} - 2\frac{\delta\mathcal{L}_{\mathrm{m}}}{\delta g^{\mu\nu}}. \tag{1.7}$$

The left-hand side of (1.6) is the *Einstein tensor* and is denoted by $G_{\mu\nu}$. From (1.6) we see that the geometry of spacetime affects the dynamics of the matter ($T_{\mu\nu}$), but also the reverse is true, i.e. the presence of matter modifies the geometry of the spacetime. From the contracted Bianchi identities it follows that $\nabla_\mu R^{\mu\nu} = \frac{1}{2}\nabla^\nu R$, which leads to the conservation of the Einstein tensor and consequentially to the conservation of the total stress-energy tensor, i.e,

$$\nabla_\mu G^{\mu\nu} = 0, \qquad \nabla_\mu T^{\mu\nu} = 0. \tag{1.8}$$

The system of equations (1.6) is highly non-linear in the metric and its derivatives which can be challenging when trying to find an exact solution.

Although GR went through numerous validity tests, there are some concerns that need to be addressed such as the strong gravity regime that arises from the gravitational collapse or even the fact that GR is not suitable to be formulated as a quantum theory. This indicates that GR is not complete and modified theories of gravity might be relevant [9–11]. Some important modified theories of gravity are *$F(R)$-theories* [12–15] and *scalar-tensor theories* [16–18] for example, but in this thesis we will focus on GR only.

1.2 Principles of FLRW Cosmology

Modern cosmology is based on two important assumptions, the fact GR gives a valid spacetime description and the so-called *cosmological principle* that states:

- *At sufficiently large scales the universe is spatially homogeneous and isotropic.*

This basically implies the so-called *Copernican principle* that states:

- *Earth does not occupy a special place in the universe.*

This means that the universe, from a statistical point for view, is equivalent to any observer regardless of observation location (homogeneity) or observation direction (isotropy) on a sufficiently large scale.

The cosmological principle statement seems to be a simple, however it presents important consequences when dealing with the theoretical modeling of cosmology implying that the universe is highly symmetric. This leads to the Friedman-Lemaître-Robertson-Walker (FLRW) class of universes that in spherical coordinates (r, θ, ϕ) can be described by the *Robertson-Walker metric* (RW).

$$ds^2 = -dt^2 + a(t)^2 \left(\frac{dr^2}{1 - kr^2} + r^2 d\theta^2 + r^2 \sin^2 \theta d\phi^2 \right) \tag{1.9}$$

where k the Gaussian spatial curvature which is agreement with the cosmological principle. In particular, k can present three different values $k = 1$ (positive curvature) which corresponds to a spherical space, $k = 0$ (null curvature) that corresponds to the flat space and, $k = -1$ (negative curvature) that corresponds to a hyperbolic space. The evolution function $a(t) > 0$ is called the *scale factor* and physically describes the evolution of the spacetime.

1.3 Evolution in a FLRW Universe

As mentioned in Sec 1.1 the dynamics of the metric tensor $g_{\mu\nu}$ is described by (1.6). We can describe the matter inside the universe as a *perfect fluid* which means that the stress-energy tensor is solely determined by the energy density $\rho_{\rm pf}(t)$ and isotropic pressure $p_{\rm pf}(t)$ and takes the form

$$T_{{\rm pf}_{\mu\nu}} = (\rho_{\rm pf} + p_{\rm pf}) u_\mu u_\nu + p_{\rm pf} g_{\mu\nu}, \tag{1.10}$$

where u^μ denotes the 4-velocity of the fluid. The stress-energy tensor for the perfect fluid also satisfies the Euler equation (1.8).

We also need to prescribe a relation between the energy and pressure density given by an *equation of state* (EoS). For a barotropic perfect fluid,

$$p_{\rm pf} = (\gamma_{\rm pf} - 1)\rho_{\rm pf}, \tag{1.11}$$

where $\gamma_{\rm pf}$ is the adiabatic index. It is assumed that $\gamma_{\rm pf} \in (0, 2)$ in order to satisfy the dominant energy conditions, however, there exist some phenomenological models that rely on values outside of this range to match astronomical observations. There are also some important values for $\gamma_{\rm pf}$ such as $\gamma_{\rm pf} = 1$ corresponding to a dust-like fluid, $\gamma_{\rm pf} = \frac{4}{3}$ to a radiation fluid. The extreme case $\gamma_{\rm pf} = 0$ corresponds to matter content described by the cosmological constant i.e, $\rho_{\rm pf} = \Lambda$, while $\gamma_{\rm pf} = 2$ describes the a stiff fluid.

We use Einstein field equations (1.6) alongside the metric ansatz (1.9) to obtain the so-called *cosmological equations* that consist of two coupled differential equations for the scale factor $a(t)$ and for the matter ($\rho_{\rm pf}(t)$ and $p_{\rm pf}(t)$). These two equations are given by

$$H^2 = \frac{\rho_{\rm pf}}{3} - \frac{k}{a^2} \tag{1.12a}$$

$$3H^2 + 2\dot{H} = -p_{\rm pf} - \frac{k}{a^2}. \tag{1.12b}$$

The first equation is called *Friedmann equation* [19, 20] and the second *acceleration equation*, where the *Hubble function* is defined as

$$H = \frac{\dot{a}}{a} \tag{1.13}$$

with an over-dot that denotes the differentiation with respect to the time, t. Using the Friedmann equation (1.12a), the acceleration equation (1.12b) can be rewritten as

$$\frac{\ddot{a}}{a} = -\frac{1}{6}\left(\rho_{\rm pf} + 3p_{\rm pf}\right), \tag{1.14}$$

which is referred as the *Raychaudhuri equation* [21]. As we can see from (1.14): If $\rho_{\rm pf} + 3p_{\rm pf} > 0 (< 0)$ the universe is decelerating (accelerating). So if (1.11) holds, this implies that $\gamma_{\rm pf} > \frac{2}{3} (< \frac{2}{3})$ for deceleration (acceleration) for a universe only containing a perfect fluid. From the equation (1.8), we can obtain the *energy conservation equation* for the perfect fluid

$$\dot{\rho}_{\rm pf} + 3H(\rho_{\rm pf} + p_{\rm pf}) = 0 \tag{1.15}$$

Using (1.11) together with (1.15) it is possible to obtain a solution for $\rho_{\rm pf}$ in terms of the scale factor, i.e.

$$\rho_{\rm pf} \propto a^{-3\gamma_{\rm pf}}. \tag{1.16}$$

It is useful to introduce, the so-called *deceleration parameter*, that will be used later on and is defined via the equation

$$\dot{H} = -(1+q)H, \qquad q = -\frac{\ddot{a}a}{\dot{a}^2} \tag{1.17}$$

As one may see the sign of (1.17) will depend on the sign of $\ddot{a}$ and this will have direct implications when analyzing $\dot{a}$ and therefore the Hubble function. In the next section, we will explore the consequences of the sign of $H(t)$ and we will provide some special solutions for the scale-factor $a(t)$.

1.4 The Big Bang: A Theory of Universe Expansion

In 1929 Hubble observed that galaxies were moving away from each other, which lead to the conclusion that the universe was expanding. For expanding cosmologies we have $H > 0$ or equivalently $\dot{a} > 0$. Taking this condition into consideration and using (1.14) and (1.15) leads to the following singularity theorem [22]:

Theorem 1.1. *(Singularity)*

Consider a FLRW cosmological model with a perfect fluid. Let $\rho_{\rm pf} > 0$ *and* $\rho_{\rm pf} + 3p_{\rm pf} > 0 \;\; \forall \;\; t$ *and* $\dot{a}(t_0) > 0$ *that represents the scale-factor in the present day, then their exists a time* $t_{BB} < t_0$ *such that* $a(t_{BB}) = 0$ *and* $\lim_{t \to t_{BB}^+} \rho_{\rm pf} = +\infty$.

This theorem tells us that, at the beginning, under those conditions the universe is in a state of extremely high density and temperature due to constraints in space. This state allowed primordial nucleosynthesis to take place leading to the creation of the lighter elements present in the universe (Hydrogen, Helium,...). After the primordial nucleosynthesis, the universe started to cool down enabling the creation of complex cosmological structures (galaxies, stars, planets,...). The Big Bang theory is, in the modern era, the most accurate model to describe the beginning of the universe.

Recent observations, in particular of the cosmic microwave background radiation (CMB)[1] tell us that the spatial curvature $k \simeq 0$. We now introduce the *density parameter* $\Omega_{\rm pf}$ that describes the dynamical effect of the matter density as

$$\Omega_{\rm pf} = \frac{\rho_{\rm pf}}{3H^2}. \tag{1.18}$$

So using (1.18) into (1.12a) we get

$$\Omega_{\rm pf} - 1 = \frac{k}{\dot{a}^2} \tag{1.19}$$

[1]CMB is an electromagnetic radiation that exists since the early stage of the universe that fills all space. The CMB was discovered accidentally by Penzias and Wilson in 1964 .

that has a dependence in the spatial curvature

$$\Omega_{\rm pf} > 1, \quad \text{corresponds to closed 3-spaces,} \qquad (k = +1), \tag{1.20a}$$

$$\Omega_{\rm pf} = 1, \quad \text{corresponds to flat 3-spaces,} \qquad (k = 0), \tag{1.20b}$$

$$\Omega_{\rm pf} < 1, \quad \text{corresponds to open 3-spaces,} \qquad (k = -1). \tag{1.20c}$$

As we mentioned before, the CMB observations tell us that $k \simeq 0$ which implies that $\Omega_{\rm pf} \simeq 1$, in agreement with the observational measurements of the density matter of the universe today. Bearing this in mind we can calculate $\rho_{\rm pf}$ (using (1.16)) and subsequently a (using (1.12a)) for a variety of values of $\gamma_{\rm pf}$ that can be found in Table 1.1. It is important to notice that the Big

$\gamma_{\rm pf}$	energy density	scale factor
0	$\rho_{\rm pf} \propto const$	$a(t) \propto e^{\kappa\sqrt{\frac{const}{2}}t}$
2/3	$\rho_{\rm pf} \propto a^{-2}$	$a(t) \propto t$
1	$\rho_{\rm pf} \propto a^{-3}$	$a(t) \propto t^{2/3}$
4/3	$\rho_{\rm pf} \propto a^{-4}$	$a(t) \propto \sqrt{t}$
2	$\rho_{\rm pf} \propto a^{-6}$	$a(t) \propto t^{1/3}$

TABLE 1.1: Energy density of the universe depending on the values of the adiabatic index $\gamma_{\rm pf}$.

Bang theory requires that in the early stages of the universe the radiation will dominate and will be followed by a matter-dominated epoch. This happens since in high-energy situations the radiation dominates over matter, however in low-energy situations it is the other way around.

1.5 Problems in the Big Bang Model

Despite the Big Bang being the most accurate theory given observational experiments (since it explains: *The expansion of the universe* , *the age of the universe*, *the origin and spectrum of CMB* and *the origin and abundance of light elements in the universe*), there are still some problems inherent in this model. The most crucial problems are *the Horizon problem*, *the Flatness problem* and *the Magnetic Monopole problem* [2–4]. In the next subsections, we will provide some explanations regarding these problems.

The Flatness Problem

As we mentioned before, nowadays $\Omega_{\rm pf} \simeq 1$, more precisely $|\Omega_{\rm pf} - 1| < 0.01$ and since $\Omega_{\rm pf}$ would be closer to one in the beginning of the universe ($|\Omega_{\rm pf} - 1| < 10^{-62}$) [23] it suggests one of two things. First, the universe could be perfectly flat with $k = 0$. Alternatively, $k \neq 0$ will not be, at any point in the history of the universe, identically to zero. In fact experimental observations of the Plank measurements [24] show that today $k = 0 \pm 10^{-2}$.

The later scenario is the one that presents a problem, since it shows that if the curvature of the universe is small, as allowed today, this implies that the primordial curvature of the universe had to be extremely finely tuned to be very close to zero. So the Flatness Problem is in reality a *fine-tuning problem* and it is not resolved for the Big Bang model.

The Horizon Problem

The cosmological principle tells us that the universe, on large-scales, is homogeneous and isotropic which is in agreement with the CMB measurements. In fact, $\Delta T/T \simeq 10^{-5}$, where ΔT is the CMB temperature variation. So apparently causality disconnected regions in the universe have the same temperature. This is a remarkable feature since we know that information cannot travel faster than the speed of light. So two photons that are coming from a distance that is greater than the maximum angular distance between two correlated points have never been causally connected which should imply a inhomogeneity in the CMB. So basically the Horizon Problem is a *Causality problem* that the Big Bang theory cannot solve.

The Magnetic Monopole Problem

If we accept the idea that in the early stages of the universe the laws of physics are described by the so-called *Ground Unified Theories* (GUT)[2] it would be expected that objects with few orders of magnitude of the Plank mass should be produced [25]. These are topological defects, like magnetic monopoles, that are commonly called *"relics"* of the universe. This presents a problem in the Big Bang scenario since it implies that they should dominate the universe [26] and as we mentioned, a radiation-dominated epoch is needed until the primordial nucleosynthesis takes place.

1.6 Inflation

In order to solve the previous problems while still having the Big Bang as the main model for the origin of the universe, the theory of inflation was developed in the late 1970s and early 1980s. This theory had the contribution of several theoretical physicists having as main pioneers Guth [27], Starobinsky [28] and Linde [25, 29]. The inflationary theory states that the universe underwent a fast period of accelerated expansion that lasted from 10^{-36} seconds

[2] GUT is part of the Standard Model and consists in the merger of three forces, electromagnetic, weak and strong forces.

until 10^{-32} seconds after the Big Bang. This model can be viewed as an extension of the Big Bang model and solves the problems stated in the previous section:

- *The Flatness Problem*

  The exponential expansion of the universe in the early times will flatten out any irregularity in the geometry of the universe.

- *The Horizon Problem*

  When entering the inflationary epoch the universe was in equilibrium, i.e. different regions of the universe were in casual contact with each other. The rapid expansion of the universe allows regions to maintain thermal equilibrium obtained prior to the inflationary epoch.

- *The Magnetic Monopole Problem*

  The inflationary theory allows the existence of magnetic monopoles, however, they needed to be created before the inflationary period. During inflation, the density of the monopoles drops exponentially leading to a drop in the abundance of such ”relics” to a current undetected level.

We define inflation as a phase of accelerated expansion of the early universe, i.e $\ddot{a} > 0$ which is equivalent to say that in the inflationary epoch the Hubble radius $(aH)^{-1}$ shrinks $(\frac{d}{dt}(aH)^{-1} < 0)$. Then, equation (1.14) implies

$$\rho + 3p < 0. \tag{1.21}$$

Since ρ is always positive then inflation must be generated by negative pressure.

The question that now emerges is: What can drive inflation?

For many years numerous theories were developed to understand what can drive inflation and we will consider two types of inflationary categories: *Scalar Field Inflation* and *Vector Field Inflation*.

1.6.1 Scalar Field Inflation

Scalar fields provide a simple mechanism to implement the inflationary theory [25, 27, 30]. Let us assume a RW metric described in (1.9). The simplest action that we can write the scalar field in GR is given by

$$S = S_{EH} + S_\phi = \int d^4x\sqrt{-g}R + \int d^4x\sqrt{-g}\left(-\frac{1}{2}\partial^\mu\phi\partial_\mu\phi - V(\phi)\right). \tag{1.22}$$

where $V(\phi)$ os the scalar field potential.

The stress-energy tensor for the scalar field is

$$T^{(\phi)}_{\mu\nu} = \partial_\mu\phi\partial_\nu\phi - g_{\mu\nu}\left(\frac{1}{2}\partial^\lambda\phi\partial_\lambda\phi + V(\phi)\right). \tag{1.23}$$

From the (1.23) we get the wave-equation

$$\Box_g\phi + V_\phi(\phi) = 0, \tag{1.24}$$

where $\Box_g$ is the usual D'Alembertian operator associated to the metric g and $V_\phi(\phi)$ denotes the derivative of the potential with respect to the field ϕ. This leads to the equation of motion

$$\ddot{\phi} + 3H\dot{\phi} + V_\phi(\phi) = 0. \tag{1.25}$$

The EFE for the scalar field are given by

$$3H^2 = \frac{1}{2}\dot{\phi}^2 + V(\phi), \tag{1.26a}$$

$$\dot{H} = -\frac{1}{2}\dot{\phi}^2, \tag{1.26b}$$

$$0 = \ddot{\phi} + 3H\dot{\phi} + V_\phi(\phi). \tag{1.26c}$$

Assuming that $\partial^\mu\phi$ is timelike, it is possible to write the stress-energy tensor for the scalar field in a perfect-fluid form using the identifications $u^\mu_{(\phi)} = (\partial^\mu\phi)/\sqrt{-(\partial\phi)^2}$ and

$$\rho_\phi = \frac{1}{2}\dot{\phi}^2 + V(\phi) \tag{1.27a}$$

$$p_\phi = \frac{1}{2}\dot{\phi}^2 - V(\phi) \tag{1.27b}$$

We can define, as well, the effective equation of state parameter γ_ϕ via

$$\gamma_\phi = 1 + \frac{p_\phi}{\rho_\phi} = 1 + \frac{\frac{1}{2}\dot{\phi}^2 - V(\phi)}{\frac{1}{2}\dot{\phi}^2 + V(\phi)} = \frac{\dot{\phi}^2}{\frac{1}{2}\dot{\phi}^2 + V(\phi)}. \tag{1.28}$$

It is important to notice that if the scalar field is the only contribution to the total energy density in early universe then the spacetime stress-energy tensor violates the *Strong Energy Condition* (SEC)

$$3\gamma_\phi - 2 > 0, \tag{1.29}$$

if $\frac{1}{2}\dot{\phi}^2 < V(\phi)$. The inflationary period can only happen if the rolling of the scalar field on the slope of its potential is not too fast. The velocity of the scalar field can be parameterized by the first Hubble slow-roll parameter, ϵ, defined via

$$\epsilon = -\frac{\dot{H}}{H^2} = -\frac{d\log H}{d\log N} = \frac{\dot{\phi}}{2H^2} \tag{1.30}$$

where $N := \int H dt$ is the number of e-folds of inflation. From (1.30) it is possible to see that the necessary condition for violating SEC and having inflation is $\epsilon < 1$. Moreover, in order for inflation to last long enough to solve the flatness and horizon problems ϵ should remain smaller than one during the inflationary period. So we can define the logarithmic rate of evolution for ϵ called the second slow-roll parameter given by

$$\eta = \frac{\dot{\epsilon}}{\epsilon H} = -\frac{\ddot{H}}{\dot{H}H} = 2\left(\epsilon + \frac{\ddot{\phi}}{H\dot{\phi}}\right), \tag{1.31}$$

where $|\eta| < 1$. For deeper intricacies of the scalar field inflation we refer the reader to [31].

Inflation can thus be achieved by a scalar field which we call *inflaton*. The nature of this process can be divided two possibilities: *cold* and *warm* inflation.

1.6.1.1 Cold Inflation

Cold inflation is also commonly known as the *slow-roll* inflation since it is assumed that the field rolls down in the potential very slowly compared to the expansion of the universe. This can be physically translated into the fact that the acceleration of ϕ in (1.26c) is small compared to the friction-like term that is proportional to $\dot{\phi}$. This leads to the following approximations

$$\frac{1}{2}\dot{\phi} << V(\phi) \tag{1.32a}$$

$$|\ddot{\phi}| << 3H|\dot{\phi}|, \tag{1.32b}$$

called the slow-roll conditions, which allows to set

$$\dot{\phi} \simeq -\frac{V_\phi(\phi)}{3H}. \tag{1.33}$$

We can now express the Hubble function as:

$$H = \frac{d\ln a}{dt} = \dot{\phi}\frac{d\ln a}{dt} \simeq -\frac{V_\phi(\phi)}{3H}\frac{d\ln a}{d\phi} \tag{1.34}$$

So integrating over the scalar field ϕ we get

$$a = a_0 e^{\int d\phi (\partial_\phi \ln V)^{-1}}. \tag{1.35}$$

We can also define the slow-roll parameter for the potential, from which we can extract the inflation behavior, via

$$\epsilon_\phi := \frac{1}{2}\left(\frac{V_\phi(\phi)}{V(\phi)}\right)^2 \tag{1.36a}$$

$$\eta_\phi := \frac{V_{\phi\phi}(\phi)}{V}, \tag{1.36b}$$

where $V_{\phi\phi}(\phi) = \frac{d^2V(\phi)}{d\phi^2}$. These slow-roll parameters are different from the ones defined in (1.30) and (1.31). However, it is possible to relate them as: $\epsilon_\phi \approx \epsilon$ and $\eta_\phi \approx 2\epsilon - \frac{1}{2}\eta$.

1.6.1.2 Warm Inflation

A drawback from the cold inflation models is the separation between the inflationary and the reheating periods[3]. Since the process of reheating is crucial a question that arises is: How can one have a smooth transition between the inflationary and reheating period? One of the most successful answers to this question is the *warm inflation* model that was first introduced by Berera [33, 34]. The main idea of warm inflation is that the interaction between the inflaton and the other fields (thermal bath) can lead to the dissipation of the inflaton energy to other degrees of freedom. This implies that particle production (radiation) can occur simultaneously with the inflationary expansion as long the vacuum energy density dominates the energy budget of the universe. This model allows a smooth transition between the inflationary period and the radiation-dominated era.

The difference between cold and warm inflation is that radiation and inflaton are coupled to the scalar curvature. This coupling is introduced by an *ad hoc* term, $\Gamma\dot{\phi}^2$. So the equation of motion for inflation is given by

$$\ddot{\phi} + (3H + \Gamma)\,\dot{\phi} + V_\phi(\phi) = 0, \tag{1.37}$$

and the energy density equation for radiation reads:

$$\dot{\rho}_{\rm pf} + 4H\rho_{\rm pf} = \Gamma\dot{\phi}\dot{}2 \tag{1.38}$$

where Γ is called the dissipation coefficient. It is important to notice, as pointed out in [33], that the damping coefficient $\Gamma\dot{\phi}$ is only a suitable description for the dissipation and energy transfer from the inflaton to the thermal bath if the system is not far from thermal equilibrium. The dissipation coefficient Γ can have a dependence in the scalar field ϕ, in the

[3] During the inflationary period, depending on the model, the temperature of the universe drops typically by a factor of $10^5 K$. When inflation ends, the temperature will rise again and return to the pre-inflationary temperature, this is what we call the *reheating period.*[32]

temperature T or both [35–39]. The shape of Γ will be highly dependent on the model that we choose. We are interested only in the polynomial interaction between the scalar field and the thermal bath, in this case, we may consider Γ with a power-law dependence [40] in ϕ.

It is also possible in this scenario to define the slow-roll parameters for the warm inflation model. In this case, in the slow regime we have:

$$\phi \simeq -\frac{V_\phi}{3H+\Gamma}, \tag{1.39a}$$

$$\rho_{\rm pf} \simeq \frac{\Gamma}{4H}\dot{\phi}^2. \tag{1.39b}$$

The cold inflation can be seen as the limit of the warm inflation when $\Gamma \to 0$. We can also have two other distinct scenarios for the warm inflation model, the *week dissipative regime* $(\Gamma < H)$,

$$3H\dot{\phi} \simeq -V_\phi(\phi), \quad 4H\rho_{\rm pf} \simeq \Gamma\dot{\phi}^2, \tag{1.40}$$

and the *strong dissipative regime* $(\Gamma > H)$,

$$3(1+\frac{\Gamma}{3H})H\dot{\phi} \simeq -V_\phi(\phi, T), \quad 4H\rho_{\rm pf} \simeq \Gamma\dot{\phi}^2. \tag{1.41}$$

The strong dissipative scenario leads to the dependence on the temperature for some observable. The warm inflation model can then be characterized by four parameters:

$$\epsilon_\phi < 1 + \frac{\Gamma}{3H}, \quad |\eta_\phi| < 1 + \frac{\Gamma}{3H}, \quad \beta_\Gamma := \frac{\Gamma_\phi V_\phi}{\Gamma V} < 1, \quad \delta_T := \frac{T V_{\phi,T}}{V_\phi} < 1. \tag{1.42}$$

Building a realist warm inflation model is actually a challenge because of the explicit form of the dissipation coefficient. Explicit formulations have been obtained in the following works: for the approach in *particle production* [41, 42], *linear response theory* [43], and the *Schwinger-Keldysh* [44–47]. In Fig. 1.1 we can see a schematic comparison between the two inflationary models.

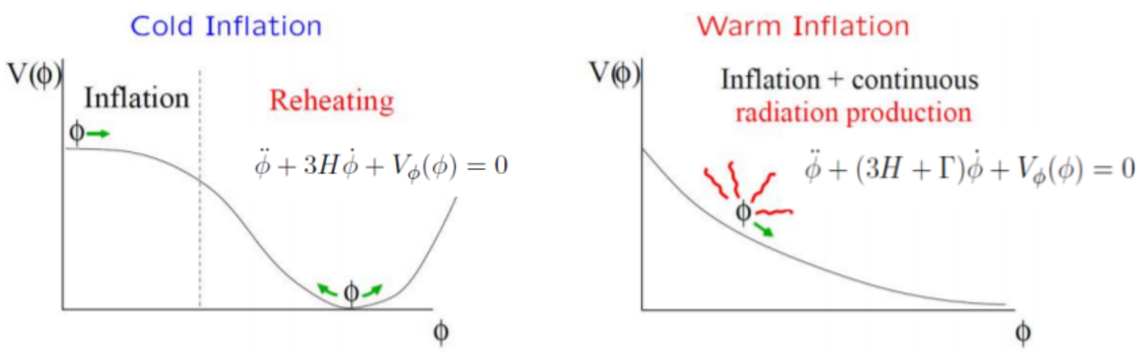

FIGURE 1.1: Comparison between cold and warm inflation as far of potential energy [1].

1.6.2 Vector Field Inflation

Despite the success achieved by both cold inflation and warm inflation and due to the difficulty in finding the proper scalar field that drives inflation, vector fields can present an interesting alternative.

It is natural to think of vector fields as they are present in the Standard Model and multiple ideas were proposed for vector fields to drive inflation [48–50].

Two main ideas that present some success when considering the vector field inflation are the *Einstein-Æther* and the *Bumblebee* model.

The Einstein-Æther theory can be seen as a modification of GR that contains a vector field called Æther non-minimal coupled to curvature. One of the main result of this model is the appearance of the *Nambu-Goldstone Bosons*, [51–53] leading to new kinds of Cherenkov radiation.

The Bumblebee model arises in the context of the *Standard Model Extension* theory, which contains the Standard Model, GR and a vector field (Bumblebee) that break Lorentz symmetry. This vector field has a non-zero expectation value and when coupled to gravity can lead to a de-Sitter type of inflation [54].

Although these vector field theories have their merit in achieving great results, in this particular work we are interested in another type of vector field, namely the *Yang-Mills* (YM) field. This field describes the dynamics of elementary particles and plays an important role in cosmology, string theory and particle physics. Although some results regarding the inflationary possibility of the Yang-Mills field were already found [50], a detailed and rigorous mathematical analysis of the global dynamics is scarce.

1.6.2.1 Introducing the Yang-Mills Field

We assume a universe that is spatially homogeneous and isotropic (FLRW) of the type

$$M = \mathbb{R} \times E^3/SO(3) \tag{1.43}$$

where the euclidean group E^3 is the isometry group of the spatial hypersurfaces. Since in FLRW, single vector fields are not allowed we will consider a multiplet of vector fields A^a_μ, $a = 1, ...N$, more precisely, a triplet of massive vector fields with global $SO_I(3)$ symmetry. Although it is true that A^a_μ is not E^3-invariant, it is possible to use relations between the asymmetries of different vector fields in such a way that the stress-energy tensor is E^3-invariant. As already shown in [55–57], in the non-Abelian case, the $SU(2)$[4] triplet of the YM fields admits

[4] $SU(n)$, the special unitary group, is a Lie group of $n \times n$ matrices with determinant 1.

a non-Abelian configuration whose stress-energy tensor has a 3-dimensional homogeneity and isotropy group.

To be able to define this multiplet one needs to consider the generators of the internal group $SO_I(3)$, L_a that obey the following relation [58]

$$[L_a, L_b] = L_a L_b - L_b L_a = \epsilon_{abc} L_c. \tag{1.44}$$

where ϵ_{abc} is the Levi-Civita symbol.

In the fundamental representation, the Lie algebra generators are normalized via

$$\mathrm{Tr}[L^a L^b] = -\frac{1}{2}\delta^{ab} \tag{1.45}$$

where we use the minus sign convention.

For each element of the algebra, it is possible to introduce a gauge field A^a_μ that can be related to the multiplet vector field by the equation

$$A_\mu = A^a_\mu L_a. \tag{1.46}$$

From the gauge potential it is possible to construct the gauge field strength [58]

$$F_{\mu\nu} = \partial_\mu A_\nu - \partial_\nu A_\mu + [A_\mu, A_\nu]. \tag{1.47}$$

1.6.2.2 Yang-Mills Action

The action for the massive YM field takes the form

$$S_{\mathrm{YM}} = \int_M d^4x\sqrt{-g}\left(\frac{1}{8e^2}\,\mathrm{Tr}[F_{\mu\nu}F^{\mu\nu}] + \frac{1}{2}\mu^2\,\mathrm{Tr}[A_\mu A^\mu]\right), \tag{1.48}$$

where $e > 0$ is the gauge coupling and $\mu \geq 0$ is the mass of the gauge field. From this, we can obtain the Yang-Mills stress-energy tensor (T_{YM}) that is given by

$$T_{\mathrm{YM}_{\mu\nu}} = -\frac{1}{2e^2}\,\mathrm{Tr}\left[F_{\mu\lambda}F^\lambda_\nu - \frac{1}{4}g_{\mu\nu}F_{\lambda\sigma}F^{\lambda\sigma}\right] - \frac{\mu^2}{2}\left[2A_\mu A_\nu - g_{\mu\nu}A_\lambda A^\lambda\right] \tag{1.49}$$

If we minimize the action with respect to each gauge field A^a_μ we obtain the classical equation of motion, called the Yang-Mills equation

$$\nabla_\mu F_{\alpha\beta} + [A_\mu, F_{\alpha\beta}] = 0. \tag{1.50}$$

1.6.2.3 Yang-Mills And Perfect Fluid

In this work we are particularly interested in understanding the dynamics of the massless and massive YM field in co-evolution with a perfect fluid with a linear equation of state, on Robertson-Walker geometries. As we shall see, this results in the problem of analyzing a nonlinear ODE system of Einstein-Euler-Yang-Mills equations.

The most general form of g which is invariant under the E^3 group is the flat Robertson-Walker metric that is obtained by making the Gaussian spatial, $k=0$, in (1.9). In Cartesian coordinates it takes the form

$$g = -dt^2 + a^2(t)(dx^2 + dy^2 + dz^2). \tag{1.51}$$

In this particular case, we will consider the action

$$S = S_{EH} + S_{\mathrm{YM}} + S_{\mathrm{pf}} = \int_M d^4x\sqrt{-g}\left(\frac{1}{2}R + \frac{1}{8e^2}\,\mathrm{Tr}[F_{\mu\nu}F^{\mu\nu}] + \frac{\mu^2}{2}\,\mathrm{Tr}[A_\mu A^\mu] + \mathcal{L}_{\mathrm{pf}}\right) \tag{1.52}$$

We have now two types of fields that are encoded in

$$T_{\mu\nu} = T_{\mathrm{pf}\mu\nu} + T_{\mathrm{YM}\mu\nu} \tag{1.53}$$

and satisfy the Euler equation

$$\nabla^\mu T_{\mathrm{pf}\mu\nu} = 0, \quad \nabla^\mu T_{\mathrm{YM}\mu\nu} = 0. \tag{1.54}$$

In our coordinate system, $u^\mu = \delta^\mu_0$, we simply get $T_{\mathrm{pf}\mu\nu} = diag(\rho_{\mathrm{pf}}, p_{\mathrm{pf}}, p_{\mathrm{pf}}, p_{\mathrm{pf}})$.

Following [59], we assume that the vector fields $\vec{A}$ have global $SO(3)$ symmetry, and fixing the gauge freedom with the temporal (Hamiltonian) gauge leads to

$$A_0 = 0, \quad A^a_i(t) = \chi(t)\delta^a_i, \tag{1.55}$$

where $\chi(t)$ is a C^2 function of t and we denote space indices with $i =, 1, 2, 3$.

It turns out that, under our symmetry assumptions, the Yang-Mills field has only a single "scalar" degree of freedom [50, 59, 60] and, using the relations

$$\mathrm{Tr}[F_{\mu\nu}F^{\mu\nu}] = 3\left(\frac{\dot{\chi}^2}{a^2} - \frac{\chi^4}{4a^4}\right), \tag{1.56a}$$

$$\mathrm{Tr}[A_\mu A^\mu] = -\frac{3\chi^2}{2a^2}, \tag{1.56b}$$

$$\mathrm{Tr}[F_{0i}F^{0i}] = -\frac{3\dot{\chi}^2}{2a^2}, \tag{1.56c}$$

then the tensor $T_{\mathrm{YM}_{\mu\nu}}$ can also be decomposed with respect to $\vec{u}$ on a "perfect fluid" form as in (1.10):

$$T_{\mathrm{YM}_{\mu\nu}} = (\rho_{\mathrm{YM}} + p_{\mathrm{YM}})u_\mu u_\nu + p_{\mathrm{YM}} g_{\mu\nu}, \tag{1.57}$$

for appropriate identifications of the quantities in (1.49) with $\rho_{\mathrm{YM}} = T_{\mathrm{YM}_{00}}$ and $p_{\mathrm{YM}} = (1/3)T^{i}_{\mathrm{YM}_{\mathrm{i}}}$, as we shall see later.

1.7 Anisotropic Universes

As mentioned in Sec. 1.6 the Flatness and Horizon problems are basically problems of fine-tuning. It is generally assumed that the universe can be modelled by a flat FLRW spacetime. However observations are compatible with small anisotropies [8]. Bianchi cosmologies are spatially homogeneous and anisotropic models that generalise FLRW cosmologies. The first studies about Bianchi models were presented by Taub [61] and Ellis, and MacCallum [62].

A Bianchi spacetime (M, g) is endowed with a metric g that admits a 3-dimensional isometry group acting simply transitively on spacelike hypersurfaces which are surfaces of homogeneity. These spacetimes then admit a Lie algebra of Killing vectors field which has been classified according to the isometry group structure into different types [62]. Bianchi type I is the simplest case when, in an appropriate basis, the structure constants are zero and the group is Abelian.

We consider that the unit vector field normal to the orbits of the isometry group is the 4-velocity vector $\mathbf{u}$ of the spacetime fluid matter field. In that case one can project spacetime quantities into the 3-spaces orthogonal to $\mathbf{u}$ with the projection tensor

$$h_{\mu\nu} = g_{\mu\nu} + u_{\mu\nu},$$

where $h_\mu{}^\alpha h_\alpha{}^\nu = h_\mu{}^\nu$, $h_\mu{}^\nu u_\nu = 0$ and $h_\alpha{}^\alpha = 3$. One can make the decomposition of the covariant derivative of the 4-velocity as (see e.g. [8])

$$\nabla_\mu u_\nu = \sigma_{\mu\nu} + H h_{\mu\nu} + u_\mu u^\alpha \nabla_\alpha u_\nu$$

where we assumed that the fluid has no vorticity. The symmetric and trace-free tensor $\sigma_{\mu\nu}$ is called shear and satisfies $u^\mu \sigma_{\mu\nu} = 0$ and

$$\begin{aligned} \sigma_{\mu\nu} &= \nabla_{(\mu} u_{\nu)} - H h_{\mu\nu} + u_{(\mu} u^\alpha \nabla_\alpha u_{\nu)} \\ H &= \frac{1}{3}\nabla^\alpha u_\alpha \end{aligned} \tag{1.58}$$

where H is the expansion scalar or Hubble function.

It is also useful to define

$$\sigma^2 = \frac{1}{2}\sigma_{\mu\nu}\sigma^{\mu\nu}.$$

1.7.1 Bianchi algebras and Classification

The Lie Algebra of *Killing Vector Fields* with basis ξ_α, $\alpha = 1, 2, 3$ satisfies

$$[\xi_\alpha, \xi_\beta] = C^\mu_{\alpha\beta}\xi_\mu, \tag{1.59}$$

where $C^\mu_{\alpha\beta}$ are the structure constants and can be decomposed as [8]

$$C^\mu_{\alpha\beta} = \epsilon_{\alpha\beta\nu}n^{\mu\nu} + a_\alpha\delta^\mu_\beta - a_\beta\delta^\mu_\alpha, \tag{1.60}$$

where $n^{\mu\nu} = n^{\nu\mu}$ and a_α are constants.

$$n^{\alpha\beta}a_\beta = 0. \tag{1.61}$$

It turns out that by choice of frame one can diagonalize $n^{\mu\nu}$ and choose $a_\alpha = (a, 0, 0)$. The classification of the Bianchi groups in GR takes into consideration the sign of $n^{\mu\nu}$ and the value of a. This classification was first introduced by Ellis and MacCallum [62] and divides the spacetime into two classes: *Class A* and *Class B*. Later on in 1973 Collins and Hawking [63] introduced an additional parameter, h defined via

$$h = \frac{a^2}{n_2 n_3}. \tag{1.62}$$

The Bianchi classification can be seen in Table. 1.2.

Group class	Group type	n_1	n_2	n_3	Contains RW?
$A(a=0)$	I	0	0	0	$k=0$
	II	+	0	0	−
	VI_0	0	+	−	−
	VII_0	0	+	+	$k=0$
	$VIII$	−	+	+	−
	IX	+	+	+	$k=+1$
$B(a\neq 0)$	V	0	0	0	$k=-1$
	IV	0	0	0	−
	VI_h	0	+	−	−
	VII_h	0	+	+	$k=-1$

Table 1.2: Bianchi models divided into two classes (A and B) alongside with the parameter h. We also indicate the possibility of admitting a RW metric.

1.7.2 Bianchi I Model

The Bianchi I model has $n_1 = n_2 = n_3 = 0$ (see Table 1.2) and the metric for this model in Cartesian coordinates (t, x, y, z) takes the form

$$ds^2 = -dt^2 + b_1(t)^2 dx^2 + b_2(t)^2 dy^2 + b_3(t)^2 dz^2 \tag{1.63}$$

where b_i are C^2 functions of time that represent the scale factor in each direction. We can also define the Hubble function

$$H(t) = \frac{\dot{a}}{a}, \tag{1.64}$$

where the dot denotes the derivative with respect to time and

$$a = (b_1, b_2, b_3)^{1/3}.$$

In this case $\sigma_{\mu\nu}$ is diagonal and since it is also trace-free it has only two degrees of freedom which can be written as

$$\sigma_+ = \frac{1}{2}\left(\sigma_{22} + \sigma_{33}\right), \qquad \sigma_- = \frac{1}{2}\sqrt{2}(\sigma_{22} - \sigma_{33}). \tag{1.65}$$

Using the shear equation and (1.64) we can obtain the non-vanishing components of $\sigma_{\mu\nu}$ as

$$\sigma_{11} = \frac{4}{3}\frac{\dot{b}_1}{b_1} - \frac{2}{3}\left(\frac{\dot{b}_2}{b_2} + \frac{\dot{b}_3}{b_3}\right) \tag{1.66a}$$

$$\sigma_{22} = \frac{4}{3}\frac{\dot{b}_2}{b_2} - \frac{2}{3}\left(\frac{\dot{b}_3}{b_3} + \frac{\dot{b}_1}{b_1}\right) \tag{1.66b}$$

$$\sigma_{33} = \frac{4}{3}\frac{\dot{b}_3}{b_3} - \frac{2}{3}\left(\frac{\dot{b}_1}{b_1} + \frac{\dot{b}_2}{b_2}\right) \tag{1.66c}$$

In turn the shear scalar σ^2 can be written as

$$\sigma^2 = \frac{1}{3}\left(\frac{\dot{b}_1^2}{b_1^2} + \frac{\dot{b}_2^2}{b_2^2} + \frac{\dot{b}_3^2}{b_3^2} - \frac{\dot{b}_1\dot{b}_2}{b_1 b_2} - \frac{\dot{b}_2\dot{b}_3}{b_2 b_3} - \frac{\dot{b}_1\dot{b}_3}{b_1 b_3}\right). \tag{1.67}$$

and taking the time derivative in (1.67) we obtain the evolution equation

$$\frac{\dot{\sigma}}{\sigma} = -\left(\frac{\dot{b}_1}{b_1} + \frac{\dot{b}_2}{b_2} + \frac{\dot{b}_3}{b_3}\right) = -3H. \tag{1.68}$$

1.8 Dynamical Systems in Cosmology

The EFE are partial differential equations but in the case of spatially homogeneous spacetimes they become ordinary differential equations. In that case one can use dynamical system's theory in order to study the qualitative behaviour of the solutions[5]. This has been particularly successful in cosmology where far reaching rigorous results have been achieved using dynamical systems [8, 66, 67]. The most common procedure in those approaches is to replace the metric variables with dimensionless variables using some form of conformal rescalings as well as suitable normalization factors to compact the state-space that allows us to write the system as an autonomous system.

The majority of studies in this context are restricted to the linear analysis of hyperbolic fixed points, overlooking cases where the linearization gives zero eigenvalues. However many cases of interest in cosmology lead precisely to non-hyperbolic fixed points in the space of solutions. Then, more advanced methods need to be used and further developed for each problem at hand. Recent works using central manifold theory include Alho et. al [68], Escobar et. al [69], Bohemer et. al [70], Cid et. al [71] and Miritzis [72, 73].

Works developing other methods using monotone functions and a careful asymptotic analysis include Heinzle & Uggla [74, 75], Norman et. al [76], Sandin & Uggla [77], Heinzle & Calogero [78] and Rendall & Uggla [79] and Alho & Uggla [80].

In turn the existence of asymptotic period orbits has also recently been studied using averaging methods in the works of Leon et al [81–83], Fajman et al [84] and Alho et al [68, 85].

Motivated by the previews reviews and works we will use a compactification of the state space that will produce a regular and compact global dynamical system that will allow us to obtain a global dynamics for a variety of cosmological models. Regarding the study of dynamical systems in cosmology, the most common way is to introduce the so-called Poincaré compactification on the plane. However this method does not consider some important features inherent to each cosmological model such as the natural geometry of the space and may lead to expensive computations [50]. To avoid this complications, we will use, dimensionless, expansion normalized variables that will provide a natural compactification of the state-space. We will consider a variety of cosmological models in which we will infer the possibility of inflation.

These cosmological scenarios include the study of global dynamics of a scalar field and a perfect fluid in both an isotropic and anisotropic universes. We will also study the dynamics inherent to the Yang-Mills field with a perfect fluid in a flat, homogeneous, and isotropic spacetime.

[5] In appendix we revise some of the relevant techniques of dynamical systems.

Chapter 2

Global Dynamics of Yang-Mills Field and Perfect-Fluid Robertson-Walker Cosmologies

In this chapter we apply a new global dynamical systems formulation to flat Robertson-Walker cosmologies with a massless and massive Yang-Mills field and a perfect-fluid with linear equation of state as the matter sources. This allows us to give proofs concerning the global dynamics of the models including asymptotic source-dominance towards the past and the future time directions. For the pure massless Yang-Mills field, we also contextualize well-known explicit solutions in a global (compact) state space picture.

The chapter is structured as follows: In Sec. 2.1 we will introduce the basic dynamics inherent to the interaction between scalar field and perfect-fluid. in Section 2.2, we consider the simplest model of a massless Yang-Mills field and a fluid with linear equation of state. We reformulate the Einstein field equations to a 3-dimensional dynamical system on a compact state-space, followed by an analysis of the flow which yields a global description of the solution space including its asymptotic behavior. For the pure massless Yang-Mills invariant subset ($\rho_{\rm pf} = 0$), the field equations can be further reduced to an analytical 2-dimensional unconstrained dynamical system which is integrable in terms of elliptic functions, thus contextualizing this well-known explicit solutions in a global (compact) state-space picture. In Section 2.3, we consider the massive Yang-Mills field together with the fluid matter model. In this case, the field equations are reformulated as a 4-dimensional dynamical system with a constraint[1]. We make a global analysis of the flow and give rigorous proofs concerning the asymptotic behavior of general solutions both in the past and future time directions.

[1]For a study of constraint systems in cosmology see [8, 87].

2.1 Dynamics and Einstein Field Equations for the Yang-Mills Field and Perfect Fluid in Robertson-Walker

We assume that (M, g) is spatially homogeneous and isotropic and given by (1.43). The most general form for g which is invariant under the E^3 group is the flat RW metric, which in Cartesian coordinates is given by (1.51). We consider scalar fields as well as vector fields defined on M which are compatible with our symmetry assumptions. In particular, we shall consider perfect fluid (scalar) matter with density $\rho_{\rm pf}(t)$ and pressure $p_{\rm pf}(t)$ and Yang-Mills (4-vector) fields that was already described in Sec. 1.6.2. These two types of fields will be encoded in two tensors $T_{\rm pf}$ and $T_{\rm YM}$ defined on M that can be seen in (1.53).

Considering a globally defined timelike vector field $\vec{u}$ corresponding, physically, to the 4-velocity of the fluid, we may decompose $T_{{\rm pf}\mu\nu}$ with respect to $\vec{u}$ as seen in (1.10), which must satisfy the Euler equations, eq. (1.54).

It turns out that, under our symmetry assumptions, the Yang-Mills field has only a single "scalar" degree of freedom [59, 60] which allows us to write the stress-energy tensor $T_{{\rm YM}_{\mu\nu}}$ similar to the one of the perfect fluid as we can see in (1.57). In particular the level sets of χ coincide with the surfaces of simultaneity of observers comoving with the fluid.

For the (conformal invariant) massless Yang-Mills field ($\mu = 0$), the resulting stress-energy tensor is trace-free, so that its effective equation of state is that of a radiation fluid and the model is explicitly solvable [59, 60]. The massive case, $\mu \neq 0$, has been studied in [59] using a dynamical systems approach, and the inclusion of a dust and radiation fluid has been discussed in [88].

The evolution and constraint equations are then obtained from (1.6), using (1.51) on the left-hand-side (which gives the Ricci tensor ($R_{\mu\nu}$) and the scalar of curvature R), and using (1.53) on the right-hand-side satisfying (1.8) and (1.50), under the above assumptions. So, the Einstein-Euler-Yang-Mills system in a flat Robertson-Walker geometry reduces to the following system of nonlinear ODEs:

$$H^2 = \left(\frac{\dot{\chi}}{2\sqrt{2}ae}\right)^2 + \left(\frac{\chi}{2^{\frac{1}{4}}2a\sqrt{e}}\right)^4 + \left(\frac{\mu\chi}{2a}\right)^2 + \frac{\rho_{\rm pf}}{3}. \tag{2.1a}$$

$$\ddot{\chi} = -H\dot{\chi} - \frac{\chi^3}{2a^2} - 2\mu^2 e^2 \chi \tag{2.1b}$$

$$\dot{\rho}_{\rm pf} = -3H\gamma_{\rm pf}\rho_{\rm pf} \tag{2.1c}$$

$$\dot{H} = -\left(\frac{\dot{\chi}}{2ae}\right)^2 - \left(\frac{\chi}{2a\sqrt{e}}\right)^4 - \left(\frac{\mu\chi}{2a}\right)^2 - \frac{\gamma_{\rm pf}}{2}\rho_{\rm pf} \tag{2.1d}$$

$$\dot{a} = Ha \tag{2.1e}$$

where the overdot denotes a derivative with respect to t and $H(t) := \dot{a}/a$ is the Hubble function.

Regarding $\dot{\chi}$ as a new dependent variable, the first equation can be seen as a constraint for the variables $(\chi, \dot{\chi}, \rho_{\rm pf}, H, a)$. By further introducing

$$\phi(t) := \frac{\chi}{\sqrt{2}a} \quad \text{and} \quad \psi(t) := \frac{\dot{\chi}}{\sqrt{2}ae}, \tag{2.2}$$

the equation for $a(t)$ decouples, and leaves a reduced dynamical system for the state vector $(\phi, \psi, \rho_{\rm pf}, H)$ given by

$$\dot{\phi} = -H\phi + e\psi \tag{2.3a}$$

$$\dot{\psi} = -2H\psi - \frac{\phi^3}{e} - 2\mu^2 e\phi \tag{2.3b}$$

$$\dot{\rho}_{\rm pf} = -3H\gamma_{\rm pf}\rho_{\rm pf} \tag{2.3c}$$

$$\dot{H} = -\frac{\psi^2}{2} - \frac{\phi^4}{4e^2} - \mu^2\frac{\phi^2}{2} - \frac{\gamma_{\rm pf}}{2}\rho_{\rm pf}, \tag{2.3d}$$

with constraint

$$H^2 = \frac{\psi^2}{4} + \frac{\phi^4}{8e^2} + \frac{\mu^2}{2}\phi^2 + \frac{\rho_{\rm pf}}{3}. \tag{2.4}$$

The Yang-Mills field generates an effective energy density $\rho_{\rm YM} \geq 0$ and pressure $p_{\rm YM}$, given by

$$\rho_{\rm YM}(t) := 3\Big[\frac{\psi^2}{4} + \frac{\phi^4}{8e^2} + \frac{\mu^2}{2}\phi^2\Big] \tag{2.5a}$$

$$p_{\rm YM}(t) := \frac{\psi^2}{4} + \frac{\phi^4}{8e^2} - \frac{\mu^2}{2}\phi^2, \tag{2.5b}$$

from which we define the function

$$\gamma_{\rm YM}(t) := 1 + \frac{p_{\rm YM}}{\rho_{\rm YM}}. \tag{2.6}$$

In (1.6), we have fixed physical units such that $8\pi G = c = 1$, where G is the Newton gravitational constant and c the speed of light. With this choice, we have that $[t] = L$, $[H] = L^{-1}$, $[e] = L^{-1}$, $[\phi] = L^{-1}$, $[\psi] = L^{-1}$, whereas μ is dimensionless.

Our aim is to apply a new global dynamical systems formulation adapted from the problem of a minimally coupled scalar field having a zero local minimum of the potential, such as the Klein-Gordon field [80] or more general monomial potentials [68]. Similar methods have also been applied to α-attractor E and T-models of inflation in [89] as well as to the Starobinsky model of modified $f(R)$ gravity theory [15].

The new formulation has several advantages with respect to the original variables and which are commonly used in the literature, see e.g. [50, 59]. To see this, consider for simplicity the state vector (ϕ, ψ, H), i.e. with no fluid matter content. The state space consists of a surface defined by the constraint (2.4) with the fixed point M located at $(0,0,0)$, which is the only fixed point of system (2.3)-(2.4), see Figure 2.1. This fixed point joins the two disconnected parts, having either $H > 0$ or $H < 0$, i.e., preserving the sign of H. We are interested in expanding cosmologies so, from now on, we will restrict the analysis to the upper half of the state space where $H > 0$. By solving for H in (2.4) and inserting the positive root in the evolution equations, leads to an unconstrained two-dimensional dynamical system on the plane. This system might have differentiability problems at the origin, where lies the full degenerated Minkowski fixed point M. The blow up of such fixed point can be found in [59] where it was shown that it is a local focus.

However, as it will be shown here, in the present formulation this fixed point appears naturally as a periodic orbit and provides indeed the correct picture [2]. This fact is related to the existence of a conserved quantity for the system: the expansion normalized effective energy density due to the Yang Mills field

$$\Omega_{\mathrm{YM}} := \frac{\rho_{\mathrm{YM}}}{3H^2}. \tag{2.7}$$

Another relevant aspect of this formulation concerns the compactification of the state space on the plane, in which Poincaré method is usually the standard approach which presents some problems as mentioned in section 1.8. Instead, the use of (dimensionless) expansion normalized variables, gives a very natural compactification of the state space (where $H \to +\infty$), in which self-similar solutions appear as hyperbolic fixed points.

Furthermore, when introducing matter in the form of a perfect fluid with a linear equation of state, the state space becomes the region limited by a quartic surface (see Figure 2.1), and the old formulation would also lead to difficulties when discussing asymptotic source dominance since all orbits tend to a single degenerated fixed point M. Instead, the correct picture of attractors being periodic orbits leads naturally to the use of averaging techniques from dynamical systems theory, see e.g. [90]. This, in turn, allows us to give rigorous proofs concerning the asymptotics when matter models other than the Yang-Mills field are present.

Finally, this framework is the starting point for considering less restrictive geometries like in the spatially homogeneous but anisotropic spacetimes, an issue we shall discuss further in Section 2.4.

[2] This also clarifies the issue of asymptotic self-similarity and manifest self-similarity breaking as discussed in [68].

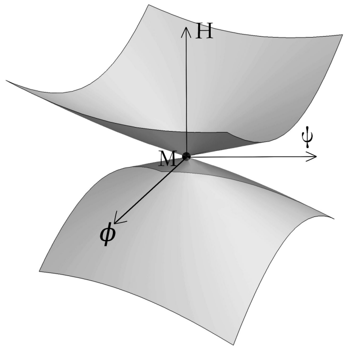

Figure 2.1: The state-space of system (2.3) defined by the constraint (2.4).

2.2 Massless Yang-Mills field (case $\mu = 0$)

For the massless Yang-Mills field, the ratio $p_{\mathrm{YM}}/\rho_{\mathrm{YM}}$ is constant and the function $\gamma_{\mathrm{YM}}(t)$, defined in (2.6), is simply given by

$$\gamma_{\mathrm{YM}} = \frac{4}{3}. \tag{2.8}$$

Hence, the massless Yang-Mills field can be view as an effective radiation fluid, which basically turns the problem into that of a two-fluid cosmology. However, it is instructive to consider first this simple model, since it allows us to introduce some basic definitions and illustrate how a global dynamical systems formulation of the original equations can be constructed. It will also allow us to situate well-known explicit solutions in a global state space picture, as well as emphasizing the differences that arise in the more complicated case of the massive Yang-Mills field.

We assume an expanding cosmology $H(t) > 0$, and introduce the (dimensionless) H-normalised variables

$$X_1 = \frac{\phi}{2^{\frac{3}{4}}\sqrt{eH}}, \qquad \Sigma_{\mathrm{YM}} = \frac{\psi}{2H}, \qquad \tilde{T} = \sqrt{\frac{\sqrt{2}e}{H}}, \qquad \Omega_{\mathrm{pf}} = \frac{\rho_{\mathrm{pf}}}{3H^2}, \tag{2.9}$$

together with the number of $e-$folds $N = \ln(a/a_0)$, where a_0 is some reference epoch at which $N = 0$, and

$$\frac{dN}{dt} = H. \tag{2.10}$$

Then, the system of equations (2.3)-(2.4), in the new variables, reduces to a *local* 3-dimensional dynamical system

$$\frac{dX_1}{dN} = -\frac{1}{2}\left[(1-q)X_1 - 2\tilde{T}\Sigma_{\mathrm{YM}}\right] \tag{2.11a}$$

$$\frac{d\Sigma_{\mathrm{YM}}}{dN} = -\left[(1-q)\Sigma_{\mathrm{YM}} + 2\tilde{T}X_1^3\right] \tag{2.11b}$$

$$\frac{d\tilde{T}}{dN} = \frac{1}{2}(1+q)\tilde{T}, \tag{2.11c}$$

where we make use of the fact that the constraint

$$1 - \Omega_{pf} = X_1^4 + \Sigma_{\rm YM}^2 \tag{2.12}$$

is linear in $\Omega_{\rm pf}$, to solve for $\Omega_{\rm pf}$, and where we introduced the so-called *deceleration parameter* q, defined via (1.17), i.e.

$$\begin{aligned} q &= -1 + 2\left(\Sigma_{\rm YM}^2 + X_1^4\right) + \frac{3}{2}\gamma_{pf}\Omega_{pf} \\ &= 1 + \frac{3}{2}\left(\gamma_{pf} - \frac{4}{3}\right)\left(1 - \Sigma_{\rm YM}^2 - X_1^4\right). \end{aligned} \tag{2.13}$$

Since $\Omega_{\rm pf} \geq 0$, the constraint equation (2.12) implies that

$$-1 \leq X_1 \leq 1, \qquad -1 \leq \Sigma_{\rm YM} \leq 1, \qquad 0 \leq \Omega_{\rm pf} \leq 1. \tag{2.14}$$

Moreover, since $0 < \gamma_{\rm pf} \leq 2$, it follows from (2.13) that

$$-1 < q \leq 2\,. \tag{2.15}$$

Hence, the right-hand side of (2.11) becomes unbounded only when $\tilde{T} \to +\infty$ ($H \to 0$). In order to obtain a global dynamical systems formulation on a compact state space, we further introduce

$$T = \frac{\tilde{T}}{1+\tilde{T}} \tag{2.16}$$

so that $T \to 0$ as $\tilde{T} \to 0$, and $T \to 1$ as $\tilde{T} \to +\infty$. We also introduce a new independent variable τ defined by

$$\frac{d\tau}{dt} = \frac{H}{1-T}. \tag{2.17}$$

The τ variable is constructed such that it interpolates between the two asymptotic regimes described by the different scales inherent to the model, i.e. the Hubble scale H, when $H \to +\infty$, and the scale associated with gauge-coupling constant e, when $H \to 0$, see [80] for more details on this issue. This leads to a *global* 3-dimensional dynamical system

$$\frac{dX_1}{d\tau} = -\frac{1}{2}\left[(1-q)(1-T)X_1 - 2T\Sigma_{\rm YM}\right] \tag{2.18a}$$

$$\frac{d\Sigma_{\rm YM}}{d\tau} = -\left[(1-q)(1-T)\Sigma_{\rm YM} + 2TX_1^3\right] \tag{2.18b}$$

$$\frac{dT}{d\tau} = \frac{1}{2}(1+q)T(1-T)^2, \tag{2.18c}$$

where the constraint (2.12) is used to globally solve for $\Omega_{\rm pf}$ and q is given by (2.13). It is also useful to consider the auxiliary evolution equation for $\Omega_{\rm YM} := \rho_{\rm YM}/(3H^2) = \Sigma_{\rm YM}^2 + X_1^4$

(equivalently $\Omega_{\rm pf} = 1 - \Omega_{\rm YM}$), which is given by

$$\frac{d\Omega_{\rm YM}}{d\tau} = 3(1-T)(\gamma_{\rm pf} - \frac{4}{3})\Omega_{\rm YM}(1-\Omega_{\rm YM}). \tag{2.19}$$

The state space $\mathbf{S}$ is a 3-dimensional space consisting of a deformed solid cylinder of height $0 < T < 1$. The outer shell of the cylinder corresponds to the *pure Yang-Mills* invariant subset $\Omega_{pf} = 0$ ($\Omega_{\rm YM} = 1$) which we denote by $\mathbf{S}_{\rm YM}$. The axis of the cylinder is a straight line with $\Omega_{pf} = 1$ ($\Omega_{\rm YM} = 0$) and corresponds to the invariant subset associated with the (self-similar) flat Friedmann-Lemaître (FL) spacetime. The state space $\mathbf{S}$ can be analytically extended to include its closure, i.e., the invariant boundaries $T = 0$ and $T = 1$, and form the extended state space $\overline{\mathbf{S}}$, while the extension of $\mathbf{S}_{\rm YM}$ to $T = 0$ and $T = 1$ will be denoted by $\overline{\mathbf{S}}_{\rm YM}$. This extension is crucial since all attracting sets are located on these boundaries as shown by the following simple lemma:

Lemma 2.1. *The α-limit set of all interior orbits in $\mathbf{S}$ is located at $T = 0$, while the ω-limit set of all interior orbits in $\mathbf{S}$ is located at $T = 1$.*

Proof. Since $1 + q > 0$, then T is strictly monotonically increasing in the interval $(0, 1)$. By the monotonicity principle (see proposition.A.23), it follows that there are no fixed points, recurrent or periodic orbits in the interior of the state space $\mathbf{S}$, and the α and ω-limit sets of all orbits in $\mathbf{S}$ are contained at $T = 0$ and $T = 1$, respectively. $\square$

We now give a detailed description of the invariant boundaries $T = 0$, associated with the asymptotic past ($H \to +\infty$), and $T = 1$, associated with the asymptotic future ($H \to 0$), as well as the pure massless Yang-Mills invariant subset $\mathbf{S}_{\rm YM}$ and the Friedmann-Lemaître invariant subset.

2.2.1 The invariant boundary $T = 0$

The flow induced on the $T = 0$ boundary is given by

$$\frac{dX_1}{d\tau} = \frac{3}{4}\left(\gamma_{\rm pf} - \frac{4}{3}\right)\Omega_{pf}X_1, \tag{2.20a}$$

$$\frac{d\Sigma_{\rm YM}}{d\tau} = \frac{3}{2}\left(\gamma_{pf} - \frac{4}{3}\right)\Omega_{pf}\Sigma_{\rm YM} \tag{2.20b}$$

with the constraint $\Omega_{pf} = 1 - \Omega_{\rm YM} = 1 - X_1^4 - \Sigma_{\rm YM}^2$. For $\gamma_{\rm pf} = 4/3$, this subset consists only of fixed points, forming the deformed disk:

$$\mathrm{D_R}: \qquad 0 \leq \Sigma_{\rm YM}^2 + X_1^4 \leq 1, \qquad \text{for} \qquad T = 0.$$

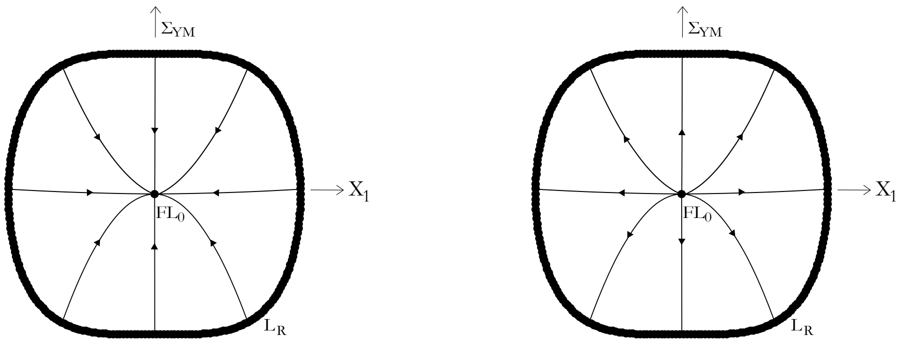

(A) Invariant boundary $T=0$ for $\gamma_{\mathrm{p}f}=1<4/3$.

(B) Invariant boundary $T=0$ for $\gamma_{\mathrm{p}f}=\frac{3}{2}>4/3$.

Figure 2.2: The invariant boundary $T=0$ of phase-space $\mathbf{S}$ for two different values of $\gamma_{\mathrm{p}f}$. The picture for $\gamma_{\mathrm{p}f}=4/3$ consists of a disk of fixed points.

For $\gamma_{\rm pf}\neq 4/3$, the invariant subset $\Omega_{\rm pf}=0$ consists of a deformed circle of fixed points given by

$$\mathrm{L}_\mathrm{R}: \qquad \Sigma_{\rm YM}^2+X_1^4=1, \qquad \text{for} \qquad T=0,$$

and there is one more isolated fixed point FL_0 located at $\Omega_{\rm YM}=0$, i.e.

$$\mathrm{FL}_0: \quad \Sigma_{\rm YM}=X_1=0, \qquad \text{for} \qquad T=0.$$

At the invariant boundary $T=0$, the trajectories of the solutions are easily found by quadrature giving

$$\Sigma_{\rm YM}=CX_1^2, \tag{2.21}$$

where C is a real constant that parametrizes the solutions. This equation clearly shows that the flow is invariant under the transformation $(X_1,\Sigma_{\rm YM})\to(-X_1,\Sigma_{\rm YM})$. Moreover, since $\Omega_{\mathrm{p}f}>0$, a straightforward inspection of the flow, shows that, if $\gamma_{\mathrm{p}f}>\frac{4}{3}$ (resp. $\gamma_{\mathrm{p}f}<\frac{4}{3}$), then L_R is a sink (resp. source) of a 1-parameter set of solutions with a single solution ending (resp. originating) from each fixed point and FL_0 is a source (resp. sink) of a 1-parameter set of solutions, see Figure 2.2.

2.2.2 The invariant boundary $T=1$

On the $T=1$ invariant boundary, the system (2.18a)-(2.18b) reduces to

$$\frac{dX_1}{d\tau}=\Sigma_{\rm YM}, \tag{2.22a}$$

$$\frac{d\Sigma_{\rm YM}}{d\tau}=-2X_1^3, \tag{2.22b}$$

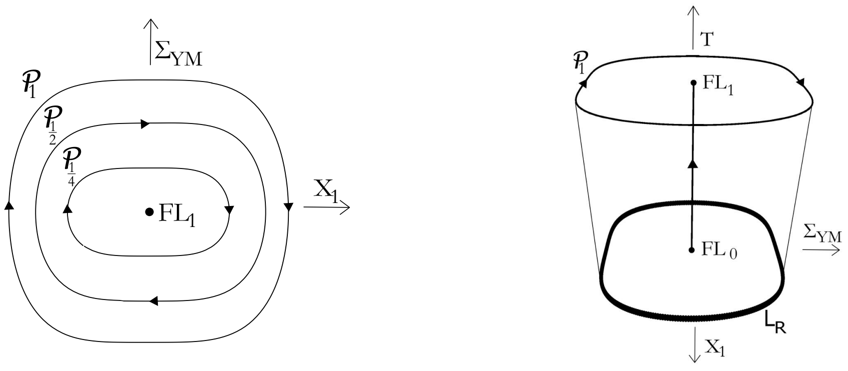

(A) Invariant boundary $T = 1$.

(B) Invariant subset $\Omega_m = 1$.

Figure 2.3: Representation of the invariant boundary $T = 1$ and the invariant subset $\Omega_{\rm pf} = 1$.

which has a single fixed point:

$$\mathrm{FL}_1: \quad \Sigma_{\rm YM} = X_1 = 0, \qquad \text{for} \qquad T = 1.$$

In this case, it also follows that $d\Omega_{\rm YM}/d\tau = 0$, implying

$$\Omega_{\rm YM} = C, \tag{2.23}$$

where $C \in [0, 1]$. The $T = 1$ boundary is then foliated by a 1-parameter set of periodic orbits $\mathcal{P}_{\Omega_{\rm YM}}$ and, therefore, the fixed point FL_1 (corresponding to $C = 0$) is a center (see Figure 2.3a). Note that $C = 1$ gives the outer periodic orbit $\mathcal{P}_1$ with $\Omega_{\rm YM} = 1$ ($\Omega_{pf} = 0$).

2.2.3 The Friedmann-Lemaître invariant subset: $\mathrm{FL}_0 \to \mathrm{FL}_1$

The invariant subset $\Omega_{pf} = 1$ consists of a straight heteroclinic orbit connecting the FL_0 fixed point, located at the origin, to the fixed point FL_1 located at $(X_1, \Sigma_{\rm YM}, T) = (0, 0, 1)$. This orbit is associated with the flat Friedmann-Lemaître solution, where T describes the evolution of H, see Figure 2.3b.

2.2.4 The pure massless Yang-Mills subset $\overline{\mathrm{S}}_{\rm YM}$

On the invariant set $\Omega_{\rm pf} = 0$, it follows that the deceleration parameter q is constant, with $q = 1$, and the dynamical system simplifies to

$$\frac{dX_1}{d\tau} = T\Sigma_{\rm YM}\,, \quad \frac{d\Sigma_{\rm YM}}{d\tau} = -2TX_1^3\,, \quad \frac{dT}{d\tau} = T(1-T)^2, \tag{2.24}$$

subject to the constraint

$$\Sigma_{\rm YM}^2 + X_1^4 = 1. \tag{2.25}$$

This constraint can be globally solved by introducing the angular variable θ as

$$X_1 = \cos\theta, \qquad \Sigma_{\rm YM} = G(\theta)\sin\theta, \tag{2.26}$$

where

$$G(\theta) = \sqrt{1+\cos^2\theta}. \tag{2.27}$$

This leads to a 2-dimensional unconstrained dynamical system for the state vector (θ, T), given by

$$\frac{d\theta}{d\tau} = -TG(\theta) \tag{2.28a}$$

$$\frac{dT}{d\tau} = T(1-T)^2. \tag{2.28b}$$

The intersection with the invariant boundary $T = 0$, consists of the circle of fixed points $\mathrm{L_R}$ whose linearisation yields the eigenvalues 1 and 0, with the center manifold being the line itself, i.e., the circle of fixed points is normally hyperbolic, so that a unique solution originates from each fixed point $(\theta_0, 0)$, $\theta_0 \in [0, 2\pi)$, and a one-parameter set of solutions (parameterised by θ_0) originates from the circle into the interior of the state space $\mathbf{S}_{\rm YM}$. At $T = 1$, it follows that

$$\frac{d\theta}{d\tau} = -G(\theta) < 0, \tag{2.29}$$

which corresponds to the periodic orbit $\mathcal{P}_1$. From the monotonicity of T, see Lemma 2.1, it follows that all solutions originate from the circle of fixed points at $T = 0$ and end at the periodic orbit at $T = 1$ which, therefore, constitutes a limit cycle. In fact, using (2.28a)-(2.28b), we find that, in this case, the orbits are the solutions to the equation

$$\frac{d\theta}{dT} = -\frac{G(\theta)}{(1-T)^2}, \tag{2.30}$$

and which are given by

$$\theta(T) = F\left(\sqrt{2}\left(\frac{1}{1-T_0} - \frac{1}{1-T}\right)\Big|\frac{1}{\sqrt{2}}\right), \tag{2.31}$$

where $F(x|k)$ is the Jacobi elliptic amplitude, satisfying $F(0|k) = 0$. This 1-parameter set of solutions parameterised by T_0, corresponds to the well-known solutions for the pure massless Yang-Mills field in a flat Robertson-Walker geometry found in [59, 60] by solving $d^2\chi/d\eta^2 = -\chi^3/2$, where η is the conformal time $d\eta = dt/a(t)$. These solutions are depicted in Figure 2.4 for different initial conditions.

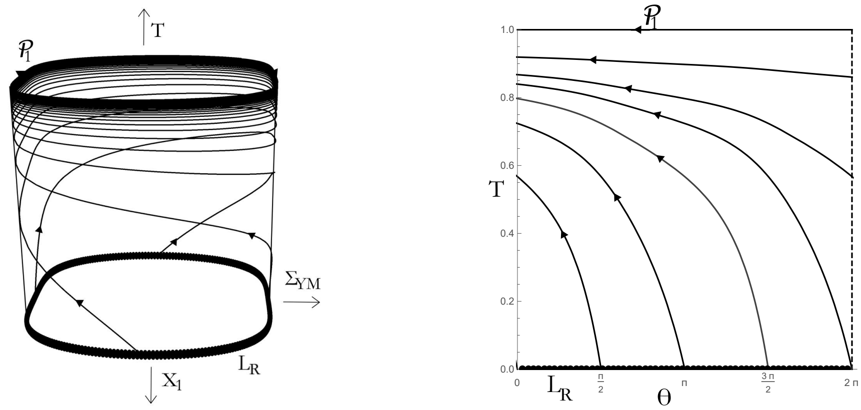

(A) Dynamics on the invariant boundary $\overline{\mathbf{S}}_{\mathrm{YM}}$.

(B) 'Unwrapped' solution space, corresponding to solutions (2.31) for different values of θ_0.

Figure 2.4: Dynamics on the invariant set $\overline{\mathbf{S}}_{\mathrm{YM}}$.

2.2.5 Global dynamics for massless Yang-Mills field and perfect fluid

We now make use of the previous analysis to prove the following result:

Proposition 2.2. *Consider solutions of the system (2.18) with* $0 < \Omega_{\mathrm{pf}} < 1$*:*

(i) If $\gamma_{\mathrm{pf}} > \frac{4}{3}$*, then all solutions converge, for* $\tau \to -\infty$*, to the fixed point* FL_0 *with* $\Omega_{\mathrm{pf}} = 1$ *and, for* $\tau \to +\infty$*, to the outer periodic orbit* $\mathcal{P}_1$ *with* $\Omega_{\mathrm{pf}} = 0$*.*

(ii) If $0 < \gamma_{\mathrm{pf}} < \frac{4}{3}$*, a 1-parameter set of solutions converges, for* $\tau \to -\infty$*, to each point on the circle of fixed point* $\mathrm{L_R}$ *with* $\Omega_{\mathrm{pf}} = 0$*, while all solutions converge, for* $\tau \to +\infty$*, to the fixed point* FL_1 *with* $\Omega_{\mathrm{pf}} = 1$*.*

(iii) If $\gamma_{\mathrm{pf}} = \frac{4}{3}$*, a unique solution converges, for* $\tau \to -\infty$*, to each point on the disk of fixed points* $\mathrm{D_R}$*, while a 1-parameter set of solutions converges, for* $\tau \to +\infty$*, to each inner periodic orbit* $\mathcal{P}_{\Omega_{\mathrm{YM}}}$*.*

This means that in case $\gamma_{\mathrm{pf}} > \frac{4}{3}$ (resp. $\gamma_{\mathrm{pf}} < \frac{4}{3}$), the model is past (resp. future) asymptotic fluid dominated and future (resp. past) asymptotic Yang-Mills field dominated. In the critical case, $\gamma_{\mathrm{pf}} = \frac{4}{3}$, the model in neither fluid nor Yang-Mills dominated towards the asymptotic past nor the asymptotic future, see Figure 2.5 for representative solutions.

Proof. The proof makes use of Lemma 2.1 and the simple orbit structure on the invariant boundaries, given in the subsections 2.2.1-2.2.4, which imply that the only possible α-limit sets are fixed points on $T = 0$, while the ω-limit sets can be either periodic orbits or the fixed point FL_1 on $T = 1$.

In order to prove the general asymptotic behavior, we make use of the auxiliary equation (2.19) for $\Omega_{\rm YM}$. Since $\gamma_{\rm YM} = 4/3$ is constant, then equation (2.19), together with the evolution equation for T, can be easily solved for $\Omega_{\rm YM}$ in terms of T. For solutions with $0 < \Omega_{\rm YM} < 1$, and $\gamma_{\rm pf} \neq \frac{4}{3}$, we get

$$\left(\frac{\Omega_{\rm YM}^{\frac{3\gamma_{\rm pf}}{4}}}{1-\Omega_{\rm YM}}\right)^{\frac{1}{3\gamma_{\rm pf}-4}} = C\frac{T}{1-T},$$

where $C > 0$ is a real constant parameterising the solutions. The last equation clearly shows that if $\gamma_{\rm pf} > \frac{4}{3}$, then $\Omega_{\rm YM} \to 0$ as $T \to 0$, and $\Omega_{\rm YM} \to 1$ as $T \to 1$, i.e. all solutions with $0 < \Omega_{\rm YM} < 1$ start at FL_0 and end at $\mathcal{P}_1$. In turn, if $\gamma_{\rm pf} < \frac{4}{3}$, then $\Omega_{\rm YM} \to 1$ as $T \to 0$, and $\Omega_{\rm YM} \to 0$ as $T \to 1$, i.e. all solutions start at $\mathrm{L}_{\rm R}$ and end at FL_1. If $\gamma_{\rm pf} = \frac{4}{3}$, then $\Omega_{\rm YM} = C$, with $C \in (0,1)$ for all T, i.e. the solutions start at $\mathrm{D}_{\rm R}$ and end at $\mathcal{P}_{\Omega_{\rm YM}}$.

Now, we give a more precise description of the flow near the invariant boundaries $T = 0$ and $T = 1$. The linearisation of the system (2.18) around the fixed points located at $T = 0$ yields (see A.8):

- FL_0: eigenvalues $\frac{3}{4}\left(\gamma_{\rm pf} - \frac{4}{3}\right)$, $\frac{3}{2}\left(\gamma_{\rm pf} - \frac{4}{3}\right)$ and $\frac{3}{4}\gamma_{\rm pf}$, with associated eigenvectors $(1,0,0)$, $(0,1,0)$ and $(0,0,1)$.

- $\mathrm{L}_{\rm R}$: eigenvalues 0, $-3\left(\gamma_{\rm pf} - \frac{4}{3}\right)$ and 1, with associated eigenvectors $(\Sigma_{\rm YM}, -2X_1^3, 0)$, $(X_1, 2\Sigma_{\rm YM}, 0)$ and $(0,0,1)$ where $\Sigma_{\rm YM}^2 + X_1^4 = 1$.

- $\mathrm{D}_{\rm R}$: eigenvalues 0, 0 and 1, with eigenvectors $(1,0,0)$, $(0,1,0)$ and $(0,0,1)$.

For all interior orbits in $\bar{\mathbf{S}}$: When $\gamma_{\rm pf} > 4/3$, FL_0 is a source of a 2-parameter set of orbits and, from $\mathrm{L}_{\rm R}$, originates a 1-parameter set of orbits lying on $\mathbf{S}_{\rm YM}$. All these solutions end up at $\mathcal{P}_1$, except the heteroclinic orbit $\mathrm{FL}_0 \to \mathrm{FL}_1$. When $\gamma_{\rm pf} < 4/3$, only this heteroclinic orbit originates from FL_0, while each point on $\mathrm{L}_{\rm R}$ has a center manifold ($\mathrm{L}_{\rm R}$ itself) and a two dimensional unstable manifold, being the source of a 1-parameter set of interior orbits (a 2-parameter set from the whole circle $\mathrm{L}_{\rm R}$). In this case, all solutions end at FL_1 except the ones on $\mathbf{S}_{\rm YM}$ which end at $\mathcal{P}_1$. If $\gamma_{\rm pf} = 4/3$, each fixed point on the disk $\mathrm{D}_{\rm R}$ is the source of a unique interior orbit. Since $\Omega_{\rm YM} = $ const., each periodic orbit $\mathcal{P}_{\Omega_{\rm YM}}$, at $T = 1$, attracts a 1-parameter set of interior orbits, i.e. those solutions which originate from the circle of fixed points on the intersection of $\mathrm{D}_{\rm R}$ with $\Omega_{\rm YM} = $ const.. $\square$

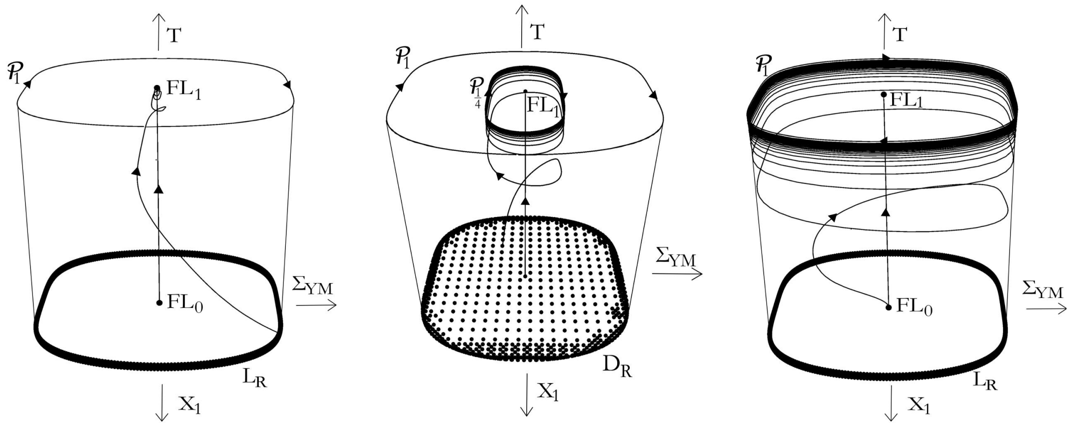

(A) Solution space for $\gamma_{\rm pf} = 1$.

(B) Solution space for $\gamma_{\rm pf} = \frac{4}{3}$.

(C) Solution space for $\gamma_{\rm pf} = \frac{3}{2}$.

Figure 2.5: Qualitative global evolution of dynamical system (2.18) in $\overline{\mathbf{S}}$ for the three different cases $\gamma_{\rm pf} < \frac{4}{3}$, $\gamma_{\rm pf} = \frac{4}{3}$ and $\gamma_{\rm pf} > \frac{4}{3}$, illustrating the results of Proposition 2.2.

2.3 Massive Yang-Mills field (case $\mu \neq 0$)

In this section, we analyse the system (2.3)-(2.4), with $\mu \neq 0$. We, therefore, introduce a new dimensionless variable associated with the mass parameter μ,

$$X_2 = \frac{\mu\phi}{\sqrt{2}H}. \tag{2.32}$$

Using e-fold time N as defined in (2.10), we obtain the *local* dynamical system

$$\frac{d\Sigma_{\rm YM}}{dN} = -\left[(1-q)\Sigma_{\rm YM} + 2\tilde{T}X_1^3 + \mu\tilde{T}^2 X_2\right] \tag{2.33a}$$
$$\frac{dX_1}{dN} = -\frac{1}{2}\left[(1-q)X_1 - 2\tilde{T}\Sigma_{\rm YM}\right] \tag{2.33b}$$
$$\frac{dX_2}{dN} = qX_2 + \mu\tilde{T}^2\Sigma_{\rm YM} \tag{2.33c}$$
$$\frac{d\tilde{T}}{dN} = \frac{1}{2}(1+q)\tilde{T}, \tag{2.33d}$$

subject to the constraint

$$X_2 = \mu\tilde{T}X_1, \tag{2.34}$$

and where we use

$$1 - \Omega_{\rm pf} = \Sigma_{\rm YM}^2 + X_1^4 + X_2^2 \tag{2.35}$$

to solve for $\Omega_{\rm pf}$. The deceleration parameter q is given by

$$q = 1 - X_2^2 + \frac{3}{2}\left(\gamma_{\rm pf} - \frac{4}{3}\right)\Omega_{\rm pf}. \tag{2.36}$$

As in the massless case, the constraint (2.35) implies that X_1, $\Sigma_{\rm YM}$, $\Omega_{\rm pf}$, and X_2 are bounded. In particular, the bounds in (2.14) hold and, in addition,

$$-1 \leq X_2 \leq 1, \tag{2.37}$$

which, given $0 < \gamma_{\rm pf} \leq 2$ and (2.36), yields

$$-1 < q \leq 2\,. \tag{2.38}$$

Since the constraint (2.34) is linear in X_2, it can be used to solve for X_2 giving a *local* 3-dimensional dynamical system for $(X_1, \Sigma_{\rm YM}, \tilde{T})$, which is particularly useful for analysing the asymptotics when $H \to +\infty$ ($\tilde{T} \to 0$), where $X_2 \to 0$. One could, as well, construct a local dynamical systems formulation appropriated to study the dynamics when $\tilde{T}$ becomes unbounded, i.e. $H \to 0$. This can be achieved by replacing $\tilde{T}$ with $\bar{T} = \tilde{T}^{-1}$, together with a new time variable $\tilde{N}$ defined via $d/d\tilde{N} = \bar{T}^3 d/dN$ and where, now, the constraint becomes linear in $X_1 = \mu^{-1}\bar{T}X_2$ and, hence, can be solved for X_1 to obtain a *local* dynamical system for $(X_2, \Sigma_{\rm YM}, \bar{T})$, with $X_1 \to 0$ as $\bar{T} \to 0$.

To obtain a *global* dynamical systems formulation on a compact state space, we proceed as in the massless case, and introduce the bounded variable

$$T = \frac{\tilde{T}}{1+\tilde{T}}\ , \tag{2.39}$$

which satisfies $0 < T < 1$. By introducing a new independent variable $\bar{\tau}$, such that

$$\frac{d}{d\bar{\tau}} = (1-T)^2 \frac{d}{dN}, \tag{2.40}$$

we obtain, from (2.33)-(2.34), a *global* dynamical system

$$\frac{d\Sigma_{\rm YM}}{d\bar{\tau}} = -\Big[(1-q)(1-T)^2\Sigma_{\rm YM} + 2(1-T)TX_1^3 + \mu T^2 X_2\Big] \tag{2.41a}$$

$$\frac{dX_1}{d\bar{\tau}} = -\frac{1}{2}\Big[(1-q)(1-T)^2 X_1 - 2(1-T)T\Sigma_{\rm YM}\Big] \tag{2.41b}$$

$$\frac{dX_2}{d\bar{\tau}} = q(1-T)^2 X_2 + \mu T^2 \Sigma_{\rm YM} \tag{2.41c}$$

$$\frac{dT}{d\bar{\tau}} = \frac{1}{2}(1+q)(1-T)^3 T, \tag{2.41d}$$

subject to the constraint

$$(1-T)X_2 = \mu T X_1, \tag{2.42}$$

and where we use (2.35) to globally solve for $\Omega_{\rm pf}$. The deceleration parameter q is, then, given by

$$q = 1 - X_2^2 + \frac{3}{2}\left(\gamma_{\rm pf} - \frac{4}{3}\right)(1 - \Sigma_{\rm YM}^2 - X_1^4 - X_2^2). \tag{2.43}$$

It is also useful to consider the *auxiliary* evolution equation for the effective energy density of the Yang-Mills field which, in the present case, reads

$$\Omega_{\rm YM} := \frac{\rho_{\rm YM}}{3H^2} = \Sigma_{\rm YM}^2 + X_1^4 + X_2^2, \tag{2.44}$$

with $\Omega_{\rm YM} = 1 - \Omega_{\rm pf}$. From (2.5)-(2.6), we can write

$$\gamma_{\rm YM} := 1 + \frac{p_{\rm YM}}{\rho_{\rm YM}} = 1 + \frac{1}{3}\frac{\Sigma_{\rm YM}^2 + X_1^4 - X_2^2}{\Omega_{\rm YM}} = \frac{4}{3} - \frac{2}{3}\frac{X_2^2}{\Omega_{\rm YM}}. \tag{2.45}$$

Furthermore, rewriting (2.43) as

$$q = -1 + \frac{3}{2}\left(\gamma_{\rm YM}\Omega_{\rm YM} + \gamma_{\rm pf}\Omega_{\rm pf}\right), \tag{2.46}$$

we obtain

$$\frac{d\Omega_{\rm YM}}{d\bar{\tau}} = 3(1-T)^2(\gamma_{\rm pf}\Omega_{\rm YM} - \gamma_{\rm YM}\Omega_{\rm YM})(1 - \Omega_{\rm YM}). \tag{2.47}$$

The price to pay, in order to have a global relatively compact state space picture, is that the constraint (2.42) cannot be solved globally. However, it forms an invariant set for the flow. This can be seen by writing $G(X_1, X_2, T) = (1-T)X_2 - \mu T X_1 = 0$ and noticing that

$$\frac{dG}{d\bar{\tau}} = \left(q - \frac{1}{2}(1+q)T\right)(1-T)^2 G. \tag{2.48}$$

The state-space $\mathbf{S}$ for the variables $(\Sigma_{\rm YM}, X_1, X_2, T)$ is, therefore, the subset defined by $G = 0$ on the set $\{0 \leq \Sigma_{\rm YM}^2 + X_1^4 + X_2^2 \leq 1 \wedge 0 < T < 1\}$. The state-space $\mathbf{S}$ contains other important invariant subsets: the pure Yang-Mills subset $\Omega_{\rm pf} = 0$ and the Friedmann-Lemaître invariant subset for which $\Omega_{\rm pf} = 1$. In addition, it can be regularly extended to include the invariant boundaries $T = 0$ and $T = 1$ to obtain the compact state-space $\overline{\mathbf{S}}$.

As a starting point for our analysis, we study the past and future limit sets:

Lemma 2.3. *Consider the system (2.41)-(2.42). The α-limit set of all interior orbits in $\mathbf{S}$ is located at the invariant boundary $T = 0$, with $X_2 = 0$, and the ω-limit set is at the invariant boundary $T = 1$, with $X_1 = 0$.*

Proof. We make use of the *monotonicity principle.* Due to $1 + q > 0$, a quick inspection of equation (2.41d) reveals that $T(\bar{\tau})$ is monotonically increasing in $\mathbf{S}$ and, therefore, there are no periodic nor recurrent orbits in the interior of the state space. We conclude that the α-limit set of all solutions is located at the $T = 0$ invariant boundary associated to the asymptotic past $H \to +\infty$, while the ω-limit set is located on the $T = 1$ invariant boundary, associated with the asymptotic future $H \to 0$. Moreover, the constraint (2.42) implies that $X_1 \to 0$ as $T \to 1$, and $X_2 \to 0$ as $T \to 0$. □

Remark 2.4. *This lemma implies, in particular, the result in [59], that for the pure Yang-Mills field, the past asymptotics is dominated by the "massless potential", while the future asymptotics it is dominated by the "mass potential".*

We now proceed with a detailed analysis of the past and future asymptotics.

2.3.1 Past asymptotics for massive Yang-Mills fields and perfect fluids

Since along $G = 0$, we have $X_2 \to 0$ as $T \to 0$, then the invariant boundary $T = 0$ coincides with the $T = 0$ boundary of the massless Yang-Mills state space. It follows that there exist the fixed points FL_0, as well as the deformed circle $\mathrm{L_R}$ and the disk $\mathrm{D_R}$ of fixed points now for:

$$\mathrm{D_R}: \quad 0 \leq \Sigma_{\mathrm{YM}}^2 + X_1^4 \leq 1, \ T = 0, \ X_2 = 0 \tag{2.49}$$

$$\mathrm{L_R}: \quad \Sigma_{\mathrm{YM}}^2 + X_1^4 = 1, \ T = 0, \ X_2 = 0 \tag{2.50}$$

$$\mathrm{FL}_0: \quad \Sigma_{\mathrm{YM}} = X_1 = 0, \ T = 0, \ X_2 = 0\,. \tag{2.51}$$

The goal of this subsection is to prove the next theorem which gives a description of the past asymptotics of the model.

Theorem 2.5. *Consider solutions of the system (2.41)-(2.42) with $0 < \Omega_{\mathrm{p}f} < 1$. For $\bar{\tau} \to -\infty$:*

(i) If $0 < \gamma_{\mathrm{pf}} < \frac{4}{3}$, all solutions converge to the circle of fixed points $\mathrm{L_R}$. More precisely, each fixed point on $\mathrm{L_R}$ is the α-limit point of a 2-parameter set of solutions.

(ii) If $\gamma_{\mathrm{pf}} = \frac{4}{3}$, all solutions converge to the disk of fixed points $\mathrm{D_R}$. More precisely, each fixed point on $\mathrm{D_R}$ is the α-limit point of a unique solution.

(iii) If $\gamma_{\mathrm{pf}} > \frac{4}{3}$, all solutions converge to the fixed point FL_0.

Proof. The proof uses Lemma 2.3 and the fact that $X_2 = 0$ at $T = 0$, which means that the orbit structure on this boundary coincides with that of the massless case studied in Subsection 2.2.2. In fact, this boundary consists of heteroclinic orbits when $\gamma_{\mathrm{pf}} \neq \frac{4}{3}$, or only of fixed points when $\gamma_{\mathrm{pf}} = \frac{4}{3}$, see Figure 2.2. Therefore, the possible past attracting sets are fixed points located at $T = 0$. In order to deduce the stability properties of the fixed points, we need to solve the constraint (2.42). Although it is not possible to solve this constraint globally, we can uniquely solve it locally at the points where $\nabla G \neq 0$ by making use of the implicit function theorem. Since $\partial_{X_2} G|_{T=0} = 1$, in a neighbourhood of the $T = 0$ boundary, then we can eliminate the variable X_2 from the eigenvalue analysis of the fixed points on $T = 0$. This yields the same results as the linearisation around the corresponding similar fixed points of the massless case. □

The physical interpretation of the above theorem is that, if $\gamma_{\rm pf} < 4/3$, the dynamics are past asymptotically dominated by the massless Yang-Mills field while, if the fluid content has an equation of state stiffer than radiation, the past asymptotics is governed by the Friedmann-Lemaître solution. If $\gamma_{\rm pf} = 4/3$, then the model is neither fluid of massless Yang-Mills dominated towards the past.

2.3.2 Future asymptotics for massive Yang-Mills fields and perfect fluids

We start by describing the future invariant subset $T = 1$. Since $X_1 = 0$ at $T = 1$, the induced flow on this boundary is given by

$$\frac{d\Sigma_{\rm YM}}{d\bar{\tau}} = -\mu X_2 \tag{2.52a}$$
$$\frac{dX_2}{d\bar{\tau}} = \mu \Sigma_{\rm YM} \ , \tag{2.52b}$$

where now

$$1 - \Omega_{\rm pf} = \Sigma_{\rm YM}^2 + X_2^2. \tag{2.53}$$

The $T = 1$ boundary is foliated by periodic orbits $\mathcal{P}_{\Omega_{\rm YM}}$, parameterised by constant values of $\Omega_{\rm YM} = \Sigma_{\rm YM}^2 + X_2^2$, with the fixed point FL_1 given by

$$\mathrm{FL}_1 : \qquad \Sigma_{\rm YM} = X_2 = 0, \ T = 1, \ X_1 = 0 \tag{2.54}$$

and located at the center, see Figure 2.6. The objective of this subsection is to prove the

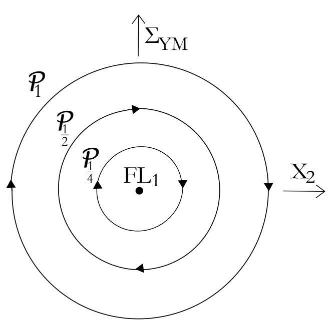

Figure 2.6: Representation of the invariant boundary $T = 1$ when $\mu > 0$.

following result:

Theorem 2.6. *Consider solutions of the system (2.41)-(2.42) with* $0 < \Omega_{\text{pf}} < 1$*. For* $\bar{\tau} \longrightarrow +\infty$*:*

(i) If $\gamma_{\text{pf}} > 1$*, then all solutions converge to the outer periodic orbit* $\mathcal{P}_1$ *with* $\Omega_{\text{pf}} = 0$*.*

(ii) If $\gamma_{\text{pf}} < 1$*, then all solutions converge to fixed point* FL_1 *with* $\Omega_{\text{pf}} = 1$*.*

(iii) If $\gamma_{\text{pf}} = 1$*, then a 1-parameter set of solutions converge to each inner periodic orbit* $\mathcal{P}_{\Omega_{\text{YM}}}$*.*

Proof. The proof is based on Lemma 2.3 together with averaging techniques and consists of an adaptation of the methods used in [68]. An important difference with respect to the standard averaging theory is that the perturbation parameter ε will not be a constant, but a function of time here. We start by recalling that each periodic orbit on $T = 1$ has an associated time period $P(\Omega_{\text{YM}})$, so that, for a given function f, its average over a time period characterized by Ω_{YM} is given by

$$\langle f \rangle_{\Omega_{\text{YM}}} = \frac{1}{P(\Omega_{\text{YM}})} \int_{\bar{\tau}_0}^{\bar{\tau}_0 + P(\Omega_{\text{YM}})} f(\bar{\tau})\, d\bar{\tau}. \tag{2.55}$$

Differentiating (2.52b) and using (2.52a) gives

$$\frac{d}{d\bar{\tau}}\left(X_2 \frac{dX_2}{d\bar{\tau}}\right) - \left(\frac{dX_2}{d\bar{\tau}}\right)^2 + \mu^2 X_2^2 = 0. \tag{2.56}$$

Taking the average for a periodic orbit gives,

$$\left\langle \left(\frac{dX_2}{d\bar{\tau}}\right)^2 \right\rangle = \mu^2 \langle X_2^2 \rangle, \tag{2.57}$$

which implies

$$\langle \Sigma_{\text{YM}}^2 \rangle = \langle X_2^2 \rangle. \tag{2.58}$$

Thus, on the $T = 1$ invariant subset

$$\langle \gamma_{\text{YM}} \rangle = \frac{4}{3} - \frac{2}{3} \frac{\langle X_2^2 \rangle}{\langle \Sigma_{\text{YM}}^2 \rangle + \langle X_2^2 \rangle} = 1, \tag{2.59}$$

which does not depend on Ω_{YM} and, on average, the Yang-Mills field behaviour resembles that of dust.

We now set $\varepsilon(\bar{\tau}) = 1 - T(\bar{\tau})$ and consider the system

$$\frac{d\Omega_{\text{YM}}}{d\bar{\tau}} = 3\varepsilon^2 \left(\gamma_{\text{pf}} \Omega_{\text{YM}} - \gamma_{\text{YM}} \Omega_{\text{YM}}\right)(1 - \Omega_{\text{YM}}) := \varepsilon^2 f(\Omega_{\text{YM}}, \bar{\tau}, \varepsilon) \tag{2.60a}$$

$$\frac{d\varepsilon}{d\bar{\tau}} = -\frac{1}{2}(1+q)\varepsilon^3(1-\varepsilon), \tag{2.60b}$$

where

$$\gamma_{\rm YM}\Omega_{\rm YM} = \frac{4}{3}\Omega_{\rm YM} - \frac{2}{3}X_2^2 \quad , \quad 1+q = \frac{3}{2}(\gamma_{\rm pf} - (\gamma_{\rm pf} - \gamma_{\rm YM})\Omega_{\rm YM}) \tag{2.61}$$

and $(X_1, X_2, \Sigma_{\rm YM})$ solves (2.41)-(2.42) with the equation for T replaced by the equation for ε. Recall that $1+q>0$ and, therefore, ε is monotonically decreasing, so that, $\varepsilon(\bar{\tau}) \to 0$ as $\bar{\tau} \to +\infty$. Moreover, since $\partial_{X_1} G|_{T=1} = \mu \neq 0$, we can use the implicit function theorem to solve (2.42) uniquely for X_1, in a neighbourhood of the $T=1$ boundary.

We start by applying the near-identity transformation depending on ε,

$$\Omega_{\rm YM}(\bar{\tau}) = y(\bar{\tau}) + \varepsilon^2(\bar{\tau}) w(y, \bar{\tau}, \varepsilon). \tag{2.62}$$

The evolution equation for y is obtained using (2.60a) and (2.60b), which gives

$$\begin{aligned}\frac{dy}{d\bar{\tau}} &= \left(1+\varepsilon^2\frac{\partial w}{\partial y}\right)^{-1}\left[\frac{d\Omega_{\rm YM}}{d\bar{\tau}} - \left(2\varepsilon w + \varepsilon^2\frac{\partial w}{\partial \varepsilon}\right)\frac{d\varepsilon}{d\bar{\tau}} - \varepsilon^2\frac{\partial w}{\partial \bar{\tau}}\right] \\ &= \frac{\varepsilon^2}{1+\varepsilon^2\frac{\partial w}{\partial y}}\Big[3(\gamma_{\rm pf}-1)y(1-y) + 3(1-\gamma_{\rm YM})y(1-y) + 3w\varepsilon^4(\gamma_{\rm pf}-\gamma_{\rm YM}) + 3\varepsilon^6(\gamma_{\rm pf}-\gamma_{\rm YM}) - \\ &\quad - \frac{\partial w}{\partial \bar{\tau}} + \left(2w + \varepsilon\frac{\partial w}{\partial \varepsilon}\right)\left(\frac{1+q}{2}\right)(1-\varepsilon)\varepsilon^2\Big]\end{aligned} \tag{2.63}$$

and where we used (2.59). Setting

$$\begin{aligned}\frac{\partial w}{\partial \bar{\tau}} &= f(y, \bar{\tau}, \varepsilon) - \langle f(y, \cdot, 0)\rangle \\ &= 3(1-\gamma_{\rm YM})y(1-y) \\ &= \left(-y + 2X_2^2\right)(1-y)\end{aligned} \tag{2.64}$$

and expanding (2.63) in powers of ε, for ε sufficiently small, the equation for $\Omega_{\rm YM}$ is transformed into the full averaged equation

$$\frac{dy}{d\bar{\tau}} = \varepsilon^2\langle f\rangle(y) + \varepsilon^4 h(y, w, \bar{\tau}, \varepsilon) + \varepsilon^5(1+q)\left(\frac{1}{2}\frac{\partial w}{\partial \varepsilon} - w\right) + \mathcal{O}(\varepsilon^6), \tag{2.65}$$

where

$$\langle f\rangle(y) = \langle f(y, \cdot, 0)\rangle = 3(\gamma_{\rm pf}-1)y(1-y) \tag{2.66}$$

$$h(y, w, \bar{\tau}, \varepsilon) = w(1+q) + 3w(1-2y)(\gamma_{\rm pf}-\gamma_{\rm YM})(1-2y) - 3(\gamma_{\rm pf}-\gamma_{\rm YM})\frac{\partial w}{\partial y}y(1-y) \tag{2.67}$$

Note that, due to the previous analysis of the invariant set $T=1$, i.e. $\varepsilon = 0$, the right-hand-side of (2.64) is, for large times, almost-periodic and has zero mean, which, in particular, implies that w is bounded. Then, it follows from (2.62) that y is also bounded. Moreover, for sufficiently small ε, equation (2.65) implies that y is monotonic, either increasing or decreasing depending on the sign of $\gamma_{\rm pf}-1\neq 0$ and, hence, y has a limit when $\bar{\tau}\to+\infty$.

Now, we study the evolution of the truncated averaged equation, which is obtained by dropping all higher order terms in (2.65) as

$$\begin{aligned} \frac{d\bar{y}}{d\bar{\tau}} &= 3\varepsilon^2(\gamma_{\rm pf}-1)\bar{y}(1-\bar{y}) \qquad (2.68)\\ \frac{d\varepsilon}{d\bar{\tau}} &= -\frac{1}{2}(1+q)(1-\varepsilon)\varepsilon^3. \qquad (2.69)\end{aligned}$$

In this system, the $\varepsilon=0$ axis consists of a non-hyperbolic line of fixed points. Making the change of time variable

$$\frac{1}{\varepsilon^2}\frac{d}{d\bar{\tau}}=\frac{d}{d\tilde{\tau}},$$

which does not affect the behavior of interior orbits, i.e. orbits with $\varepsilon>0$, we get

$$\begin{aligned} \frac{d\bar{y}}{d\tilde{\tau}} &= 3(\gamma_{\rm pf}-1)\bar{y}(1-\bar{y}) \qquad (2.70)\\ \frac{d\varepsilon}{d\tilde{\tau}} &= -\frac{1}{2}\varepsilon(1+q)(1-\varepsilon). \qquad (2.71)\end{aligned}$$

For $\gamma_{\rm pf}-1\neq 0$, the above dynamical system has the two fixed points $\mathrm{P}_1=(\bar{y}=0;\varepsilon=0)$ and $\mathrm{P}_2=(\bar{y}=1;\varepsilon=0)$, where the $\varepsilon=0$ axis consists now of the heteroclinic orbit $\mathrm{P}_1\to\mathrm{P}_2$ (resp. $\mathrm{P}_2\to\mathrm{P}_1$), in case $\gamma_{\rm pf}-1>0$ (resp. $\gamma_{\rm pf}-1<0$). Thus, for $\gamma_{\rm pf}>1$ (resp. $\gamma_{\rm pf}<1$), solution trajectories of the system (2.68)-(2.69) will converge to the fixed point P_2 (resp. P_1), tangentially to the $\varepsilon=0$ axis.

Next, we show that solutions y, of the full averaged equation (2.65), have the same limit as the solutions $\bar{y}$ of the truncated averaged equation when $\bar{\tau}\to+\infty$. For this, we define the sequences $\{\bar{\tau}_n\}$ and $\{\varepsilon_n\}$ such that $\varepsilon_n=\varepsilon(\bar{\tau}_n)$, with $n\in\mathbb{N}$, and

$$\begin{aligned} \bar{\tau}_{n+1}-\bar{\tau}_n &= \frac{1}{\varepsilon_n^2} \qquad (2.72)\\ \bar{\tau}_0 &= 0 \qquad (2.73)\\ \varepsilon_0 &> 0, \qquad (2.74)\end{aligned}$$

where $\lim\bar{\tau}_n=+\infty$ and $\lim\varepsilon_n=0$, since $\varepsilon(\bar{\tau})\to 0$ as $\bar{\tau}\to+\infty$. We estimate $|\eta(\bar{\tau})|=|y(\bar{\tau})-\bar{y}(\bar{\tau})|$ as follows

$$\begin{aligned} |\eta(\bar{\tau})| &= \left|\int_{\bar{\tau}_n}^{\bar{\tau}}\left(3\varepsilon^2(\gamma_{\rm pf}-1)y(1-y)+\varepsilon^4 h(y,w,\varepsilon,s)\right)ds-\int_{\bar{\tau}_n}^{\bar{\tau}}3\varepsilon^2(\gamma_{\rm pf}-1)\bar{y}(1-\bar{y})ds+\mathcal{O}(\varepsilon^5)\right|\\ &\leq \varepsilon^2\int_{\bar{\tau}_n}^{\bar{\tau}}3\underbrace{|\gamma_{\rm pf}-1|}_{|\cdot|\leq C}|(y-\bar{y})\underbrace{(1-(y+\bar{y}))}_{|\cdot|\leq 1}|ds+\varepsilon^4\int_{\bar{\tau}_n}^{\bar{\tau}}\underbrace{|h(y,w,\varepsilon,s)|}_{|\cdot|\leq M}ds+\mathcal{O}(\varepsilon^5)\\ &\leq 3C\varepsilon_n^2\int_{\bar{\tau}_n}^{\bar{\tau}}|\eta(s)|ds+\varepsilon_n^4 M(\bar{\tau}-\bar{\tau}_n)+\mathcal{O}(\varepsilon_n^5),\end{aligned}$$

where C and M are some positive constants. By Gronwall's inequality

$$|\eta(\bar{\tau})| \leq \frac{\varepsilon_n^2 M}{3C}(e^{3C\varepsilon_n^2(\bar{\tau}-\bar{\tau}_n)} - 1) + \mathcal{O}(\varepsilon_n^3), \tag{2.75}$$

and using the fact that $\bar{\tau} - \bar{\tau}_n \in [0, 1/\varepsilon_n^2]$, we find

$$|\eta(\bar{\tau})| \leq K\varepsilon_n^2, \tag{2.76}$$

with K a positive constant. As $\varepsilon_n \to 0$, then $|\eta(\bar{\tau})| \to 0$, and so y and $\bar{y}$ have the same limit. Finally, from equation (2.62), the triangular inequality, and the fact that $\varepsilon \to 0$ as $\bar{\tau} \to +\infty$, it follows that Ω_{YM} has the same limit as $\bar{y}$ and, therefore, converges to 0 or 1, depending on the sign of $\gamma_{\mathrm{pf}} - 1 \neq 0$. This proves cases (i) and (ii) of the theorem.

Now, we analyse the case when $\gamma_{\mathrm{pf}} = 1$. In that case, the equation for y is given by

$$\frac{dy}{d\bar{\tau}} = \varepsilon^4 h(y, w, \varepsilon, \bar{\tau}) + \mathcal{O}(\varepsilon^5). \tag{2.77}$$

Taking the average of h, given in (2.67), at $\varepsilon = 0$,

$$\begin{aligned}
\langle h\rangle(y, w) &= \langle h(y, \cdot, 0)\rangle = \frac{1}{P}\int_0^P h(y, w, 0, \bar{\tau})d\bar{\tau} \\
&= \frac{1}{P}\int_0^P w(y, \bar{\tau}, 0)(1+q)d\bar{\tau} \\
&= \frac{1}{P}\int_0^P \frac{3}{2}w(y, \bar{\tau}, 0)(1 + (\gamma_{\mathrm{YM}} - 1)y)d\bar{\tau} \\
&= \frac{3}{2}\langle w(y, \cdot, 0)\rangle = \frac{3}{2}\langle w\rangle(y),
\end{aligned} \tag{2.78}$$

we consider the truncated averaged equation

$$\frac{d\bar{z}}{d\bar{\tau}} = \frac{3}{2}\varepsilon^4\langle w\rangle(\bar{z}) \tag{2.79}$$

$$\frac{d\varepsilon}{d\bar{\tau}} = -\frac{3}{4}\varepsilon^4(1-\varepsilon)\,. \tag{2.80}$$

To resolve the non-hyperbolicity of the line of fixed points at $\varepsilon = 0$, we make the change of time variable $\varepsilon^{-3}d/d\bar{\tau} = d/d\tilde{\tau}$, to obtain

$$\frac{d\bar{z}}{d\tilde{\tau}} = \frac{3}{2}\varepsilon\langle w\rangle(\bar{z}) \tag{2.81}$$

$$\frac{d\varepsilon}{d\tilde{\tau}} = -\frac{3}{4}\varepsilon(1-\varepsilon). \tag{2.82}$$

In this case, the $\varepsilon = 0$ axis consists of a line of fixed points with $\bar{z}_0 \in [0, 1]$, whose linearisation yields the eigenvalues $\lambda_1 = 0$ and $\lambda_2 = -\frac{3}{4}$ with associated eigenvectors $v_1 = (\bar{z} = 1; \varepsilon = 0)$

and $v_2 = (\bar{z} = -2\langle w\rangle(\bar{z}_0); \varepsilon = 1)$. Therefore, the line is normally hyperbolic and each point on the line is exactly the ω-limit point of a unique interior orbit. This means that there also exists an orbit of the dynamical system (2.79)-(2.80) with $\varepsilon > 0$ initially, that converges to $(\bar{z}_0, 0)$, for each $\bar{z}_0$, as $\tilde{\tau} \to +\infty$.

Just as in the proof of cases (i) and (ii), we can estimate the term $\mathcal{O}(\varepsilon^5)$ that provides bootstrapping sequences. This defines a pseudo-trajectory $\Omega^n_{\mathrm{YM}}(\bar{\tau}_n) = \bar{z}(\bar{\tau}_n)$ of system (2.60a)-(2.60b), with

$$|\Omega^n_{\mathrm{YM}}(\bar{\tau}) - \bar{z}(\bar{\tau})| \leq K\varepsilon_n^2 \,, \tag{2.83}$$

where $\bar{\tau} \in [\bar{\tau}_n, \bar{\tau}_{n+1}]$ and K is a positive constant. Compactness of the state space and the regularity of the flow implies that exists a set of initial values whose solution trajectory $\Omega_{\mathrm{YM}}(\bar{\tau})$ shadows the pseudo-trajectory $\Omega^n_{\mathrm{YM}}(\bar{\tau})$, in the sense that

$$\forall n \in \mathbb{N}, \quad \forall \bar{\tau} \in [\bar{\tau}_n, \bar{\tau}_{n+1}] : \quad |\Omega^n_{\mathrm{YM}}(\bar{\tau}) - \Omega_{\mathrm{YM}}(\bar{\tau})| \leq K\varepsilon_n^2 \,. \tag{2.84}$$

Finally, using the triangle inequality, we get

$$\begin{aligned}
|\Omega_{\mathrm{YM}}(\bar{\tau}) - \bar{z}(\bar{\tau})| &= |\Omega_{\mathrm{YM}}(\bar{\tau}) - \Omega^n_{\mathrm{YM}}(\bar{\tau}) + \Omega^n_{\mathrm{YM}}(\bar{\tau}) - \bar{z}(\bar{\tau})| \\
&\leq \underbrace{|\Omega^n_{\mathrm{YM}}(\bar{\tau}) - \Omega_{\mathrm{YM}}(\bar{\tau})|}_{\leq K\varepsilon_n^2} + \underbrace{|\Omega^n_{\mathrm{YM}}(\bar{\tau}) - \bar{z}(\bar{\tau})|}_{\leq K\varepsilon_n^2} \\
&\leq 2K\varepsilon_n^2 \underbrace{\to}_{\bar{\tau}_n \to \infty} 0 \,,
\end{aligned} \tag{2.85}$$

and, therefore, for each $\bar{z}_0 \in [0, 1]$, there exists a solution trajectory $\Omega_{\mathrm{YM}}(\bar{\tau})$ that converges to a periodic orbit at $\varepsilon = 0$ i.e. $T = 1$, characterized by $\Omega_{\mathrm{YM}} = \bar{z}_0$, which concludes the proof of (iii). □

2.4 Concluding Remarks

This chapter considered spatially homogeneous and isotropic massless and massive Yang-Mills field cosmologies with perfect fluid. In particular the well-known explicitly solvable massless Yang-Mills isotropic cosmologies [59, 60] have been contextualized in a global state-space picture. The dynamical systems formulations introduced here can be used to shed light on the dynamics of more general anisotropic cosmological models, where massless Yang-Mills fields are known to exhibit past asymptotic chaotic behaviour reminiscent of the Mixmaster universe as well as future asymptotic oscillatory behaviour similar to Yang-Mills field in Minkowski space [88, 91–94]. General spatially homogeneous Yang-Mills fields under the Hamiltonian gauge can be written in diagonal form $A_i^a = \chi_{(i)}(t)\delta_i^a$, where for the diagonal Bianchi class A, if the off-diagonal components are zero initially, then they will remain so for the whole evolution. Isotropy requires all diagonal components $\chi_{(i)}$ to be equal, thus reducing the Yang-Mills field degrees of freedom to a single scalar field with a quartic potential, which excludes its chaotic behaviour. A general treatment of diagonal Yang-Mills Bianchi class A spacetimes using an orthonormal frame approach and expansion normalized variables can be found in [94]. However, a lack of suitable renormalized matter variables has prevented so far to obtain a global dynamical systems formulation on a compact state-space suitable for asymptotic description of those models. The present formulation can be extended to more general Bianchi models, where the isotropic case treated here appears as a special invariant set. The physical interpretation of Theorem 2.6 is as follows: In if $\gamma_{\rm pf} < 1$, then the general solutions of the massive system behave like the Friedmann-Lemaître solution asymptotically towards the future. However, if the fluid content has an equation of state stiffer than dust, then the future asymptotics is governed by the pure massive Yang-Mills solution, which, in particular, exhibits oscillatory behaviour. If $\gamma_{\rm pf} = 1$, then the model is neither fluid of massive Yang-Mills dominated towards the future.

Chapter 3

Dynamics of interacting monomial scalar field potentials and perfect fluids

In this chapter we investigate the dynamical interaction between scalar fields and perfect fluid. We consider the Einstein equations for a spatially homogeneous and isotropic metric (1.51) having a scalar field with monomial potentials interacting with perfect fluids with linear equation of state. Our main goal is to obtain a global dynamical picture of the resulting non-linear ODEs and in particular about is past and future asymptotics. Our analysis relies on the introduction a new set of dimensionless variables which results on a regular dynamical system on a compact state-space consisting of a 3-dimensional cylinder. This allow us to describe the global evolution of these cosmological models identifying all possible past and future attractors set which, as will see, in many situations, can be isolated non-hyperbolic fixed points, non-normally hyperbolic lines of fixed points or even bands of periodic orbits. So, our analysis will require on one hand center manifold theory and blow-up techniques around the non-hyperbolic fixed points and, on the other hand, averaging methods involving a time dependent perturbation parameter.

The chapter is mostly self-contained and is organized as follows: In Section 3.1 we explain how the non-linear system of ODEs is obtain from physical principles. In Section 3.2 we find the appropriate dimensionless variables that transform the ODE system into a 3-dimensional regular autonomous dynamical system on relatively compact state space. This construction naturally shows that a significant bifurcation occurs for $p = \frac{n}{2}$. We therefore split the analysis into three cases according to the different exponents of the scalar field potential and the interaction term: Section 3.3 treat the case $p < n/2$, where the analysis is further split in two distinct subcases corresponding to $p = \frac{1}{2}(n-1)$ and $p < \frac{1}{2}(n-1)$. The case $p = n/2$ is treated in Section 3.4, and when $p > n/2$ in Section 3.5. Interestingly, in some situations we encounter non-hyperbolic fixed points whose exceptional divisor of the blow-up space consists of generalised Liénard systems. We provide proofs as well as conjectures about the global dynamics complemented by numerical pictures of representative cases.

3.1 Non-linear ODE system

Motivated by the warm inflation scenario of the early universe, here we assume a minimally coupled scalar field ϕ with self-interaction potential $V(\phi)$ interacting with a perfect fluid. The evolution equations can be derived from an action principle and the most general action for this case is given by

$$S = \int_M \Big(\frac{R}{2} + \frac{1}{2}(\partial\phi)^2 - V(\phi) + \mathcal{L}_{\text{pf}} + \mathcal{L}_{\text{int}}\Big)\sqrt{-\det(g)}d^4x^\mu, \tag{3.1}$$

where as standard, we use Greek indices $\mu, \nu, ... = 0, 1, 2, 3$ for each coordinate in spacetime. Here $(\partial\phi)^2 := \partial_\mu\phi\partial^\mu\phi$, $\mathcal{L}_{\text{pf}}$ is the Lagrangian density of the perfect fluid and $\mathcal{L}_{\text{int}}$ describes the interaction between the scalar field and the thermal bath. Varying the Lagrangian density with respect to the metric we obtain the Einstein equations (1.6) with stress-energy tensor components

$$\mathcal{T}_{\mu\nu} = \mathcal{T}^{(\phi)}_{\mu\nu} + \mathcal{T}^{(\text{pf})}_{\mu\nu} \tag{3.2}$$

with

$$\mathcal{T}^{(\text{pf})}_{\mu\nu} = (\rho_{\text{pf}} + p_{\text{pf}})u_\mu u_\nu + p_{\text{pf}}g_{\mu\nu} + g_{\mu\nu}\mathcal{L}_{\text{int}} \tag{3.3a}$$

$$\mathcal{T}^{(\phi)}_{\mu\nu} = \partial_\mu\phi\partial_\nu\phi - (\frac{1}{2}(\partial\phi)^2 - V(\phi))g_{\mu\nu} - g_{\mu\nu}\mathcal{L}_{\text{int}} \tag{3.3b}$$

where u^μ denotes the unit 4-velocity vector field of the perfect fluid, with $\rho_{\text{pf}} > 0$ and p_{pf} being the fluid energy density and pressure, respectively.

The stress-energy tensor for the scalar field can be written in a perfect-fluid form, with the identifications $u^\mu_{(\phi)} = (\partial^\mu\phi)/\sqrt{-(\partial\phi)^2}$, that lead to eq. (1.27).

The total stress-energy tensor $\mathcal{T}_{\mu\nu}$ obeys the conservation law $\nabla_\nu\mathcal{T}^\nu_\mu = 0$. However each component of the total stress-energy tensor, $\mathcal{T}^{(\phi)}_{\mu\nu}$ and $\mathcal{T}^{(\text{pf})}_{\mu\nu}$, is not conserved, in contrast to the case when the scalar field does not interact with the thermal bath. In the presence of interactions

$$\nabla^\nu\mathcal{T}^{(\phi)}_{\mu\nu} = Q^{(\phi)}_\mu, \qquad \nabla^\nu\mathcal{T}^{(\text{pf})}_{\mu\nu} = Q^{(\text{pf})}_\mu \tag{3.4}$$

where $Q_\mu^{(\phi)}$ and $Q_\mu^{(\text{pf})}$ describe the energy exchange between the scalar field and the perfect-fluid. It follows from the conservation equation that

$$\nabla^\nu \mathcal{T}_{\mu\nu} = Q_\mu^{(\phi)} + Q_\mu^{(\text{pf})} = 0. \tag{3.5}$$

In this work we consider a phenomenological friction-like interaction term for which

$$Q_\mu^{(\phi)} = -Q_\mu^{(\text{pf})} = -\Gamma(\phi) u^\nu \partial_\mu \phi \partial_\nu \phi. \tag{3.6}$$

where we assume that $\Gamma = \Gamma(\phi)$ is a function of the scalar field ϕ only. In more general warm inflationary models, the function Γ can also depend on the thermal bath temperature [38, 95–98], although, as mentioned in sec. 1.6.1.2, recent studies suggest that temperature dependence is redundant [40]. Equation (3.3a) then gives the modified energy "conservation" equation and the Euler equation

$$-u^\mu \nabla_\mu \rho_{\text{pf}} + (\rho_{\text{pf}} + p_{\text{pf}}) \nabla_\mu (u^\mu u_\nu) = \Gamma(\phi) \partial^\mu \phi \partial_\mu \phi \tag{3.7a}$$

$$(\rho_{\text{pf}} + p_{\text{pf}}) u^\mu \nabla_\mu u^\nu + u^\nu u^\mu \nabla_\mu p_{\text{pf}} + \nabla^\nu p_{\text{pf}} = 0. \tag{3.7b}$$

The above system is closed once an equation of state relating the pressure and the energy density is given. Here we assume that the fluid obeys a linear equation of state (1.11) with $\gamma_{\text{pf}} \in (0, 2)$. Equation (3.3b) yields the wave-equation

$$\Box_g \phi = -\frac{dV}{d\phi} + \Gamma(\phi) u^\mu \partial_\mu \phi, \tag{3.8}$$

Motivated by the current cosmological models, we will use a flat spatial homogeneous and isotropic metric g, called Robertson-Walker (RW) metric, that in the Cartesian coordinates $(t, x, y, z) \in (t_-, t_+) \times \mathbb{R}^3$ takes the form given in eq. (1.51). A solution is said to be global to the past (future) if $t_- = -\infty$ $(t_+ = +\infty)$. Then the Einstein equations coupled to the nonlinear scalar field equation (3.8), and the energy conservation equation for the fluid component (3.7a), form the following non-linear ODE system for the unknowns $\{a, H, \phi, \rho_{\text{pf}}\}$:

$$\dot{a} = aH \tag{3.9a}$$

$$\dot{H} = -\frac{1}{2}\gamma_{\text{pf}} \rho_{\text{pf}} - \frac{\dot{\phi}^2}{2} \tag{3.9b}$$

$$\ddot{\phi} = -(3H + \Gamma(\phi))\dot{\phi} - \frac{dV}{d\phi} \tag{3.9c}$$

$$\dot{\rho}_{\text{pf}} = -3\gamma_{\text{pf}} H \rho_{\text{pf}} + \Gamma(\phi)\dot{\phi}^2 \tag{3.9d}$$

together with the Gauss (Hamiltonian) constraint

$$H^2 = \frac{\rho_{\rm pf}}{3} + \frac{\dot{\phi}^2}{6} + \frac{V(\phi)}{3}, \tag{3.10}$$

where H is the Hubble function (see eq.(1.13)). For expanding cosmologies $H > 0$. Note also that the equation for the scale factor $a(t)$ decouples leaving a reduced system of equations for the unknowns $\{H, \phi, \rho_{\rm pf}\}$. The scale-factor can then be obtained by quadrature $a = a_0 e^{\int H dt}$. The $\Gamma(\phi)$ term appearing in (3.9c) and (3.9d) acts as a friction term which describes the decay of the scalar field ϕ due to the interactions encoded in the Lagrangian $\mathcal{L}_{int}$. Here we assume monomial scalar field potentials which are popular examples of inflaton models

$$V(\phi) = \frac{(\lambda\phi)^{2n}}{2n} \quad , \quad \lambda > 0 \quad , \quad n = 1, 2, 3, ... \tag{3.11}$$

and a monomial scalar field interaction term

$$\Gamma(\phi) = \mu\phi^{2p} \quad , \quad \mu > 0 \quad , \quad p = 0, 1, 2, 3, ... \tag{3.12}$$

The exponent $2p$ reflects the parity invariance of the potential and the condition $\mu > 0$ ensures that the second law of thermodynamics is satisfied (see e.g. [37, 99]). For example, interactions described by $\mathcal{L}_{int} \sim \phi\psi$ and $\mathcal{L}_{int} \sim g^2\phi^2\chi^2$, where ψ is the particle of the thermal bath, leads in the first case to the simplest constant interaction term with $\Gamma(\phi) = \mu$, i.e. $p = 0$. and in the other case to $\Gamma(\phi) = \mu\phi^2$, i.e. $p = 1$, see e.g. [100].

To summarise, we will analyse the system (3.9) for the unknowns $\{H, \phi, \rho_{\rm pf}\}$ having the free parameters $\{n, p, \lambda, \mu, \gamma_{\rm pf}\}$ besides the initial conditions $\{\rho_0, \phi_0, \dot{\phi}_0, H_0\}$. Note that n, p and $\gamma_{\rm pf}$ are dimensionless parameters while λ and μ have dimensions. We shall see ahead that it is the dimensionless ratio (see (3.17) ahead) of these two quantities that plays an important role on the qualitative behaviour of solutions.

3.2 Dynamical systems' formulation

In order to obtain a regular dynamical system on a compact state-space, we start by introducing dimensionless variables normalized by the Hubble function H (which is positive for ever expanding models)

$$\Omega_{\rm pf} := \frac{\rho_{\rm pf}}{3H^2} > 0 \quad , \quad \Sigma_\phi := \frac{\dot{\phi}}{\sqrt{6}H} \quad , \quad X := \frac{\lambda\phi}{(6nH^2)^{\frac{1}{2n}}} \quad , \quad \tilde{T} := \frac{c}{H^{\frac{1}{n}}} > 0, \tag{3.13}$$

where $c = \left(\frac{6^{n-1}}{n}\right)^{\frac{1}{2n}} \lambda$ is a positive constant. We also introduce a new time variable $\tilde{N}$ defined by

$$\frac{d}{d\tilde{N}} := \frac{\left(\frac{c}{H^{\frac{1}{n}}}\right)^{\delta}}{H} \frac{d}{dt}, \tag{3.14}$$

where

$$\delta = \begin{cases} 0 & \text{if} \quad p \leq \dfrac{n}{2} \\ 2p - n & \text{if} \quad p > \dfrac{n}{2} \end{cases}$$

When $\delta = 0$, i.e. $p \leq \frac{n}{2}$, then $\tilde{N} = N = \ln(a/a_0)$ is the number of e-folds N from some reference epoch at which $a = a_0$, i.e., $N = 0$. When written in terms of the new variables, the system (3.9), reduces to a regular *local* 3-dimensional dynamical system

$$\frac{dX}{d\tilde{N}} = \frac{1}{n}(1+q)\tilde{T}^{\delta} X + \tilde{T}^{1+\delta}\Sigma_\phi \tag{3.15a}$$

$$\frac{d\Sigma_\phi}{d\tilde{N}} = -\left[(2-q)\tilde{T}^{\delta} + \nu \tilde{T}^{\delta+n-2p} X^{2p}\right]\Sigma_\phi - n\tilde{T}^{1+\delta} X^{2n-1} \tag{3.15b}$$

$$\frac{d\tilde{T}}{d\tilde{N}} = \frac{1}{n}(1+q)\tilde{T}^{1+\delta}, \tag{3.15c}$$

where the constraint equation

$$\Omega_{\rm pf} = 1 - \Sigma_\phi^2 - X^{2n} \tag{3.16}$$

is used to globally solve for $\Omega_{\rm pf}$. Since $\Omega_{\rm pf} > 0$, the above equation implies that $\Omega_{\rm pf}$ is bounded since $\Omega_{\rm pf} \in (0,1)$, while $\Sigma_\phi \in (-1,1)$, and $X \in (-1,1)$. The positive dimensionless constant ν is given explicitly by

$$\nu = 6^p \mu c^{-n} = \sqrt{n 6^{2p-(n-1)}} \frac{\mu}{\lambda^n}, \tag{3.17}$$

and q is the usual deceleration "parameter" defined via (1.17),

$$q = -1 + 3\Sigma_\phi^2 + \frac{3}{2}\gamma_{\rm pf}\Omega_{\rm pf} = -1 + \frac{3}{2}\left(\gamma_\phi \Omega_\phi + \gamma_{\rm pf}\Omega_{\rm pf}\right), \tag{3.18}$$

where we introduced

$$\Omega_\phi = \frac{\rho_\phi}{3H^2} = \Sigma_\phi^2 + X^{2n} = 1 - \Omega_{\rm pf}, \quad \Omega_\phi \in (0,1), \tag{3.19}$$

and the scalar field effective equation of state parameter γ_ϕ is given by

$$\gamma_\phi := 1 + \frac{p_\phi}{\rho_\phi} = \frac{\dot{\phi}^2}{\frac{1}{2}\dot{\phi}^2 + \frac{1}{2n}(\lambda\phi)^{2n}} = \frac{2\Sigma_\phi^2}{\Omega_\phi}. \tag{3.20}$$

Moreover, since $\gamma_{\rm pf} \in (0,2)$, it follows from (3.16), and (3.18) that

$$-1 \leq q \leq 2, \tag{3.21}$$

with $q = 1$ when $\Sigma_\phi = 0$, and $\Omega_{\rm pf} = 0$; $q = 2$ when $X = 0$, and $\Omega_{\rm pf} = 0$; and $q = \frac{1}{2}(3\gamma_{\rm pf} - 2)$ when $X = 0$, and $\Sigma_\phi = 0$. These special constant values of q correspond to well-known solutions: de-Sitter (dS) spacetime when $q = 1$, kinaton or massless scalar field self-similar solution when $q = 2$ and whose scale factor is given by $a(t) = t^{1/3}$, and the flat Friedmann-Lemâitre (FL) self-similar solution when $q = \frac{1}{2}(3\gamma_{\rm pf} - 2)$ with scale factor given by $a(t) = t^{\frac{2}{3\gamma_{\rm pf}}}$. Although the constraint is used to solve for $\Omega_{\rm pf}$, it is nevertheless useful to consider the auxiliary equation for $\Omega_{\rm pf}$ (equivalently $\Omega_\phi = 1 - \Omega_{\rm pf}$) given by

$$\begin{aligned}\frac{d\Omega_{\rm pf}}{d\tilde{N}} &= 2(1 + q - \frac{3}{2}\gamma_{\rm pf})\tilde{T}^{\delta}\Omega_{\rm pf} + 2\nu\tilde{T}^{\delta+n-2p}X^{2p}\Sigma_\phi^2 \\ &= 3(\gamma_\phi - \gamma_{\rm pf})\Omega_{\rm pf}(1 - \Omega_{\rm pf})\tilde{T}^{\delta} + 2\nu\tilde{T}^{\delta+n-2p}X^{2p}\Sigma_\phi^2.\end{aligned} \tag{3.22}$$

Although the variables (X, Σ_ϕ) are bounded, the variable $\tilde{T}$ becomes unbounded $\tilde{T} \to +\infty$ when $H \to 0$. In order to obtain a *regular* and *global* 3-dynamical system, we introduce

$$T = \frac{\tilde{T}}{1 + \tilde{T}}, \tag{3.23}$$

so that $T \in (0,1)$ with $T \to 0$ as $\tilde{T} \to 0$, and $T \to 1$ as $\tilde{T} \to +\infty$, as well as a new independent time variable τ defined by

$$\frac{d}{d\tau} = (1 - T)^k \frac{d}{d\tilde{N}} = \frac{T^{\delta}(1 - T)^{k-\delta}}{H}\frac{d}{dt}, \tag{3.24}$$

where

$$k = \begin{cases} n - 2p + \delta & \text{if} \quad p < \dfrac{n}{2}, \\ 1 + \delta & \text{if} \quad p \geq \dfrac{n}{2}. \end{cases}$$

This leads to a *regular* and *global* 3-dimensional dynamical system for the state-vector (X, Σ_ϕ, T)

$$\frac{dX}{d\tau} = \frac{1}{n}(1 + q)T^{\delta}(1 - T)^{k-\delta}X + T^{1+\delta}(1 - T)^{k-(1+\delta)}\Sigma_\phi \tag{3.25a}$$

$$\frac{d\Sigma_\phi}{d\tau} = -\left[(2 - q)T^{\delta}(1 - T)^{k-\delta} + \nu T^{\delta+n-2p}(1 - T)^{k-(\delta+n-2p)}X^{2p}\right]\Sigma_\phi - nT^{1+\delta}(1 - T)^{k-(1+\delta)}X^{2n-1} \tag{3.25b}$$

$$\frac{dT}{d\tau} = \frac{1}{n}(1 + q)T^{1+\delta}(1 - T)^{1+k-\delta}, \tag{3.25c}$$

The auxiliary equation (3.22) written in terms of the new time variable τ becomes

$$\frac{d\Omega_{\rm pf}}{d\tau} = 2(1+q-\frac{3}{2}\gamma_{\rm pf})T^{\delta}(1-T)^{k-\delta}\Omega_{\rm pf} + 2\nu T^{\delta+n-2p}(1-T)^{k-(\delta+n-2p)}X^{2p}\Sigma_{\phi}^{2}. \tag{3.26}$$

The state space $\mathbf{S}$ is thus a 3-dimensional space consisting of a (deformed when $n>1$) open and bounded solid cylinder without its axis

$$\mathbf{S} = \{(X,\Sigma_\phi,T)\in\mathbb{R}^3 : 0 < X^{2n}+\Sigma_\phi^2 < 1, \quad 0<T<1\}. \tag{3.27}$$

The state space $\mathbf{S}$ can be regularly extended to include the axis of the cylinder with $\Omega_{\rm pf}=1$ ($\Omega_\phi = X^{2n}+\Sigma_\phi^2 = 0$) which is an invariant boundary subset as follows from (3.26), and the outer shell of the cylinder which consists of the pure *scalar field boundary subset*, $\Omega_{\rm pf}=0$ ($\Omega_\phi = X^{2n}+\Sigma_\phi^2 = 1$). Due to the interaction term when $\nu\neq 0$, the $\Omega_{\rm pf}=0$ boundary subset is not invariant for the flow. Furthermore at $\Omega_{\rm pf}=0$ it follows that

$$\left.\frac{d\Omega_{\rm pf}}{d\tau}\right|_{\Omega_{\rm pf}=0} = 2\nu T^{\delta+n-2p}(1-T)^{k-(\delta+n-2p)}X^{2p}\Sigma_\phi^2 \geq 0, \qquad \left.\frac{d^2\Omega_{\rm pf}}{d\tau^2}\right|_{\Omega_{\rm pf}=0} = 0 \qquad \left.\frac{d^3\Omega_{\rm pf}}{d\tau^3}\right|_{\Omega_{\rm pf}=0} = 0 \tag{3.28a}$$

$$\begin{aligned}\left.\frac{d^4\Omega_{\rm pf}}{d\tau^4}\right|_{\Omega_{\rm pf}=0} &= 6n^2(1-T)^{k-\delta-1}(3(1-T)^{3k-3\delta-1}T^{1+3\delta}\gamma_{\rm pf}^2 + \\ &+ (1-T)^{2k-2\delta-1}T^{1+2\delta}\gamma_{\rm pf}(3(1-T)^{k-\delta}T^{\delta} + (1-T)^{k-n+2p-\delta}T^{n-2p-\delta}\nu)) > 0.\end{aligned} \tag{3.28b}$$

Since $\nu>0$, this shows that the surface $\Omega_{\rm pf}=0$ not being invariant, it is future-invariant, which motivates the following definition:

Definition 3.1. The orbits in $\mathbf{S}$ with initial data $\Omega_{\rm pf}(\tau_0)>0$ are said to be of class B if there is a finite $\tau_* < \tau_0$ such that $\Omega_{\rm pf}(\tau_*)=0$. The complement of such orbits in $\mathbf{S}$ are said to be of class A.

Class B orbits enter the state-space $\mathbf{S}$ by crossing the outer cylindrical shell with $\Omega_\phi = \Sigma_\phi^2 + X^{2n} = 1$. Moreover $\mathbf{S}$ can be regularly extended to include the invariant boundaries $T=0$ and $T=1$. Although these boundaries are unphysical, it is essential to include them since all possible past attractor sets for class A orbits are located at $T=0$ and all possible future attractors for both class A and B orbits are located at $T=1$ as follows from the following lemma:

Lemma 3.2. *The α-limit set of class* A *interior orbits in* $\mathbf{S}$ *is located at* $T=0$*, while the* ω*-limit set of all interior orbits in* $\mathbf{S}$ *is located at* $T=1$.

Proof. Since $1+q \leq 0$, then T is strictly monotonically increasing in the interval $(0,1)$ except when $q=-1$ in which case

$$\left.\frac{dT}{d\tau}\right|_{q=-1} = 0, \qquad \left.\frac{d^2T}{d\tau^2}\right|_{q=-1} = 0,$$
$$\left.\frac{d^3T}{d\tau^3}\right|_{q=-1} = n(1-T)^{2k-3(1+\delta)}T^{1+2\delta}\Big(3(1-T)^k T^\delta\big(n(k-\delta)T+(1-T)^2T^2\gamma_{\rm pf}\big)+\nu nk(1-T)^{1+\delta}T^k\Big) > 0.$$

This shows that the points in **S** with $q=-1$ are just inflection points in the graph of $T(\tau)$. By the *monotonicity principle* (see A.23), it follows that there are no fixed points, recurrent or periodic orbits in the interior of the state space **S**, and the α-limit sets of class A orbits are contained at $T=0$ and ω-limit sets of all orbits in **S** are located at $T=1$. □

Thus the global behavior of both class of orbits can be inferred by a complete detailed description of the invariant subsets $T=0$ and $T=1$, which are associated with the asymptotic past $(H \to +\infty)$ and future $(H \to 0)$ respectively. Due to their distinct properties, we split our analysis into three cases: $p < n/2$, $p = n/2$ and $p > n/2$.

3.3 Dynamical systems' analysis when $p < \frac{n}{2}$

When $p < \frac{n}{2}$ the global dynamical system (3.25) takes the form

$$\frac{dX}{d\tau} = \left[\frac{1}{n}(1+q)(1-T)X + T\Sigma_\phi\right](1-T)^{n-2p-1} \tag{3.29a}$$
$$\frac{d\Sigma_\phi}{d\tau} = -\nu T^{n-2p}X^{2p}\Sigma_\phi - \Bigg[(2-q)(1-T)\Sigma_\phi + nTX^{2n-1}\Bigg](1-T)^{n-2p-1} \tag{3.29b}$$
$$\frac{dT}{d\tau} = \frac{1}{n}(1+q)T(1-T)^{n-2p+1} \tag{3.29c}$$

and the auxiliary equation becomes

$$\frac{d\Omega_{\rm pf}}{d\tau} = 2(1-T)^{n-2p}(1+q-\frac{3}{2}\gamma_{\rm pf})\Omega_{\rm pf} + 2\nu T^{n-2p}X^{2p}\Sigma_\phi^2. \tag{3.30}$$

3.3.1 Invariant boundary $T=0$

The flow induced in the $T=0$ boundary is given by

$$\frac{dX}{d\tau} = \frac{1}{n}(1+q)X \quad , \quad \frac{d\Sigma_\phi}{d\tau} = -(2-q)\Sigma_\phi, \tag{3.31}$$

where $q = -1 + 3\Sigma_\phi^2 + \frac{3}{2}\gamma_{\rm pf}\Omega_{\rm pf}$, and $\Omega_{\rm pf} = 1 - \Omega_\phi = 1 - X^{2n} - \Sigma_\phi^2$, satisfies

$$\frac{d\Omega_{\rm pf}}{d\tau} = 2(1+q-\frac{3}{2}\gamma_{\rm pf})\Omega_{\rm pf}. \tag{3.32}$$

Thus

$$\left.\frac{d\Omega_{\rm pf}}{d\tau}\right|_{\Omega_{\rm pf}=0} = 0, \qquad \left.\frac{d\Omega_{\rm pf}}{d\tau}\right|_{\Omega_{\rm pf}=1} = 0, \tag{3.33}$$

and the intersection of the sets $\Omega_{\rm pf} = 0$, and $\Omega_{\rm pf} = 1$ with the invariant boundary $T = 0$ yields an invariant boundary subset. On $T = 0$ the system (3.29) admits five fixed points, one at the center with $\Omega_{\rm pf} = 1$, and four on the invariant scalar field subset with $\Omega_{\rm pf} = 0$.

The fixed point that lies on the intersection of $T = 0$ with the pure matter subset $\Omega_{\rm pf} = 1$ is given by

$$\mathrm{FL}_0: \quad X = 0, \qquad \Sigma_\phi = 0, \qquad T = 0, \tag{3.34}$$

with $q = \frac{1}{2}(3\gamma_{\rm pf} - 2)$ corresponding to the flat FL self-similar solution. The linearisation around this fixed point yields the eigenvalues $\frac{3}{2n}\gamma_{\rm pf}$, $-\frac{3}{2}(2-\gamma_{\rm pf})$ and $\frac{3}{2n}\gamma_{\rm pf}$ with eigenvectors the canonical basis for $\mathbb{R}^3$. Since $0 < \gamma_{\rm pf} < 2$, FL_0 has two positive real eigenvalues and a negative real eigenvalue, being a hyperbolic saddle, and the α-limit point of a 1-parameter set of class A orbits in $\mathbf{S}$.

On the intersection of the invariant boundary $T = 0$ with the subset $\Omega_m = 0$ there are two equivalent fixed points

$$\mathrm{K}^\pm: \quad X = 0, \qquad \Sigma_\phi = \pm 1, \qquad T = 0. \tag{3.35}$$

with $q = 2$ corresponding to the self-similar massless scalar field or kinaton solution. The linearisation of the full system around these fixed points yields the eigenvalues $\frac{3}{n}$, $3(2-\gamma_{\rm pf})$ and $\frac{3}{n}$ whose generalised eigenvectors are $(1,0,0)$, $(0,1,0)$, and $(\mp 1, 0, 1)$. Since $\gamma_{\rm pf} \in (0,2)$ it is easy to conclude that $\mathrm{K}^\pm$ are hyperbolic sources, and the α-limit point of a 2-parameter set of class A orbits in $\mathbf{S}$.

The remaining other two equivalent fixed points are

$$\mathrm{dS}_0^\pm: \quad X = \pm 1, \qquad \Sigma_\phi = 0, \qquad T = 0 \tag{3.36}$$

and correspond to a quasi-de-Sitter state with $q = -1$. The linearisation around these fixed points yields the eigenvalues $-3\gamma_{\rm pf}$, -3 and 0 with eigenvectors $(1,0,0)$, $(0,1,0)$ and $(0, \mp\frac{n}{3}, 1)$ respectively. The fixed points $\mathrm{dS}_0^\pm$ have two negative real eigenvalues (since $\gamma_{\rm pf} > 0$) and a zero eigenvalue corresponding to a center manifold. Due to the monotonicity of T it is clear that a single class A orbit originates from each $\mathrm{dS}_0^\pm$ into $\mathbf{S}$ corresponding to the 1-dimensional center manifold of each fixed point. This center manifold its what is usually called the *inflationary attractor solution*. In order to simplify the analysis of the center manifold we use instead system (3.15) for the unbounded variable $\tilde{T}$, and introduce the adapted variables

$$\bar{X} = X \mp 1, \qquad \bar{\Sigma}_\phi = \Sigma_\phi \pm \frac{n}{3}\tilde{T}, \qquad \bar{T} = \tilde{T}. \tag{3.37}$$

This leads to the transformed adapted system

$$\frac{d\bar{X}}{dN} = -3\gamma_{\rm pf}\bar{X} + F(\bar{X},\bar{\Sigma}_\phi,\tilde{T}), \qquad \frac{d\bar{\Sigma}_\phi}{dN} = -3\bar{\Sigma}_\phi + G(\bar{X},\bar{\Sigma}_\phi,\tilde{T}), \qquad \frac{d\tilde{T}}{dN} = N(\bar{X},\bar{\Sigma}_\phi,\tilde{T}) \tag{3.38}$$

where the fixed points $\mathrm{dS}_0^\pm$ are now located at the origin of coordinates $(\bar{X},\bar{\Sigma}_\phi,\tilde{T}) = (0,0,0)$, and F, G and N are functions of higher order terms. The 1-dimensional center manifold $W^{\rm c}$ at $\mathrm{dS}_0^\pm$ can be locally represented as the graph $h : E^c \to E^s$, i.e. $(\bar{X},\bar{\Sigma}_\phi) = (h_1(\tilde{T}), h_2(\tilde{T}))$, satisfying the fixed point $h(0) = 0$ and the tangency $\frac{dh(0)}{d\tilde{T}} = 0$ conditions (see A.5). Using this in the above equation and, using $\tilde{T}$ as an independent variable, we get

$$\frac{1}{n}(1+q)\Big(\frac{dh_1}{d\tilde{T}}(\tilde{T})\tilde{T} - h_1(\tilde{T}) \mp 1\Big) - \tilde{T}\Big(h_2(\tilde{T}) \mp \frac{n}{3}\tilde{T}\Big) = 0, \tag{3.39a}$$

$$\frac{1}{n}(1+q)\tilde{T}\Big(\frac{dh_2}{d\tilde{T}}(\tilde{T}) \mp \frac{n}{3}\Big) + (2-q)\Big(h_2(\tilde{T}) \mp \frac{n}{3}\tilde{T}\Big) + \\ + \nu\tilde{T}^{n-2p}\Big(h_1(\tilde{T}) \pm 1\Big)^{2p}\Big(h_2(\tilde{T}) \mp \frac{n}{3}\tilde{T}\Big) + n\tilde{T}\Big(h_1(\tilde{T}) \pm 1\Big)^{2n-1} = 0. \tag{3.39b}$$

where $q = -1 + 3\Big(h_2(\tilde{T}) \mp \frac{n}{3}\tilde{T}\Big)^2 + \frac{3}{2}\gamma_{\rm pf}\Big(1 - (h_1(\tilde{T}) \pm 1)^{2n} - (h_2(\tilde{T}) \mp \frac{n}{3}\tilde{T})^2\Big)$. The problem of finding the inflationary attractor solution amounts to solving the above system of non-linear ordinary differential equations. Although in general the existence of an explicit solution for the above system is not expected, it is possible however to approximate the solution by a formal truncated power series expansion in $\tilde{T}$:

$$h_1(\tilde{T}) = \sum_{i=1}^{N} a_i\tilde{T}^i, \qquad h_2(\tilde{T}) = \sum_{i=1}^{N} b_i\tilde{T}^i. \tag{3.40}$$

Plugging in (3.40) into (3.39a)-(3.39b), and using the expansions $(\bar{X} \pm 1)^{2n} = 1 \pm 2n\bar{X} + \binom{2n}{2n-2}\bar{X}^2 + \dots$, $\tilde{T}^{n-2p} = \tilde{T}\delta_1^{n-2p} + \tilde{T}^2\delta_2^{n-2p} + \dots$, and solving the resulting linear system of equations for the coefficients of the expansions yields as $\tilde{T} \to 0$,

$$X = \pm 1 \mp \frac{n}{18}\tilde{T}^2 \pm \left(\frac{n^2}{648}(5-2n) + \frac{\nu n}{27\gamma_{\rm pf}}\delta_1^{n-2p}\right)\tilde{T}^4 + \mathcal{O}(\tilde{T}^4) \tag{3.41a}$$

$$\Sigma_\phi = \mp\frac{n}{3}\tilde{T}\Big[1 \mp \left(\frac{n}{18} + \frac{\nu}{3}\delta_1^{n-2p}\right)\tilde{T}^2 \pm \tag{3.41b}$$

$$\left(\frac{n^2}{648}(17-6n) - \frac{\nu}{3}\left(\delta_2^{n-2p} - \frac{n(2-4n+(7+2p)\gamma_{\rm pf}) + 6\gamma_{\rm pf}}{18\gamma_{\rm pf}}\delta_1^{n-2p}\right)\right)\tilde{T}^4 + \mathcal{O}(\tilde{T}^6)\Big] \tag{3.41c}$$

$$\Omega_{\rm pf} = \frac{2\nu n^2}{27\gamma_{\rm pf}}\delta_1^{n-2p}\tilde{T}^4 + \mathcal{O}(\tilde{T}^6). \tag{3.41d}$$

Therefore, it follows that to leading order on the center manifold

$$\frac{d\tilde{T}}{dN} = \frac{n}{3}\tilde{T}^3 + \mathcal{O}(\tilde{T}^4) \quad \text{as} \quad \tilde{T} \to 0, \tag{3.42}$$

which shows explicitly that $\mathrm{dS}_0^{\pm}$ are center saddles with a unique center manifold orbit originating from each fixed point into the interior of $\mathbf{S}$.

We now show that on $T = 0$ the above fixed points are the only possible α-limit sets, and that the orbit structure on $T = 0$ is very simple consisting only of heteroclinic orbits connecting these fixed points.

Lemma 3.3. *Let $p < \frac{n}{2}$. Then the $T = 0$ invariant boundary consists of heteroclinic orbits connecting the fixed points as depicted in Figure 3.1.*

Proof. It is straightforward to check that $\{\Sigma_\phi = 0\}$ and $\{X = 0\}$ are invariant 1-dimensional subsets consisting of heteroclinic orbits $\mathrm{FL}_0 \to \mathrm{dS}_0^{\pm}$, and $\mathrm{K}^{\pm} \to \mathrm{FL}_0$ respectively. Therefore the two axis divide the (deformed) circle with boundary $X^{2n} + \Sigma_\phi^2 = 1$ consisting of the heteroclinic orbits $\mathrm{K}^+ \to \mathrm{dS}_0^{\pm}$ and $\mathrm{K}^- \to \mathrm{dS}_0^{\pm}$ into 4-invariant quadrants. On each quadrant there are no interior fixed points and hence by the *index theorem* (theorem A.28) no closed curves. It follows by the *Poincaré-Bendixson theorem* (A.25) that each quadrant consists of heteroclinic orbits connecting the fixed points. Moreover in this case the $T = 0$ invariant boundary admits the following conserved quantity

$$\Sigma_\phi^{\gamma_{\rm pf}} X^{(2-\gamma_{\rm pf})n}\Omega_{\rm pf}^{-1} = \text{const.}, \quad \Omega_{\rm pf} = 1 - \Sigma_\phi^2 - X^{2n} \tag{3.43}$$

which determines the solution trajectories on $T = 0$, see Figure 3.1. □

Theorem 3.4. *Let $p < \frac{n}{2}$. The α-limit set for class* A *orbits in* $\mathbf{S}$*, consists of fixed points on $T = 0$. In particular as $\tau \to -\infty$ ($N \to -\infty$), a 2-parameter set of orbits converge to each*

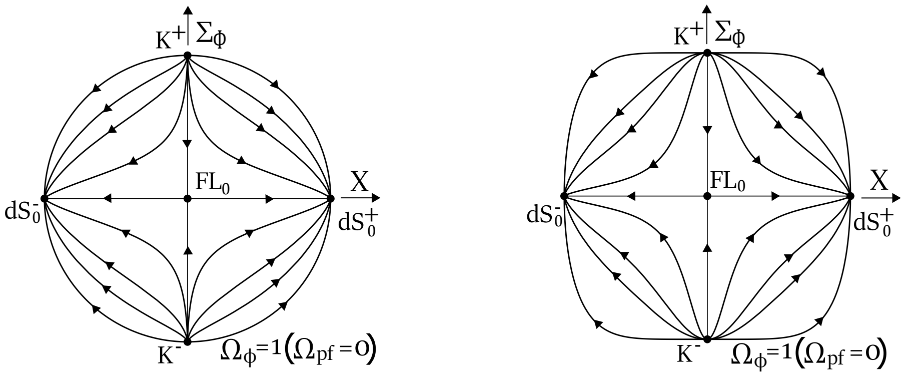

(A) $(p,n)=(0,1)$. (B) $(p,n)=(1,3)$.

Figure 3.1: The invariant boundary $T=0$.

$\mathrm{K}^{\pm}$, *with asymptotics*

$$X(N)=(C_X \pm C_T N)e^{\frac{3}{n}N}, \qquad \Sigma_\phi(N)=\pm 1 \mp C_\Sigma e^{3(2-\gamma_{\mathrm{pf}})N}, \qquad \tilde{T}(N)=C_T e^{\frac{3}{n}N} \tag{3.44}$$

with C_X, $C_\Sigma>0$, *and* $C_T>0$ *constants. A 1-parameter set converges to* FL_0 *with asymptotics*

$$X(N)=C_X e^{\frac{3\gamma_{\mathrm{pf}}}{2n}N}, \qquad \Sigma_\phi(N)=0, \qquad \tilde{T}(N)=C_T e^{\frac{3\gamma_{\mathrm{pf}}}{2n}N} \tag{3.45}$$

with C_X, *and* $C_T>0$ *constants, and a unique center manifold orbit converge to each* $\mathrm{dS}_0^{\pm}$ *with asymptotics*

$$X=\pm 1 \mp \frac{n}{18}\left(1-\frac{2n}{3}N\right)^{-1}, \qquad \Sigma_\phi=\mp\frac{n}{3}\left(1-\frac{2n}{3}N\right)^{-1/2}, \qquad \tilde{T}(N)=\left(1-\frac{2n}{3}N\right)^{-1/2}. \tag{3.46}$$

When $p=\frac{1}{2}(n-1)$ *we also get from (3.41d) the asymptotics* $\Omega_{\mathrm{pf}}=\frac{2\nu n^2}{27\gamma_{\mathrm{pf}}}\left(1-\frac{2n}{3}N\right)^{-2}$. *For* $p<\frac{1}{2}(n-1)$ *one needs to go higher orders on the center manifold of* Ω_{pf}.

Proof. The proof follows by Lemmas 3.2, and 3.3, and the local analysis of the fixed points. ☐

Remark 3.5. *Solutions of class* A *which approach* $\mathrm{K}^{\pm}$ *behave as the self-similar massless scalar field or kinaton solution, and the ones approaching* FL_0 *as the self-similar Friedmann-Lemâitre solution whose asymptotics towards the past exhibit well-known Big-Bang singularities. In the context of cosmological inflation the physical interesting solution is the center* *manifold originating from each* $\mathrm{dS}_0^{\pm}$ *whose asymptotics are given by*

$$n = 1: \qquad H \sim -t \quad , \quad \phi \sim -t \quad , \quad \rho_{\rm pf} \sim (-t)^2, \qquad as \quad t \to -\infty \tag{3.47a}$$

$$n = 2: \qquad H \sim e^{-\frac{2}{3}t} \quad , \quad \phi \sim e^{-\frac{t}{3}} \quad , \quad \rho_{\rm pf} \sim e^{-\frac{4}{3}t}, \qquad as \quad t \to -\infty \tag{3.47b}$$

$$n \geq 3: \qquad H \sim (-t)^{\frac{n}{n-2}} \quad , \quad \phi \sim (-t)^{\frac{2}{n-2}} \quad , \quad \rho_{\rm pf} \sim (-t)^{\frac{2n(2p+1)}{n-2}}, \qquad as \quad t \to -\infty. \tag{3.47c}$$

with $p < \frac{n}{2}$.

3.3.2 Invariant boundary $T = 1$

On the $T = 1$ invariant boundary, the system (3.29a) and (3.29b) reduces to

$$\frac{dX}{d\tau} = \Sigma_\phi \delta_1^{n-2p} \qquad , \qquad \frac{d\Sigma_\phi}{d\tau} = -nX^{2n-1}\delta_1^{n-2p} - \nu X^{2p}\Sigma_\phi. \tag{3.48}$$

and the auxiliary equation for $\Omega_{\rm pf}$, satisfies for $n > 2p$

$$\frac{d\Omega_{\rm pf}}{d\tau} = 2\nu X^{2p}\Sigma_\phi^2. \tag{3.49}$$

The analysis can be divided in two subcases, $p < \frac{1}{2}(n-1)$, i.e. $(p, n) = (0, 2), (0, 3), ...$, $(p, n) = (1, 4), (1, 5), ...$, *etc.*, and $p = \frac{1}{2}(n-1)$, i.e., $(p, n) = (0, 1), (1, 3), (2, 5), ...$

3.3.2.1 Case $p < \frac{1}{2}(n-1)$

In the first case $p < \frac{1}{2}(n-1)$, for all $p \geq 0$ there is a line of fixed points

$$\mathrm{L}_1: \quad X = X_0, \qquad \Sigma_\phi = 0, \qquad T = 1, \tag{3.50}$$

with $X_0 \in [-1, 1]$. In addition to L_1 there exists another line of fixed points when $p > 0$,

$$\mathrm{L}_2: \quad X = 0, \qquad \Sigma_\phi = \Sigma_{\phi 0}, \qquad T = 1, \tag{3.51}$$

with $\Sigma_{\phi 0} \in [-1, 1]$. We shall refer to the non-isolated fixed point at the origin of the $T = 1$ invariant set as FL_1, and the end points of L_1 with $X = \pm 1$ as $\mathrm{dS}_1^{\pm}$. The description of the induced flow on $T = 1$ when $p < \frac{1}{2}(n-1)$ is given by the following simple lemma:

Lemma 3.6. *When* $p < \frac{1}{2}(n-1)$*, the set* $\{T = 1\} \backslash \mathrm{L}_1$ *for* $p = 0$*, and the set* $\{T = 1\} \backslash \mathrm{L}_1 \cup \mathrm{L}_2$ *for* $p > 0$ *are foliated by invariant subsets* $X = const.$ *consisting of regular orbits which enter the region* $\Omega_{\rm pf} > 0$ *by crossing the set* $\Omega_{\rm pf} = 0$ *and converging to the line of fixed points* L_1 *as* $\tau \to +\infty$*. See Figure 3.2.*

Proof. When $p < \frac{1}{2}(n-1)$, the system (3.48) admits the following conserved quantity

$$X = \text{const.} \tag{3.52}$$

which determine the solutions trajectories on the $T = 1$ invariant boundary. The remaining properties of the flow follows from the fact that on $\{T = 1\} \setminus \mathrm{L}_1$ for $p = 0$, and the set $\{T = 1\} \setminus \mathrm{L}_1 \cup \mathrm{L}_2$ for $p > 0$, $d\Sigma_\phi/d\tau < 0$, and $d\Omega_{\mathrm{pf}}/d\tau < 0$. $\square$

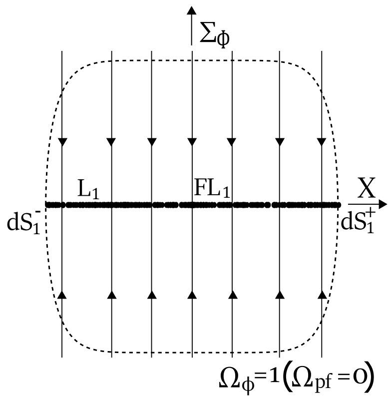

(A) $p = 0$

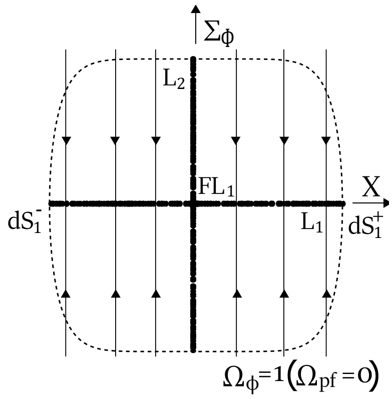

(B) $p > 0$

FIGURE 3.2: The invariant boundary $T = 1$ for $p < \frac{1}{2}(n-1)$.

Theorem 3.7. *Let $p < \frac{1}{2}(n-1)$. Then the ω-limit set all orbits in $\mathbf{S}$ is contained on L_1. In particular:*

i) If $p < \frac{1}{2}(n-2)$, then as $\bar{\tau} \to +\infty$, a 2-parameter set of orbits converge to each of the two fixed points $\mathrm{dS}_1^{\pm}$ on the line L_1 with $X_0 = \pm 1$, and when $p = 0$ a 1-parameter set of orbits converge to FL_1 with $X_0 = 0$.

ii) If $p = \frac{1}{2}(n-2)$, then as $\bar{\tau} \to +\infty$, a 2-parameter set of orbits converge to each of the two fixed points on the line with

$$X_0 = \pm \left(\frac{n^2}{3\gamma_{\mathrm{pf}}\nu} \left(-1 + \sqrt{1 + \left(\frac{3\gamma_{\mathrm{pf}}\nu}{n^2} \right)^2} \right) \right)^{1/n}.$$

and when $p = 0$ a 1-parameter set of orbits converge to FL_1 with $X_0 = 0$.

Proof. The first statement follows by lemmas 3.2 and 3.6 for $p = 0$, while for $p > 0$, it is shown in lemma 3.13 by doing a cylindrical blow-up of L_2 on top of the blow up of FL_1.

The linearised system around L_1 has eigenvalues 0, $-\nu X_0^{2p}$ and 0, with associated eigenvectors $(1,0,0)$, $(0,1,0)$, and $(0, -\frac{2}{\nu}(p - \frac{1}{2}(n-1))X_0^{2(n-p)-1}\delta_2^{n-2p}, 1)$. On the $\{T = 1\}$ invariant boundary the line of fixed points L_1 is normally hyperbolic, i.e. the linearisation yields one negative eigenvalue for all $X_0 \in [-1,1]$, except at $X_0 = 0$ when $p > 0$ where the two lines intersect, and one zero eigenvalue with eigenvector tangent to the line itself, see e.g. [101]. On $\bar{\mathbf{S}}$, the line L_1 is said to be *partially hyperbolic*. Each fixed point on the line, including the point at the center when $p = 0$, has a 1-dimensional stable manifold, and a 2-dimensional center manifold, while the point with $X_0 = 0$ is non-hyperbolic for $p > 0$. In this case the blow up of FL_1 is done in Section 3.3.3. To analyse the 2-dimensional center manifold of each partially hyperbolic fixed point on the line. We start by making the change of coordinates given by

$$\bar{X} = X - X_0, \qquad \bar{\Sigma}_\phi = \Sigma_\phi + \frac{2n}{\nu}(p - \frac{1}{2}(n-1))X_0^{2(n-p)-1}(1-T)\delta_2^{n-2p}, \qquad \bar{T} = 1 - T \quad (3.53)$$

which takes a point in the line L_1 to the origin $(\bar{X}, \bar{\Sigma}_\phi, \bar{T}) = (0,0,0)$ with $\bar{T} \geq 0$. The resulting system of equations takes the form

$$\frac{d\bar{X}}{d\tau} = F(\bar{X}, \bar{\Sigma}_\phi, \bar{T}), \qquad \frac{d\bar{\Sigma}_\phi}{d\tau} = -\nu X_0^{2p}\bar{\Sigma}_\phi + G(\bar{X}, \bar{\Sigma}_\phi, \bar{T}), \qquad \frac{d\bar{T}}{d\tau} = N(\bar{X}, \bar{\Sigma}_\phi, \bar{T}) \quad (3.54)$$

where F, G and N are functions of higher order. The center manifold reduction theorem (see A.5)yields that the above system is locally topological equivalent to a decoupled system on the 2-dimensional center manifold, which can be locally represented as the graph $h:\ E^c \to E^s$, i.e., $\bar{\Sigma}_\phi = h(\bar{X}, \bar{T})$ which solves the nonlinear partial differential equation

$$F(\bar{X}, h(\bar{X}, \bar{T}), \bar{T})\partial_{\bar{X}} h(\bar{X}, \bar{T}) + N(\bar{X}, h(\bar{X}, \bar{T}), \bar{T})\partial_{\bar{T}} h(\bar{X}, \bar{T}) = -\nu X_0^{2p} h(\bar{X}, \bar{T}) + G(\bar{X}, h(\bar{X}, \bar{T}), \bar{T}) \quad (3.55)$$

subject to the fixed point and tangency conditions $h(0,0) = 0$ and $\nabla h(0,0) = 0$ respectively. A quick look at the nonlinear terms suggests that we approximate the center manifold at $(\bar{X}.\bar{T}) = (0,0)$, by making a formal multi-power series expansion for h of the form $h(\bar{X}, \bar{T}) = \bar{T}^{n-2p}\sum_{i,j=0}^{N} \tilde{a}_{ij}\bar{X}^i\bar{T}^j$. Solving for the coefficients of expansion it is easy to verify that all coefficients of type $\tilde{a}_{i0}$ are identically zero, so that h can be written as a series expansion in $\bar{T}$ with coefficients depending on $\bar{X}$, i.e.,

$$h(\bar{X}, \bar{T}) = \bar{T}^{n-2p}\sum_{j=1}^{N} \bar{a}_j(\bar{X})\bar{T}^j, \qquad \bar{a}_j(X) = \sum_{i=0}^{N} a_{ij}\bar{X}^i \quad (3.56)$$

where for example

$$a_{01} = 0, \qquad a_{11} = -\frac{(2(n-p)-1)!}{\nu(n-1)!(n-2p-1)!}X_0^n$$
$$a_{02} = \frac{n}{\nu}X_0^{2(n-p)-1}, \qquad a_{12} = -\frac{n(2n-2p-1)}{\nu}X_0^{2(n-p-2)}$$
$$a_{03} = -\frac{n(n-2p-1)}{\nu}X_0^{2(n-p)-1} + \frac{\left(3(n-1)!\nu - (2(n-p)-1)!X_0^{2(n-p-1)}\right)}{(n-1)!\nu^3}X_0^{n-2p+1}\delta_2^{n-2p}$$

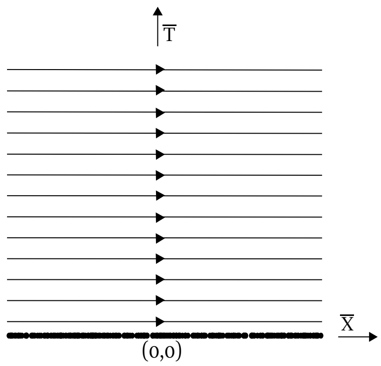

(A) $b_{01} > 0$. For $b_{01} < 0$ the direction of the flow is reversed.

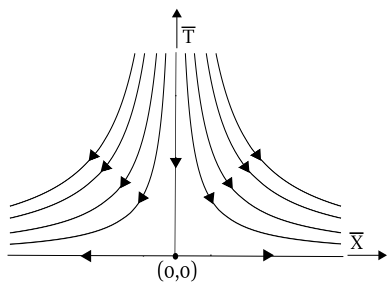

(B) $X_0 = 0$ when $p = 0$

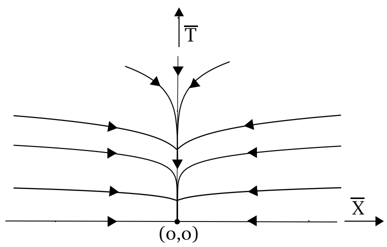

(C) $X_0 = X_\pm$ when $p = \frac{1}{2}(n-2)$.

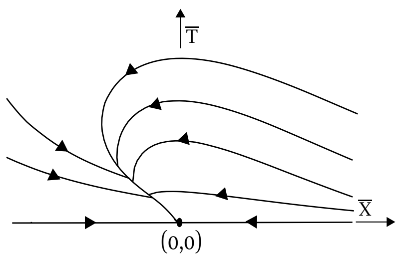

(D) $X_0 = \pm 1$ when $p < \frac{1}{2}(n-2)$.

FIGURE 3.3: Flow on the 2-dimensional center manifold of each point on L_1.

After a change of time $d/d\tau = \bar{T}^{n-2p-1}d/d\bar{\tau}$, the flow on the 2-dimensional center manifold is given by

$$\frac{d\bar{X}}{d\bar{\tau}} = \sum_{j=1}^{N}\bar{b}_j(\bar{X})\bar{T}^j, \qquad \bar{b}_j(\bar{X}) = \sum_{i=0}^{N}b_{ij}\bar{X}^i \tag{3.58a}$$

$$\frac{d\bar{T}}{d\bar{\tau}} = \bar{T}\sum_{j=1}^{N}\bar{c}_j(X)\bar{T}^j \qquad \bar{c}_j(\bar{X}) = \sum_{i=0}^{N}c_{ij}\bar{X}^i \tag{3.58b}$$

with

$$
\begin{aligned}
b_{01} &= X_0\left(\frac{3\gamma_{\rm pf}}{2n}(1-X_0^{2n}) - \frac{n(n-2p-1)}{\nu}X_0^{2(n-p-1)}\delta_2^{n-2p}\right)\\
b_{11} &= \left(\frac{3\gamma_{\rm pf}}{2n}\left(1-(1+2n)X_0^{2n}\right) - \frac{(2(n-p)-1)!}{\nu(n-1)!(n-2p-1)!}X_0^{2(n-p-1)}\delta_2^{n-2p}\right)\\
b_{02} &= \frac{n}{\nu}X_0^{2(n-p)}\\
c_{01} &= -\frac{3\gamma_{\rm pf}}{2n}(1-X_0^{2n}), \qquad c_{11} = 0\\
c_{02} &= \frac{3\gamma_{\rm pf}}{2n}(1-X_0^{2n}), \qquad c_{12} = -3\gamma_{\rm pf}X_0^{2n}.
\end{aligned}
$$

For $p=\frac{1}{2}(n-2)$, with n even, the coefficient b_{01} vanishes at $X_0=0$ and $X_0=X_\pm$ where

$$
X_\pm = \pm\left[\frac{n^2}{3\gamma_{\rm pf}\nu}\left(-1+\sqrt{1+\left(\frac{3\gamma_{\rm pf}\nu}{n^2}\right)^2}\right)\right]^{1/n}. \tag{3.60}
$$

Note that $X_- \in (-1,0)$ and $X_+ \in (0,1)$. Moreover $b_{01}<0$ for $X_0 \in (X_-,0)\cup(X_+,1]$, and $b_{01}>0$ for $X_0\in[-1,X_-)\cup(0,X_+)$ and the origin $(0,0)$ is a nilpotent singularity. Since the coefficient $\bar{c}_{01}(\bar{X}) \neq 0$ for all X_0, then the formal normal form is zero with

$$
\frac{d\bar{X}_*}{d\bar{\tau}_*} = \text{sign}(b_{01})\bar{T}_*, \qquad \frac{d\bar{T}_*}{d\bar{\tau}_*} = \bar{T}_*^2\Phi(\bar{X}_*,\bar{T}_*) \tag{3.61}
$$

and Φ an analytic function. The phase-space is the flow-box multiplied by the function $\bar{T}_*$, with the direction of the flow given by the sign of b_{01}, see Figure 3.3a. For $X_0=0$ (when $p=0$), then $b_{11}(0)=\frac{3\gamma_{\rm pf}}{2n}>0$, and $c_{01}(0)=-\frac{3\gamma_{\rm pf}}{2n}<0$ which after Euler multiplication by $\bar{T}^{-1}$ yields a hyperbolic saddle, see Figure 3.3b. For $X_0=X_\pm$, we have

$$
\begin{aligned}
b_{11}(X_\pm) &= -\left(\frac{n^2}{\nu\sqrt{3\gamma_{\rm pf}}}\right)^2\left(1+\left(\frac{3\gamma_{\rm pf}\nu}{n^2}\right)^2 - \sqrt{1+\left(\frac{3\gamma_{\rm pf}\nu}{n^2}\right)^2}\right)<0,\\
c_{01}(X_\pm) &= -\frac{n^3}{6\gamma_{\rm pf}\nu^2}\left(-1+\sqrt{1+\left(\frac{3\gamma_{\rm pf}\nu}{n^2}\right)^2}\right)<0,
\end{aligned}
$$

and after Euler multiplication by $\bar{T}^{-1}$ the origin is a hyperbolic sink, see Figure 3.3c.

For $p<\frac{1}{2}(n-2)$, the coefficient b_{01} vanishes at $X_0=0$ and $X_0=\pm1$, being negative for $X_0\in(-1,0)$, and positive for $X_0\in(0,1)$. For $b_{01}\neq 0$, the phase-space is again as depicted in Figure 3.3a with the direction of the flow given by the sign of b_{01}, i.e. of X_0. When $X_0=0$ (and restricting to $p=0$), $b_{01}=0$, and $b_{11}=\frac{3\gamma_{\rm pf}}{2n}>0$ which after Euler multiplication by $\bar{T}^{-1}$ yields that FL_1 is a hyperbolic saddle, see Figure 3.3b. For $X_0=\pm1$, we have that $b_{11}=-3\gamma_{\rm pf}<0$, $c_{01}=0$, $c_{02}=0$ and $c_{12}=-3\gamma_{\rm pf}<0$ after changing time variable to

$d/d\tilde{\tau} = \bar{T}^{-1} d/d\bar{\tau}$, then

$$\begin{aligned}
\frac{d\bar{X}}{d\tilde{\tau}} &= -3\gamma_{\rm pf}\bar{X} + \frac{n}{\nu}\bar{T} + \frac{n}{\nu}\bar{T}^2 + \frac{n(n-2p)}{2}\bar{X}\bar{T} - \frac{3}{2}(2n+1)\bar{X}^2 + \mathcal{O}(\|(\bar{X},\bar{T})\|^3)\\
\frac{d\bar{T}}{d\tilde{\tau}} &= -3\gamma_{\rm pf}\bar{X}\bar{T} + \mathcal{O}(\|(\bar{X},\bar{T})\|^3)
\end{aligned}$$

and the origin is a semi-hyperbolic fixed point with eigenvalues $-3\gamma_{\rm pf}$, 0 and associated eigenvectors $(1,0)$ and $(-\frac{n}{3\gamma_{\rm pf}\nu}, 1)$. To analyse the 1-dimensional center manifold we introduce the adapted variable $\tilde{X} = \bar{X} + \frac{n}{3\gamma_{\rm pf}\nu}\bar{T}$. The 1-dimensional center manifold W^c at $(0,0)$ can be locally represented as the graph $h: E^c \to E^s$, i.e. $\tilde{X} = h(\bar{T})$, satisfying the fixed point $h(0) = 0$ and tangency $\frac{dh(0)}{d\bar{T}} = 0$ conditions, i.e. using $\bar{T}$ as an independent variable. Approximating the solution by a formal truncated power series expansion $h(\bar{T}) = \sum_{i=2}^{N} a_i \bar{T}^i$ and solving for the coefficients yields to leading order on the center manifold

$$\frac{d\bar{T}}{d\tilde{\tau}} = -\frac{n}{\nu}\bar{T}^2 + \mathcal{O}(\bar{T}^3), \quad \text{as} \quad \bar{T} \to 0. \tag{3.63}$$

Therefore for $X_0 = \pm 1$, the origin is the ω-limit set of a 1-parameter set of orbits on the 2-dimensional center manifold, see Figure 3.3d. □

The global qualitative behavior for solutions of the dynamical system 3.29 when $p < \frac{1}{2}(n-1)$ is shown in Figure 3.4.

Remark 3.8. *The asymptotic for solutions converging to* $\mathrm{dS}_1^{\pm}$ *are given by*

$$H \sim t^{-\frac{n}{2(n-p)}}, \quad \phi \sim const, \quad \rho_{\rm pf} \sim t^{-\frac{n}{n-p}}, \quad as \quad t \to +\infty \tag{3.64}$$

while those converging to $\mathrm{S}^{\pm}$ *are given by*

$$H \sim t^{-\frac{n}{n+3}}, \quad \phi \sim const, \quad \rho_{\rm pf} \sim t^{-\frac{2n}{n+3}}, \quad as \quad t \to +\infty. \tag{3.65}$$

3.3.2.2 Case $p = \frac{1}{2}(n-1)$

In the second case $p = \frac{1}{2}(n-1)$, there is single fixed point lying in the intersection of $T = 1$ with the pure matter subset $\Omega_{\rm pf} = 1$

$$\mathrm{FL}_1: \quad X = 0, \qquad \Sigma_\phi = 0, \qquad T = 1. \tag{3.66}$$

The linearisation around this fixed point on $T = 1$ boundary yields the characteristic polynomial $\lambda^2 + \nu\delta_1^n\lambda + n\delta_1^n = 0$. Since $\nu > 0$, when $n = 1$ ($p = 0$), FL_1 has two eigenvalues with negative real part being a hyperbolic sink on $T = 1$ (stable node if $\nu \geq 2$, and a stable focus

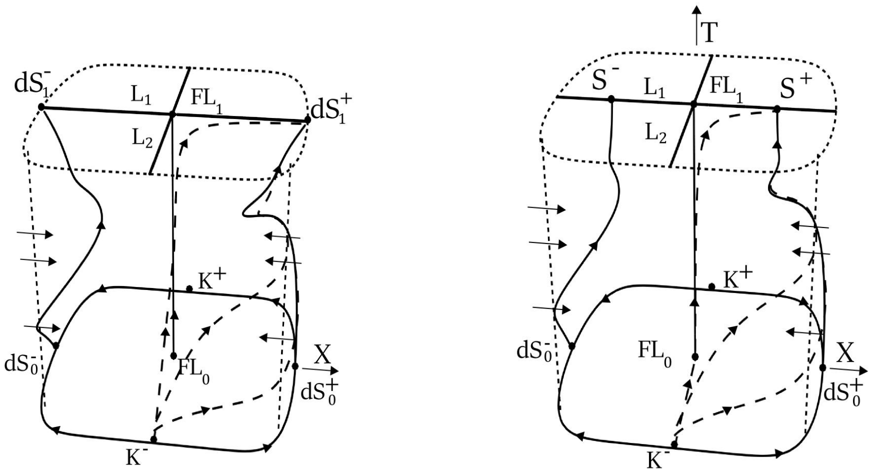

(A) Case $p < \frac{1}{2}(n-2)$ with $(p,n) = (1,5)$, $\gamma_{\rm pf} = \frac{4}{3}$ and $\nu = 1$.

(B) Case $p = \frac{1}{2}(n-2)$ with $(p,n) = (1,4)$, $\gamma_{\rm pf} = \frac{4}{3}$ and $\nu = 1$.

Figure 3.4: Qualitative global evolution of the dynamical system (3.29) for $p < \frac{n}{2}(n-1)$

if $0 < \nu < 2$), while on the full state space FL_1 has a 1-dimensional center manifold with center tangent space $E^c = \langle(0,0,1)\rangle$, i.e., consisting of the $\Omega_{\rm pf} = 1$ invariant set. Therefore FL_1 is the ω-limit point of a 2-parameter set of orbits, converging to FL_1 tangentially to the center manifold when $\nu \geq 2$, or spiraling around the center manifold when $0 < \nu < 2$. When $n - 2p = 1$ but $p \neq 0$ and $n > 1$ all eigenvalues of the fixed point FL_1 are zero. The blow-up of the fixed point FL_1 is given in Section 3.3.3.

Lemma 3.9. *Let $p = \frac{1}{2}(n-1)$. Then the $T = 1$ invariant boundary consists of orbits entering the region $\Omega_{\rm pf} > 0$ by crossing the set $\Omega_{\rm pf} = 0$ and converging to the fixed point* FL_1 *at the center as $\tau \to +\infty$.*

Proof. It suffices to note that the bounded function $\Omega_{\rm pf}$ is strictly monotonically increasing along the orbits, except at the axis of coordinates $\Sigma_\phi = 0$ or $X = 0$ when $p > 0$. However since $d\Sigma_\phi/d\tau \neq 0$ on $\Sigma_\phi = 0$ and $dX/d\tau \neq 0$ on $X = 0$, except at origin where the axis intersect, it follows by the *LaSalle's invariance principle* (A.10) that $(\Sigma_\phi, X) \to (0,0)$, and $\Omega_{\rm pf} \to 1$. In fact, when $p = \frac{1}{2}(n-1)$, the system (3.48) admits the following conserved quantity on $T = 1$:

$$-\frac{\arctan\left[\frac{\frac{2n}{\nu}\frac{\Sigma_\phi}{X^n}+1}{\sqrt{\left(\frac{2n}{\nu}\right)^2-1}}\right]}{\sqrt{\left(\frac{2n}{\nu}\right)^2-1}}+\frac{1}{2}\log\left[\nu\Sigma_\phi X^n+n(1-\Omega_{\mathrm{pf}})\right]=\text{const.},\qquad \text{if}\quad 0<\nu<2n, \tag{3.67a}$$

$$\log\left[\Sigma_\phi+X^n\right]+\frac{X^n}{\Sigma_\phi+X^n}=\text{const.},\qquad \text{if}\quad \nu=2n, \tag{3.67b}$$

$$\frac{\operatorname{arctanh}\left[\frac{\frac{2n}{\nu}\frac{\Sigma_\phi}{X^n}+1}{\sqrt{1-\left(\frac{2n}{\nu}\right)^2}}\right]}{\sqrt{1-\left(\frac{2n}{\nu}\right)^2}}+\frac{1}{2}\log\left[\nu\Sigma_\phi X^n+n(1-\Omega_{\mathrm{pf}})\right]=\text{const.},\qquad \text{if}\quad \nu>2n \tag{3.67c}$$

which determine the solutions trajectories on the $T=1$ invariant boundary. □

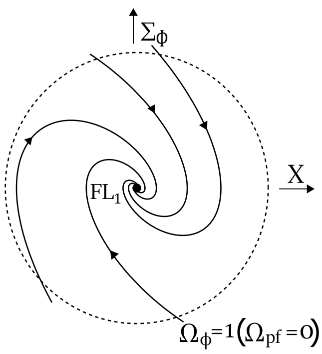

(A) $(p,n)=(0,1)$.

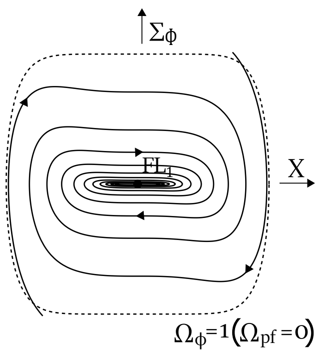

(B) $(p,n)=(1,3)$.

Figure 3.5: The invariant boundary $T=1$ for $p=\frac{1}{2}(n-1)$.

Theorem 3.10. *Let $p=\frac{1}{2}(n-1)$. Then as $\tau\to+\infty$, all orbits in $\mathbf{S}$ converge to the fixed point FL_1.*

Proof. The proof follows by Lemmas 3.2, and 3.9. □

Remark 3.11. *It is possible to deduce the asymptotics towards the fixed point FL_1. For $(n,p)=(1,0)$, and all $\gamma_{\mathrm{pf}}\in(0,2)$ the preceding analysis yields to leading order on the center manifold*

$$T(\tau)=1-\left(1+\frac{3\gamma_{\mathrm{pf}}}{2}C_T\tau\right)^{-1}\qquad \textit{as}\qquad \tau\to+\infty. \tag{3.68}$$

Moreover if $0<\nu<2$, then

$$X(\tau)=e^{-\frac{\nu}{2}\tau}\Big(C_X\cos(\frac{1}{2}\sqrt{4-\nu^2}\tau)+\frac{(\nu C_X+2C_\Sigma)\sin(\frac{1}{2}\sqrt{4-\nu^2}\tau)}{\sqrt{4-\nu^2}}\Big), \tag{3.69a}$$

$$\Sigma_\phi(\tau)=e^{-\frac{\nu}{2}\tau}\Big(C_\Sigma\cos(\frac{1}{2}\sqrt{4-\nu^2}\tau)-\frac{(2\nu C_X+\nu C_\Sigma)\sin(\frac{1}{2}\sqrt{4-\nu^2}\tau)}{\sqrt{4-\nu^2}}\Big). \tag{3.69b}$$

as $\tau \to +\infty$. If $\nu = 2$,

$$X(\tau) = e^{-\tau}\Big((1+\tau)C_X + \tau C_\Sigma\Big), \tag{3.70a}$$

$$\Sigma_\phi(\tau) = e^{-\tau}\Big(C_\Sigma - \tau(C_X + C_\Sigma)\Big), \tag{3.70b}$$

as $\tau \to +\infty$, and if $\nu > 2$, then

$$X(\tau) = e^{-\frac{\nu}{2}\tau}\Big(C_X \cosh(\frac{1}{2}\sqrt{\nu^2-4}\tau) + \frac{(\nu C_X + 2C_\Sigma)\sinh(\frac{1}{2}\sqrt{\nu^2-4}\tau)}{\sqrt{\nu^2-4}}\Big), \tag{3.71a}$$

$$\Sigma_\phi(\tau) = e^{-\frac{\nu}{2}\tau}\Big(C_\Sigma \cosh(\frac{1}{2}\sqrt{\nu^2-4}\tau) - \frac{(2\nu C_X + \nu C_\Sigma)\sinh(\frac{1}{2}\sqrt{\nu^2-4}\tau)}{\sqrt{\nu^2-4}}\Big). \tag{3.71b}$$

as $\tau \to +\infty$. For $p > 0$, i.e., $(p, n) = (1, 3), (2, 5), (3, 7), etc.$, the asymptotics can be obtained by the analysis of the blow-up of FL_1 *done in Section 3.3.3.*

The global qualitative behavior for solutions of the dynamical system 3.29 when $p = \frac{n}{2}(n-1)$ is shown in Figure 3.6.

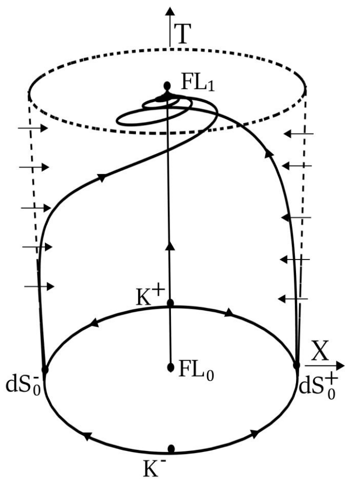

(A) $(p, n) = (0, 1)$.

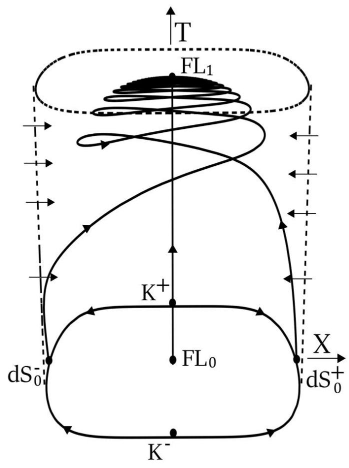

(B) $(p, n) = (1, 3)$.

Figure 3.6: Qualitative global evolution of the dynamical system (3.29) for $p = \frac{n}{2}(n-1)$.

3.3.3 Blow-up of FL_1 when $p > 0$

To analyse the non-hyperbolic fixed point FL_1 of the dynamical system (3.29) when $p > 0$, we start by relocating FL_1 at the origin, i.e., we introduce $\bar{T} = 1 - T$, to obtain the dynamical system

$$\frac{dX}{d\tau} = \frac{1}{n}(1+q)\tilde{T}^{n-2p}X + (1-\tilde{T})\tilde{T}^{n-2p-1}\Sigma_\phi \tag{3.72a}$$
$$\frac{d\Sigma_\phi}{d\tau} = -\left[(2-q)\tilde{T}^{n-2p} + \nu(1-\tilde{T})^{n-2p}X^{2p}\right]\Sigma_\phi - n(1-\tilde{T})\tilde{T}^{n-2p-1}X^{2n-1} \tag{3.72b}$$
$$\frac{d\tilde{T}}{d\tau} = -\frac{1}{n}(1+q)(1-\tilde{T})\tilde{T}^{n-2p+1} \tag{3.72c}$$

where recall

$$q = -1 + 3\Sigma_\phi^2 + \frac{3}{2}\gamma_{\mathrm{pf}}\left(1 - X^{2n} - \Sigma_\phi^2\right). \tag{3.73}$$

In order to understand the dynamics near the origin $(X, \Sigma_\phi, \bar{T}) = (0,0,0)$, which is a non-hyperbolic fixed point for $p > 0$ we employ the spherical blow-up method [102–104] (see A.7.3). This is, we transform the fixed point at the origin to the unit 2-sphere $\mathbb{S}^2 = \{(x,y,z) \in \mathbb{R}^3 : x^2 + y^2 + z^2 = 1\}$, and define the blow-up space manifold as $\mathcal{B} := \mathbb{S}^2 \times [0, u_0]$ for some fixed $0 < u_0 < 1$. We further define the quasi-homogeneous blow-up map

$$\Psi : \mathcal{B} \to \mathbb{R}^3, \qquad \Psi(x,y,z,u) = (u^{n-2p}x, u^n y, u^{2p} z) \tag{3.74}$$

which after canceling a common factor $u^{2p(n-2p)}$ (i.e. by changing time variable $d/d\tau = u^{2p(n-2p)} d/d\bar{\tau}$, where $p < \frac{n}{2}$, with $p > 0$) leads to a desingularisation of the non-hyperbolic fixed point on the blow-up locus $\{u = 0\}$. Since Φ is a diffeomorphism outside of the sphere $\mathbb{S}^2 \times \{u = 0\}$, which corresponds to the fixed point $(0,0,0)$, the dynamics on the blow-up space $\mathcal{B} \setminus \mathbb{S}^2 \times \{u = 0\}$ are topological conjugate to $\mathbb{R}^3 \setminus \{0,0,0\}$.

It usually simplifies the computations if instead of standard spherical coordinates on $\mathcal{B}$, one uses different local charts $\kappa_i : \mathcal{B} \to \mathbb{R}^3$ such that $\psi_i : \Psi \circ \kappa_i^{-1}$ and the resulting vector fields are simpler to analyse. We choose six charts κ_i such that

$$\psi_{1\pm} = (\pm u_{1\pm}^{n-2p}, u_{1\pm}^n y_{1\pm}, u_{1\pm}^{2p} z_{1\pm}) \tag{3.75a}$$
$$\psi_{2\pm} = (u_{2\pm}^{n-2p} x_{2\pm}, \pm u_{2\pm}^n, u_{2\pm}^{2p} z_{2\pm}) \tag{3.75b}$$
$$\psi_{3\pm} = (u_{3\pm}^{n-2p} x_{3\pm}, u_{3\pm}^n y_{3\pm}, \pm u_{3\pm}^{2p}) \tag{3.75c}$$

where $\psi_{1\pm}$, $\psi_{2\pm}$ and $\psi_{3\pm}$ are called the directional blows ups in the positive/negative x, y, and z-directions respectively. It is easy to check that the different charts are given explicitly by

$$\kappa_{1+}: \quad (u_{1+}, y_{1+}, z_{1+}) = (ux^{\frac{1}{n-2p}}, yx^{-n}, zx^{-2p}) \tag{3.76a}$$
$$\kappa_{2+}: \quad (x_{2+}, u_{2+}, z_{2+}) = (xy^{-\frac{n-2p}{n}}, uy^{\frac{1}{n}}, zy^{-\frac{2p}{n}}) \tag{3.76b}$$
$$\kappa_{3+}: \quad (x_{3+}, u_{3+}, z_{3+}) = (xz^{-\frac{n-2p}{2p}}, yz^{-\frac{n}{2p}}, uz^{\frac{1}{2p}}) \tag{3.76c}$$

Later transition maps $\kappa_{ij} = \kappa_j \circ \kappa_i^{-1}$ allows us to identify fixed points and special invariant manifolds on different charts, and to deduce all dynamics on the blow up space. In this case, we will need the following transition charts.

$$\kappa_{1+2+} \quad : \quad (x_{2+}, u_{2+}, z_{2+}) = (y_{1+}^{-\frac{n-2p}{n}}, u_{1+}y_{1+}^{\frac{1}{n}}, y_{1+}^{-\frac{2p}{n}} z_{1+}), \quad y_{1+} > 0; \tag{3.77a}$$

$$\kappa_{2+1+} \quad : \quad (u_{1+}, y_{1+}, z_{1+}) = (u_{2+}x_{2+}^{\frac{1}{n-2p}}, x_{2+}^{-n}, z_{2+}x_{2+}^{-2p}), \quad x_{2+} > 0; \tag{3.77b}$$

$$\kappa_{1+3+} \quad : \quad (x_{3+}, y_{3+}, u_{3+}) = (z_{1+}^{-\frac{n-2p}{2p}}, y_{1+}z_{1+}^{-\frac{n}{2p}}, u_{1+}z_{1+}^{\frac{1}{2p}}), \quad z_{1+} > 0; \tag{3.78a}$$

$$\kappa_{3+1+} \quad : \quad (u_{1+}, y_{1+}, z_{1+}) = (u_{3+}x_{3+}^{\frac{1}{n-2p}}, y_{3+}, y_{3+}x_{3+}^{-n}, x_{3+}^{-2p}), \quad x_{3+} > 0; \tag{3.78b}$$

$$\kappa_{2+3+} \quad : \quad (x_{3+}, y_{3+}, u_{3+}) = (x_{2+}z_{2+}^{-\frac{n-2p}{2p}}, z_{2+}^{-\frac{n}{2p}}, u_{2+}z_{2+}^{\frac{1}{2p}}), \quad z_{2+} > 0; \tag{3.79a}$$

$$\kappa_{3+2+} \quad : \quad (x_{2+}, u_{2+}, z_{2+}) = (x_{3+}y_{3+}^{-\frac{n-2p}{n}}, u_{3+}y_{3+}^{\frac{1}{n}}, y_{3+}^{-\frac{2p}{n}}), \quad y_{3+} > 0; \tag{3.79b}$$

Since the physical state-space has $\bar{T} \geq 0$, we are only interested in the region $\{z \geq 0\}$, i.e. the union of the upper hemisphere of the unit sphere $\mathbb{S}^2$ and the equator of the sphere $\{z = 0\}$ which constitutes an invariant boundary. This motivates that we start the analysis by using chart κ_{3+}, i.e., the directional blow-up map in the positive z-direction, on which the northern hemisphere is mapped into an invariant plane of coordinates $(x_3, y_3, 1)$. After canceling a common factor $u_3^{2p(n-2p)}$ (i.e. by changing the time variable $d/d\tau = u_3^{2p(n-2p)} d/d\bar{\tau}_3$) leads to

$$\frac{dx_3}{d\bar{\tau}_3} = \frac{1}{2np}(1+q)(2p + (n-2p)(1-u_3^{2p}))x_3 + (1-u_3^{2p})y_3 \tag{3.80a}$$

$$\frac{dy_3}{d\bar{\tau}_3} = \frac{1}{2p}(1+q)(1-u^{2p})y_3 - (2 - q + \nu(1-u_3^{2p})^{n-2p}x_3^{2p})y_3 - n(1-u_3^{2p})x_3^{2n-1}u_3^{2n(n-1-2p)} \tag{3.80b}$$

$$\frac{du_3}{d\bar{\tau}_3} = -\frac{1}{2np}(1+q)(1-u_3^{2p})u_3 \tag{3.80c}$$

where

$$q = -1 + \frac{3\gamma}{2}\left(1 + \frac{2-\gamma}{\gamma}y_3^2u_3^{2n} - x_3^{2n}u_3^{2n(n-2p)}\right).$$

In these coordinates the equator of the sphere is at infinity, and it is better analyzed using charts $\kappa_{1\pm}$ and $\kappa_{2\pm}$. Moreover since the above system is symmetric under the transformation $(x_3, y_3) \to -(x_3, y_3)$ it suffices to consider the charts in the positive direction. To study the points at infinity, we notice that both the directional blow-ups in the positive x and y direction already tell how such local chart must be given. To study the region where x_3 blows up, we use the chart

$$(y_1, z_1, u_1) = \left(\frac{y_3}{x_3^n}, \frac{1}{x_3^{2p}}, u_3 x_3^{\frac{1}{n-2p}}\right) \tag{3.81}$$

together with change of time variable $d/d\bar{\tau}_1 = z_1 d/d\bar{\tau}_3$, i.e. $d/d\tau = u_1^{2p(n-2p)} d/d\bar{\tau}_1$, leads to the system of equations

$$\frac{dy_1}{d\bar{\tau}_1} = -n(1-u_1^{2p}z_1)z_1^{n-2p-1}u_1^{2n(n-2p-1)} - \left(2-q+\frac{1+q}{n-2p}\right)y_1 z_1^{n-2p} - \nu y_1(1-u_1^{2p})^{n-2p} \tag{3.82a}$$
$$- \frac{n}{n-2p}\left(1-u_1^{2p}z_1\right)y_1^2 z_1^{n-2p-1}$$
$$\frac{dz_1}{d\bar{\tau}_1} = -\left(\frac{1+q}{n}\left(\frac{n}{n-2p} - u_1^{2p}z_1\right)z_1^{n-2p} + \frac{2p}{n-2p}(1-u_1^{2p}z_1)y_1 z_1^{n-2p-1}\right)z_1 \tag{3.82b}$$
$$\frac{du_1}{d\bar{\tau}_1} = \frac{1}{n-2p}\left(\frac{1+q}{n}z_1 + \left(1-u_1^{2p}z_1\right)y_1\right)u_1 z_1^{n-2p-1} \tag{3.82c}$$

where

$$q = -1 + \frac{3\gamma_{\rm pf}}{2}\left(1 + \frac{2-\gamma_{\rm pf}}{\gamma_{\rm pf}}y_1^2 u_1^{2n} - u_1^{2n(n-2p)}\right).$$

To study the region where y_3 blows up, we use the chart κ_{3+2+}

$$(x_2, z_2, u_2) = \left(\frac{x_3}{y_3^{\frac{n-2p}{n}}}, \frac{1}{y_3^{-\frac{2p}{n}}}, u_3 y_3^{\frac{1}{n}}\right) \tag{3.83}$$

and changing the time variable $d/\bar{\tau}_2 = z_2 d/d\bar{\tau}_3$ i.e. $d/d\tau = u_2^{2p(n-2p)} d/\bar{\tau}_2$ we get

$$\frac{dx_2}{d\bar{\tau}_2} = \frac{1}{n}\left(2(n-2p+\frac{1}{2}) - (n-2p-1)q\right)x_2 z_2^{n-2p} + \left(1+(n-2p)x_2^{2n}\right)(1-u_2^{2p}z_2)z_2^{n-2p-1}$$
$$+ \nu\frac{n-2p}{n}(1-u_2^{2p}z_2)^{n-2p}x_2^{2p+1} \tag{3.84a}$$
$$\frac{dz_2}{d\bar{\tau}_2} = \frac{2p}{n}\left(\left(2-q+\frac{1+q}{2p}(1-u_2^{2p}z_2)\right)z_2^{n-2p} + \nu(1-u_2^{2p}z_2)^{n-2p}x_2^{2p}\right)z_2$$
$$+ 2p(1-u_2^{2p}z_2)x_2^{2n-1}z_2^{n-2p}u_2^{2n(n-2p-1)}$$
$$\frac{du_2}{d\bar{\tau}_2} = -\left((2-q)z_2^{n-2p} + \frac{\nu}{n}(1-u_2^{2p}z_2)^{n-2p}x_2^{2p} + \left(1-u_2^{2p}z_2\right)z_2^{n-2p-1}x_2^{2n-1}u_2^{2n(n-2p-1)}\right)u_2 \tag{3.84b}$$

where

$$q = -1 + \frac{3\gamma_{\rm pf}}{2}\left(1 + \frac{2-\gamma_{\rm pf}}{\gamma_{\rm pf}}u_2^{2n} - x_2^{2n}u_2^{2n(n-2p)}\right). \tag{3.85}$$

The general structure of the blow-up space for the two different cases with $p < \frac{1}{2}(n-1)$ and $p = \frac{1}{2}(n-1)$ is shown in Figure 3.7. In the first case, we shall see ahead that the points $R^{\pm}$ are still non-hyperbolic and therefore needed a further blow-up, while in the second case the number of fixed points on the equator depends on if $\nu < 2n$, $\nu = 2n$ or $\nu > 2n$.

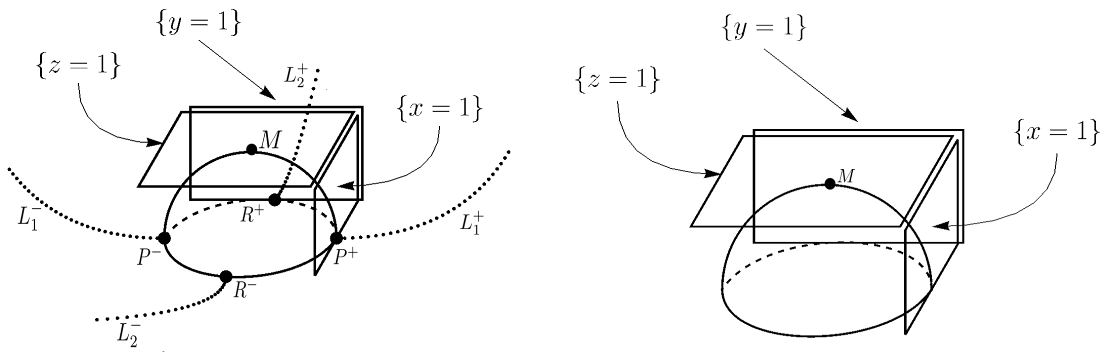

(A) Case $p < \frac{1}{2}(n-1)$. (B) Case $p = \frac{1}{2}(n-1)$.

FIGURE 3.7: Blow-up space $\mathcal{B}$.

To obtain a global phase-space description, we shall also, instead of projecting the upper-half of the unit 2-sphere on the $z = 1$ plane, to project it into the open unit disk $x^2 + y^2 < 1$ which can be joined with the equator (unit circle on $\{z = 0\}$), thus obtaining a global understanding of the flow on the Poincaré-Lyapunov unit cylinder $\mathbb{D}^2 \times [0, \bar{u}_0]$ for some $\bar{u} \in (0, 1)$. Usually generalised angular variable Θ are used on the invariant subset $\{u_3 = 0\}$, see e.g. [105, 106]. Here we use a different type of transformation, based on [68], which makes the analysis somewhat simpler:

$$(x_3, y_3, u_3) = \left(\left(\frac{r}{1-r}\right)^{\frac{1}{2p}} \cos\theta, \left(\frac{r}{1-r}\right)^{\frac{2p+1}{2p}} F(\theta)\sin\theta, (1-r)^{\frac{1}{2p}}\,\bar{u}\right), \tag{3.86}$$

where

$$F(\theta) = \sqrt{\frac{1-\cos^{2(2p+1)}\theta}{1-\cos^2\theta}} = \sqrt{\sum_{k=0}^{2p} \cos^{2k}\theta} \tag{3.87}$$

is bounded and analytical in $\theta \in [0, 2\pi)$, satisfying $F(\theta) \geq 1$ (with $F \equiv 1$ when $p = 0$), and $F(0) = \sqrt{2p+1}$. The above transformation leads to

$$x_3^{2(2p+1)} + y_3^2 = \left(\frac{r}{1-r}\right)^{\frac{2p+1}{p}} \tag{3.88}$$

and make a further change of time variable

$$\frac{d}{d\bar{\xi}} = (1-r)\frac{d}{d\bar{\tau}_3}. \tag{3.89}$$

we obtain the dynamical system

$$\frac{dr}{d\xi} = 2p(1-r)r\Bigg(\frac{(1+q)(1-r)}{2pn(2p+1)}\Big((2p+1)\Big(n-(n-2p)(1-r)\bar{u}^{2p}\Big)-n(1-\bar{u}^{2p})F^2(\theta)\sin^2\theta\Big)$$
$$+\frac{F^2(\theta)\sin^2\theta}{2p+1}\Big((2-q)(1-r)+r(1-(1-r)\bar{u}^{2p})^{n-2p}\nu\cos^{2p}\theta\Big)+r(1-(1-r)\bar{u}^{2p})F(\theta)\sin\theta$$
$$-\frac{n(1-\bar{u}^{2p})}{2p+1}\bar{u}^{2n(n-2p-1)}(1-r)^{\frac{(n-1)(n-2p-1)}{p}}r^{\frac{n-1}{p}-1}F(\theta)\sin\theta\Bigg) \tag{3.90a}$$

$$\frac{d\theta}{d\xi} = -\frac{F(\theta)^2}{2np}\Big((1+q)(1-r)(n-(1-r)(n-2p)\bar{u}^{2p})\cos\theta+2pnr(1+(1-r)\bar{u}^{2p})F(\theta)\sin\theta\Big)\sin\theta$$
$$-\frac{4n}{4(2p+1)}(1-r)^{\frac{(n-2p-1)(n-1)}{p}}r^{\frac{n-p-1}{p}}\bar{u}^{2n(n-2p-1)}(1-\bar{u}^{2p})\cos^{2n}\theta F(\theta)$$
$$+\frac{(1-r)}{4p(2p+1)}(1+q)(1-\bar{u}^{2p}-2p(2-q))F(\theta)^2\sin 2\theta+2r(1+(1-r)\bar{u}^{2p})^{n-2p}\nu F(\theta)\cos^{2p}\theta\sin 2\theta \tag{3.90b}$$

$$\frac{d\bar{u}}{d\xi} = -\frac{(1+q)(1-(1-r)\bar{u}^{2p})}{2np}(1-r)\bar{u}-\frac{\bar{u}}{4p(2p+1)}\Big(2(1-r)r\Big(2p(2-q)-(1+q)(1-\bar{u}^{2p})\Big)F^2(\theta)$$
$$+4p\nu r^2(1-(1-r)\bar{u}^{2p})^{n-2p}F^2(\theta)+4pn(1-r)^{\frac{(n-2p-1)(n-1)}{p}}r^{\frac{(n-1)}{p}}\bar{u}^{2n(n-2p-1)}(1-\bar{u}^{2p})\cos^{n-1}\theta F(\theta)\Big)\sin^2\theta$$
$$+\frac{\bar{u}r\cos^{4p+1}\theta}{2np}\Big((1+q)(1-r)(n-(1-r)(n-2p)\bar{u}^{2p})\cos\theta+2pnr(1+(1-r\bar{u}^{2p}))F(\theta)\Big) \tag{3.90c}$$

where

$$q=-1+\frac{3\gamma_{\rm pf}}{2}\left(1-(1-r)^{\frac{n(n-2p-1)}{p}}r^{n/p}\bar{u}^{2n(n-2p)}\cos^{2n}\theta+\frac{2-\gamma_{\rm pf}}{\gamma_{\rm pf}}(1-\cos^{2p(2p+1)}\theta)(1-r)^{\frac{n-2p-1}{p}}r^{2+\frac{1}{p}}\bar{u}^{2n}\right).$$

The right-hand side of the above dynamical system is regular and can be extended up to $\{r=0\}$ and $\{r=1\}$ at least in a C^1 manner. The general structure of the Poincaré-Lyapunov cylinders in both cases when $p<\frac{1}{2}(n-1)$ and $p=\frac{1}{2}(n-1)$ are shown in Figure 3.8a. In this way all fixed points are hyperbolic or semi-hyperbolic, and in particular when $p<\frac{1}{2}(n-1)$ the line L_2 does no longer exists.

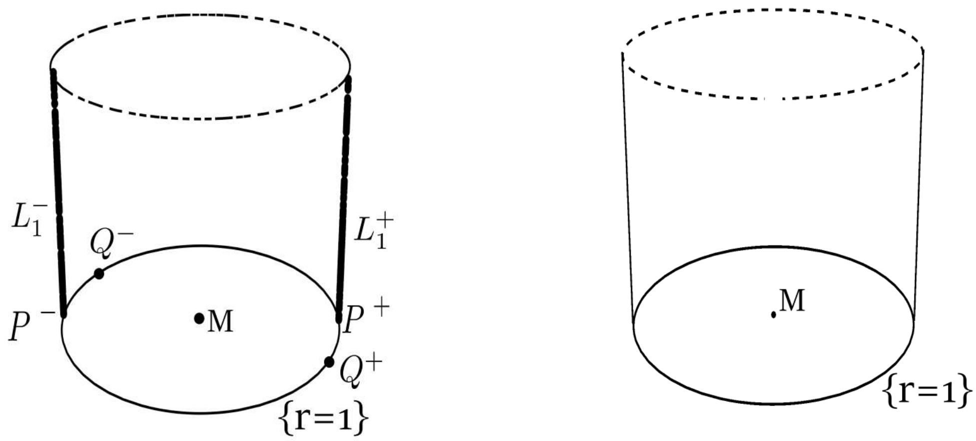

(A) Case $p < \frac{1}{2}(n-1)$.

(B) Case $p = \frac{1}{2}(n-1)$.

Figure 3.8: Blow-up space on the Poincaré-Lyapunov cylinder.

3.3.3.1 Case $p < \frac{1}{2}(n-1)$:

Consider the case $p < \frac{1}{2}(n-1)$ with $p > 0$, i.e. $n > 2$, for example $(p, n) = (1, 4), (1, 5), (1, 6), \ldots$, $(p, n) = (2, 6), (2, 7), \ldots$, etc.

Positive z-direction

For $u_3 < 1$ all fixed points are located at the invariant subset $\{u_3 = 0\}$. The flow induced on $\{u_3 = 0\}$ is given by

$$\frac{dx_3}{d\bar{\tau}_3} = \frac{3\gamma_{\rm pf}}{4p}x_3 + y_3 \quad , \quad \frac{dy_3}{d\bar{\tau}_3} = \left(\frac{3(2p+1)\gamma_{\rm pf}}{4p}K - \nu x_3^{2p}\right) y_3 \tag{3.91}$$

where we introduced

$$K(\gamma_{\rm pf}, p) = 1 - \frac{4p}{(2p+1)\gamma_{\rm pf}}. \tag{3.92}$$

Due to that $\gamma_{\rm pf} \in (0, 2)$, it follows that $K \in (-\infty, \frac{1}{1+2p})$.

Remark 3.12. *By changing coordinates to $(\bar{x}, \bar{y}) = \left(x_3, \frac{3\gamma_{\rm pf}}{4p}x_3 + y_3\right)$ the system of equations (3.91) is transformed into an equivalent Liénard-type system*

$$\frac{d\bar{x}}{d\bar{\tau}_3} = \bar{y}, \quad \frac{d\bar{y}}{d\bar{\tau}_3} = -f(\bar{x})\bar{y} - g(\bar{x}) \tag{3.93}$$

where

$$f(\bar{x}) = -\frac{3\gamma_{\text{pf}}}{4p}\frac{(1+p)}{2p}K + \nu\bar{x}^{2p} \tag{3.94a}$$

$$g(\bar{x}) = \frac{3\gamma_{\text{pf}}}{4p}\bar{x}\left(\frac{3\gamma_{\text{pf}}(1+2p)}{4p}K - \nu\bar{x}^{2p}\right). \tag{3.94b}$$

which arises from the second-order Liénard-type differential equation

$$\frac{d^2\bar{x}}{d\bar{\tau}_3^2} + f(\bar{x})\frac{d\bar{x}}{d\bar{\tau}_3} + g(\bar{x}) = 0. \tag{3.95}$$

Introducing the functions

$$F(\bar{x}) = \int_0^{\bar{x}} f(s)ds, \qquad G(\bar{x}) = \int_0^{\bar{x}} g(s)ds \tag{3.96}$$

the energy of the system is is $E = \frac{1}{2}\bar{y}^2 + G(\bar{x})$*, and making a further change of variable* $Y = \bar{y} + F(\bar{x})$ *leads to the Liénard plane*

$$\frac{d\bar{x}}{d\bar{\tau}_3} = Y - F(\bar{x}), \qquad \frac{dY}{d\bar{\tau}_3} = -g(\bar{x}). \tag{3.97}$$

There is vast amount of literature on Liénard type systems, see e.g.,[102, 104, 107, 108] and reference therein. The most difficult problem concerns the existence, number, relative position and bifurcations of limit cycles arising on Liénard equations.

The fixed points are the real solutions of

$$\left(\frac{3(2p+1)\gamma_{\text{pf}}}{4p}K - \nu x_3^{2p}\right)y_3 = 0 \quad , \quad y_3 = -\frac{3\gamma_{\text{pf}}}{4p}x_3. \tag{3.98}$$

In this case there are at most 3 fixed points. The fixed point at the origin of coordinates

$$\text{M}: \quad x_3 = 0, \quad y_3 = 0. \tag{3.99}$$

The linearised system at M has eigenvalues $\lambda_1 = \frac{3\gamma_{\text{pf}}}{4p}$, $\lambda_2 = 3\frac{(2p+1)\gamma_{\text{pf}}}{4p}K$, $\lambda_3 = -\frac{3\gamma_{\text{pf}}}{4np}$, and associated eigenvectors $v_1 = (1,0,0)$, $v_2 = (-\frac{2}{3(2-\gamma_{\text{pf}})}, 1, 0)$, $v_3 = (0,0,1)$. Hence on $\{u_3 = 0\}$, M is a hyperbolic fixed point if and only if $K \neq 0$, being a saddle if $K < 0$, $(0 < \gamma_{\text{pf}} < \frac{4p}{2p+1})$, and a source if $K > 0$, $(\frac{4p}{2p+1} < \gamma_{\text{pf}} < 2)$. When $K = 0$, $(\gamma_{\text{pf}} = \frac{4p}{2p+1})$, there is a bifurcation leading to a center manifold associated with a zero eigenvalue. To analyse the center manifold we introduce the adapted variable $\bar{y}_3 = y_3 - \frac{2}{3(2-\gamma_{\text{pf}})}\bar{x}_3$. The center manifold can be locally represented as the graph $h: E^c \to E^u$, i.e. $x_3 = h(\bar{y}_3)$, which solves the initial value problem.

$$\frac{3\gamma_{\rm pf}}{4p}h(\bar{y}_3) - \frac{2\nu}{3(2-\gamma_{\rm pf})}\left(h(\bar{y}_3) - \frac{2\bar{y}_3}{3(2-\gamma_{\rm pf})}\right)\bar{y}_3 = \bar{y}\left(\frac{3(2p+1)\gamma_{\rm pf}}{4p} - \nu\left(h(\bar{y}_3) - \frac{2\bar{y}_3}{3(2-\gamma_{\rm pf})}\right)^{2p}\right)\frac{dh}{d\bar{y}_3} \tag{3.100a}$$

$$h(0) = 0 \qquad \frac{dh}{d\bar{y}_3}(0) = 0. \tag{3.100b}$$

Approximating the solution by formal truncated power series expansion, and solving coefficients yields to the leading order

$$\frac{d\bar{y}_3}{d\bar{\tau}_3} = -\nu\left(\frac{2p+1}{3}\right)^{2p}\bar{y}_3^{2p+1} + \mathcal{O}(\bar{y}_3^{2p+3}), \qquad \bar{y}_3 \to 0 \tag{3.101}$$

and therefore it is one dimensional stable center manifold. In addition to M there are more two fixed point when $K > 0$, while no additional fixed points exists when $K \leq 0$. When $K > 0$, the fixed points are

$$\mathrm{S}^{\pm}: \quad x_3 = \pm\left(\frac{3(2p+1)\gamma_{\rm pf}}{4p\nu}K\right)^{\frac{1}{2p}}, \quad y_3 = \mp\left(\frac{3\gamma_{\rm pf}}{4p}\right)\left(\frac{3(2p+1)\gamma_{\rm pf}}{4p\nu}K\right)^{\frac{1}{2p}} \tag{3.102}$$

The linearisation around these fixed points yields the eigenvalues

$$\lambda_1 = \frac{3\gamma_{\rm pf}}{8p}\left(1 - \sqrt{1+8p(1+2p)K}\right), \quad \lambda_2 = \frac{3\gamma_{\rm pf}}{8p}\left(1 + \sqrt{1+8p(1+2p)K}\right), \quad \lambda_3 = -\frac{3\gamma_{\rm pf}}{4np} \tag{3.103}$$

with associated eigenvectors

$$v_1 = \left(\frac{1-\sqrt{1+8p(1+2p)K}}{3(1+2p)\gamma_{\rm pf}K}, 1, 0\right), \quad v_2 = \left(\frac{1+\sqrt{1+8p(1+2p)K}}{3(1+2p)\gamma_{\rm pf}K}, 1, 0\right), \quad v_3 = (0,0,1). \tag{3.104}$$

It follows that $\mathrm{S}^{\pm}$ are hyperbolic saddles.

Fixed points at infinity

When $p < \frac{1}{2}(n-1)$, the flow on the invariant subset $\{u_1 = 0\}$ is given by

$$\frac{dy_1}{d\bar{\tau}_1} = -3\left(1 - \frac{n-2p-1}{n-2p}\gamma_{\rm pf}\right)y_1 z_1^{n-2p} - \nu y_1, \quad \frac{dz_1}{d\bar{\tau}_1} = -\frac{1}{n-2p}\left(\frac{3\gamma_{\rm pf}}{2}z_1 - 2py_1\right)z_1^{n-2p} \tag{3.105}$$

and analyse the invariant set $\{z_1 = 0\}$ on $\{u_1 = 0\}$, which results

$$\frac{dy_1}{d\bar{\tau}_1} = -\nu y_1. \tag{3.106}$$

and has one fixed point

$$\mathrm{P}^+ \quad : \quad y_1 = 0, \quad z_1 = 0 \quad u_1 = 0. \tag{3.107}$$

The linearisation yields the eigenvalues $\lambda_1 = -\nu$, $\lambda_2 = 0$, and $\lambda_3 = 0$ with associated eigenvectors $v_1 = (1,0,0)$, $v_2 = (0,1,0)$, and $v_3 = (0,0,1)$. The zero eigenvalue in the u_1-direction is associated with a line of fixed points parameterized by constant values of $u_1 = u_0 \in (0,1)$, and which corresponds to the half of the line of fixed points L_1 with $X_0 < 0$. Thus on $u_1 = 0$ invariant set, the fixed point P^+ is semi-hyperbolic. The center manifold reduction theorem yields that the above system is locally topological equivalent to the 1-dimensional decoupled equation on the center manifold, which can be locally represented as graph $h : E^c \to E^s$, i.e. $y_1 = h(z_1)$ which solves the nonlinear ordinary differential equation

$$-\frac{1}{n-2p}\left(\frac{3\gamma_{\rm pf}}{2} - 2ph(z1)\right) z_1^{n-2p}\frac{dh}{dz_1} = -\nu h(z_1) - 3\left(1 - \frac{n-2p-1}{n-2p}\gamma_{\rm pf}\right) h(z_1) z_1^{n-2p} \tag{3.108}$$

subject to the fixed point, $h(0) = 0$, and tangency, $\frac{dh(0)}{dz_1} = 0$, conditions. In general it is not possible to solve for h explicitly. However we can approximate the solutions by making a formal multi-power series expansion for $h(z_1)$ and solving for the coefficients gives as $z_1 \to 0$: In this case, the flow on the center manifold is

$$\frac{dz_1}{d\bar{\tau}_1} = -\frac{3\gamma_{\rm pf}}{2(n-2p)} z_1^{n-2p+1} + \mathcal{O}\left(z_1^{n-2p+2}\right), \quad z_1 \to 0. \tag{3.109}$$

and so P^+ is the ω-limit point of a 1-parameter set of orbits.

On the positive y-direction, when $p < \frac{1}{2}(n-1)$, the flow induced on the invariant subset $\{u_2 = 0\}$ is given by

$$\frac{dx_2}{d\bar{\tau}_2} = \nu\frac{n-2p}{n}x_2^{2p+1} + \left(\frac{1}{n}\left((n-2p) - \frac{3(n-2p-1)\gamma_{\rm pf}}{2}\right) x_2 z_2 + (1 + (n-2p)x_2^{2n})\right) z_2^{n-2p-1} \tag{3.110a}$$

$$\frac{dz_2}{d\bar{\tau}_2} = \frac{2p}{n}\left(3\left(1 - \frac{(2p+1)\gamma_{\rm pf}}{2}\right) z_2^{n-2p} + \nu x_2^{2p}\right) z_2 \tag{3.110b}$$

and analyse the invariant set $\{z_2 = 0\}$ on $\{u_2 = 0\}$, which results

$$\frac{dx_2}{d\bar{\tau}_2} = \nu\frac{n-2p}{n}x_2^{2p+1} \tag{3.111}$$

which admits one fixed point

$$\mathrm{R}^+ \quad : \quad x_2 = 0, \quad z_2 = 0 \quad u_2 = 0 \tag{3.112}$$

and whose linearised system has all eigenvalues zero. The zero eigenvalue in the u_2 direction is due to the line of fixed points L_2^+. Nevertheless it follows from (3.106), and (3.111), that the equator of the Poincaré sphere consists of heteroclinic orbits $\mathrm{R}^+ \to \mathrm{Q}^\pm$, and $\mathrm{R}^- \to \mathrm{Q}^\pm$.

To blow-up of R^+ or better the complete line L_2^+, we perform a cylindrical blow up, i.e. we transform each point on the line to a circle $\mathbb{S}^1 = \{(v, w) \in \mathbb{R}^2 : v^2 + w^2 = 1\}$. The blow-up space is $\bar{\mathcal{B}} = \mathbb{S}^1 \times [0, u_{20}) \times [0, s_0)$ and define the quasi-homogeneous blow-up map

$$\bar{\Psi} : \bar{\mathcal{B}} \to \mathbb{R}^3, \quad \bar{\Psi}(v, w, u_2, s) = (s^{n-2p-1}v, s^{2p+1}w, u_2)$$

We choose four charts such that

$$\bar{\psi}_{1\pm} = \left(\pm s_{1\pm}^{n-2p-1}, s_{1\pm}^{2p+1} w_{1\pm}, u_2\right) \tag{3.113a}$$

$$\bar{\psi}_{2\pm} = \left(s_{2\pm}^{n-2p-1} v_{2\pm}, \pm s_{2\pm}^{2p+1}, u_2\right) \tag{3.113b}$$

In fact we only consider the semi-circle with $w \geq 0$ since $z_2 \geq 0$. This in particular means that we only need to consider the blow-up in the positive w-direction, i.e. the directional blow-up defined by $\bar{\psi}_{2+}$. We start with the v-direction $\{v = \pm 1\}$ which after canceling the common factor $s_{1\pm}^{2p(n-2p-1)}$ (i.e by changing the time variable $d/d\bar{\tau}_2 = s_{1\pm}^{2p(n-2p-1)} d/d\tilde{\tau}_{1\pm}$) leads to

$$\begin{aligned}
\frac{dw_{1\pm}}{d\bar{\tau}_{1\pm}} &= \nu \frac{(1 - s_{1\pm}^{2p+1} u_2^{2p} w_{1\pm})^{n-2p}}{2p - n + 1} w_{1\pm} - \frac{n(2-q) + (1+2p)(1+q)}{n(n-2p-1)} s_{1\pm}^n w_{1\pm}^{n-2p-1} \\
&\mp \left(\frac{(1+2p)(1 + (n-2p) s_{1\pm}^{2n(n-2p-1)})}{n-2p-1} - 2p (s_{1\pm} u_2)^{2n(n-2p-1)} \right) w_{1\pm}^{n-2p} (1 - s_{1\pm}^{2p+1} u_2^{2p} w_{1\pm}) \\
&+ \frac{(1+q)(1 - s_{1\pm}^{2p+1} u_2^{2p} w_{1\pm})}{n} w_{1\pm}^{n-2p+1} s_{1\pm}^n
\end{aligned} \tag{3.114a}$$

$$\begin{aligned}
\frac{ds_{1\pm}}{d\bar{\tau}_{1\pm}} &= \frac{1}{n-2p-1} \left(\frac{1 + q + (n-2p)(2-q)}{n} s_{1\pm}^n w_1^{n-2p} + \frac{\nu (n-2p)(1 - s_{1\pm}^{2p+1} u_2^{2p} w_{1\pm})}{n} \right) s_{1\pm} \\
&\pm \frac{1}{n-2p-1} \left(1 + (n-2p) s_{1\pm}^{2n(n-2p-1)}\right) \left(1 - s_{1\pm}^{2p+1} u_2^{2p} w_{1\pm}\right) w_{1\pm}^{n-2p-1} s_{1\pm}
\end{aligned} \tag{3.114b}$$

$$\begin{aligned}
\frac{du_2}{d\bar{\tau}_{1\pm}} &= -\Bigg((2-q) s_{1\pm}^n w_1^{n-2p} \pm (s_{1\pm} u_2)^{2n(n-2p-1)} (1 - s_{1\pm}^{2p+1} u_2^{2p} w_{1\pm}) w_1^{n-2p-1} \\
&+ \frac{\nu \left(1 - s_{1\pm}^{2p+1} u_2^{2p} w_{1\pm}\right)^{n-2p}}{n} \Bigg) u_2
\end{aligned} \tag{3.114c}$$

where

$$q = -1 + \frac{3\gamma_{\mathrm{pf}}}{2} \left(1 + \frac{2 - \gamma_{\mathrm{pf}}}{\gamma_{\mathrm{pf}}} u_2^{2n} - u_2^{2n(n-2p)} s_{1\pm}^{2n(n-2p-1)}\right) \tag{3.115}$$

The system above presents the following fixed point:

$$T^\pm : \quad w_{1\pm} = 0, \quad s_{1\pm} = 0, \quad u_2 = 0 \tag{3.116}$$

whose linearised system has eigenvalues $-\frac{\nu}{n-2p-1}$, $\frac{(n-2p)\nu}{n(n-2p-1)}$, and $-\frac{\nu}{n}$ with eigenvectors the canonical basis of $\mathbb{R}^3$, and the fixed points

$$Q^{\pm}: \quad w_{1\pm} = \mp\left(\frac{\nu}{2p+1}\right)^{\frac{1}{n-2p-1}}, \quad s_{1\pm} = 0, \quad u_2 = 0 \tag{3.117}$$

where only Q^- exists in the region $w_{1\pm} > 0$. The eigenvalues of the linearised system around $Q^{\pm}$ are ν, $\frac{2p\nu}{n(2p+1)}$ and $-\frac{\nu}{n}$ with associated eigenvectors the canonical basis of $\mathbb{R}^3$.

In the w-direction and after canceling a common factor $s_{2\pm}^{2p(n-2p-1)}$ (i.e. by changing the time variable $d/d\bar{\tau}_2 = s_{2\pm}^{2p(n-2p-1)} d/d\tilde{\tau}_{2+}$) leads to the system

$$\begin{aligned}\frac{dv_{2\pm}}{d\bar{\tau}_{2\pm}} &= \frac{n(2-q)+(2p+1)(1+q)}{n(2p+1)} s_{2\pm}^{n} v_2 + \nu\frac{(1-s_{2\pm}^{2p+1}u_2^{2p})^{n-2p}}{2p+1} v_{2\pm}^{2p+1} \\ &\left(1+\frac{\left((n-2p)(2p+1)-2p(n-2p-1)u_2^{2n(n-2p-1)}\right) v_{2\pm}^{2n} s_{2\pm}^{2n(n-2p-1)}}{1+2p}\right)\left(1-s_{2\pm}^{2p+1}u_2^{2p}\right) \\ &+\frac{(n-2p-1)(1+q)}{n(2p+1)}\left(1-s_{2\pm}^{2p+1}u_2^{2p}\right) s_{2\pm}^{n} v_{2\pm}\end{aligned} \tag{3.118a}$$

$$\begin{aligned}\frac{ds_{2\pm}}{d\bar{\tau}_{2\pm}} &= \frac{\nu(1-s_{2\pm}^{2p+1}u_2^{2p})^{n-2p}}{n(2p+1)} v_{2\pm}^{2p} s_{2\pm} + \frac{2p(2-q)+(1+q)(1-s_{2\pm}^{2p+1})u_2^{2p}}{n(2p+1)} s_{2\pm}^{n+1} \\ &\frac{2p(1-s_{2\pm}^{2p+1}u_2^{2p})}{2p+1} s_{2\pm}^{2n(n-2p-1)+1} u_2^{2n(n-2p-1)} v_{2\pm}^{2n-1}\end{aligned} \tag{3.118b}$$

$$\frac{du_2}{d\bar{\tau}_{2\pm}} = -\left((2-q)s_{2\pm}^{n} + (1-s_{2\pm}^{2p+1}u_{2\pm}^{2p})v_{2\pm}^{2n-1} s_{2\pm}^{2n(n-2p-1)} u_2^{2n(n-2p-1)} + \frac{\nu(1-s_{2\pm}^{2p+1}u_2^{2p})^{n-2p}}{n} v_{2\pm}^{2p}\right) u_2 \tag{3.118c}$$

where

$$q = -1 + \frac{3\gamma_{\rm pf}}{2}\left(1 + \frac{2-\gamma_{\rm pf}}{\gamma_{\rm pf}} u_2^{2n} - u_2^{2n(n-2p)} s_{2\pm}^{2n(n-2p-1)} v_{2\pm}^{2n}\right) \tag{3.119}$$

The system only has the fixed points

$$Q^{\mp}: \quad v_{2\pm} = \mp\left(\frac{2p+1}{\nu}\right)^{\frac{1}{2p+1}}, \quad s_{2\pm} = 0, \quad u_2 = 0 \tag{3.120}$$

which has eigenvalues $\left(\frac{2p+1}{\nu}\right)^{\frac{2p}{2p+1}}$, $\frac{\nu}{n(2p+1)}\left(\frac{2p+1}{\nu}\right)^{\frac{2p}{2p+1}}$, and $-\frac{\nu}{n}\left(\frac{2p+1}{\nu}\right)^{\frac{2p}{2p+1}}$ with associated eigenvectors are the canonical basis of $\mathbb{R}^3$. The blow-up of L_2^+ is shown Figure 3.9. Since all fixed points are located on $u_2 = 0$, we have the following result concerning the line L_2 on the cylinder state-space $\mathbf{S}$.

Lemma 3.13. *No interior orbit in* $\mathbf{S}$ *converges to the points on the set* $\mathrm{L}_2 \setminus \mathrm{FL}_0$.

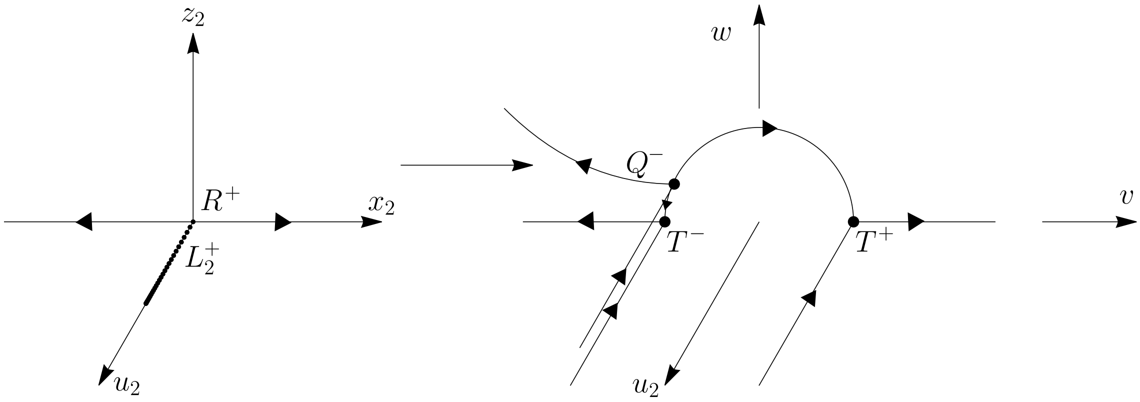

Figure 3.9: Blow-up of the non-hyperbolic line of fixed points L_2.

Global phase-space on the Poincaré-Lyapunov disk

The previous results can be collected in a global phase-space by employing the Poincaré-Lyapunov compactification. This compactification has the advantage that all fixed points are hyperbolic, or partially hyperbolic, and in particular on the cylinder the line L_2 is absent. When $p < \frac{1}{2}(n-1)$, the induced flow on the $\{\bar{u} = 0\}$ invariant subset (to see the cylindrical Poincaré-Lyapunov compactification see), is given by

$$\begin{aligned}
\frac{dr}{d\bar{\xi}} &= 2p(1-r)r\left(-\frac{\nu}{2p+1}r\left(1-\cos^{2(2p+1)}\theta\right)\cos^{2p}\theta + \frac{3\gamma_{\mathrm{pf}}}{(2p+1)}(1-r)\left(\frac{(2p+1)K\gamma_{\mathrm{pf}}}{4p} + \cos^{2(2p+1)}\theta\right)\right) \\
&\quad + 2p(1-r)r^2F(\theta)\sin\theta, \\
\frac{d\theta}{d\bar{\xi}} &= -F(\theta)\left(\frac{3}{2p+1}F(\theta)\sin 2\theta(1-r) + \left(1 + \frac{\nu}{2(2p+1)}\sin 2\theta F(\theta)\cos^{2p}\theta - \cos^{2(2p+1)}\theta\right)r\right).
\end{aligned}$$

At $\{r = 0\}$ lies the fixed point M which is the origin (x_3, y_3) plane. The fixed point M is a saddle for $K \leq 0$ and a source when $K > 0$. When $K > 0$ we have two additional saddle fixed points $\mathrm{S}^{\pm}$ that are located at

$$\begin{aligned}
\frac{r_{\mathrm{S}^{\pm}}}{1-r_{\mathrm{S}^{\pm}}} &= \left(\left(\frac{3\gamma_{\mathrm{pf}}}{4p}\right)^2 \frac{(2p+1)K}{\nu}\right)^{\frac{1}{2p+1}} \left[\left(\frac{(2p+1)K}{\nu}\right)^2 + 1\right]^{\frac{p}{2p+1}} \\
\theta_{\mathrm{S}^{\pm}} &= \arccos\left(\pm\left(1 + \left(\frac{(2p+1)K}{\nu}\right)^{-2}\right)^{-\frac{1}{2(2p+1)}}\right).
\end{aligned}$$

The points at the infinity in the (x_3, y_3) plane are now located at the $\{r = 1\}$ invariant set. The hyperbolic sinks $\mathrm{P}^{\pm}$ and the hyperbolic sources $\mathrm{Q}^{\pm}$ are given by

$$\theta_{\mathrm{P}^+} = 0, \qquad \theta_{\mathrm{P}^-} = \pi$$
$$\theta_{\mathrm{Q}^{\pm}} = \arccos\left(\pm\left(\frac{(2p+1)^2}{(2p+1)^2+4\nu^2}\right)^{\frac{1}{2(2p+1)}}\right).$$

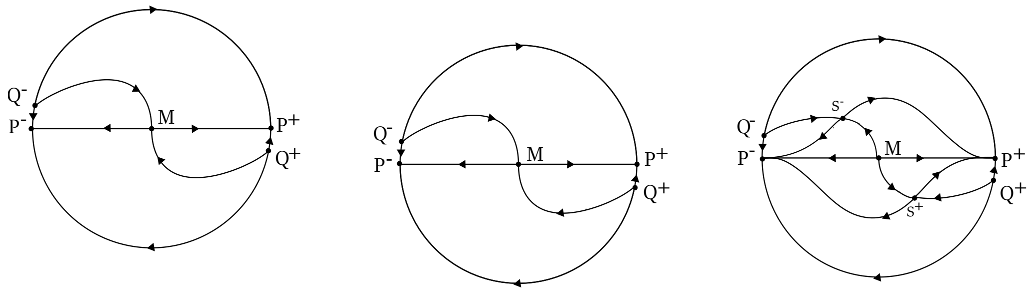

(A) Case $0 < \gamma_{\mathrm{pf}} < \frac{4p}{2p+1}$, i.e., $K \in (-\infty, 0)$.

(B) Case $\gamma_{\mathrm{pf}} = \frac{4p}{2p+1}$, i.e., $K = 0$.

(C) Case $\frac{4p}{2p+1} < \gamma_{\mathrm{pf}} < 2$, i.e., $K \in (0, \frac{1}{1+2p})$.

FIGURE 3.10: Poincaré-Lyapunov disk when $p < \frac{1}{2}(n-1)$ with $p > 0$.

Theorem 3.14. *Let $p < \frac{1}{2}(n-1)$ with $p > 0$. Then for all $\nu > 0$ the Poincaré-Lyapunov disk consists of heteroclinic orbits connecting the fixed points M, $P^{\pm}$, $Q^{\pm}$, and $S^{\pm}$ when they exist, with the separatrix skeleton as depicted in Figure 3.10.*

Proof. First notice that $\{y_3 = 0\}$ is an invariant subset consisting of heteroclinic orbits $\mathrm{M} \to \mathrm{P}^{\pm}$ which splits the phase-space into two invariant sets $\{y_3 > 0\}$ and $\{y_3 < 0\}$. On each of these invariant sets there are no fixed points when $K \leq 0$, and if $K > 0$ there is a single fixed point which is a saddle. Therefore by the index theorem (A.28) there are no periodic orbits on each of these regions. Since close saddle connections cannot exist either, by the Poincaré-Bendixson theorem (A.25), the ω and α-limit sets of all orbits in the Poincaré-Lyapunov disk are the fixed points M, $\mathrm{P}^{\pm}$, $\mathrm{Q}^{\pm}$ and $\mathrm{S}^{\pm}$ when they exist, the phase-space consisting of heteroclinic orbits connecting these fixed points. In particular whe $K \leq 0$ there are two separatrices $\mathrm{Q}^{\pm} \to M$ which further split the regions $y_3 > 0$, and $y_3 < 0$ into two invariant subsets, the flow on these subsets being trivial, and when $K > 0$ there are four separatrices $\mathrm{Q}^- \to \mathrm{S}^-$, $M \to \mathrm{S}^-$, and $\mathrm{Q}^+ \to \mathrm{S}^+$, $M \to \mathrm{S}^+$ which further splits the invariant regions $y_3 > 0$ and $y_3 < 0$ into four invariant subsets where the flow is also trivial.

□

Remark 3.15. *It is interesting to obtain the asymptotics for the orbits on the cylinder* **S** *towards* FL_1. *For example when $0 < \gamma_{\mathrm{pf}} < \frac{2n}{n+1}$, there exists a one parameter family of orbits* *in* $\mathbf{S}$ *with the following asymptotics towards* FL_1 *as* $\tau \to +\infty$

$$
\begin{aligned}
X(\tau) &= -\frac{2C_T C_\Sigma}{3(2-\gamma_{\rm pf})}\left(1+\frac{3\gamma_{\rm pf}}{2n}(n-2p)\tau\right)^{\frac{n+1}{(n-2p)\gamma_{\rm pf}}\left(\gamma_{\rm pf}-\frac{2n}{n+1}\right)} \\
\Sigma_\phi(\tau) &= C_\Sigma C_T\left(1+\frac{3\gamma_{\rm pf}}{2n}(n-2p)\tau\right)^{-\frac{n\gamma_{\rm pf}}{n-2p}(2-\gamma_{\rm pf})} \\
T(\tau) &= 1-\left(1+\frac{3\gamma_{\rm pf}}{2n}(n-2p)\tau\right)^{-\frac{1}{n-2p}}
\end{aligned}
$$

with $C_T > 0$, C_Σ *constants, which is obtained via the linearised solution at* M *restricted to the 2-dimensional unstable manifold when* $K<0$.

3.3.3.2 Case $p = \frac{1}{2}(n-1)$:

Positive z-direction

Consider now the case $p=\frac{1}{2}(n-1)$ with $p>0$, $n>1$ with n odd, i.e., $(p,n) = (1,3), (2,5), (3,7), etc.$. Setting $p=\frac{1}{2}(n-1)$ in (3.80) leads to

$$\frac{dx_3}{d\bar{\tau}_3} = \frac{1}{n-1}\left(1-\frac{u^{n-1}}{n}\right)(1+q)x_3 + (1-u_3^{n-1})y_3 \tag{3.125a}$$

$$\frac{dy_3}{d\bar{\tau}_3} = \frac{1}{n-1}(1+q)(1-u^{n-1})y_3 - (2-q+\nu(1-u_3^{n-1})x_3^{n-1})y_3 - n(1-u_3^{n-1})x_3^{2n-1} \tag{3.125b}$$

$$\frac{du_3}{d\bar{\tau}_3} = -\frac{1}{n(n-1)}(1+q)(1-u_3^{n-1})u_3 \tag{3.125c}$$

where

$$q = -1+\frac{3\gamma}{2}+\frac{3\gamma}{2}\left(\frac{(2-\gamma)}{\gamma}y_3^2 - x_3^{2n}\right)u_3^{2n}.$$

Since n is odd, the system is symmetric under the transformation $(x_3, y_3, u_3) \to (-x_3, -y_3, u_3)$, and all fixed points with $u_3 < 1$ lie on the invariant subset $\{u_3 = 0\}$ where the induced flow is given by

$$\frac{dx_3}{d\bar{\tau}_3} = \frac{3\gamma_{\rm pf}}{2(n-1)}x_3 + y_3 \quad , \quad \frac{dy_3}{d\bar{\tau}_3} = \frac{3\gamma_{\rm pf}}{2(n-1)}nKy_3 - nx_3^{2n-1} - \nu y_3 x_3^{n-1} \tag{3.126}$$

and where we introduced the notation

$$K = 1-\frac{2(n-1)}{n\gamma_{\rm pf}}, \tag{3.127}$$

Due to that $\gamma_{\rm pf} \in (0,2)$, it follows that $K \in (-\infty, \frac{1}{n})$.

Remark 3.16. *The system (3.126) can be transformed to Liénard type system (3.93), where now the functions $f(x)$ and $g(x)$ are given by*

$$f(x) = \nu x^{n-1} - \frac{3(1+nK)}{n(1-K)} \tag{3.128a}$$

$$g(x) = nx^{2n-1} - \frac{3\gamma_{\rm pf}}{2(n-1)}\nu x^n + \left(\frac{3\gamma_{\rm pf}}{2(n-1)}\right)^2 nKx. \tag{3.128b}$$

The fixed points of (3.126) are the real solutions to

$$-x_3\left(nx_3^{2(n-1)} - \frac{3\gamma_{\rm pf}}{2(n-1)}\nu x_3^{n-1} + \left(\frac{3\gamma_{\rm pf}}{2(n-1)}\right)^2 nK\right) = 0 \quad , \quad y_3 = -\frac{3\gamma_{\rm pf}}{2(n-1)}x_3 \tag{3.129}$$

The first equation admits at most five real solutions. The origin of coordinates is always a fixed point

$$\mathrm{M}: \quad x_3 = 0, \quad y_3 = 0. \tag{3.130}$$

and the linearised system at M has eigenvalues $\frac{3\gamma_{\rm pf}}{2n(n-1)}$, $\frac{3n\gamma_{\rm pf}}{2(n-1)}K$, and $-\frac{3\gamma_{\rm pf}}{2n(n-1)}$, with associated eigenvectors $(1,0,0)$, $(-\frac{2}{3(2-\gamma_{\rm pf})},1,0)$, and $(0,0,1)$. On $\{u_3=0\}$, and for all $\gamma_{\rm pf}\in(0,2)$ and $n>1$, M is a hyperbolic fixed point if and only if $K\neq 0$, being a saddle if $K<0$, $(0<\gamma_{\rm pf}<\frac{2(n-1)}{n})$, and a source if $K>0$, $(\frac{2(n-1)}{n}<\gamma_{\rm pf}<2)$. When $K=0$, $(\gamma_{\rm pf}=\frac{2(n-1)}{n})$, there is a bifurcation leading to a center manifold associated with a zero eigenvalue. To analyse the center manifold we introduce the adapted variables $\bar{y}_3 = y_3 - \frac{2}{3(2-\gamma_{\rm pf})}\bar{x}_3$. The center manifold can be locally represented as the graph $h: E^c \to E^u$, i.e. $\bar{x}_3 = h(\bar{y}_3)$, which solves the differential equation

$$\begin{aligned}&\frac{3\gamma_{\rm pf}}{2(n-1)}h(\bar{y}_3) + \frac{2}{3(2-\gamma_{\rm pf})}\left(h(\bar{y}_3) - \frac{2\bar{y}_3}{3(2-\gamma_{\rm pf})}\right)^{2n-1} + \frac{2}{2-\gamma_{\rm pf}}\left(1-\frac{2}{n}-\frac{2}{3}\left(h(\bar{y}_3)-\frac{2\bar{y}_3}{3(2-\gamma_{\rm pf})}\right)^{n-1}\right)\bar{y}_3\\ &= \left(\frac{3\gamma_{\rm pf}}{2(n-1)}K\bar{y}_3 - \nu\bar{y}_3\left(h(\bar{y}_3)-\frac{2\bar{y}_3}{3(2-\gamma_{\rm pf})}\right)^{n-1} - n\left(h(\bar{y}_3)-\frac{2\bar{y}_3}{3(2-\gamma_{\rm pf})}\right)^{2n-1}\right)\frac{dh}{d\bar{y}_3}\end{aligned} \tag{3.131a}$$

satisfying the fixed point $h(0)=0$ and tangency $\frac{dh(0)}{d\bar{y}_3}=0$ conditions. Approximating the solution by a formal truncated power series expansion and solving for the coefficients yields to the leading order on the center manifold

$$\frac{dy_3}{d\bar{\tau}_3} = -\nu\left(\frac{n}{3}\right)^{n-1} y_3^n\left(1-\frac{n}{\nu}\left(\frac{n}{3}\right)^n y_3^{n-1}\right), \quad y_3\to 0, \tag{3.132}$$

and therefore M is a center-saddle in this case. The remaining four fixed points that may or not exist depending on the parameters range are

$$\mathrm{S}^{\pm}_{\pm}: \quad x_3 = \pm\left(\frac{3\gamma_{\rm pf}A_\pm}{2(n-1)}\right)^{\frac{1}{n-1}} \qquad , \qquad y_3 = \mp\left(\frac{3\gamma_{\rm pf}}{2(n-1)}\right)^{\frac{n}{n-1}} A_\pm^{\frac{1}{n-1}} \tag{3.133}$$

where

$$A_\pm = \frac{\nu}{2n} \pm \sqrt{\left(\frac{\nu}{2n}\right)^2 - K}. \tag{3.134}$$

and the superscripts $\pm$ on the nomenclature of the fixed points stand for A_+ or A_- respectively, and the subscripts $\pm$ stand for the sign of the value of x_3 at the fixed point. The linearisation around the fixed points $\mathrm{S}^{\pm}_{\pm}$, yields the eigenvalues

$$\begin{aligned}
\lambda_{1\pm} &= \frac{3\gamma_{\rm pf}}{4(n-1)}\left[1 + nK - \nu A_\pm\right] + \sqrt{\frac{(1-K)^2(2-\gamma_{\rm pf})^2}{9}n^2 + (1-K)(2+\gamma_{\rm pf})nA_\pm + (4n - 8n^2 + \nu^2)A_\pm} \\
\lambda_{2\pm} &= \frac{3\gamma_{\rm pf}}{4(n-1)}\left[1 + nK - \nu A_\pm\right] - \sqrt{\frac{(1-K)^2(2-\gamma_{\rm pf})^2}{9}n^2 + (1-K)(2+\gamma_{\rm pf})nA_\pm + (4n - 8n^2 + \nu^2)A_\pm} \\
\lambda_3 &= -\frac{3\gamma_{\rm pf}}{2n(n-1)}
\end{aligned} \tag{3.135a}$$

with associated eigenvectors

$$v_1 = (a_1, 1, 0), \quad v_2 = (a_2, 1, 0), \quad v_3 = (0, 0, 1) \quad a_i = \frac{2\lambda_i - 3\gamma_{\rm pf}}{\left(\frac{3\gamma_{\rm pf}A_\pm}{2(n-1)}\right)\left(2n(2n-1)\left(\frac{3\gamma_{\rm pf}A_\pm}{2(n-1)}\right) + 3\gamma_{\rm pf}\nu\right)} \tag{3.136}$$

Just as the stability properties of the fixed point M, the sign of K plays a prominent role in the qualitative properties of the phase space. Hence we shall split the analysis into two subcases $K \leq 0$, and $K > 0$. Moreover it is helpful to introduce the quantity

$$\begin{aligned}
f_\pm(\gamma_{\rm pf}, n) = &\sqrt{n}\Bigg[(2n-1)(1-K)\frac{1 - nK\left(n\frac{10n-9}{2n-1} - \frac{\gamma_{\rm pf}(3n-1)^2}{2(n-1)}\right)}{1 + 4n(n-1)K} \pm \\
&\pm\sqrt{2n^2\gamma_{\rm pf}}(1-K)^2\frac{\left|-1 - nK\left(n + \frac{(n+1)}{2}\gamma_{\rm pf}\right)\right|}{1 + 4n(n-1)K}\Bigg]^{1/2}.
\end{aligned}$$

a) **SUBCASE** $K \leq 0$ $(0 < \gamma_{\rm pf} \leq \frac{2(n-1)}{n})$: In addition to M, and for all $\nu > 0$, only $\mathrm{S}^{+}_{\pm}$ exist. For $\mathrm{S}^{+}_{\pm}$, the pair of eigenvalues $\lambda_{1+}, \lambda_{2+}$ are real if $\nu \geq f_-(\gamma_{\rm pf}, n)$ and imaginary otherwise. Moreover, if $0 < \nu < (1+nK)\sqrt{n}$, then $\lambda_{1+}, \lambda_{2+}$ have positive real part, and if $\nu > (1+nK)\sqrt{n}$ then $\lambda_{1+}, \lambda_{2+}$ have negative real part. Finally, if if $\nu = (1+nK)\sqrt{n} > 0$ both eigenvalues are purely imaginary. Notice that the cases $\nu \leq (1+nK)\sqrt{n}$ only exists when $-\frac{1}{n} < K < 0$, i.e., $\frac{2(n-1)}{n+1} < \gamma_{\rm pf} < \frac{2(n-1)}{n}$ holds. Therefore on the $\{u_3 = 0\}$ invariant subset, $\mathrm{S}^{\pm}$ are an unstable (strong) focus if $\nu < (1+nK)\sqrt{n}$, a center or weak focus if $\nu = (1+nK)\sqrt{n}$, a stable strong focus if $(1+nK)\sqrt{n} < \nu < f_-(n, \gamma_{\text{pf}})$ and a stable node if $\nu \geq f_-(\gamma_{\text{pf}}, n)$.

The case $\nu = (1+nK)\sqrt{n}$ consists of a bifurcation where stability is changed, from an unstable focus to a stable focus leading to a center-focus problem, which will not be treated here, although numerical results indicate that they are centers.

As a final remark, note that when $K = 0$ the expression for the fixed points reduce to $x_3 = \pm\left(\frac{3\nu}{n^2}\right)^{\frac{1}{n-1}}$, $y_3 = \mp\left(\frac{\nu}{n}\right)^{\frac{1}{n-1}}\left(\frac{3}{n}\right)^{\frac{n}{n-1}}$, and $f_\pm$ is solely a function of n, given by $f_\pm(n) = \sqrt{n}\sqrt{2n-1\pm\sqrt{4n(n-1)}}$. Moreover for $\nu < \sqrt{n}$, the solution of Equation 3.132 describes globally the center manifold which consists of the two heteroclinic orbits $\mathrm{S}^+_\pm \to \mathrm{M}$.

b) **SUBCASE** $0 < K < 1/n$ $\left(\frac{2(n-1)}{n} < \gamma_{\text{pf}} < 2\right)$: In addition to M, there are fixed points only for $\nu \geq 2n\sqrt{K}$, while no additional fixed points exists for $0 < \nu < 2n\sqrt{K}$. When $\nu > 2n\sqrt{K}$ there are four fixed points $\mathrm{S}^\pm_\pm$, which merge into two fixed points $\mathrm{S}^0_\pm$ when $\nu = 2n\sqrt{K}$,

$$\mathrm{S}^0_\pm \;:\quad x_3 = \pm\left(\frac{3\gamma_{\text{pf}}K}{(n-1)}\right)^{\frac{1}{n-1}} \quad , \quad y_3 = \mp\left(\frac{3\gamma_{\text{pf}}K}{(n-1)}\right)^{\frac{1}{n-1}}. \tag{3.137}$$

For $\nu > 2n\sqrt{K}$, The eigenvalues λ_{1+} and λ_{2+} of the linearisation around $\mathrm{S}^+_\pm$ are real if $2n\sqrt{K} < \nu \leq f_+(n,K)$ or $\nu \geq f_-(n,K)$, and imaginary otherwise. Moreover if $2n\sqrt{K} < \nu < (1+nK)\sqrt{n}$, then $\lambda_{1+}, \lambda_{2+}$ have positive real part and if $\nu > (1+nK)\sqrt{n}$ then $\lambda_{1+}, \lambda_{2+}$ have negative real part. Finally if $\nu = (1+nK)\sqrt{n}$ both eigenvalues are purely imaginary. Therefore on $\{u_3 = 0\}$ the fixed points $\mathrm{S}^\pm_\pm$ are unstable nodes if $2n\sqrt{K} < \nu \leq f_+(n,K)$, an unstable focus if $f_+(n,K) < \nu < (1+nK)\sqrt{n}$, a center if $\nu = (1+nK)\sqrt{n}$ a stable focus if $(1+nK)\sqrt{n} < \nu < f_-(n,K)$ and a stable node if $\nu \geq f_-(n,K)$.

The eigenvalues λ_{1-} and λ_{2-} of the linearisation around $\mathrm{S}^-_\pm$ are real for all $\nu > 2n\sqrt{K}$. Moreover, $\lambda_{1\_}$ is negative and $\lambda_{2\_}$ is positive, so that $S^-_\pm$ are hyperbolic saddles.

When $\nu = 2n\sqrt{K}$, λ_1 and λ_2 are always complex. Moreover since $0 < K < 1/n$ the real part of the eigenvalues λ_1 and λ_2 is always positive, and the fixed points $\mathrm{S}^0_\pm$ are unstable strong focus.

3.3.3.3 Fixed points at infinity

Due to that when $p = \frac{1}{2}(n-1)$ the power of u in front of x and y in (3.74) is odd, it is enough to consider the blow up in positive direction. Setting $p = \frac{1}{2}(n-1)$, the flow induced on the

$\{u_1 = 0\}$ invariant subset is given by

$$\frac{dy_1}{d\bar{\tau}_1} = -n - \nu y_1 - n y_1^2 - 3 y_1 z_1 \quad , \quad \frac{dz_1}{d\bar{\tau}_1} = -(n-1)\left(\frac{3\gamma_{\rm pf}}{2(n-1)} z_1 + y_1\right) z_1 \tag{3.138}$$

We are interested in the invariant subset $\{z_1 = 0\}$ on $\{u_1 = 0\}$, where the system reduces further to

$$z_1 \frac{dy_1}{d\bar{\tau}_3} = -n - \nu y_1 - n y_1^2 \tag{3.139}$$

and yields two fixed points when $\nu > 2n$:

$$\mathrm{P}^{\pm} \quad : \quad y_1 = B_{\pm}, \quad z_1 = 0, \quad u_1 = 0 \tag{3.140}$$

where we introduced the notation

$$B_{\pm} = -\frac{\nu}{2n} \pm \sqrt{\left(\frac{\nu}{2n}\right)^2 - 1} < 0. \tag{3.141}$$

The linearised system at $\mathrm{P}^{\pm}$ has eigenvalues $\lambda_1 = -(n-1)B_{\pm}$, $\lambda_2 = \mp 2n\sqrt{\left(\frac{\nu}{2n}\right)^2 - 1}$, and $\lambda_3 = B_{\pm}$, with associated eigenvectors $v_1 = (1, a, 0)$, $v_2 = (0, 1, 0)$, and $v_3 = (0, 0, 1)$, where $a = -\frac{3}{n-1}\frac{B_{\pm} + \frac{\lambda_2}{2n}}{B_{\pm} + \lambda_2}$. Since P^{+} has $\lambda_2, \lambda_3 < 0$, and $\lambda_1 > 0$, and P_{-} has $\lambda_3 < 0$, and $\lambda_1, \lambda_2 > 0$, they are both hyperbolic saddles, but on $\{u_1 = 0\}$, P_{-} is a source and P^{+} is a saddle, in particular, a one-parameter set of orbits originate from P^{-}, and a single orbit from P^{+} into the region $\{z_1 > 0\}$. When $\nu = 2n$, the fixed points $\mathrm{P}_{\pm}$ merge into a single fixed point

$$\mathrm{P}^{0} \quad : \quad y_1 = -1, \quad z_1 = 0, \quad u_1 = 0 \tag{3.142}$$

where the eigenvalues reduce to $\lambda_1 = (n-1)$, $\lambda_2 = 0$, and $\lambda_3 = -1$. Hence the $z_1 = 0$ axis is the center manifold of P^0. Finally when $0 < \nu < 2n$ there are no fixed points on the $\{z_1 = 0\}$ axis.

Using the directional blow-up in the positive y-direction, the flow induced on $\{u_2 = 0\}$ is given by

$$\frac{dx_2}{d\bar{\tau}_2} = 1 + \frac{\nu}{n} x_2^n + x_2^{2n} + \frac{3}{2} x_2 z_2, \quad \frac{dz_2}{d\bar{\tau}_2} = \frac{(n-1)}{n}\left(n x_2^{2n-1} + \nu x_2^{n-1} + \frac{3n\gamma_{\rm pf}}{2(n-1)}\left(\frac{2}{n} - K\right) z_2\right) z_2. \tag{3.143}$$

Further restricting to the invariant subset $\{z_2 = 0\}$ results in

$$\frac{dx_2}{d\bar{\tau}_2} = 1 + \frac{\nu}{n} x_2^n + x_2^{2n}. \tag{3.144}$$

Since n is odd, there are two fixed points when $\nu > 2n$, corresponding to the fixed points $\mathrm{P}^{\pm}$ studied above and which in these coordinates are located at $(x_2, z_2, u_2) = \left(B_{\pm}^{1/n}, 0, 0\right)$, and which for $\nu = 2n$ merge into a single fixed point P^0. When $0 < \nu < 2n$ there are no fixed points on $\{z_2 = 0\} \cap \{u_2 = 0\}$. Therefore the equator of the Poincaré sphere has fixed points when $\nu \geq 2n$ on the second and fourth quadrants, which are α-limit points for orbits in the northern hemisphere. When $0 < \nu < 2n$ the equator consists of a periodic orbit. In order to study the stability of the periodic orbit at infinity in the (x_3, y_3) plane when $0 < \nu < 2n$ we shall employ a Poincaré-Lyapunov compactification on the unit disk.

The Poincaré-Lyapunov disk

When $p = \frac{1}{2}(n-1)$, using(3.86) on (3.90) leads to the regular system of equations

$$\frac{dr}{d\bar{\xi}} = (n-1)r(1-r)\left[-\frac{\nu}{n}r(1-\cos^{2n}\theta)\cos^{n-1}\theta + \frac{3}{n}(1-r)\left(\frac{n\gamma_{\mathrm{pf}}K}{2(n-1)} + \cos^{2n}\theta\right)\right] \quad (3.145a)$$

$$\frac{d\theta}{d\bar{\xi}} = -F(\theta)\left[\frac{3}{2n}F(\theta)\sin 2\theta(1-r) + \left(1 + \frac{\nu}{2n}\sin 2\theta F(\theta)\cos^{n-1}\theta\right)r\right]. \quad (3.145b)$$

At $\{r = 0\}$ lies the fixed point M which is the origin of the (x_3, y_3) plane. The previous analysis showed that M is a saddle if $K < 0$, a center saddle if $K = 0$, and a source if $K > 0$. The fixed points $\mathrm{S}^{\pm}_{\pm}$ are located at

$$\frac{r_{\mathrm{S}}}{1-r_{\mathrm{S}}} = \left(\frac{3\gamma_{\mathrm{pf}}A_{\pm}}{2(n-1)}\right)\left(1 + A_{\pm}^{-2}\right)^{\frac{n-1}{2n}}, \quad \theta_{\mathrm{S}} = \arccos\left(\pm\frac{1}{\left(1 + A_{\pm}^{-2}\right)^{\frac{1}{2n}}}\right) \quad (3.146)$$

while the points at infinity in the (x_3, y_3) plane are now located at $\{r = 1\}$. When $\nu > 2n$ there are two fixed points corresponding to $\mathrm{P}^{\pm}$:

$$\theta_{\mathrm{P}} = \arccos\left(\pm\left(\frac{\nu - \sqrt{\nu^2 - 4n^2}}{\nu\sqrt{2}}\right)^{\frac{1}{2n}}\right) \quad (3.147)$$

which merge into a single fixed point P^0 when $\nu = 2n$, with

$$\theta_0 = \arccos\left(-\left(\frac{1}{\sqrt{2}}\right)^{\frac{1}{n}}\right) \quad (3.148)$$

which we have seen to be α-limit points for interior orbits on the disk. Finally, when $\nu \in (0, 2n)$ there exists a periodic orbit Γ_∞:

$$\frac{d\theta}{d\xi} = -F(\theta)\left(1 + \frac{\nu}{2n}F(\theta)\cos^{n-1}\theta\sin 2\theta\right) < 0. \quad (3.149)$$

Lemma 3.17. *For all $0 < \nu < 2n$, with $n > 1$, n odd, Γ_∞ is an unstable limit cycle.*

Proof. To analyse the periodic orbit we introduce the variable $s = (1-r)/r$, so that the periodic orbit is now located at $s = 0$, and a new time variable ξ by $d/d\bar{\tau}_3 = (1-r)/rd/d\xi$, which leads to a regular system that close to $s = 0$,

$$\frac{ds}{d\theta} = S_1(\theta)s + S_2(\theta)s^2 + \cdots \tag{3.150}$$

where

$$S_1 = \frac{-\frac{\nu}{n}(n-1)F^2(\theta)\sin^2\theta\cos^{n-1}\theta}{F(\theta)\left(1+\frac{\nu}{2n}F(\theta)\cos^{n-1}\theta\sin 2\theta\right)}, \tag{3.151a}$$

$$S_2 = \frac{\frac{3}{2n}\left(2-(2-\gamma_{\mathrm{pf}})n+2(n-1)\cos^{2n}\theta\right) - \frac{3}{2n}F(\theta)\sin 2\theta\left(-\frac{\nu}{n}(n-1)F^2(\theta)\sin^2\theta\cos^{n-1}\theta\right)}{F(\theta)\left(1+\frac{\nu}{2n}F(\theta)\cos^{n-1}\theta\sin 2\theta\right)} \tag{3.151b}$$

Denoting by $s(\theta, s_0)$ the solution of the above differential equation such that $s(0, s_0) = s_0$, then close to $s = 0$ we have

$$S(\theta) = \beta_1(\theta)s_0 + \beta_2(\theta)s_0^2 + \cdots \tag{3.152}$$

where β_1 and β_2 solve the initial value problem

$$\frac{d\beta_1}{d\theta} = S_1(\theta)\beta_1(\theta), \qquad \beta_1(0) = 1, \tag{3.153a}$$

$$\frac{d\beta_2}{d\theta} = S_1(\theta)\beta_2(\theta) + S_2(\theta)\beta_1^2(\theta), \qquad \beta_2(0) = 0. \tag{3.153b}$$

The solutions are

$$\beta_1(\theta) = e^{\alpha(\theta)}, \qquad \beta_2(\theta) = -e^{\alpha(\theta)}\int_0^\theta e^{\alpha(\psi)}S_2(\psi)d\psi, \tag{3.154}$$

with

$$\alpha(\theta) = -\frac{\nu}{n}(n-1)\int_0^\theta \frac{F(\tilde{\theta})\sin^2\tilde{\theta}\cos^{n-1}\tilde{\theta}}{1+\frac{\nu}{2n}F(\tilde{\theta})\sin 2\tilde{\theta}\cos^{n-1}\tilde{\theta}}d\tilde{\theta} \tag{3.155}$$

The Poincaré return map near $s = 0$ is $P(s_0) = s(2\pi, s_0)$. Since $P(0) = 0$, and for n odd, $P'(0) = e^{\alpha(2\pi)} < 1$, and that θ is striclty monotonically decreasing, the periodic orbit Γ_∞ is an unstable limit cycle for all $0 < \nu < 2n$ and $n > 1$. □

Proposition 3.18. *Let $p = \frac{1}{2}(n-1)$ with $p > 0$ ($n > 1$ with n odd). Then the infinity is a repeller.*

Proof. The proof follows by the local analysis of the fixed points $\mathrm{P}^{\pm}$, P^0 and Lemma 3.17. □

Figure 3.11, shows the three different types of orbit structure at the boundary of the disk $\{r = 1\}$.

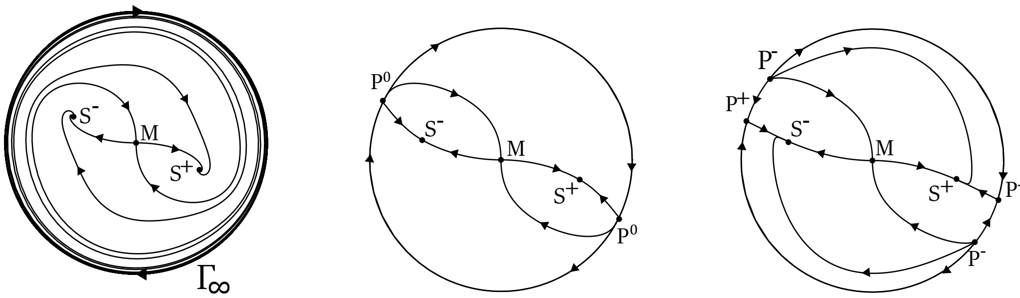

(A) $(p, n) = (1, 3)$, $\gamma_{\rm pf} = 1$ i.e. $K = -1/3$, and $\nu < 6$.

(B) $(p, n) = (1, 3)$, $\gamma_{\rm pf} = 1$ i.e. $K = -1/3$, and $\nu = 6$.

(C) $(p, n) = (1, 3)$, $\gamma_{\rm pf} = 1$ i.e. $K = -1/3$, and $\nu > 6$.

Figure 3.11: Poincaré-Lyapunov disk when $K \leq -\frac{1}{n}$, for $0 < \nu < 2n$, $\nu = 2n$, and $\nu > 2n$.

Theorem 3.19. *Let $p = \frac{1}{2}(n-1)$ with $p > 0$ ($n > 1$ with n odd). If $K \in (-\infty, -\frac{1}{n}]$, i.e., $\gamma_{\rm pf} \in (0, \frac{2(n-1)}{n+1})$, and $\nu > 0$, then the ω-limit set of all orbits on the Poincaré-Lyapunov disk is contained on the set $\mathrm{M} \cup \mathrm{S}^{+}_{\pm}$. In particular, as $\bar{\tau}_3 \to +\infty$ exactly 2 orbits converge to the fixed point M and a 1-parameter family of orbits converge to each fixed point $\mathrm{S}^{+}_{\pm}$, the separatrix skeleton being trivial.*

Proof. From Proposition 3.18 every regular orbits on the (x_3, y_3) plane remains bounded for all future times. The divergence of the vector field (3.126) yields

$$\frac{3\gamma_{\rm pf}}{2(n-1)}(1 + nK) - \nu x_3^{n-1}, \tag{3.156}$$

which for $K \leq -1/n$ and $\nu > 0$, does not change sign and vanishes at a set of measure zero, by the *the Bendixson-Dulac criteria* (see A.24) there are no periodic orbits. Moreover the origin M is a saddle, and $\mathrm{S}^{\pm}$ are sinks for all $\nu > 0$. Since closed saddle connections are not possible it follows by the Poincaré-Bendixson theorem (see A.25) that the only possible ω-limit sets in this case are the fixed points $\mathrm{S}^{+}_{\pm}$ and M. The last statement follows by the local stability properties of the fixed points. □

Besides the possible orbit structure on the invariant boundary $\{r = 1\}$, Figure 3.11, also shows the trivial separatrix skeleton on the Poincaré-Lyapunov disk for $K \in (-\infty, -\frac{1}{n})$ and $\nu > 0$.

Theorem 3.20. *Let $p = \frac{1}{2}(n-1)$ with $p > 0$ ($n > 1$ with n odd). If $K \in (0, \frac{1}{n})$ i.e., $\gamma_{\rm pf} \in (\frac{2(n-1)}{n}, 2)$, and $0 < \nu < 2n\sqrt{K}$, then, as $\tau_3 \to +\infty$, all orbits converge to a unique interior stable limit cycle $\Gamma_{\rm in}$.*

Proof. Here we make use of the equivalent system (3.97), and apply *Liénard's Theorem* (A.7.2), see e.g. [102]. The functions $g(\bar{x})$ and $F(\bar{x}) = \int_0^{\bar{x}} f(s)ds$ in (3.128), are odd functions

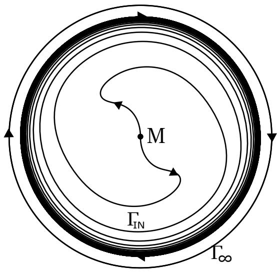

FIGURE 3.12: Poincaré-Lyapunov disk when $0 < K < \frac{1}{n}$, and $0 < \nu < \sqrt{2nK} < 2n$.

of $\bar{x}$, and if $\nu < 2n\sqrt{K}$, then $\bar{x}g(\bar{x}) > 0$ for $\bar{x} \neq 0$. Moreover, $F(0) = 0$, $F'(0) < 0$, $F(\bar{x})$ has unique positive zero at $\bar{x} = \left(\frac{n}{\nu}\frac{3\gamma_{\text{pf}}}{2(n-1)}(1+nK)\right)^{\frac{1}{n-1}}$, and for $\bar{x} \geq \left(\frac{n}{\nu}\frac{3\gamma_{pf}}{2(n-1)}(1+nK)\right)^{\frac{1}{n-51}}$, $F(\bar{x})$ is monotonically increasing to infinity as $\bar{x} \to +\infty$. Therefore the system has a unique stable limit cycle. Since in this case $\nu < 2n\sqrt{K}$, by Lemma 3.17 the infinity consists of an unstable limit cycle, and M is a hyperbolic source, the only possible ω-limit set is the unique interior stable limit cycle. $\square$

Remark 3.21. *In fact Liénards theorem also gives the relative location of the interior stable limit cycle.*

Figure 3.12 shows the Poincaré-Lyapunov disk for $K \in (0, \frac{1}{n})$ and $\nu < 2n\sqrt{K}$, where the orbits accumulate at the interior stable limit cycle Γ_{in}.

Remark 3.22. *We now briefly discuss what we have not proved. The cases $K \in (-\frac{1}{n}, 0]$ with $\nu < (1+nK)\sqrt{n}$, $\nu = (1+nK)\sqrt{n}$ or $\nu > (1+nK)\sqrt{n}$, and the cases $K \in (0, \frac{1}{n})$ with $\nu \geq 2n\sqrt{K}$, and $\nu < (1+nK)\sqrt{n}$, $\nu = (1+nK)\sqrt{n}$ or $\nu > (1+nK)\sqrt{n}$. Numerical results indicate that in the first case a unique stable interior limit cycle Γ_{in} exists if $\nu \leq (1+nK)\sqrt{n}$, with $\mathrm{S}_{\pm}^{+}$ sources when $\nu < (1+nK)\sqrt{n}$, and centers with an unstable outer periodic orbit when $\nu = (1+nK)\sqrt{n}$, while no interior limit cycle exists when $\nu > (1+nK)\sqrt{n}$, and $\mathrm{S}_{\pm}^{+}$ are sinks, see Figure 3.13, for representative examples. In the second sub-case for which $K \in (0, \frac{1}{n})$ with $\nu \geq 2n\sqrt{K}$, numerical results suggest that an interior stable limit cycle exists if $\nu \leq (1+nK)\sqrt{n}$, in which case $\mathrm{S}_{\pm}^{+}$ are sources for the strict inequality and centers if $\nu = (1+nK)\sqrt{n}$ with an unstable outer periodic orbit, while no interior periodic orbit exists when $\nu > (1+nK)\sqrt{n}$. Recall that when $K > 0$, the fixed point M are sources, and $\mathrm{S}_{\pm}^{-}$ are saddles when they exist, i.e., when $\nu > 2n\sqrt{K}$. If $\nu = 2n\sqrt{K}$, then $\mathrm{S}_{\pm}^{+}$ and $\mathrm{S}_{\pm}^{-}$ merge into the fixed points $\mathrm{S}_{\pm}^{0}$, which are unstable strong focus, see Figure 3.14, for some representative cases.*

Most of the results on existence of limit cycles for Liénard system rely on the strong assumption that $\bar{x}g(\bar{x}) > 0$ for $\dot{x} \neq 0$, i.e., that the fixed point at the origin is the only fixed point of the system, see e.g. [109] and references therein. Recent works on which such assumptions is relaxed are for e.g. [110] and references therein. In trying to apply Theorem 3.4 of [110] with $V(x,Y) = Y^2 + 2G(x) - YF(x)$ for which $H(x) = -2F(x)G'(x) + 4F'(x)G(x) = \frac{6(n-1)x^{n+1}}{n^2(n+1)(1-K)}\left((n(1+n)(1+nK) - \nu^2)x^{n-1} - 3\nu\right)$, which does not seem enough to prove the numerical results discussed on Remark 3.22.

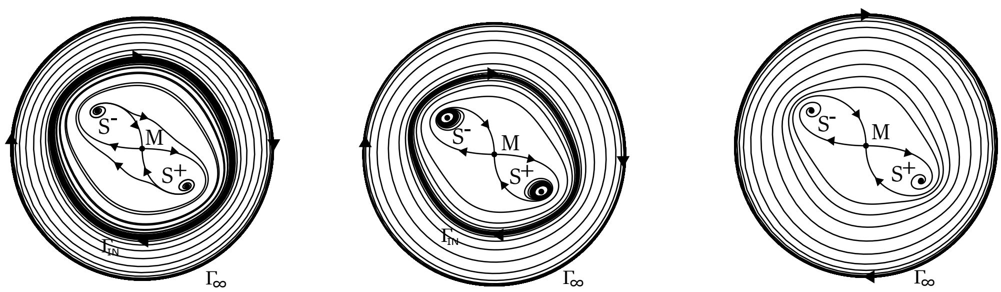

(A) $\nu < (1+nK)\sqrt{n}$.

(B) $\nu = (1+nK)\sqrt{n}$.

(C) $(1+nK)\sqrt{n} < \nu < f_-(\gamma_{\rm pf}, n)$.

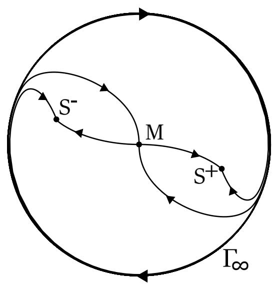

(D) $f_-(\gamma_{\rm pf}, n) \leq \nu < 2n$.

FIGURE 3.13: Poincaré-Lyapunov disk when $K \in (0, \frac{1}{n})$, exemplified with $n = 3$, and $\gamma_{\rm pf} = 5/4$, i.e. $K = -\frac{1}{15}$.

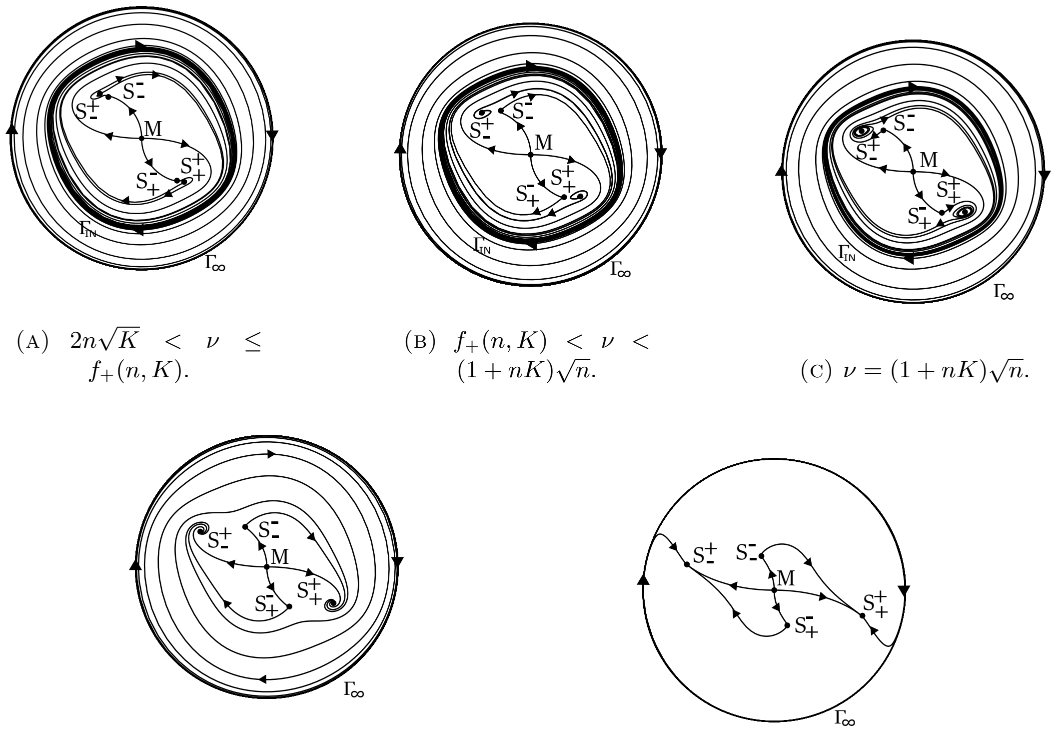

(A) $2n\sqrt{K} < \nu \leq f_+(n,K)$.

(B) $f_+(n,K) < \nu < (1+nK)\sqrt{n}$.

(C) $\nu = (1+nK)\sqrt{n}$.

(D) $(1+nK)\sqrt{n} < \nu < f_-(n,K)$.

(E) $\nu \geq f_-(n,K)$.

FIGURE 3.14: Poincaré-Lyapunov disk when $K \in (0, \frac{1}{n})$, exemplified with $n=3$ and $\gamma_{\rm pf} = 3/2$, i.e. $K = \frac{1}{9}$.

Remark 3.23. *It is interesting to obtain the asymptotics for the orbits on the cylinder* $\mathbf{S}$ *towards* FL_1*. For example when* $0 < \gamma_{\rm pf} < \frac{2n}{n+1}$*, there exists an one parameter family of orbits in* $\mathbf{S}$ *with the asymptotics towards* FL_1 *as in 3.124 with* $n - 2p = 1$*.*

3.4 Dynamical systems' analysis when $p = \frac{n}{2}$

By setting $p = \frac{n}{2}$ with n even, i.e., $(p,n) = (1,2),(2,4),(3,4),\ldots$, global dynamical system (3.25) becomes

$$\frac{dX}{d\tau} = \frac{1}{n}(1+q)(1-T)X + T\Sigma_\phi \tag{3.157a}$$
$$\frac{d\Sigma_\phi}{d\tau} = -(2-q)(1-T)\Sigma_\phi - nTX^{2n-1} - \nu(1-T)X^{2p}\Sigma_\phi \tag{3.157b}$$
$$\frac{dT}{d\tau} = \frac{1}{n}(1+q)T(1-T)^2 \tag{3.157c}$$

where the deceleration parameter q is given by (3.18). The auxiliary equation takes the form

$$\frac{d\Omega_\phi}{d\tau} = -3(1-T)\left[(\gamma_{\rm pf}-\gamma_\phi)\Omega_\phi(1-\Omega_\phi)+\frac{2}{3}\nu\sigma_\phi\Omega_\phi^{\frac{3}{2}}\right]. \tag{3.158}$$

where

$$\gamma_\phi = \frac{2\Sigma_\phi}{3\Omega_\phi}, \qquad \sigma_\phi = \frac{2\Sigma_\phi^2 X^n}{\Omega_\phi^{3/2}}. \tag{3.159}$$

3.4.1 Invariant boundary $T = 0$

The flow at $T = 0$ is given by

$$\frac{dX}{d\tau} = \frac{1}{n}(1+q)X \tag{3.160a}$$

$$\frac{d\Sigma_\phi}{d\tau} = -\Big[2-q+\nu X^{2p}\Big]\Sigma_\phi. \tag{3.160b}$$

From auxiliary equation for $\Omega_{\rm pf}$ we have that

$$\left.\frac{d\Omega_{\rm pf}}{d\tau}\right|_{\Omega_{\rm pf}=1} = 0, \qquad \left.\frac{d\Omega_{\rm pf}}{d\tau}\right|_{\Omega_{\rm pf}=0} = 2\nu X^{2p}\Sigma_\phi^2 \geq 0. \tag{3.161}$$

On the $T = 0$ invariant boundary, the system (3.157) admits five fixed points, one at the origin with $\Omega_{\rm pf} = 1$,

$$\mathrm{FL}_0: \quad X = 0 \quad , \quad \Sigma_\phi = 0, \qquad T = 0, \tag{3.162}$$

at which $q = \frac{1}{2}(3\gamma_{\rm pf}-2)$ corresponding to the flat Friedmann-Lemâitre solution. The linearisation around FL_0 yields the eigenvalues $\frac{3}{2n}$, $-\frac{3}{2}(2-\gamma_{\rm pf})$ and $\frac{3}{2n}$ with associated eigenvectors the canonical basis for $\mathbb{R}^3$. This fixed point as one negative real eigenvalue and two positive real eigenvalues, and is therefore a hyperbolic saddle, from which departs a 1-parameter family of orbits in $\mathbf{S}$. On $T = 0$ the subset $\Omega_{\rm pf} = 0$ ($X^{2n}+\Sigma_\phi^2 = 1$) is not invariant (except at $\Sigma_\phi = 0$ or $X = 0$), but it is future invariant since $\nu > 0$. On this subset there are four fixed points. The first two equivalent fixed points on the intersection of the invariant boundary $T = 0$ with the pure scalar field subset $\Omega_{\rm pf} = 0$ are given by

$$\mathrm{K}^\pm: \quad X = 0 \quad , \quad \Sigma_\phi = \pm 1, \qquad T = 0 \tag{3.163}$$

which correspond to a massless scalar field states or kinaton states, with $q = 2$. The linearisation around this fixed point yields to the eigenvalues $\frac{3}{n}$, $\frac{3}{n}$ and $3(2-\gamma_{\rm pf})$, with associated eigenvectors the canonical basis for $\mathbb{R}^3$. It follows that $\mathrm{K}^\pm$ are hyperbolic sources, so that a 2-parameter family of orbits in $\mathbf{S}$ originate from each $\mathrm{K}^{\pm}$. The other two equivalent fixed points are

$$\mathrm{dS}_0^{\pm}: \quad X = \pm 1 \quad , \quad \Sigma_\phi = 0, \qquad T = 0 \tag{3.164}$$

and correspond to a quasi-de-Sitter state with $q = -1$. The linearisation yields the eigenvalues $-3\gamma_{\mathrm{pf}}$, $-(3+\nu)$ and 0 with eigenvectors $(1,0,0)$, $(0,1,0)$ and $(0, \mp\frac{n}{3+\nu}, 1)$. These fixed points have two negative real eigenvalues and a null eigenvalue, possessing a 2-dimensional stable manifold contained in the boundary $T = 0$, and a 1-dimensional center manifold (the inflationary attractor solution). Just as in section 3.3.1, the monotonicity of T implies that $\mathrm{dS}_{\pm}$ are center-saddles with a unique orbit, the center manifold orbit, entering the state-space $\mathrm{dS}_0^{\pm}$. However, due its physical meaning, it is important to obtain approximations for the center manifold solution. In order to analyse the center manifold of $\mathrm{dS}_0^{\pm}$ we use instead system (3.15) for the unbounded variable $\tilde{T}$. To analyze the center manifold of the fixed points $(X, \Sigma_\phi, \tilde{T}) = (\pm 1, 0, 0)$ for $p = \frac{n}{2}$, we introduce adapted variables

$$\bar{X} = X \mp 1, \qquad \bar{\Sigma}_\phi = \Sigma_\phi \pm \frac{n}{3+\nu}\tilde{T}, \qquad \bar{T} = \tilde{T} \tag{3.165}$$

where the fixed points $\mathrm{dS}_0^{\pm}$ are now located at the origin of coordinates $(\bar{X}, \bar{\Sigma}_\phi, \tilde{T}) = (0,0,0)$. This leads to the system

$$\frac{d\bar{X}}{dN} = -3\gamma_{\mathrm{pf}}\bar{X} + F(\bar{X}, \bar{\Sigma}_\phi, \tilde{T}), \qquad \frac{d\bar{\Sigma}_\phi}{dN} = -(3+\nu)\bar{\Sigma}_\phi + G(\bar{X}, \bar{\Sigma}_\phi, \tilde{T}), \qquad \frac{d\tilde{T}}{dN} = N(\bar{X}, \bar{\Sigma}_\phi, \tilde{T}) \tag{3.166}$$

where F, G and N are functions of higher order terms. The 1-dimensional center manifold W^c at $\mathrm{dS}_0^{\pm}$ can be represented locally as the graph $h : E^c \to E^s$, i.e. $(\bar{X}, \bar{\Sigma}_\phi) = (h_1(\tilde{T}), h_2(\tilde{T}))$, satisfying the fixed point $h(0) = 0$ and the tangency $\frac{dh(0)}{d\tilde{T}} = 0$ conditions. Using this in the above equation and, using $\tilde{T}$ as an independent variable, we get

$$\frac{1}{n}(1+q)\Big(h_1'(\tilde{T})\tilde{T} - (h_1(\tilde{T}) \pm 1)\Big) - \tilde{T}\Big(h_2(\tilde{T}) \mp \frac{n}{3+\nu}\tilde{T}\Big) = 0, \tag{3.167a}$$

$$\begin{aligned}\frac{1}{n}(1+q)\tilde{T}\Big(h_2'(\tilde{T}) \mp \frac{n}{3+\nu}\Big) + (2-q)\Big(h_2(\tilde{T}) \mp \frac{n}{3+\nu}\Big) + \\ + \nu\Big(h_1(\tilde{T}) \pm 1\Big)^n\Big(h_2(\tilde{T}) \mp \frac{n}{3+\nu}\tilde{T}\Big) - \tilde{T}\Big(h_1(\tilde{T}) \pm 1\Big)^{2n-1} = 0.\end{aligned} \tag{3.167b}$$

Finding the attractor solution amounts to solve the above non-linear ordinary differential equation. We can however approximate the solution by performing a formal power series expansion

$$h_1(\tilde{T}) = \sum_{i=1}^{N} a_i \tilde{T}^i, \qquad h_2(\tilde{T}) = \sum_{i=1}^{N} b_i \tilde{T}^i, \tag{3.168}$$

Inserting (3.168) into (3.167) subject to the fixed point and tangency conditions, and solving the resulting linear system of equations for the coefficients results in

$$X = \pm 1 + \mp \frac{n}{6\gamma_{\rm pf}} \frac{3\gamma_{\rm pf} + 2\nu}{(3+\nu)^2} \tilde{T}^2 + \mathcal{O}(\tilde{T}3) \tag{3.169a}$$

$$\Sigma_\phi = \mp \frac{n}{3+\nu} \tilde{T} \left[1 - \frac{n^2}{6\gamma_{\rm pf}(3+\nu)^4} \left(\gamma_{\rm pf}\left(9 + (3-3n)\nu\right) - 2\nu\left(3 + \nu + n\nu - 2n(3+\nu)\right)\right) \tilde{T}^2 + \mathcal{O}(\tilde{T}^3) \right] \tag{3.169b}$$

$$\Omega_{\rm pf} = \frac{2n^2\nu}{3\gamma_{\rm pf}(3+\nu)^2} \tilde{T}^2 + \mathcal{O}(\tilde{T}^3). \tag{3.169c}$$

Therefore, it follows that to leading order on the center manifold

$$\frac{d\tilde{T}}{dN} = \frac{n}{3+\nu} \tilde{T}^3 + \mathcal{O}(\tilde{T})^4, \qquad \text{as} \quad \tilde{T} \to 0 \tag{3.170}$$

which shows explicitly that $\mathrm{dS}_0^\pm$ are center saddles with a unique class A center manifold orbit originating from each fixed point into the interior of $\mathbf{S}$.

We now show that on $T = 0$ the above fixed points are the only possible α-limit sets for class A orbits in $\mathbf{S}$, and that the orbit structure on $T = 0$ is very simple consisting only of heteroclinic orbits connecting these fixed points.

Lemma 3.24. *Let $n = \frac{p}{2}$. Then the $T = 0$ invariant boundary consists of heteroclinic orbits connecting the fixed points, and semi-orbits crossing the set $\Omega_{\rm pf} = 0$ and converging to $\mathrm{dS}_0^\pm$, as depicted in figure 3.15*

Proof. The proof is identical to the proof of Lemma 3.3, although in this case there are no conserved quantities, and the $\Omega_{\rm pf} = 0$ set is not invariant but future invariant. □

Theorem 3.25. *Let $p = \frac{n}{2}$. Then the α-limit set of class A orbits in $\mathbf{S}$, consists of fixed points on $T = 0$. In particular as $\tau \to -\infty$ a 2-parameter set of orbits converge to each $\mathrm{K}^\pm$, a 1-parameter set to FL_0, and a unique center manifold orbit converge to each $\mathrm{dS}_0^\pm$.*

Proof. The proof follows by lemmas, 3.2, 3.24, and the local analysis of the fixed points. □

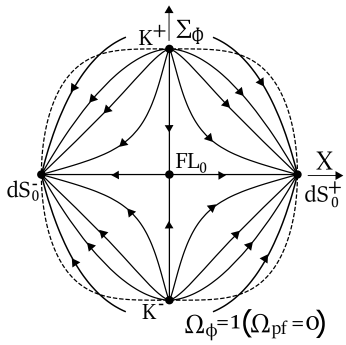

Figure 3.15: The invariant boundary $T = 0$ exemplified with $n = 2$ and $p = 1$.

3.4.2 Invariant Boundary $T = 1$

The induced flow in the boundary $T = 1$ is given by

$$\frac{dX}{d\tau} = \Sigma_\phi \tag{3.171a}$$
$$\frac{d\Sigma_\phi}{d\tau} = -nX^{2n-1} \tag{3.171b}$$

while the auxiliary equation for $\Omega_{\rm pf}$ is given by

$$\frac{d\Omega_{\rm pf}}{d\tau} = 0 \quad \Rightarrow \quad \Omega_{\rm pf} = 1 - (X^{2n} + \Sigma_\phi^2) = \text{const.} \tag{3.172}$$

Hence the $T = 1$ invariant boundary is foliated by periodic orbits characterized by $\Omega_{\rm pf} =$ const., where $\Omega_{\rm pf} = 1$ corresponds to the fixed point

$$\mathrm{FL}_1: \quad X = 0, \qquad \Sigma_\phi = 0, \qquad T = 1, \tag{3.173}$$

being a center, see Figure 3.16.

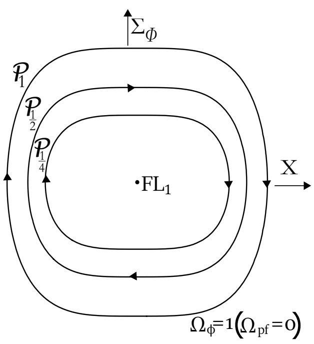

Figure 3.16: The invariant boundary $T = 1$ exemplified with $n = 2$ and $p = 1$.

Theorem 3.26. *Let* $p = \frac{n}{2}$*:*

(i) If $\gamma_{\rm pf} \leq \frac{2n}{n+1}$*, then all orbits in* $\mathbf{S}$ *converge for* $\tau \to +\infty$*, to the fixed point* FL_1 *with* $\Omega_{\rm pf} = 1$*;*

(ii) If $\gamma_{\rm pf} > \frac{2n}{n+1}$*, then all orbits in* $\mathbf{S}$ *converge for* $\tau \to +\infty$*, to an inner periodic orbit* $\mathcal{P}_{\Omega_{\rm pf}}$ *with* $0 < \Omega_{\rm pf} < 1$*.*

Proof. The proof is based on Lemma 3.2 together with generalised averaging techniques based on the methods introduced in [50, 68]. Standard averaging techniques and theorems can be found in [111] for the periodic case and [90] for the general case. In these theorems a key role is played by the perturbation parameter ϵ, (see A.8). In the present situation the role of ϵ-parameter is instead played by the function $\epsilon = 1 - T$. Therefore, we have to prove an averaging theorem for the case where ϵ is not a constant, but a variable that slowly goes to zero.

Each periodic orbit on $T = 1$ ($\epsilon = 0$) has an associated time period, $P(\Omega_\phi)$, so that for a given real function f, its average over time period associated with Ω_ϕ is given by

$$\langle f \rangle = \frac{1}{P(\Omega_\phi)} \int_{\tau_0}^{\tau_0 + P(\Omega_\phi)} f(\tau) d\tau. \tag{3.174}$$

In what follows we will need to compute several averaged quantities, such as $\langle \Sigma_\phi^2 \rangle$, or $\langle X^n \Sigma_\phi^2 \rangle$. We therefore use a differential formulation, which is more adapted to the problem at hand, by introducing new polar variables (r, θ) that solves the constraint equation $\Omega_\phi = \Sigma_\phi^2 + X^{2n}$, where Ω_ϕ can be seen as the square of the radial coordinate, i.e., $r = \sqrt{\Omega_\phi}$, and

$$(X, \Sigma_\phi) = (r^{\frac{1}{n}} \cos\theta, r G(\theta) \sin\theta), \qquad G(\theta) = \sqrt{\frac{1 - \cos^{2n}\theta}{1 - \cos^2\theta}} = \sqrt{\sum_{k=0}^{n-1} \cos^{2k}\theta}. \tag{3.175}$$

The resulting system of equation takes the form

$$\frac{dr}{d\tau} = \frac{3}{2}\epsilon \left[(\gamma_{\rm pf} - \gamma_\phi)(1 - r^2) - \nu\sigma_\phi r^2 \right] = \epsilon f(\omega, \tau, \epsilon) \tag{3.176a}$$

$$\frac{d\epsilon}{d\tau} = -\frac{1}{n}\epsilon^2 (1 - \epsilon)(1 + q) \tag{3.176b}$$

where

$$q + 1 = \frac{3}{2}(2r^2 G(\theta)^2 \sin^2\theta + \gamma_{\rm pf}(1 - r^2)), \tag{3.177}$$

and θ solves

$$\frac{d\theta}{d\tau} = -\frac{\epsilon}{2n}\left(3 + \nu r \cos^n\theta\right) G^2(\theta) \sin 2\theta + (1 - \epsilon) G(\theta) r^{\frac{n-1}{n}}. \tag{3.178}$$

On $T=1$, the average of a real function f over a time period associated with $\Omega_\phi=$ const., is then

$$\langle f\rangle = \frac{\Gamma[\frac{n+1}{2n}]}{4\sqrt{\pi}\Gamma[1+\frac{1}{2n}]}\int_0^{2\pi}\frac{f}{G(\theta)}d\theta \tag{3.179}$$

where $\Gamma[x]$ is the usual Γ-function. This yields

$$\langle X^{2n}\rangle = \frac{\Omega_\phi}{n+1}, \qquad \langle\Sigma_\phi^2\rangle = \frac{n\Omega_\phi}{n+1}, \qquad \langle\Sigma_\phi^2 X^n\rangle = \frac{\Gamma^2[\frac{1}{2}+\frac{1}{2n}]\Omega_\phi^{3/2}}{2(1+2n)\Gamma^2[1+\frac{1}{2n}]}. \tag{3.180}$$

Note that the above implies $\langle\Sigma_\phi^2\rangle = n\langle X^{2n}\rangle$, which is in accordance with the result in [68], obtained by averaging the dynamical system. In particular, it follows that the scalar field equation of state $\gamma_\phi = 2\Sigma_\phi^2/\Omega_\phi = 2G(\theta)^2\sin^2\theta$ has an average

$$\langle\gamma_\phi\rangle = \frac{2n}{n+1} \tag{3.181}$$

while for the interaction term $\sigma_\phi = 2\Sigma_\phi^2 X^n/(3\Omega_\phi^{3/2}) = 2/3G(\theta)^2\sin^2\theta\cos^n\theta$, we obtain

$$\langle\sigma_\phi\rangle = \frac{\Gamma^2[\frac{1}{2}+\frac{1}{2n}]}{3(1+2n)\Gamma^2[1+\frac{1}{2n}]}, \tag{3.182}$$

both independent of $r^2=\Omega_\phi$. The general idea of this averaging method is to start with the near identity transformation

$$r(\tau) = y(\tau) + \epsilon(\tau)g(y,\tau,\epsilon) \tag{3.183}$$

and then prove that the evolution of the variable y is approximated, at first order, by the solution $\bar{y}$ of the averaged equation. The evolution equation for y can be obtained using equations (3.176a) and (3.176b) alongside with the evolution equation for ω. This then gives

$$\begin{aligned}
\frac{dy}{d\tau} &= \left(1+\epsilon\frac{\partial g}{\partial y}\right)^{-1}\left[\frac{dr}{d\tau} - \left(g+\epsilon\frac{\partial g}{\partial\epsilon}\right)\frac{d\epsilon}{d\tau} - \epsilon\frac{\partial g}{\partial\tau}\right] \\
&= \left(1+\epsilon\frac{\partial g}{\partial y}\right)^{-1}\left[\frac{3}{2}\epsilon\Big((\gamma_{\rm pf}-\langle\gamma_\phi\rangle)y(1-y^2) + (\langle\gamma_\phi\rangle-\gamma_\phi)y(1-y^2) - \nu\langle\sigma_\phi\rangle y^2\right. \\
&+ \left.\nu(\langle\sigma_\phi\rangle-\sigma_\phi)y^2 - \frac{2}{3}\frac{\partial g}{\partial\tau}\Big)\right. \\
&+ \frac{3}{2}\epsilon^2 g\left((\gamma_{\rm pf}-\gamma_\phi)(1-3y^2) - 2\nu\sigma_\phi + \frac{2}{3n}(1-\epsilon)(1+q)\right) \\
&- \left.\frac{3}{2}\epsilon^3\left((\gamma_{\rm pf}-\gamma_\phi)(1-2y)g^2 - \nu\sigma_\phi g^2 + \frac{2}{3n}(1-\epsilon)(1+q)\frac{\partial g}{\partial\epsilon}\right)\right].
\end{aligned} \tag{3.184}$$

Setting

$$\begin{aligned}\frac{\partial g}{\partial \tau} &= f(y,\bar{\tau},\epsilon) - \langle f(y,.,0)\rangle \\ &= \frac{3}{2}\left(\langle\gamma_\phi\rangle - \gamma_\phi\right) y(1-y^2) + \frac{3}{2}\left(\langle\sigma_\phi\rangle - \sigma_\phi\right) y^2\end{aligned} \tag{3.185}$$

where the right-hand side is for large times almost periodic has an average that is zero that the variable g is bounded. Now using the fact that $\left(1+\epsilon\frac{\partial g}{\partial y}\right)^{-1} \approx 1-\epsilon\frac{\partial g}{\partial y} + \mathcal{O}(\epsilon^2)$ we get

$$\frac{dy}{d\tau} = \epsilon\langle f\rangle(y) + \epsilon^2 h(y,g,\tau,\epsilon) + \mathcal{O}(\epsilon^3) \tag{3.186}$$

where

$$\langle f\rangle(y) = \frac{3}{2}\Big((\gamma_{\rm pf} - \langle\gamma_\phi\rangle)y(1-y^2) - \nu\langle\gamma_\phi\rangle y^2\Big) \tag{3.187a}$$

$$\begin{aligned}h(y,g,,\tau,\epsilon) &= \frac{3}{2}\left((\gamma_{\rm pf}-\gamma_\phi)(1-3y^2)g - 2\nu\sigma_\phi + \frac{2(1+q)}{3n}\right) g \\ &- \frac{3}{2}\Big((\gamma_{\rm pf} - \langle\gamma_\phi\rangle)y(1-y^2) - \nu\langle\sigma_\phi\rangle y^2\Big)\frac{\partial g}{\partial y}.\end{aligned} \tag{3.187b}$$

Dropping the higher order terms in ϵ in (3.186), we study the truncated averaged equation coupled to an evolution equation for ϵ:

$$\frac{d\bar{y}}{d\tau} = \frac{3}{2}\epsilon\Big(\gamma_{\rm pf} - \langle\gamma_\phi\rangle\Big)\bar{y}(1-\bar{y}^2) - \frac{3}{2}\epsilon\nu\langle\sigma_\phi\rangle\bar{y}^2 \tag{3.188a}$$

$$\frac{d\epsilon}{d\tau} = -\frac{1}{n}\epsilon^2(1-\epsilon)(1+q). \tag{3.188b}$$

This system has a line of fixed points at $\epsilon = 0$ which can be removed by introducing a new time variable

$$\frac{1}{\epsilon}\frac{d}{d\tau} = \frac{d}{d\bar{\tau}}, \tag{3.189}$$

leading to

$$\frac{d\bar{y}}{d\tau} = \frac{3}{2}\Big(\gamma_{\rm pf} - \langle\gamma_\phi\rangle\Big)\bar{y}(1-\bar{y}^2) - \frac{3}{2}\nu\langle\sigma_\phi\rangle\bar{y}^2 \tag{3.190a}$$

$$\frac{d\epsilon}{d\bar{\tau}} = -\frac{1}{n}\epsilon(1-\epsilon)(1+q) \tag{3.190b}$$

which admits two fixed points on the $\epsilon = 0$ invariant subset. The first fixed point is given by

$$\mathrm{F}_1: \quad \bar{y} = 0, \quad \epsilon = 0, \tag{3.191}$$

whose linearisation yield the eigenvalues $3(\gamma_{\rm pf} - \langle\gamma_\phi\rangle)$ and $-3\gamma_{\rm pf}/2$, with associated eigenvectors the canonical basis of $\mathbb{R}^2$. When $\gamma_{\rm pf} > \langle\gamma_\phi\rangle$, F_1 is a saddle, and since $\langle\sigma_\phi\rangle \in (0,1)$ and

$\nu > 0$, there is a second fixed point

$$\mathrm{F}_2: \quad \bar{y} = \frac{1}{2}\left(-\frac{\nu\langle\sigma_\phi\rangle}{\gamma_{\mathrm{pf}} - \langle\gamma_\phi\rangle} + \sqrt{4 + \frac{\nu^2\langle\sigma_\phi\rangle^2}{(\gamma_{\mathrm{pf}} - \gamma_\phi)^2}}\right) \quad , \quad \epsilon = 0 \tag{3.192}$$

and whose linearisation yields the eigenvalues.

$$\begin{aligned} &-3(\gamma_{\mathrm{pf}} - \langle\gamma_\phi\rangle) + \frac{3}{4}\nu\langle\sigma_\phi\rangle\left(-\frac{\nu\langle\sigma_\phi\rangle}{\gamma_{\mathrm{pf}} - \gamma_\phi} + \sqrt{4 + \frac{\nu^2\langle\sigma_\phi^2\rangle}{(\gamma_{\mathrm{pf}} - \langle\gamma_\phi\rangle)^2}}\right), \\ &-\frac{3}{4n}\left(\nu\langle\sigma_\phi\rangle + 2\gamma_{\mathrm{pf}}\sqrt{4 + \frac{\nu^2\langle\sigma_\phi\rangle^2}{(\gamma_{\mathrm{pf}} - \gamma_\phi)^2}}(\langle\gamma_\phi\rangle - \gamma_{\mathrm{pf}})\right) \end{aligned}$$

with associated eigenvectors the canonical basis for $\mathbb{R}^2$. Hence F_2 is a hyperbolic sink. Notice that in the absence of interaction, i.e., $\nu = 0$ the fixed point F_2 reduces to $\bar{y} = 1$, $\epsilon = 0$ as in [68, 80]. When $\gamma_{\mathrm{pf}} = \langle\gamma_\phi\rangle$, F_2 merge into F_1, leading to center manifold as follows by the flow at $\epsilon = 0$ in this case, i.e. $d\bar{y}/d\bar{\tau} = -3/2\nu\langle\sigma_\phi\rangle\bar{y}^2$. Thus the solutions converge to F_1 tangentially to the $\epsilon = 0$ axis. When $\gamma_{\mathrm{pf}} < \langle\gamma_\phi\rangle$, F_1 is the only fixed point being a hyperbolic sink.

Next, we prove that the solutions y of the full averaged system (3.186), have the same limit as the solutions $\bar{y}$ of the truncated averaged equation when $\tau \to +\infty$, and hence also r and subsequently Ω_ϕ. For this we define sequences $\{\tau_n\}$ and $\{\epsilon_n\}$, with $n \in \mathbb{N}$, as follows

$$\tau_{n+1} - \tau_n = \frac{1}{\epsilon_n}, \quad \tau_0 = 0, \tag{3.194a}$$

$$\epsilon_{n+1} = \epsilon(\tau_{n+1}), \quad \epsilon_0 > 0 \tag{3.194b}$$

with $\lim \tau_n = +\infty$ and $\lim \epsilon_n = 0$, since $\epsilon(\tau) \to 0$ as $\tau \to +\infty$. Notice that for ϵ small enough y is monotone and bounded, and therefore has a limit as $\tau \to +\infty$. Then we estimate $|\eta(\tau)| = |y(\tau) - \bar{y}(\tau)|$ where y and $\bar{y}$ are solution trajectories with the same initial condition,

$$\begin{aligned}
|\eta(\tau)| &= \Bigg| \int_{\tau_n}^{\tau} \left(\frac{3}{2}\epsilon\Big(\gamma_{\rm pf} - \langle\gamma_\phi\rangle\Big) y\Big(1-y^2\Big) - \frac{3}{2}\epsilon\nu\langle\sigma_\phi\rangle y^2 + \epsilon^2 h(y,g,\tau,\epsilon)\right) ds \\
&- \int_{\tau_n}^{\tau} \left(\frac{3}{2}\epsilon\Big(\gamma_{\rm pf} - \langle\gamma_\phi\rangle\Big) \bar{y}\Big(1-\bar{y}^2\Big) - \frac{3}{2}\epsilon\nu\langle\sigma_\phi\rangle^2 \bar{y}^2 \right) ds \Bigg| \\
&\leq \epsilon_n \int_{\tau_n}^{\tau} \frac{3}{2} \underbrace{|\gamma_{\rm pf} - \langle\gamma_\phi\rangle|}_{|.|\leq C} |y-\bar{y}| \underbrace{|1-(y^2+\bar{y}^2+y\bar{y})|}_{|.|\leq 2} ds + \frac{3}{2}\epsilon_n\nu\langle\sigma_\phi\rangle^2 \int_{\tau_n}^{\tau} \underbrace{|1-(y+\bar{y})|}_{|.|\leq 1} |\bar{y}-y| ds \\
&+ \epsilon_n^2 \int_{\tau_n}^{\tau} \underbrace{|h(y,g,\tau,\epsilon)|}_{|.|\leq M} ds + \mathcal{O}(\epsilon_n^3) \\
&\leq 3C\epsilon_n \int_{\tau_n}^{\tau} |\eta(s)| ds + \frac{3}{2}\epsilon_n\nu\langle\sigma_\phi\rangle \int_{\tau_n}^{\tau} |\eta(s)| ds + \epsilon_n^2 M(\tau-\tau_n) + \mathcal{O}(\epsilon_n^3) \\
&= \epsilon_n \frac{3}{2}\Big(2C + \nu\langle\sigma_\phi\rangle\Big) \int_{\tau_n}^{\tau} |\eta(s)| ds + \epsilon_n^2 M(\tau-\tau_n) + \mathcal{O}(\epsilon_n^3), \qquad (3.195)
\end{aligned}$$

where C and M are positive constants. By Gronwall's inequality

$$|\eta(\tau)| \leq \frac{\epsilon_n M}{\frac{3}{2}\Big(2C + \nu\langle\sigma_\phi\rangle\Big)} \left(e^{\frac{3}{2}(2C+\nu\langle\sigma_\phi\rangle)(\tau-\tau_n)} - 1 \right) \qquad (3.196)$$

and using the fact that $\tau - \tau_n \in [0, 1/\epsilon_n]$, i.e., $\tau \in [\tau_n, \tau_{n+1}]$, it follows that

$$|\eta(\tau)| \leq K\epsilon_n, \qquad (3.197)$$

with K is a positive constant. Letting $n \to +\infty$ implies that $\eta \to 0$ as $\tau \to +\infty$. Therefore y and $\bar{y}$ have the same limit as $\tau \to +\infty$, i.e. the fixed point F_1 or F_2. Finally, from equation (3.183), using the triangle inequality and the fact that $\epsilon \to 0$ as $\tau \to +\infty$, it follows that r (and hence also Ω_ϕ) has the same limit as $\bar{y}$.

□

The above results are shown numerical in Figure 3.17, for some representative cases.

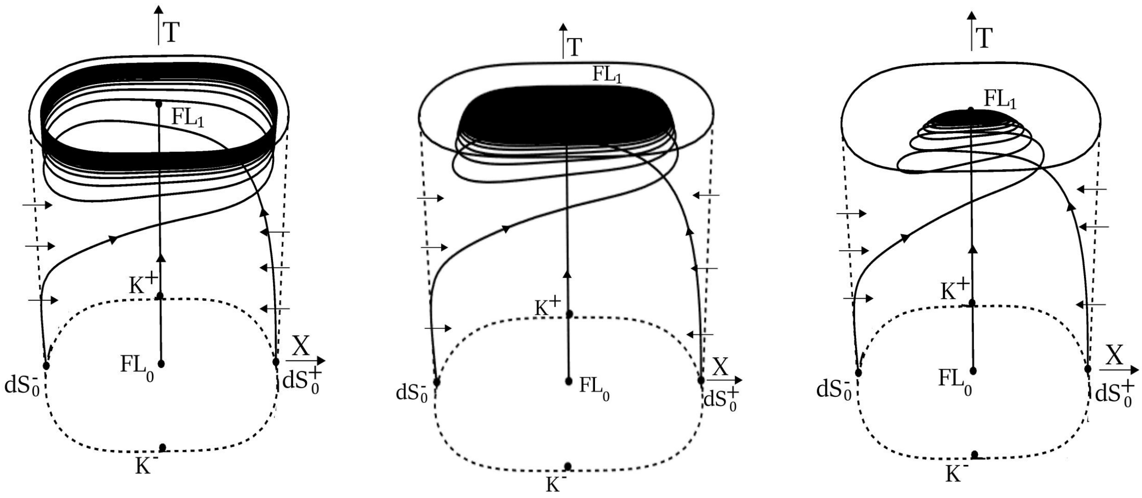

(A) $\gamma_{\rm pf} - \langle\gamma_\phi\rangle > 0$. (B) $\gamma_{\rm pf} - \langle\gamma_\phi\rangle = 0$. (C) $\gamma_{\rm pf} - \langle\gamma_\phi\rangle < 0$.

FIGURE 3.17: Qualitative global evolution of the dynamical system (3.157) for three different future asymptotic cases, exemplified with $n = 2$ and $\nu = 1$. Figure 3.17a has $\gamma_{\rm pf} = \frac{3}{2} > \frac{4}{3}$, Figure 3.17b has $\gamma_{\rm pf} = \frac{4}{3}$ and Figure 3.17c $\gamma_{\rm pf} = 1 < \frac{4}{3}$.

3.5 Dynamical systems' analysis when $p > \frac{n}{2}$

When $p > \frac{n}{2}$ the global dynamical system (3.25) reduces to

$$\frac{dX}{d\tau} = \frac{1}{n}(1+q)T^{2p-n}(1-T)X + T^{2p-n+1}\Sigma_\phi \tag{3.198a}$$

$$\frac{d\Sigma_\phi}{d\tau} = -(2-q)T^{2p-n}(1-T)\Sigma_\phi - nT^{2p-n+1}X^{2n-1} - \nu(1-T)^{2p-n+1}X^{2p}\Sigma_\phi \tag{3.198b}$$

$$\frac{dT}{d\tau} = \frac{1}{n}(1+q)T^{2p-n+1}(1-T)^2 \tag{3.198c}$$

where $q = -1 + 3\Sigma_\phi^2 + \frac{3}{2}\gamma_{\rm pf}\Omega_{\rm pf}$, and the auxiliary equation for $\Omega_{\rm pf}$ becomes

$$\frac{d\Omega_{\rm pf}}{d\tau} = 2(1 + q - \frac{3}{2}\gamma_{\rm pf})T^{2p-n}(1-T)\Omega_{\rm pf} + 2\nu(1-T)^{2p-n+1}X^{2p}\Sigma_\phi^2. \tag{3.199}$$

3.5.1 Invariant boundary $T = 0$

When $p > \frac{n}{2}$ with $n \in \mathbb{N}$, the induced flow on the $T = 0$ invariant boundary reduces to

$$\frac{dX}{d\tau} = 0, \qquad \frac{d\Sigma_\phi}{d\tau} = -\nu X^{2p}\Sigma_\phi \tag{3.200}$$

and $\Omega_{\rm pf} = 1 - \Sigma_\phi^2 - X^{2n}$, satisfies for $p > \frac{n}{2}$

$$\frac{d\Omega_{\rm pf}}{d\tau} = 2\nu X^{2p}\Sigma_\phi^2. \tag{3.201}$$

Thus, the subset $\Omega_{\rm pf}=0$ is not invariant but future invariant, except at $\Sigma_\phi=0$ or $X=0$, which are the points of intersection of the subset $\Omega_{\rm pf}=0$ with the lines of fixed points

$$\mathrm{L}_1: \quad X=X_0, \quad \Sigma_\phi=0, \quad T=0 \tag{3.202}$$

with $X_0\in[-1,1]$ and

$$\mathrm{L}_2: \quad X_0=0, \quad \Sigma_\phi=\Sigma_{\phi_0}, \quad T=0, \tag{3.203}$$

with $\Sigma_{\phi_0}\in[-1,1]$. We shall refer to the non-isolated fixed point at the origin of the $T=0$ invariant set as $\mathrm{FL}_0=\mathrm{L}_1\cap\mathrm{L}_2$. The end points of L_1 with $X=\pm1$ as $\mathrm{dS}_0^{\pm}$, and the end points of L_2 with $\Sigma_{\phi 0}=\pm1$ as $\mathrm{K}^{\pm}$. The description of the induced flow on $T=0$ is given by the following lemma:

Lemma 3.27. *When $p>\frac{n}{2}$, the set set $\{T=0\}\setminus\mathrm{L}_1\cup\mathrm{L}_2$ is foliated by invariant subsets $X=const.$ consisting of regular orbits which enter the region $\Omega_{\rm pf}>0$ by crossing the set $\Omega_{\rm pf}=0$ and converging to the line of fixed points L_1 as $\tau\to-\infty$. See Figure 3.18.*

Proof. When $p>n/2$ the system (3.200) admits the following conserved quantity

$$X=const. \tag{3.204}$$

which determine the solutions trajectories on $T=0$ invariant boundary. The remaining properties of the flow follows from the fact that on $\mathcal{U}$, $d\Sigma_\phi/d\tau<0$, and $d\Omega_{\rm pf}/d\tau<0$. $\square$

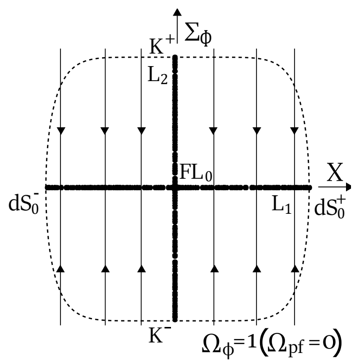

FIGURE 3.18: The invariant boundary $T=0$ exemplified with $n=2$ and $p=2$.

Theorem 3.28. *Let $p>\frac{n}{2}$. Then the α-limit set of all orbits in $\mathbf{S}$ is contained on the set $\mathrm{dS}_0^{\pm}\cup\mathrm{FL}_0\cup\mathrm{K}^{\pm}$. In particular, as $\tau\to-\infty$ a 2-parameter set of orbits converge to each fixed point $\mathrm{K}^{\pm}$, a 1-parameter set of FL_0, and a single orbit to each of the fixed points $\mathrm{dS}_0^{\pm}$.*

Proof. By Lemma 3.2, the α-limit set of all orbits in $\mathbf{S}$ is located $T=0$, the description of this boundary given in Lemma 3.27. The conclusions about the non-hyperbolic fixed point FL_0 and the line L_2 can be found in subsection 3.5.2 where we blow-up the point FL_0 and on top of that also the line L_2. For the line L_2, Lemma 3.29 says that the fixed points $\mathrm{K}^{\pm}$ are sources. We now analyse the line of fixed points L_1. The linearised system around L_1 has eigenvalues 0, $-\nu X_0^{2p}$ and 0, with associated eigenvectors $(1,0,0)$, $(0,1,0)$, and $(\frac{3(2p-n)}{2n}X_0(1-X_0^2)\delta_1^{2p-n},0,1)$. On the $\{T=0\}$ invariant boundary the line of fixed points L_1 is normally hyperbolic, i.e. the linearisation yields one negative eigenvalue for all $X_0\in[-1,1]$, except at $X_0=0$ where the two lines intersect, and one zero eigenvalue with eigenvector tangent to the line itself (similar to Sec.3.3.2.1). On $\bar{\mathbf{S}}$, the line L_1 is said to be *partially hyperbolic*. Each fixed point on the line, has a 1-dimensional stable manifold, and a 2-dimensional center manifold, while the point with $X_0=0$ is non-hyperbolic. In this case the blow up of FL_0 is done in Sec. 3.5.2. To analyse the 2-dimensional center manifold of each partially hyperbolic fixed point on the line we start by making the change of coordinates given by

$$\bar{X}=X-X_0+\frac{3(2p-n)\gamma_{\mathrm{pf}}}{2n}X_0(1-X_0^2)\bar{T}\delta_1^{2p-n},\qquad \bar{\Sigma}_\phi=\Sigma_\phi,\qquad \bar{T}=T \tag{3.205}$$

which takes a point in the line L_1 to the origin $(\bar{X},\bar{\Sigma}_\phi,\bar{T})=(0,0,0)$ with $\bar{T}\geq 0$. The resulting system of equations takes the form

$$\frac{d\bar{X}}{d\tau}=F(\bar{X},\bar{\Sigma}_\phi,\bar{T}),\qquad \frac{d\bar{\Sigma}_\phi}{d\tau}=-\nu X_0^{2p}\bar{\Sigma}_\phi+G(\bar{X},\bar{\Sigma}_\phi,\bar{T}),\qquad \frac{d\bar{T}}{d\tau}=N(\bar{X},\bar{\Sigma}_\phi,\bar{T}) \tag{3.206}$$

where F, G and N are functions of higher order. The center manifold reduction theorem yields that the above system is locally topological equivalent to a decoupled system on the 2-dimensional center manifold, which can be locally represented as the graph $h: E^c\to E^s$, i.e., $\bar{\Sigma}_\phi=h(\bar{X},\bar{T})$ which solves the nonlinear partial differential equation

$$F(\bar{X},h(\bar{X},\bar{T}),\bar{T})\partial_{\bar{X}}h(\bar{X},\bar{T})+N(\bar{X},h(\bar{X},\bar{T}),\bar{T})\partial_{\bar{T}}h(\bar{X},\bar{T})=-\nu X_0^{2p}h(\bar{X},\bar{T})+G(\bar{X},h(\bar{X},\bar{T}),\bar{T}) \tag{3.207}$$

subject to the fixed point and tangency conditions $h(0,0)=0$ and $\nabla h(0,0)=0$ respectively. A quick look at the nonlinear terms suggests that we approximate the center manifold at $(\bar{X}.\bar{T})=(0,0)$, by making a formal multi-power series expansion for h of the form $h(\bar{X},\bar{T})=\bar{T}^{2p-n+1}\sum_{i,j=0}^{N}\tilde{a}_{ij}\bar{X}^i\bar{T}^j$. Solving for the coefficients of expansion it is easy to verify that all coefficients of type $\tilde{a}_{i0}$ are identically zero, so that h can be written as a series expansion in $\bar{T}$ with coefficients depending on $\bar{X}$, i.e.,

$$h(\bar{X},\bar{T})=\bar{T}^{2p-n+1}\sum_{j=1}^{N}\bar{a}_j(\bar{X})\bar{T}^j,\qquad \bar{a}_j(X)=\sum_{i=0}^{N}a_{ij}\bar{X}^i \tag{3.208}$$

where for example

$$a_{01} = 0, \qquad a_{11} = 0 \qquad a_{02} = -\frac{n}{\nu}X_0^{2(p-n)-1} \qquad a_{12} = -\frac{n(2p+1)}{\nu}X_0^{2(p+1)}$$
$$a_{03} = \frac{1}{2\nu^2}\left(6n + 3(2p+1)\gamma_{\rm pf}\nu(1 - X_0^{2n})X_0^n\right)\delta_1^{n-2p}. \tag{3.209a}$$

After a change of time $d/d\tau = \bar{T}^{2p-n}d/d\bar{\tau}$, the flow on the 2-dimensional center manifold is given by

$$\frac{d\bar{X}}{d\bar{\tau}} = \sum_{j=1}^{N}\bar{b}_j(\bar{X})\bar{T}^j, \qquad \bar{b}_j(\bar{X}) = \sum_{i=0}^{N}b_{ij}\bar{X}^i \tag{3.210a}$$
$$\frac{d\bar{T}}{d\bar{\tau}} = \bar{T}\sum_{j=1}^{N}\bar{c}_j(X)\bar{T}^j \qquad \bar{c}_j(\bar{X}) = \sum_{i=0}^{N}c_{ij}\bar{X}^i \tag{3.210b}$$

with

$$b_{01} = \frac{3}{2}(1 - X_0^{2n})X_0$$
$$b_{11} = \frac{3\gamma_{\rm pf}}{2n}(1 - (1+2n)X_0^{2n})$$
$$b_{02} = -\frac{n}{\nu}X_0^{2(p-n)}$$
$$b_{21} = -\frac{3\gamma_{\rm pf}}{2}(2n+1)X_0^{2n}$$
$$b_{12} = -3\gamma_{\rm pf}X_0^{2n}$$
$$c_{01} = \frac{3\gamma_{\rm pf}}{2n}(1 - X_0^{2n}), \qquad c_{11} = 0$$
$$c_{02} = -\frac{9\gamma_{\rm pf}^2}{2n}X_0^{2n}(1 - X_0^{2n})\delta_1^{n-2p}, \qquad c_{12} = -3\gamma_{\rm pf}X_0^{2n}$$

b_{01} only vanishes for $X_0 = \pm 1$ or $X_0 = 0$ for any $p > n/2$, being negative for $X_0 \in (-1, 0)$, and positive for $X_0 \in (0, 1)$. In this case the origin $(0, 0)$ is a nilpotent singularity. Since the coefficient $c_{01}(\bar{X}) \neq 0$ for all X_0, then the normal formal form is zero with

$$\frac{d\bar{X}_*}{d\bar{\tau}_*} = \mathrm{sign}(b_{01})\bar{T}_*, \qquad \frac{d\bar{T}_*}{d\bar{\tau}_*} = \bar{T}_*^2\Phi(\bar{X}_*, \bar{T}_*) \tag{3.212}$$

and Φ an analytic function. The phase-space is the flow-box multiplied by the functional $\bar{T}_*$, with the direction of the flow given by the sign of b_{01}, see Figure 3.19a. When $X_0 = \pm 1$ we have that $b_{11} = -3\gamma_{\rm pf} < 0$, $c_{01} = 0$, $c_{02} = 0$ and $c_{12} < -3\gamma_{\rm pf}$ after changing the time variable to $d/d\tilde{\tau} = T^{-1} d/d\bar{\tau}$, then

$$\frac{d\bar{X}}{d\tilde{\tau}} = -3\gamma_{\rm pf}\bar{X} - \frac{n}{\nu}\bar{T} - \frac{3\gamma_{\rm pf}}{2}(2n+1)\bar{X}^2 - 3\gamma_{\rm pf}XT + \mathcal{O}\left(||(\bar{X},\bar{T})||^3\right) \tag{3.213a}$$

$$\frac{d\bar{T}}{d\tilde{\tau}} = -3\gamma_{\rm pf}\bar{X}\bar{T} + \mathcal{O}\left(||(\bar{X},\bar{T})||^3\right) \tag{3.213b}$$

and the origin is a semi-hyperbolic fixed point with eigenvalues $-3\gamma_{\rm pf}$, 0 and associated eigenvectors $(1,0)$ and $(-\frac{n}{3\gamma_{\rm pf}\nu},1)$. To analyse the 1-dimensional center manifold we introduce the adapted variable $\tilde{X} = \bar{X} + \frac{n}{3\gamma_{\rm pf}\nu}\bar{T}$. The 1-dimensional center manifold W^c at $(0,0)$can be locally represented as the graph $h: \quad E^c \to E^s$, i.e. $\tilde{X} = h(\bar{T})$, satisfying the fixed point $h(0) = 0$ and tangency $\frac{dh(0)}{d\bar{T}} = 0$ conditions, i.e. using $\bar{T}$ as an independent variable. Approximating the solution by a formal truncated power series expansion $h(\bar{T}) = \sum_{i=2}^{N} a_i \bar{T}^i$ and solving for the coefficients yields to leading order on the center manifold

$$\frac{d\bar{T}}{d\tilde{\tau}} = \frac{n}{\nu}\bar{T}^2 + \mathcal{O}(\bar{T}^3), \quad \text{as} \quad \bar{T} \to 0. \tag{3.214}$$

Therefore for $X_0 = \pm 1$, the origin is the α-limit set of 1-parameter set of orbits on the 2-dimensional center manifold, see Figure 3.19b. □

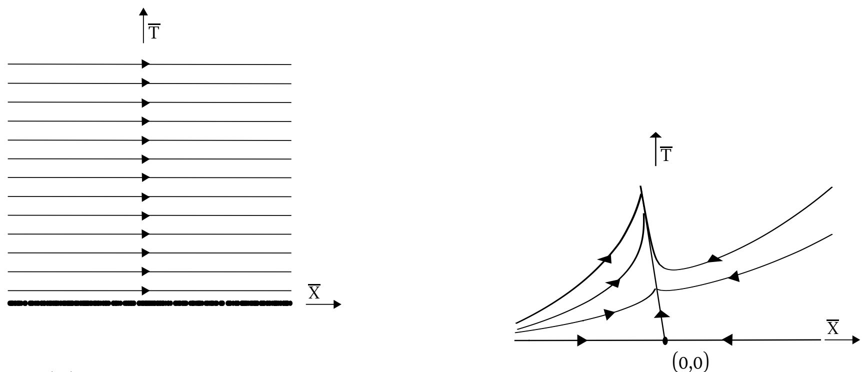

(A) $b_{01} > 0$. For $b_{01} < 0$ the direction of the flow is reversed.

(B) $X_0 = \pm 1$.

Figure 3.19: Flow on the 2-dimensional center manifold of each point on L_1.

3.5.2 Blow-up of FL_0

To analyse the non-hyperbolic fixed point FL_0 we use the unbounded dynamical system (3.15) for $p > \frac{n}{2}$ and this system reads

$$\frac{dX}{dN} = \frac{1}{n}(1+q)\tilde{T}^{2p-n}X + \tilde{T}^{2p-n+1}\Sigma_\phi \tag{3.215a}$$
$$\frac{d\Sigma_\phi}{dN} = -\left[(2-q)\tilde{T}^{2p-n} + \nu X^{2p}\right]\Sigma_\phi - n\tilde{T}^{2p-n+1}X^{2n-1} \tag{3.215b}$$
$$\frac{d\tilde{T}}{dN} = \frac{1}{n}(1+q)\tilde{T}^{2p-n+1} \tag{3.215c}$$

where recall

$$q = -1 + 3\Sigma_\phi^2 + \frac{3\gamma_{\rm pf}}{2}\left(1 - X^{2n} - \Sigma_\phi^2\right). \tag{3.216}$$

In order to understand the dynamics near the origin $(X, \Sigma_\phi, \bar{T}) = (0,0,0)$, which is a non-hyperbolic fixed point for $p > 0$ we employ the spherical blow-up method [102–104] (see A.7.3). This is, we transform the fixed point at the origin to the unit 2-sphere $\mathbb{S}^2 = \{(x,y,z) \in \mathbb{R}^3 : x^2+y^2+z^2 = 1\}$, and define the blow-up space manifold as $\mathcal{B} := \mathbb{S}^2 \times [0, u_0]$ for some fixed $0 < u_0 < 1$. We further define the quasi-homogeneous blow-up map

$$\Psi : \mathcal{B} \to \mathbb{R}^3, \qquad \Psi(x,y,z,u) = (u^{n-2p}x, u^n y, u^{2p}z) \tag{3.217}$$

which after canceling a common factor $u^{2p(n-2p)}$ (i.e. by changing time variable $d/d\tau = u^{2p(n-2p)}d/d\bar{\tau}$, where $p < \frac{n}{2}$, with $p > 0$) leads to a desingularisation of the non-hyperbolic fixed point on the blow-up locus $\{u = 0\}$.

We choose six charts κ_i such that

$$\psi_{1\pm} = (\pm u_{1\pm}^{2p-n}, u_{1\pm}^n y_{1\pm}, u_{1\pm}^{2p}z_{1\pm}) \tag{3.218a}$$
$$\psi_{2\pm} = (u_{2\pm}^{2p-n}x_{2\pm}, \pm u_{2\pm}^n, u_{2\pm}^{2p}z_{2\pm}) \tag{3.218b}$$
$$\psi_{3\pm} = (u_{3\pm}^{2p-n}x_{3\pm}, u_{3\pm}^n y_{3\pm}, \pm u_{3\pm}^{2p}) \tag{3.218c}$$

where $\psi_{1\pm}$, $\psi_{2\pm}$ and $\psi_{3\pm}$ are called the directional blows ups in the positive/negative x, y, and z-directions respectively. It is easy to check that the different charts are given explicitly by

$$\kappa_{1+}: \quad (u_{1+}, y_{1+}, z_{1+}) = (ux^{\frac{1}{2p-n}}, yx^{-n}, zx^{-2p}) \tag{3.219a}$$
$$\kappa_{2+}: \quad (x_{2+}, u_{2+}, z_{2+}) = (xy^{-\frac{2p-n}{n}}, uy^{\frac{1}{n}}, zy^{-\frac{2p}{n}}) \tag{3.219b}$$
$$\kappa_{3+}: \quad (x_{3+}, u_{3+}, z_{3+}) = (xz^{-\frac{2p-n}{2p}}, yz^{-\frac{n}{2p}}, uz^{\frac{1}{2p}}) \tag{3.219c}$$

Later transition maps $\kappa_{ij} = \kappa_j \circ \kappa_i^{-1}$ allows us to identify fixed points and special invariant manifolds on different charts, and to deduce all dynamics on the blow up space. In this case, we will need the following transition charts.

$$\kappa_{1+2+} \quad : \quad (x_{2+}, u_{2+}, z_{2+}) = (y_{1+}^{-\frac{2p-n}{n}}, u_{1+}y_{1+}^{\frac{1}{n}}, y_{1+}^{-\frac{2p}{n}} z_{1+}), \quad y_{1+} > 0; \tag{3.220a}$$

$$\kappa_{2+1+} \quad : \quad (u_{1+}, y_{1+}, z_{1+}) = (u_{2+}x_{2+}^{\frac{1}{2p-n}}, x_{2+}^{-n}, z_{2+}x_{2+}^{-2p}), \quad x_{2+} > 0; \tag{3.220b}$$

$$\kappa_{1+3+} \quad : \quad (x_{3+}, y_{3+}, u_{3+}) = (z_{1+}^{-\frac{2p-n}{2p}}, y_{1+}z_{1+}^{-\frac{n}{2p}}, u_{1+}z_{1+}^{\frac{1}{2p}}), \quad z_{1+} > 0; \tag{3.221a}$$

$$\kappa_{3+1+} \quad : \quad (u_{1+}, y_{1+}, z_{1+}) = (u_{3+}x_{3+}^{\frac{1}{2p-n}}, y_{3+}, y_{3+}x_{3+}^{-n}, x_{3+}^{-2p}), \quad x_{3+} > 0; \tag{3.221b}$$

$$\kappa_{2+3+} \quad : \quad (x_{3+}, y_{3+}, u_{3+}) = (x_{2+}z_{2+}^{-\frac{2p-n}{2p}}, z_{2+}^{-\frac{n}{2p}}, u_{2+}z_{2+}^{\frac{1}{2p}}), \quad z_{2+} > 0; \tag{3.222a}$$

$$\kappa_{3+2+} \quad : \quad (x_{2+}, u_{2+}, z_{2+}) = (x_{3+}y_{3+}^{-\frac{2p-n}{n}}, u_{3+}y_{3+}^{\frac{1}{n}}, y_{3+}^{-\frac{2p}{n}}), \quad y_{3+} > 0; \tag{3.222b}$$

Just as in the blow-up of FL_1 we are only interested in the region $\{z \geq 0\}$, i.e. the union of the upper hemisphere of the unit sphere $\mathbb{S}^2$ and the equator of the sphere $\{z = 0\}$ which constitutes an invariant boundary. This motivates that we start the analysis by using chart κ_{3+}, i.e., the directional blow-up map in the positive z-direction, on which the northern hemisphere is mapped into the $z = 1$, and the equator of the sphere is at infinity, which is better analysed using the charts κ_{1+} and κ_{2+}. Figure 3.20 shows the blow-up space of FL_0 when $p > \frac{n}{2}$. Later we shall also instead of projecting the upper-half og the unit 2-sphere on the $z = 1$ plane, to project it into the open unit disk $x^2 + y^2 < 1$ which can be joined with the equator (unite circle on $\{z = 0\}$), thus obtaining a global understanding of the flow on the Poincaré-Lyapunov disk.

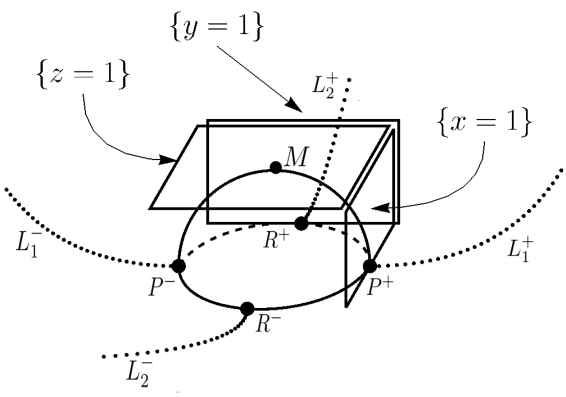

Figure 3.20: Blow-up space $\mathcal{B}$ for $p > n/2$.

3.5.2.1 Positive z-direction

We start with the positive z-direction $\{z = 1\}$ which after canceling a common factor $u_3^{2p(2p-n)}$ (i.e. by changing the time variable $d/d\tau = u_3^{2p(2p-n)} d/d\bar{\tau}_3$) leads to

$$\frac{dx_3}{d\bar{\tau}_3} = \frac{1}{2p}(1+q)x_3 + u_3^{2n} y_3 \tag{3.223a}$$

$$\frac{dy_3}{d\bar{\tau}} = -\left((2-q) + \frac{1+q}{2p} + \nu x_3^{2p}\right) y_3 - n u_3^{2n(2p-n)} x_3^{2n-1} \tag{3.223b}$$

$$\frac{du_3}{d\bar{\tau}_3} = \frac{1}{2np}(1+q)u_3 \tag{3.223c}$$

where

$$q = -1 + \frac{3\gamma_{\rm pf}}{2} + \frac{3\gamma_{\rm pf}}{2}\left(\frac{2-\gamma_{\rm pf}}{\gamma_{\rm pf}} y_3^2 u_3^{2n} - x_3^{2n} u_3^{2n(2p-n)}\right). \tag{3.224}$$

For all $u_3 < 1$ all fixed points are located at the invariant subset $\{u_3 = 0\}$. The low induced on $\{u_3 = 0\}$ is given by

$$\frac{dx_3}{d\bar{\tau}_3} = \frac{3\gamma_{\rm pf}}{4p} x_3 \qquad , \qquad \frac{dy_3}{d\bar{\tau}_3} = \left(\frac{3(2p-1)\gamma_{\rm pf}}{4p}\tilde{K} - \nu x_3^{2p}\right) y_3 \tag{3.225}$$

where

$$\tilde{K} = 1 - \frac{4p}{(2p-1)\gamma_{\rm pf}} < 0. \tag{3.226}$$

The system only presents one fixed point at the origin

$$\mathrm{M}: \quad x_3 = 0, \quad y_3 = 0 \tag{3.227}$$

and whose linearisation yields the eigenvalues $\lambda_1 = \frac{3\gamma_{\rm pf}}{4p}$, $\lambda_2 = \frac{3\gamma_{\rm pf}(2p-1)}{4p}\tilde{K}$, and $\lambda_3 = \frac{3\gamma_{\rm pf}}{4np}$, the associated eigenvectors are the canonical basis of $\mathbb{R}^3$. Hence on $\{u_3 = 0\}$, M is always a hyperbolic saddle.

3.5.2.2 Fixed points at infinity

To study the points at infinity, we notice that both directional blow-ups in the positive x and y direction already tell how such local chart must be given. To study the region where x_3 blows up, we use the chart

$$(y_1, z_1, u_1) = \left(\frac{y_3}{x_3^n}, \frac{1}{x_3^{2p}}, u_3 x_3^{\frac{1}{2p-n}}\right) \tag{3.228}$$

with change of time variable $d/d\bar{\tau}_1 = z_1 d/d\bar{\tau}_3$, i.e. $d/d\tau = u_1^{2p(2p-n)} d/d\bar{\tau}_1$, leads to the system of equations

$$\frac{dy_1}{d\bar{\tau}_1} = -\left(\left(2 - q + \frac{1+q}{2p-n}\right) z_1^{2p-n} - \nu\right) y_1 - \left(n u_2^{2n(2p-n+1)} - \frac{n^2}{2p-n} y_1^2\right) z_1^{2p-n+1} u_1^{2n} \tag{3.229a}$$

$$\frac{dz_1}{d\bar{\tau}_1} = -\frac{1+q}{2p-n} z_1^{2p-n+1} - \frac{2p}{2p-n} y_1 z_1^{2p-n+2} u_1^{2n} \tag{3.229b}$$

$$\frac{du_1}{d\bar{\tau}_1} = \frac{1}{2p-n}\left(\frac{1+q}{n} z_1^{2p-n} + y_1 z_1^{2p-n+1} u_1^{2n}\right) u_1, \tag{3.229c}$$

where

$$q = -1 + \frac{3\gamma_{\rm pf}}{2n}\left(1 + \frac{2-\gamma_{\rm pf}}{\gamma_{\rm pf}} u_1^{2n} y_1^2 - u_1^{2n(2p-n)}\right).$$

The flow on the invariant subset $\{u_1 = 0\}$ is given by

$$\frac{dy_1}{d\bar{\tau}_1} = -\left(\frac{3}{2}\left(2 - \gamma_{\rm pf} + \frac{\gamma_{\rm pf}}{2p-n}\right) z_1^{2p-n} + \nu\right) y_1, \quad \frac{dz_1}{d\bar{\tau}_1} = -\frac{3\gamma_{\rm pf}}{2(2p-n)} z_1^{2p-n+1} \tag{3.230}$$

and analyse the invariant set $\{z_1 = 0\}$ on $\{u_1 = 0\}$, which results

$$\frac{dy_1}{d\bar{\tau}_1} = -\nu y_1 \tag{3.231}$$

which has one fixed point

$$\mathrm{P}^+ \quad : \quad y_1 = 0, \quad z_1 = 0 \quad u_1 = 0 \tag{3.232}$$

whose linearisation yields to the eigenvalues $\lambda_1 = -\nu$, $\lambda_2 = 0$, and $\lambda_3 = 0$, with associated eigenvectors $v_1 = (1,0,0)$, $v_2 = (0,1,0)$, and $v_3 = (0,0,1)$. The zero eigenvalue in the u_1-direction is associated with a line of fixed points parameterized by constant values of $u_1 = u_0 \in (0,1)$, and which corresponds to the half of the line of fixed points L_1 with $X_0 < 0$. Thus on $u_1 = 0$ invariant set, the fixed point P^+ is semi-hyperbolic. The center manifold reduction theorem yields that the above system is locally topological equivalent to the 1-dimensional decoupled equation on the center manifold, which can be locally represented as the graph $h : E^c \to E^s$, i.e. $y_1 = h(z_1)$ which solves the nonlinear ordinary differential equation.

$$\frac{3\gamma_{\rm pf}}{2(2p-n)} z_1^{2p-n+1} \frac{dh}{dz_1} = \nu h(z_1) + \frac{3}{2}\left(2 - \gamma_{\rm pf} + \frac{\gamma_{\rm pf}}{2p-n}\right) h(z_1) z_1^{n-2p} \tag{3.233}$$

subject to the fixed point, $h(0) = 0$, and tangency, $\frac{dh}{dz_1}(0) = 0$, conditions. The above differential equation subject to the given initial conditions lead to an explicit solution

$$h(z_1) = C_z e^{\frac{(3(2p-n)(2-\gamma_{\rm pf})+2\gamma_{\rm pf})\log z_1 - 2\nu z_1^{n-2p}}{3\gamma_{\rm pf}}}. \tag{3.234}$$

The flow on the center manifold is, to leading order, given by

$$\frac{dz_1}{d\tau_1} = -\frac{3\gamma_{\rm pf}}{2(2p-n)} z^{2p-n+1} + \mathcal{O}(z_1^{2p-n+3}) \tag{3.235}$$

and therefore it is a stable center manifold.

To study the region where y_3 blows up, we use the chart

$$(x_2, z_2, u_2) = \left(\frac{x_3}{y_3^{\frac{2p-n}{n}}}, \frac{1}{y_3^{-\frac{2p}{n}}}, u_3 y_3^{\frac{1}{n}}\right) \tag{3.236}$$

and changing the time variable $d/\bar{\tau}_2 = z_2 d/d\bar{\tau}_3$ i.e. $d/d\tau = u_2^{2p(2p-n)} d/\bar{\tau}_2$ we get

$$\frac{dx_2}{d\bar{\tau}_2} = \frac{1}{n}\left((1+q) + (2-q)(2p-n)\right) x_2 z_2^{2p-n} + \left(1 + (2p-n) u_2^{2n(2p-n-1)} x_2^{2n}\right) z_2^{2p-n+1} + \nu \frac{2p-n}{n} x_2^{2p+1} \tag{3.237a}$$

$$\frac{dz_2}{d\bar{\tau}_2} = \left(2p u_2^{2n(2p-n)} x_2^{2n-1} z_2^{2p-n+1} + \frac{1}{n}\left(1 + q + 2p(2-q)\right) z_2^{2p-n} + 2p\nu x_2^{2p}\right) z_2 \tag{3.237b}$$

$$\frac{du_2}{d\bar{\tau}} = -\frac{1}{n}\left((2-q) z_2^{2p-n} + n u_2^{2n(2p-n)} x_2^{2n-1} z_2^{2p-n+1} + \nu x_2^{2p}\right) u, \tag{3.237c}$$

where

$$q = -1 + \frac{3\gamma_{\rm pf}}{2}\left(1 + \frac{2-\gamma_{\rm pf}}{\gamma_{\rm pf}} u_2^{2n} - x_2^{2n} u_2^{2n(2p-n)}\right).$$

The induced flow on the invariant subset $\{u_2 = 0\}$ is given by

$$\frac{dx_2}{d\bar{\tau}_2} = \left(z_2 + \frac{3\gamma_{\rm pf}}{2n} x_2\right) z_2^{2p-n} + \frac{2p-n}{n}\left(\frac{3}{2}(2-\gamma_{\rm pf}) z_2^{2p-n} + \nu x_2^{2p}\right) \tag{3.238a}$$

$$\frac{dz_2}{d\bar{\tau}_2} = \frac{3\gamma_{\rm pf}}{2n} z_2^{2p-n+1} + \frac{2p}{n}\left(\frac{3}{2}(2-\gamma_{\rm pf}) z_2^{n-2p} + \nu x_2^{2p}\right) z_2 \tag{3.238b}$$

and analyse the invariant set $\{z_2 = 0\}$ on $\{u_2 = 0\}$ which results

$$\frac{dx_2}{d\bar{\tau}_1} = \nu \frac{2p-n}{n} x_2^{2p} \tag{3.239}$$

which admits one fixed point

$$\mathrm{R}^+ : \quad x_2 = 0, \quad z_2 = 0 \tag{3.240}$$

and whose linearised system has all eigenvalues zero. The zero eigenvalue in the u_2 direction is due to the line of fixed points L_2^+. The zero eigenvalue in the u_2 direction is due to the line of fixed points L_2^+. To blow-up $\mathrm{R}^{\pm}$ or better the complete line L_2^+ we will perform a cylindrical blow-up. We will transform each point on the line to a circle $\mathbb{S}^1 = \{(v,w) \in \mathbf{R}^2 : v^2+w^2 = 1\}$. The blow-up space is $\bar{\mathcal{B}} = \mathbb{S}^1 \times [0, u_{20}) \times [0, s_0)$ and define the quasi-homogeneous blow-up map

$$\bar{\Psi} : \bar{\mathcal{B}} \to \mathbb{R}^3, \quad \bar{\Psi}(v,w,u_2,s) = (s^{2p-n}v, s^{2p}w, u_2)$$

We choose four charts such that

$$\bar{\psi}_{1\pm} = \left(\pm s_{1\pm}^{2p-n}, s_{1\pm}^{2p} w_{1\pm}, u_2\right) \tag{3.241a}$$

$$\bar{\psi}_{2\pm} = \left(s_{2\pm}^{2p-n} \bar{v}_{2\pm}, \pm s_{2\pm}^{2p}, u_2\right). \tag{3.241b}$$

We start with the v_1-direction $\{v_1 = \pm 1\}$ which after canceling the common factor $s_{1\pm}^{2p(2p-n)}$ (i.e by changing the time variable $d/d\bar{\tau}_2 = s_{1\pm}^{2p(2p-n)} d/d\bar{\tau}_{1\pm}$) leads to

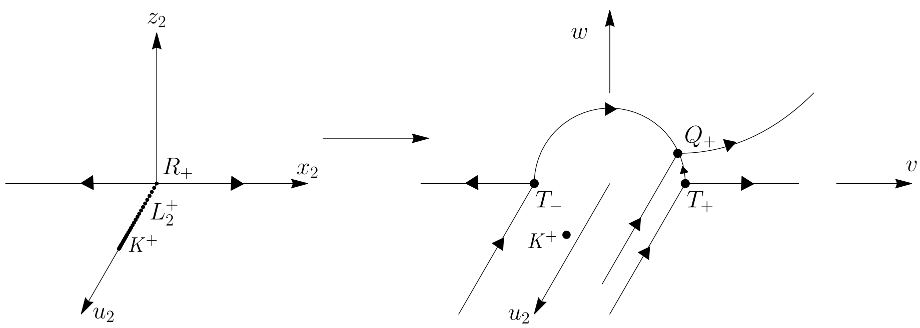

FIGURE 3.21: Blow-up of the non-hyperbolic line of fixed points L_2 for $p > n/2$.

$$\frac{dw_{1\pm}}{d\tilde{\tau}_{1\pm}} = -\frac{1+q}{2p-n} w_{1\pm}^{2p-n+1} + \frac{2p(n-1)\nu}{n} w_{1\pm} \tag{3.242a}$$
$$\mp \frac{2p}{2p-n}\left(1 + (2p-n)s_{1\pm}^{2n(2p-n)} u_2^{2n(2p-n-1)}(1-u_2^{2n})\right) w_{1\pm}^{2p-n+2} s_{1\pm}^{2n}$$

$$\frac{ds_{1\pm}}{d\tilde{\tau}_{1\pm}} = \frac{s_{1\pm}}{n(2p-n)}\Bigg(\left(1+q+(2p-n)(2-q)\right) w_{1\pm}^{2p-n} \tag{3.242b}$$
$$\pm \left(1 + (2p-n)s_{1\pm}^{2n(2p-n)} \bar{u}^{2n(2p-n-1)}\right) w_{1\pm}^{2p-n+1} + \nu(2p-n)\Bigg)$$

$$\frac{du_2}{d\tilde{\tau}_{1\pm}} = -\frac{1}{n}\left((2-q)w_{1\pm}^{2p-n} \pm n s_{1\pm}^{2p(2p-n)+1} u_2^{2n(2p-n)} w_{1\pm}^{2p-n+1} + \nu\right) u_2 \tag{3.242c}$$

where

$$q = -1 + \frac{3\gamma_{\mathrm{pf}}}{2}\left(1 + \frac{2-\gamma_{\mathrm{pf}}}{\gamma_{\mathrm{pf}}} u_2^{2n} - u_2^{2n(2p-n)} s_{1\pm}^{2n(2p-n)}\right). \tag{3.243}$$

The above system has the fixed points

$$\mathrm{T}^{\pm}: \quad w_{1\pm}=0, \quad s_{1\pm}=0 \quad u_2=0, \tag{3.244}$$

whose linearisation gives the eigenvalues $\frac{2p(n-1)\nu}{n}$, $\frac{\nu}{n}$, and $-\frac{\nu}{n}$, where the associated eigenvectors are the canonical basis of $\mathbb{R}^3$. Hence $\mathrm{T}^{\pm}$ are saddles. Moreover in the $\{u_2=0\}$ subset is a hyperbolic source. The other fixed point is

$$\mathrm{Q}^{\pm}: \quad w_{1\pm}=\pm\left(\frac{4(n-1)(2p-n)p\nu}{3\gamma_{\mathrm{pf}}n}\right)^{\frac{1}{2p-n}}, \quad s_{1\pm}=0, \quad u_2=0 \tag{3.245}$$

where only Q^{+} exists in the region $w_{1\pm}>0$. The eigenvalues of the linearised system around $\mathrm{Q}^{\pm}$ are $-\frac{2p(2p-n)(n-1)\nu}{n}$, $\frac{2p(n-1)((2p-n)(2-\gamma_{\mathrm{pf}})+\gamma_{\mathrm{pf}})\nu}{n^2\gamma_{\mathrm{pf}}}+\frac{\nu}{n}$, and $-\frac{2(n-1)(2p-n)(2-\gamma_{\mathrm{pf}})\nu}{n^2\gamma_{\mathrm{pf}}}-\frac{\nu}{n}$ where the associated eigenvectors are the canonical basis of $\mathbb{R}^3$. In the $\{u_2=0\}$ subset Q^{+} is a hyperbolic saddle, while when $n=1$, it merges with T^{+} leading to a center manifold. The center manifold reduction theorem yields that the above system is locally topological equivalent to the 1-dimensional decoupled equation on the center manifold, which can be locally represented as graph $h: E^c\rightarrow E^s$, i.e. $s_1=h(w_1)$ wich solves the nonlinear differential equation

$$\frac{4-3\gamma_{\mathrm{pf}}+4pw_1h(w_1)^2}{2p(2p-1)}=\left(\nu-\frac{3(1-\gamma_{\mathrm{pf}})-3p(2-\gamma_{\mathrm{pf}})+w_1}{2p-1}\right)h(w_1)\frac{dh}{dw_1} \tag{3.246}$$

subject to the fixed point, $h(0)$, and tangency, $\frac{dh}{dw_1}(0)=0$, conditions. In general it is not possible to solve for h explicitly. However we can approximate the solutions by making a formal power series expansion for $h(w_1)$ and solving for the coefficients gives as $w_1\rightarrow 0$, which yields on the center manifold

$$\frac{dw_{1\pm}}{d\tilde{\tau}_{1\pm}}=-\frac{3\gamma_{\mathrm{pf}}}{2(2p-1)}w_{1\pm}^{2p} \tag{3.247}$$

showing that it is a stable center manifold.

In the w-direction and after canceling the common factor $s_{2\pm}^{2p(2p-n)}$ (i.e. by changing the time variable $d/d\bar{\tau}_2=s_{2\pm}^{2p(2p-n)}d/d\tilde{\tau}_{2+}$) leads to the system

$$\frac{dv_{2\pm}}{d\tilde{\tau}_{2+}}=\frac{1+q}{2p}v_{2\pm}-\frac{(2p-n)(n-1)}{n}v_{2\pm}^{2p+1}\nu+\left(1+(2p-n)s_{2\pm}^{2n(2p-n)}u_2^{2n(2p-n-1)}(1-u_2^{2n})v_{2\pm}^{2n}\right)s_{2\pm}^{n} \tag{3.248a}$$

$$\frac{ds_{2\pm}}{d\tilde{\tau}_{2+}}=\frac{1}{2pn}\left((1+q+2p(2-q))+2pns_{2\pm}^{n(2(2p-n)+1)}v_{2\pm}^{2n-1}+2pn\nu v_{2\pm}^{2p}\right)s_{2\pm} \tag{3.248b}$$

$$\frac{du_2}{d\tilde{\tau}_{2+}}=-\frac{1}{n}\left((2-q)+ns_{2\pm}^{n(2(2p-n)+1)}u_2^{2n(2p-n)}v_{2\pm}^{2n-1}+\nu v_{2\pm}^{2p}\right)u_2 \tag{3.248c}$$

where

$$q = -1 + \frac{3\gamma_{\rm pf}}{2}\left(1 + \frac{2-\gamma_{\rm pf}}{\gamma_{\rm pf}} u_2^{2n} - s_{2\pm}^{2n(2p-n)} u_2^{2n(2p-n)} v_{2\pm}^{2n}\right) \tag{3.249}$$

The above system has the fixed points

$$\mathrm{T}^{\pm}: \quad v_{2\pm} = 0, \quad s_{2\pm} = 0, \quad u_2 = 0, \tag{3.250}$$

whose linearisation gives the eigenvalues $\frac{3\gamma_{\rm pf}}{4p}$, $\frac{3(2p(2-\gamma_{\rm pf})+\gamma_{\rm pf})}{4np}$, and $-\frac{3(2-\gamma_{\rm pf})}{2n}$, where the associated eigenvectors are the canonical basis of $\mathbb{R}^3$. In this case in the $\{u_2\}$-subset $T^{\pm}$ is a hyperbolic source. The other fixed points are

$$\mathrm{Q}^{\pm}: \quad v_{2\pm} = \pm\left(\frac{3n\gamma_{\rm pf}}{4p(n-1)(2p-n)}\right)^{\frac{1}{2p}}, \quad s_{2\pm} = 0, \quad u_2 = 0. \tag{3.251}$$

The eigenvalues of the linearised system around $\mathrm{Q}^{\pm}$ are $-\frac{3\gamma_{\rm pf}}{2}, \frac{3}{4np}\left(4p - \frac{2p(2p-n-1)\gamma_{\rm pf}}{2p-n} + \frac{n\gamma_{\rm pf}}{(n-1)(2p-n))}\right)$, and $-\frac{3(2-\gamma_{\rm pf})}{2n} - \frac{3\gamma_{\rm pf}}{4p(n-1)(2p-n)}$. In the $\{u_2\}$ subset, Q^{+} is a hyperbolic saddle.

Lastly in the positive w-direction we have one more fixed point,

$$\mathrm{K}^{+}: \quad v_{1\pm} = 0, \quad s_{2\pm} = 0, \quad u_2 = 1 \tag{3.252}$$

The eigenvalues of the linearised system around K^{+} are $\frac{3}{2p}$, $\frac{3}{2np}$, and $3(2-\gamma_{\rm pf})$, where the associated eigenvectors are the canonical basis of $\mathbb{R}^3$. Since $\gamma_{\rm pf} < 2$, $K^{\pm}$ has all eigenvalues have positive real part being a hyperbolic source.

Hence we have the following lemma:

Lemma 3.29. *No interior orbit in* $\mathbf{S}$ *converges to the points on the set* $\mathrm{L}_2 \setminus \mathrm{FL}_0 \cup \mathrm{K}^{\pm}$ *as* $\tau \to -\infty$*, while a two-parameter set converges to each* $K^{\pm}$ *and a 1-parameter set to* FL_0.

Global phase-space on the Poincaré-Lyapunov disk

In this section we introduce a new cylindrical transformation

$$(x_3, y_3) = \left(\left(\frac{r}{1-r}\right)^{\frac{1}{2p}}\cos\theta, \left(\frac{r}{1-r}\right)^{\frac{2p+1}{2p}} F(\theta)\sin\theta, (1-r)r^{\frac{2p-n+1}{2n(2p-n)}}, \bar{u}\right), \tag{3.253}$$

where

$$F(\theta) = \sqrt{\frac{1-\cos^{2(2p+1)}\theta}{1-\cos^2\theta}} = \sqrt{\sum_{k=0}^{2p}\cos^{2k}\theta} \tag{3.254}$$

The resulting dynamical system is regular and can be extended up to $\{r=0\}$ and $\{r=1\}$ at least in a C_1 manner. The general structure of the Poincaré-Lyapunov cylinder is shown in Figure 3.22 where one can see the presence of the kinaton fixed points $\mathrm{K}^{\pm}$.

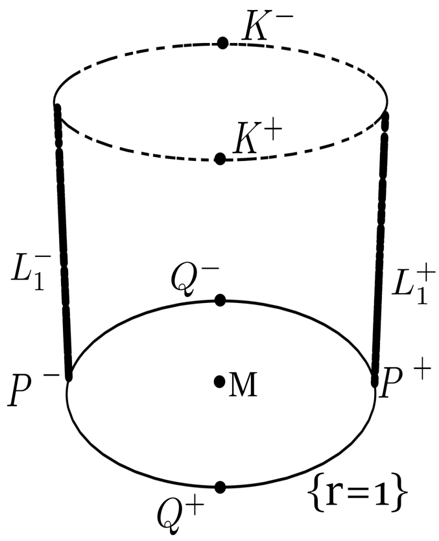

FIGURE 3.22: Blow-up space in the Poincaré-Lyapunov cylinder.

We will focus our study to the $\{u_3 = 0\}$ subset to obtain a global phase-space picture on the unit disk $\mathbb{D}^2$. Similarly to the blow-up of FL_1 done in section 3.3.3

The above transformation leads to

$$x_3^{2(2p+1)} + y_3^2 = \left(\frac{r}{1-r}\right)^{\frac{2p+1}{p}} \tag{3.255}$$

and make a further change of time variable

$$\frac{d}{d\bar{\xi}} = (1-r)\frac{d}{d\bar{\tau}_3}. \tag{3.256}$$

we get the regular system of equations

$$\frac{dr}{d\bar{\xi}} = \frac{1}{2}r(1-r)\left(\frac{(2p-1)}{(2p+1)}\tilde{K}\gamma_{\text{pf}} + \left(1 - \tilde{K}\frac{2p-1}{(2p+1)}\right)\cos^{2p(2p+1)}\theta - p\nu r F^2(\theta)\cos^{2(p-1)}\sin^2 2\theta\right) \tag{3.257a}$$

$$\frac{d\theta}{d\bar{\xi}} = -\frac{1}{4p}F^2(\theta)\sin\theta\left(-3(1-r)\gamma_{\text{pf}}\left(\frac{2p-1}{2p+1}\tilde{K} - 1\right) + 4pr\cos^{2p}\theta\right) \tag{3.257b}$$

At $\{r = 0\}$ lies the fixed point M which is the origin of the (x_3, y_3) plane, which the previous analysis showed that is a saddle since $\tilde{K} < 0$.

The fixed points at infinity in the (x_3, y_3) plane are now located at $\{r = 1\}$. The fixed points $\mathrm{R}^{\pm}$ and $\mathrm{Q}^{\pm}$ are located at

$$\theta_{P^+} = 0, \quad \theta_{P^-} = \pi, \quad \theta_{Q^+} = \frac{\pi}{2}, \quad \theta_Q^- = \frac{3\pi}{2}. \tag{3.258}$$

Theorem 3.30. *Let $p > \frac{n}{2}$ with $p > 0$ and $n > 0$. Then for all $\nu > 0$ the Poincaré-Lyapunov disk consists of heteroclinic orbits connecting the fixed points* M*,* $\mathrm{P}^{\pm}$ *and* $\mathrm{Q}^{\pm}$*.*

Proof. First notice that $\{y_3 = 0\}$ and $\{x_3 = 0\}$ are invariant subset consisting of heteroclinic orbits $\mathrm{M} \to \mathrm{P}^{\pm}$, and $\mathrm{Q}^{\pm} \to \mathrm{M}$ respectively. These separatrices split the phase-space into four invariant subsets (the quadrants). Since on both of these quadrants there are no fixed points the there are also no periodic orbits and by Poincaré-Bendixson theorem the Poincaré-Lyapunov disk consists of heteroclinic orbits connecting the fixed points. □

Figure 3.23 shows the Poincaré-Lyapunov disk for $p > \frac{n}{2}$.

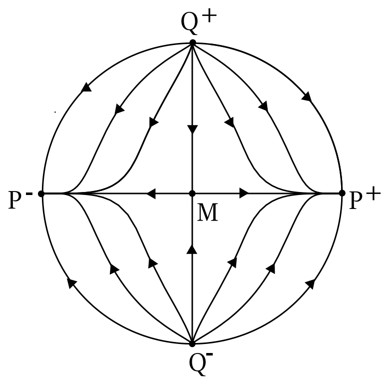

Figure 3.23: Poincaré-Lyapunov disk when $p > \frac{n}{2}$ for $(n, p, \gamma_{\mathrm{pf}}) = (1, 1, 4/3)$.

3.5.3 Invariant Boundary $T = 1$

The flow induced in the $T = 1$ boundary is given by

$$\frac{dX}{d\tau} = \Sigma_\phi \tag{3.259a}$$

$$\frac{d\Sigma_\phi}{d\tau} = -nX^{2n-1} \tag{3.259b}$$

and the system presents only the fixed point

$$\mathrm{FL}_1: \quad X = 0, \qquad \Sigma_\phi = 0, \qquad T = 1. \tag{3.260}$$

Notice that FL_1 corresponds to the intersection of the invariant subset $T = 1$ and the subset $\Omega_{\mathrm{pf}} = 1$. At $T = 1$ the auxiliary equation for Ω_{pf} gives $d\Omega_\phi/d\tau = 0$, so that the invariant boundary $T = 1$ is foliated by periodic orbits, and FL_1 is a center, see Fig.3.24.

Theorem 3.31. *Consider the system (3.198) with $0 < \Omega_{\mathrm{pf}} < 1$ and $0 < \gamma_{\mathrm{pf}} < 2$:*

(i) If $\gamma_{\mathrm{pf}} < \frac{2n}{n+1}$, then all solutions converge, for $\tau \to +\infty$, to the fixed point FL_1 *with* $\Omega_{\mathrm{pf}} = 1$.

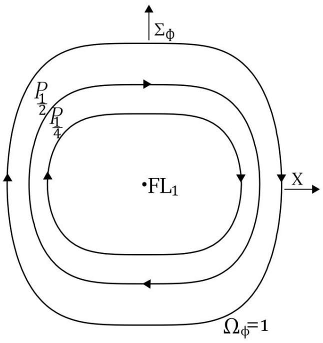

FIGURE 3.24: The invariant boundaries $T = 1$ exemplified with $(n, p) = (2, 2)$.

(ii) If $\gamma_{\rm pf} > \frac{2n}{n+1}$, then all solutions converge, for $\tau \to +\infty$, to $\Omega_\phi = 1$.

(iii) If $\gamma_{\rm pf} = \frac{2n}{n+1}$, then all solutions converge, for $\tau \to +\infty$, to each inner periodic orbit P_{Ω_ϕ}.

Proof. The proof uses the same methods as in the proof of Theorem 3.26. There are two differences, the first being that the the average of the interaction term σ_ϕ is now given by

$$\langle \sigma_\phi \rangle = \frac{\Gamma\left[\frac{1}{2} + \frac{1}{2n}\right]\Gamma\left[\frac{1}{2n} + \frac{p}{2n}\right]}{3\Gamma[1 + \frac{1}{2n}]\Gamma[\frac{1}{2n} + \frac{p}{n}]} \tag{3.261}$$

and the second one is the θ equation defined in (3.264).

The evolution for $r = \sqrt{\Omega_\phi}$ and $\epsilon = 1 - T$ are given by

$$\frac{d\omega}{d\tau} = \frac{3}{2}\epsilon\left((1-\epsilon)^{2p-n}\left(\gamma_{\rm pf} - \gamma_\phi\right) r(1-r^2) - \sigma_\phi \epsilon^{2p-n+1}\nu r^{1+\frac{2p}{n}}\right) \tag{3.262a}$$

$$\frac{d\epsilon}{d\tau} = -\frac{1}{n}\epsilon^2(1-\epsilon)(1+q) \tag{3.262b}$$

where

$$q + 1 = \frac{3}{2}\left(2r^2 G(\theta)^2 \sin^2\theta + \gamma_{\rm pf}(1-r^2)\right) \tag{3.263}$$

and θ solves

$$\frac{d\theta}{d\tau} = -\frac{\epsilon}{2n}\left(3(1-\epsilon^{2+-n}) + \epsilon 2p - n\nu r^{\frac{2p}{n}}\cos^{2p}\theta\right) G(\theta)^2 \sin 2\theta + (1-\epsilon)^{2p-n+1} r^{\frac{n-1}{n}} F(\theta). \tag{3.264}$$

Starting with the near identity transformation

$$r(\tau) = y(\tau) + \epsilon(\tau) g(y, \tau, \epsilon) \tag{3.265}$$

and expanding

$$(1-\epsilon)^{2p-n} \approx 1-(2p-n)\epsilon + \frac{1}{2}\zeta(\zeta-1)\epsilon^2 - \frac{1}{6}\zeta(\zeta-1)(\zeta-2)\epsilon^3 + \mathcal{O}(\epsilon^3) \tag{3.266a}$$
$$\epsilon^{2p-n+1} = \epsilon^2\delta_1^{2p-n} + \epsilon^3\delta_2^{2p-n} + \mathcal{O}(\epsilon^3). \tag{3.266b}$$

where $\zeta = 2p-n$. In turn, the evolution equation for y can be obtained using equations (3.262) alongside with the evolution equation for r, and gives

$$\begin{aligned}
\frac{dy}{d\tau} &= \left(1+\epsilon\frac{\partial g}{\partial y}\right)^{-1}\left[\frac{dr}{d\tau} - \left(g+\epsilon\frac{\partial g}{\partial \epsilon}\right)\frac{d\epsilon}{d\tau} - \epsilon\frac{\partial g}{\partial \tau}\right] \\
&= \left(1+\epsilon\frac{\partial g}{\partial y}\right)^{-1}\left[\epsilon\left(\frac{3}{2}(\gamma_{\mathrm{pf}}-\langle\gamma_\phi\rangle)\right)y(1-y^2) + \frac{3}{2}(\langle\gamma_\phi\rangle-\gamma_\phi)y(1-y^2) - \frac{\partial g}{\partial \tau}\right. \\
&+ \left.\epsilon^2\left(\frac{3}{2}\left((\gamma_{\mathrm{pf}}-\gamma_\phi)(1-3y^2)g + (\gamma_{\mathrm{pf}}-\gamma_\phi)\zeta y(1-y^2) - \sigma_\phi\delta_1^{2p-n}\nu y^2\right) + \frac{(1+q)}{n}g\right)\right] + \mathcal{O}(\epsilon^3).
\end{aligned} \tag{3.267}$$

Setting

$$\frac{\partial g}{\partial \tau} = \frac{3}{2}\left(\langle\gamma_\phi\rangle - \gamma_\phi\right)y(1-y^2) \tag{3.268}$$

and using the fact that $(1+\epsilon\frac{\partial g}{\partial y})^{-1} \approx 1-\epsilon\frac{\partial g}{\partial y} + \mathcal{O}(\epsilon^2)$ we get

$$\frac{dy}{d\tau} = \epsilon\langle f\rangle(y) + \epsilon^2 h(y,g,\tau,\epsilon) + (O)(\epsilon^3) \tag{3.269}$$

where

$$\langle f\rangle(y) = \frac{3}{2}(\gamma_{\mathrm{pf}}-\langle\gamma_\phi\rangle)y(1-y^2), \tag{3.270a}$$
$$\begin{aligned}
h(y,g,,\tau,\epsilon) &= \frac{3}{2}(\gamma_{\mathrm{pf}}-\langle\gamma_\phi\rangle)y(1-y^2)\frac{\partial g}{\partial y} \\
&+ \frac{3}{2}\left((\gamma_{\mathrm{pf}}-\gamma_\phi)(1-3y^2)g + (\gamma_{\mathrm{pf}}-\gamma_\phi)\zeta y(1-y^2) - \sigma_\phi\delta_1^{2p-n}\nu y^2\right) + \frac{(1+q)}{n}g.
\end{aligned} \tag{3.270b}$$

As before, the right-hand side (3.268) is almost periodic, meaning that in late times $\langle\gamma_\phi\rangle - \gamma_{\mathrm{pf}} \approx$ which implies that g is bounded.

For the truncated system (at ϵ) we get

$$\frac{d\bar{y}}{d\bar{\tau}} = 3\Big(\gamma_{\mathrm{pf}} - \langle\gamma_\phi\rangle\Big)\bar{y}\Big(1-\bar{y}\Big) \tag{3.271a}$$
$$\frac{d\epsilon}{d\bar{\tau}} = -\frac{1}{n}\epsilon(1-\epsilon)(1+q) \tag{3.271b}$$

in the independent variable $d\bar{\tau} = \epsilon d\tau$. This system is similar to the one presented in [68], so we simply refer the important results. The system presents two fixed points

$$\mathrm{F}_1: \quad \bar{y} = 1 \quad , \quad \epsilon = 0 \tag{3.272a}$$

$$\mathrm{F}_2: \quad \bar{y} = 0 \quad , \quad \epsilon = 0. \tag{3.272b}$$

The linearisation around the fixed points for $\gamma_{\rm pf} - \langle\gamma_\phi\rangle \neq 0$ gives for F_1: $\lambda_1 = -3(\gamma_{\rm pf} - \langle\gamma_\phi\rangle)$, $\lambda_2 = -\frac{3\gamma_\phi}{2n}$, where the eigenvectors are the canonical basis of $\mathbb{R}^2$ while for F_2: $\lambda_1 = 3(\gamma_{\rm pf} - \langle\gamma_\phi\rangle)$, $\lambda_2 = -\frac{3\gamma_{\rm pf}}{2n}$ and again the eigenvectors are again the canonical basis of $\mathbb{R}^2$ for F_2. The stability of each fixed points depends on the sign of $\gamma_{\rm pf} - \langle\gamma_\phi\rangle$. If $\gamma_{\rm pf} > \langle\gamma_\phi\rangle$ then F_1 is a sink and F_2 is a saddle, whereas if $\gamma_{\rm pf} < \langle\gamma_\phi\rangle$ then F_1 is a saddle and F_2 is a sink. Employing Gronwall's inequality we can show that solutions of y and r and hence Ω_ϕ have the same limit as the solutions of $\bar{y}$ of the truncated averaged equation when $\tau \to +\infty$ which proves points (i) and (ii).

For point (iii), where $\gamma_{\rm pf} = \langle\gamma_\phi\rangle$. In this case the equation for y is given by

$$\begin{aligned}\frac{dy}{d\tau} = \epsilon^2 \Bigg(& \frac{3}{2}(\gamma_{\rm pf} - \langle\gamma_\phi\rangle) y(1-y^2)\frac{\partial g}{\partial y} \\ & + \frac{3}{2}\left((\gamma_{\rm pf} - \gamma_\phi)(1-3y^2)g + (\gamma_{\rm pf} - \gamma_\phi)\zeta y(1-y^2) - \nu\sigma_\phi\delta_1^{2p-n}y^2\right) + \frac{(1+q)}{n}g\Bigg)\end{aligned} \tag{3.273}$$

Taking the average of h we get

$$\begin{aligned}\langle h\rangle(y,g) &= \langle h(y,.,0)\rangle = \frac{1}{P}\int_0^P h(y,g,0,\tau)d\tau \\ &= \frac{3}{2n}\langle w\rangle\left(\left(\underbrace{\langle\gamma_\phi\rangle - \gamma_{\rm pf}}_{=0}\right) + \gamma_{\rm pf}\right) - \frac{3}{2}\langle\sigma_\phi\rangle\delta^{n-2p}\nu y^2 \\ &= \frac{3}{n+1}\langle g\rangle(y) - \frac{3}{2}\langle\sigma_\phi\rangle\nu y^2\delta_1^{n-2p}\end{aligned} \tag{3.274}$$

where in the last step we have used integration by parts. After changing time variable $\epsilon d/d\bar{\tau} = d/d\tau$, yields the truncated averaged system

$$\frac{d\bar{z}}{d\bar{\tau}} = \epsilon\frac{3}{n+1}\langle g\rangle(\bar{z}) - \epsilon\frac{3}{2}\langle\sigma_\phi\rangle\nu\bar{z}^2\delta_1^{n-2p} \tag{3.275a}$$

$$\frac{d\epsilon}{d\bar{\tau}} = -\frac{3}{n(n+1)}\epsilon(1-\epsilon) \tag{3.275b}$$

which on $\epsilon = 0$ has a line of fixed points with $\bar{z}_0 \in [0,1]$. The linearisation around the line yields the eigenvalues $\lambda_1 = 0$ and $\lambda_2 = -\frac{3}{n(n+1)}$ with associated eigenvectors

$$v_1 = (1, \epsilon = 0) \qquad v_2 = (-n\langle g\rangle(\bar{z}_0) + \frac{n(n+1)}{2}\nu\langle\sigma_\phi\rangle\bar{z}_0^2\delta_1^{2p-n}, 1)$$

Therefore the line is normally hyperbolic and each point on the line is exactly the ω-limit point of a unique interior orbit. This means that there also exists an orbit of the dynamical system with $\epsilon > 0$ initially, that converges to $(\bar{z}_0, 0)$, for each $\bar{z}_0$ as $\bar{\tau}+ \to \infty$.

Just as in the proof of cases (i) and (ii), we can estimate the term $\mathcal{O}(\varepsilon^3)$ that provides bootstrapping sequences. This defines a pseudo-trajectory $r^n(\bar{\tau}_n) = \bar{z}(\bar{\tau}_n)$ of system (3.262), with

$$|r^n(\bar{\tau}) - \bar{z}(\bar{\tau})| \leq K\varepsilon_n^2\,, \tag{3.276}$$

where $\bar{\tau} \in [\bar{\tau}_n, \bar{\tau}_{n+1}]$ and K is a positive constant. Compactness of the state space and the regularity of the flow implies that exists a set of initial values whose solution trajectory $\Omega(\bar{\tau})$ shadows the pseudo-trajectory $r^n(\bar{\tau})$, in the sense that

$$\forall n \in \mathbb{N}, \quad \forall \bar{\tau} \in [\bar{\tau}_n, \bar{\tau}_{n+1}]: \quad |r^n(\bar{\tau}) - r(\bar{\tau})| \leq K\varepsilon_n^2\,. \tag{3.277}$$

Finally, using the triangle inequality, we get

$$\begin{aligned}
|r(\bar{\tau}) - \bar{z}(\bar{\tau})| &= |r(\bar{\tau}) - z^n(\bar{\tau}) + r^n(\bar{\tau}) - \bar{z}(\bar{\tau})| \\
&\leq \underbrace{|r^n(\bar{\tau}) - r(\bar{\tau})|}_{\leq K\varepsilon_n^2} + \underbrace{|r^n(\bar{\tau}) - \bar{z}(\bar{\tau})|}_{\leq K\varepsilon_n^2} \\
&\leq 2K\varepsilon_n^2 \underbrace{\rightarrow}_{\bar{\tau}_n \to \infty} 0\,,
\end{aligned} \tag{3.278}$$

and, therefore, for each $\bar{z}_0 \in [0,1]$, there exists a solution trajectory $r(\bar{\tau})$ that converges to a periodic orbit at $\varepsilon = 0$ i.e. $T = 1$, characterized by $r = \bar{z}_0$, which concludes the proof of (iii). □

The global representative solutions for the $p > n/2$ can be founded in Figure 3.25.

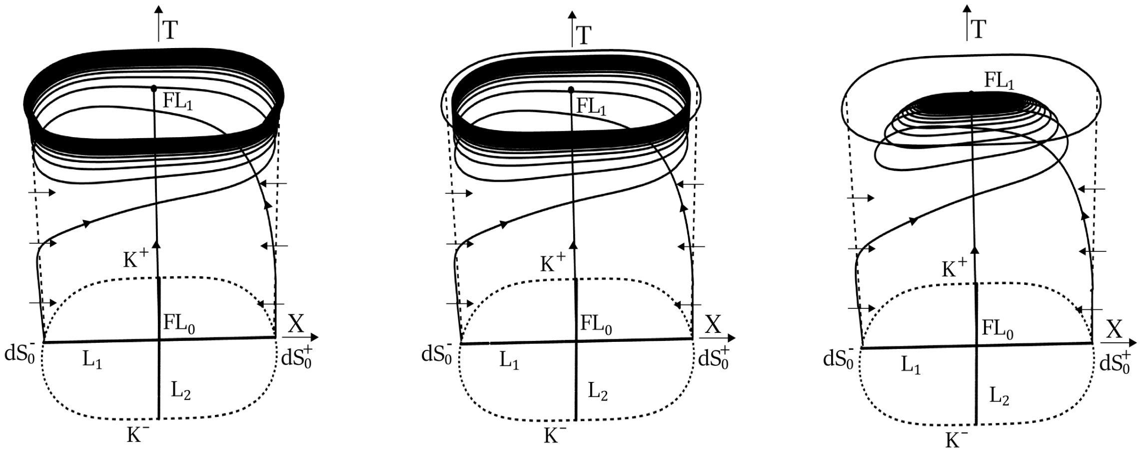

(A) Solution space for $\gamma_{\mathrm{pf}} = \frac{3}{2}$ with $n = 2$, $p = 2$ and $\nu = 1$.

(B) Solution space for $\gamma_{\mathrm{pf}} = \frac{4}{3}$ with $n = 2$, $p = 2$ and $\nu = 1$.

(C) Solution space for $\gamma_{\mathrm{pf}} = 1$ with $n = 2$, $p = 2$ and $\nu = 1$.

FIGURE 3.25: Qualitative global evolution of the dynamical system (3.198) for three different cases $\gamma_{\mathrm{pf}} < \frac{4}{3}$, $\gamma_{\mathrm{pf}} = \frac{4}{3}$ and $\gamma_{\mathrm{pf}} > \frac{4}{3}$ illustrating the results of Theorem 3.31.

3.6 Concluding Remarks

This chapter considered a spatially homogeneous and isotropic universe having a scalar field with monomial potentials interacting with perfect fluids. We were able to find a set of dimensionless bounded variables which resulted in a regular 3-dimensional regular dynamical system that allowed us to describe the global evolution of these cosmological models and identify all possible past and future attractors. This brought some mathematical challenges as new non-linearities arise in the resulting ODE system that required, for example, the use of center manifold theory and blow-up techniques around non-hyperbolic fixed points. We split our analysis into three cases for the exponents of the scalar field potential and the interaction term, $p < n/2$, $p = n/2$ and $p > n/2$,.

In the $p < \frac{n}{2}$ case we further split our analysis into two subcases, $p < \frac{1}{2}(n-1)$ and $p = \frac{1}{2}(n-1)$. When $p = \frac{1}{2}(n-1)$ all solutions at late times converge asymptotically to a Friedman-Lemaître type of universe. When $p < \frac{1}{2}(n-1)$ it was shown that our system could admit one or two lines of fixed points depending on whether p is equal or greater than zero. For any point other than the origin we see that for $p = 0$ all solutions will converge to the FL solution while for $p > 0$ all solutions will converge to a point on the line. Moreover, we found that for $p < \frac{1}{2}(n-2)$, the generic future attractor is de-Sitter, a result that seems unknown in the literature and that might offer a new model for quintessential inflation. Regarding the fixed point FL_1 located at the origin, we saw that this point is totally non-hyperbolic so we employed blow-up techniques together with a cylindrical Poincaré-compactification to better understand the dynamics in its neighbourhood.

For $p = \frac{n}{2}$ the future asymptotic regime depends on the values of γ_{pf}. Following Theorem 3.26 we have that for $\gamma_{\text{pf}} < \frac{2n}{n+1}$ the future state will be dominated by a perfect fluid model with $q = \frac{1}{2}(3\gamma_{\text{pf}} - 2)$ which is self-similar. When $\gamma_{\text{pf}} > \frac{2n}{n+1}$ the future state will be neither scalar field or perfect fluid dominated due to the existence of the interaction term $\nu \neq 0$. In this case the universe will oscillate towards the future and is characterized by a future asymptotic manifest self-similarity breaking [112].

Lastly, for $p > \frac{n}{2}$ we again have two lines of fixed points (for any p, $n > 0$) although located in the asymptotic past. In this case besides the existence of de-Sitter fixed points we also have the presence of the kinaton self-similar solution. Once again the fixed point FL_0 is not hyperbolic, which motivated once more the use of blow-up techniques together with the Poincaré compactification in order to understand the dynamics inherent to this point. The asymptotics at late times follow Theorem 3.31 and the physical interpretation is the following: In the case (i), where $\gamma_{\text{pf}} > \langle\gamma_\phi\rangle$ the future behaviour is described by a limit cycle, meaning that the deceleration parameter oscillates toward the future. The consequence of this is that this type of models exhibit a future asymptotic manifest self-similarity breaking. In turn for $\gamma_{\text{pf}} < \gamma_\phi$ the future state is dominated by the perfect fluid model with $q = \frac{1}{2}(3\gamma_{\text{pf}} - 2)$. This model is self-similar which leads us to conclude that the solutions will approach the Minkowski spacetime in a self-similar manner. Finally, for $\gamma_{\text{pf}} = \gamma_\phi$ we saw that all solutions oscillate towards the future, so the asymptotic future also manifests self-similarity breaking and is neither dominated by the scalar field nor the perfect fluid.

Chapter 4

Global dynamics of Scalar field and perfect-fluid in Bianchi I

Dynamical systems in Bianchi models have already a long history. Collins [113] obtained a compact state space using normalized variables and analysed a perfect fluid model for Bianchi types I, II, III, V and VI. This work was followed and extended by many others, for instance [114] who considered the dynamics of all Class A Bianchi models. For a review of the early works see [8].

Regarding more recent studies including the Bianchi I type, we highlight [81–83] where they use averaging theory to determine the future asymptotics for models with perfect fluids and scalar fields with an harmonic potential. Also [75] where the Bianchi type I Einstein-Vlasov equations were analysed and it was shown that all models isotropize towards the future. In [115] a dynamical systems analysis is used to study the dynamics of a Bianchi I cosmological model with a homogeneous magnetic field and a viscous fluid. In [91] the authors constructed the most general form of axially symmetric $SU(2)$ Yang Mills fields in Bianchi cosmologies and compared the dynamical evolution of the axially symmetric Yang Mills fields in Bianchi I with fully isotropic Yang Mills fields in FLRW cosmologies.

In this chapter we investigate the global dynamics of scalar fields with monomial potentials and perfect fluids on Bianchi I spacetimes. We define the dynamics on the appropriate compact phase-space using H-renormalized variables, similar to the ones defined in the Chapters 2 and 3. Due to the fact that in this case the system is 5-dimensional, it is necessary to introduce appropriate monotone functions that will exclude periodic and recurrent orbits in all invariant sets. Our analysis which involves the study of invariant boundaries including the study of fixed points, center manifolds and averaging techniques for the future attracting periodic orbits.

The chapter is organized as follows:

In Sec. 4.1 we introduce a dynamical system for the co-evolution of a monomial scalar field and a perfect fluid in a Bianchi I universe. In Sec 4.2 we consider the model without the scalar field making a global analysis of the flow and giving rigorous proofs concerning the asymptotic behaviour of general solutions in the past and in the future. A similar analysis is made in Sec. 4.3 where now we will consider the full 5-dimensional system and the scalar field in co-evolution with the perfect fluid.

4.1 The Bianchi I Dynamical System

4.1.1 Derivation of the non-linear ODE system

We consider a Bianchi I spacetime with metric g (1.63) containing a perfect fluid in co-evolution with scalar field with potential (3.11).

Substituting the metric (1.63) in the Einstein equations (1.6) we obtain the non-linear evolution system for the unknowns $\{H, \phi, \rho_{\rm pf}, \sigma_+, \sigma_-\}$:

$$\dot{H} = -\frac{1}{2}\gamma_{\rm pf}\rho_{\rm pf} - \frac{\dot{\phi}}{2} - \sigma^2 \tag{4.1a}$$

$$\ddot{\phi} = -3H\dot{\phi} + \lambda^{2n}\phi^{2n-1} \tag{4.1b}$$

$$\dot{\sigma}_\pm = -3H\sigma_\pm \tag{4.1c}$$

$$\dot{\rho}_{\rm pf} = -3H\gamma_{\rm pf}\rho_{\rm pf} \tag{4.1d}$$

together with the constraint

$$H^2 = \frac{\rho_{\rm pf}}{3} + \frac{\dot{\phi}}{6} + \frac{(\lambda\phi)^{2n}}{6n} + \frac{\sigma^2}{3}. \tag{4.2}$$

where we recall

$$\sigma^2 = 3\left(\sigma_+^2 + \sigma_-^2\right). \tag{4.3}$$

4.1.2 Dynamical Systems' Formulation

In order to obtain a regular dynamical system on compact state-space, we start by introducing dimensional variables normalized by the Hubble function H $(H(t) > 0)$.

$$\Omega_{\rm pf} := \frac{\rho_{\rm pf}}{3H^2} > 0, \quad \Sigma_\phi^2 := \frac{\dot{\phi}}{\sqrt{6}H}, \quad X := \frac{\lambda\phi}{(6nH^2)^{\frac{1}{2n}}}, \quad \Sigma_\sigma^2 = \frac{\sigma^2}{3H^2}, \quad \Sigma_\pm := \frac{\sigma_\pm}{H}, \quad \tilde{T} : \frac{c}{H^{\frac{1}{n}}} \tag{4.4}$$

where $c = \left(\frac{6^{n-1}}{n}\right)^{\frac{1}{2n}} \lambda$ is a positive constant and

$$\Sigma_\sigma^2 = \Sigma_+^2 + \Sigma_-^2 \tag{4.5}$$

where $\Sigma_\pm$ describes the anisotropy of the Hubble flow. We also introduce a new time variable N that is defined by

$$\frac{d}{dN} := \frac{1}{H}\frac{d}{dt}, \tag{4.6}$$

where $N = \ln(a/a_0)$ represents the number of e-folds in the inflationary period of cosmological exponential expansion where a_0 is some epoch at which $N = 0$.

Then, the system (4.1), in the new variables, will be reduced to a *local* 5-dimensional dynamical system

$$\frac{dX}{dN} = \frac{1}{n}(1+q)X + \tilde{T}\Sigma_\phi \tag{4.7a}$$

$$\frac{d\Sigma_\phi}{dN} = -(2-q)\Sigma_\phi - n\tilde{T}X^{2n-1} \tag{4.7b}$$

$$\frac{d\Sigma_+}{dN} = -(2-q)\Sigma_+ \tag{4.7c}$$

$$\frac{d\Sigma_-}{dN} = -(2-q)\Sigma_- \tag{4.7d}$$

$$\frac{d\tilde{T}}{dN} = \frac{1}{n}(1+q)\tilde{T}, \tag{4.7e}$$

subjected to the constraint

$$1 - \Omega_{\rm pf} = \Sigma_\phi^2 + X^{2n} + \Sigma_+^2 + \Sigma_-^2 = \Omega_\phi + \Sigma_\sigma^2, \tag{4.8}$$

which is used to globally solved $\Omega_{\rm pf}$. It's useful to introduce the full form of the deceleration parameter q defined via (1.17), i.e.

$$q := -1 + 3(\Sigma_\phi^2 + \Sigma_+^2 + \Sigma_-^2) + \frac{3}{2}\gamma_{\rm pf}\Omega_{\rm pf} = -1 + 3\Sigma_\sigma^2 + \frac{3}{2}(\gamma_\phi\Omega_\phi + \gamma_{\rm pf}\Omega_{\rm pf}) \tag{4.9}$$

where γ_ϕ is defined in (3.20).

It is also useful to consider an auxiliary equation for $\Omega_{\rm pf}$ which is given by

$$\frac{d\Omega_{\rm pf}}{dN} = \left[(2-\gamma_{\rm pf})\Sigma_\sigma - (\gamma_{\rm pf} - \gamma_\phi)\Omega_\phi\right]\Omega_{\rm pf}. \tag{4.10}$$

It is easy to notice that when $\tilde{T} \to +\infty$ ($H \to 0$), the system (4.7) becomes unbounded. In order to o obtain a *regular* and *global* 5-dimensional dynamical system, we further introduce

$$T = \frac{\tilde{T}}{1+\tilde{T}}, \tag{4.11}$$

so that when $T \to 0$ as $\tilde{T} \to 0$ and $T \to 1$ as $\tilde{T} \to +\infty$, as well a new, independent, variable τ defined by

$$\frac{d}{d\tau} := (1-T)\frac{d}{dN} = \frac{(1-T)}{H}\frac{d}{dt}. \tag{4.12}$$

This leads to a *global* 5-dimensional dynamical system on the variables $\{X, \Sigma_\phi, \Sigma_+, \Sigma_-, T\}$:

$$\frac{dX}{d\tau} = \frac{1}{n}(1+q)(1-T)X + T\Sigma_\phi \tag{4.13a}$$
$$\frac{d\Sigma_\phi}{d\tau} = -(2-q)(1-T)\Sigma_\phi - nTX^{2n-1} \tag{4.13b}$$
$$\frac{d\Sigma_\pm}{d\tau} = -(2-q)(1-T)\Sigma_\pm \tag{4.13c}$$
$$\frac{dT}{d\tau} = \frac{1}{n}(1+q)T(1-T)^2, \tag{4.13d}$$

where the constraint (4.8) is used to solve $\Omega_{\rm pf}$ globally and q is given by (4.9). The auxiliary equation (4.10) alongside with the equations for Ω_ϕ and Σ_σ in the new time τ is given by

$$\frac{d\Omega_{\rm pf}}{d\tau} = 3(1-T)\left[(2-\gamma_{\rm pf})\Sigma_\sigma^2 - (\gamma_{\rm pf}-\gamma_\phi)\Omega_\phi\right]\Omega_{\rm pf} \tag{4.14a}$$
$$\frac{d\Omega_\phi}{d\tau} = 3(1-T)\left[(\gamma_{\rm pf}-\gamma_\phi)(1-\Omega_\phi) + (2-\gamma_{\rm pf})\Sigma_\sigma^2\right]\Omega_\phi \tag{4.14b}$$
$$\frac{d\Sigma_\sigma}{d\tau} = -\frac{3}{2}(1-T)\left[(2-\gamma_{\rm pf})(1-\Sigma_\sigma^2) + (\gamma_{\rm pf}-\gamma_\phi)\Omega_\phi\right]\Sigma_\sigma \tag{4.14c}$$

From the definition of T and the constraint equation together with the fact that $\Omega_{\rm pf}$, we see the state space

$$S = \{X, \Sigma_\phi, \Sigma_+, \Sigma_-, T\}$$

is bounded since

$$-1 \leq X \leq 1 \quad , \quad -1 \leq \Sigma_\phi \leq 1 \quad , \quad -1 \leq \Sigma_\pm \leq 1 \quad , \quad 0 \leq T \leq 1. \tag{4.15}$$

Moreover, since $\gamma_{\rm pf} \in (0,2)$, it follows from (4.9) that

$$-1 \leq q \leq 2. \tag{4.16}$$

The state space $\mathbf{S}$ is 5-dimensional however it is useful to view it using two 3-dimensional point of views represented by the spaces:

$$\begin{aligned}\mathbf{S}_1 &: \{X, \Sigma_\phi, T\}\\ \mathbf{S}_2 &: \{\Sigma_+, \Sigma_-, T\}.\end{aligned} \tag{4.17}$$

The outer shell of the cylinder $\mathbf{S}_1$ is described by the pure *scalar field subset*:

$$\mathbf{S}_\phi: \quad \Omega_{\text{pf}} = \Sigma_\sigma = 0 \quad (\Omega_\phi = 1).$$

The outer shell of the cylinder $\mathbf{S}_2$ is described by the pure *Kasner subset*:

$$\mathbf{S}_\sigma: \quad \Omega_{\text{pf}} = \Omega_\phi = 0 \quad (\Sigma_\sigma = 1).$$

The state space $\mathbf{S}$ can be analytically extended to include is closure, i.e., the invariant boundaries $T = 0$ and $T = 1$, and form the extended state space $\bar{\mathbf{S}}$. In the same way we can define the extension of $\mathbf{S}_\phi$ and $\mathbf{S}_\sigma$ to $T = 0$ and $T = 1$ as $\bar{\mathbf{S}}_\phi$ and $\bar{\mathbf{S}}_\sigma$ respectively. Although this boundary in unphysical, this extension is crucial since all attracting sets are located on these boundaries as shown by the following lemma:

Lemma 4.1. *The α-limit set of all interior orbits in $\mathbf{S}$ is located at $T = 0$, while the ω-limit set of all interior orbits in $\mathbf{S}$ is located at $T = 1$.*

Proof. Since $1 + q \leq 0$, then T is strictly monotonically increasing in the interval $(0, 1)$ except when $q = -1$ in which case

$$\frac{dT}{d\tau}\Big|_{1+q=0} = 0 \ , \ \frac{d^2T}{d\tau^2}\Big|_{1+q=0} \ , \ \frac{d^3T}{d\tau}\Big|_{1+q=0} = 6n(1-T)T^3 > 0 \tag{4.18}$$

for $T \in (0, 1)$. By the monotonicity principle A.23, it follows that there are no fixed points, recurrent or periodic orbits in the interior of the state space $\mathbf{S}$ and the α and ω-limit sets of all orbits in $\mathbf{S}$ are contained at $T = 0$ and $T = 1$, respectively. □

4.1.3 Monotonic functions

In order to study the dynamics in each 4-dimensional boundary ($T = 0$ and $T = 1$) we will use some monotonic functions that will simplify the system. As a consequence of the monotonicity principle, this will allow us to exclude periodic orbits and recurrent orbits in all invariant sets (see e.g.[74]), Some monotone functions were already suggested in [76, 78, 116] however we will consider new ones.

The firs monotone function that comes into mind is the one proportional to the shear equation.

$$Z_1 = \Sigma_\sigma^2, \qquad Z_1' = -(1-T)(2-q)Z_1 \tag{4.19}$$

As one can see Z_1 is a decreasing monotone function, since $q \in [-1, 2]$. In fact $Z_1' = 0$ when $T = 1$ and $q = 2$. Following equation (4.14c) we see that in fact the Σ_σ is a conserved quantity when $T = 1$. For $q = 2$ we see $Z_1' = 0$ when $\Sigma_\sigma^2 = 1$ or when $\Sigma_\phi^2 = 1$ ($\Sigma_\sigma^2 = 0$) and since Σ_σ is bounded it follows that $\Sigma_\sigma \to 1$ in the past and $\Sigma_\sigma \to 0$ in the future.

Other monotone function is the one proportional to $\Omega_{\rm pf}$

$$Z_2 = \Omega_{\rm pf}, \qquad Z_2' = 3(1-T)\left((2-\gamma_{\rm pf})\Sigma_\sigma^2 - (\gamma_{\rm pf} - \gamma_\phi)\Omega_\phi\right) Z_2 \tag{4.20}$$

In the $\{\Omega_\phi = 0\}$-subset $Z_2' = 3(1-T)(2-\gamma_{\rm pf})\Sigma_\sigma^2 Z_2$ which is always positive everywhere except when $T = 1$ or when $\Sigma_\sigma^2 = 0$. In the first case, $T = 1$ we can see from (4.14a) that in the $T = 1$ boundary $\Omega_{\rm pf}$ it is also a conserved quantity. When $\Sigma_\sigma = 0$, we know that when $\Omega_\phi = 0$ then $\Omega_{\rm pf} + \Sigma_\sigma^2 = 1$ so when $\Sigma_\sigma^2 \to 0$, $\Omega_{\rm pf} \to 1$ and when $\Sigma_\sigma^2 \to 1$, then $\Omega_{\rm pf} \to 0$ since all variables are bounded we see that in the $\{\Omega_\phi = 0\}$-subset in the past $\Omega_{\rm pf} \to 0$ and $\Omega_{\rm pf} \to 1$ in the future.

To connect everything up we introduce another monotonic function

$$Z_3 = \frac{\Omega_\phi}{\Sigma_\sigma^2}, \qquad Z_3' = \frac{6(1-T)X^{2n}}{\Omega_{\rm pf}} Z_3 \tag{4.21}$$

We see that Z_3 is a monotonically increasing function in the $T = 0$ subset except when X^{2n} is zero. Since are variables are bounded we see that in the past $\Omega_\phi \to 0$ and in the future $\Sigma_\sigma^2 \to 0$ joining all this information we see that the Kasner circle Σ_σ^2 is the repeller in the $T = 0$ boundary.

Now we are able to give a complete detailed description of the invariant subsets $T = 0$ and $T = 1$ that are associated to the asymptotic past ($H \to +\infty$) and future ($H \to 0$), however it is interesting also to analyze a particular sub-case that arrive from this particular Bianchi-I model, the anisotropic universe without the scalar field.

4.2 Model in the absence of scalar field

This case was first analysed from a dynamical system's perspective in [113], but a more complete early analysis was done in [114], see [8]. The model is asymptotically self-similar to the past and future. One of the conclusions was that the flat FL equilibrium point is the future attractor and the Kasner circle is the past attractor for the system.

In this section, we revisit previous results within our framework before considering a model with scalar field and perfect fluid. With respect to the previous formalism's we use a different time variable which allow us to draw a 3-dimensional picture of phase-space. In this context, we also obtain explicit estimates for the asymptotic evolution of the variables in the approach the pas and future attractors.

In this particular case we $\Omega_\phi = 0$, so our constraint is now $\Omega_{\rm pf} = 1 - \Sigma_\sigma^2 = 1 - \Sigma_+^2 - \Sigma_-^2$. Due to the fact that we don't have a scalar field we need to adapt our H-normalized variables from the ones in (4.4). In this case we have

$$\Omega_{\rm pf} := \frac{\rho_{\rm pf}}{3H^2}, \quad \Sigma_\sigma^2 := \frac{\sigma^2}{3H^2}, \quad \Sigma_\pm := \frac{\sigma_\pm}{H}, \quad \tilde{T} := \frac{1}{H} \tag{4.22}$$

and using the conformal time N defined in (4.6) we obtain the system

$$\frac{d\Sigma_\pm}{dN} = -(2-q)\Sigma_\pm, \quad \frac{dT}{dN} = (1+q)T(1-T) \tag{4.23}$$

together with the auxiliary equations

$$\frac{d\Omega_{\rm pf}}{dN} = -3(2-\gamma_{\rm pf})\Sigma_\sigma\Omega_{\rm pf}, \quad \frac{d\Sigma_\sigma}{dN} = 3(2-\gamma_{\rm pf})\Sigma_\sigma\Omega_{\rm pf}. \tag{4.24}$$

In this case our state space $\mathbf{S}_{\rm pf,\sigma}$ is a 3-dimensional space consisting in a cylinder with height $0 < T < 1$. The outer shell of the cylinder is the *pure shear* invariant subset $\mathbf{S}_\sigma$ where $\Omega_{\rm pf} = 0$ ($\Sigma_\sigma = 1$). The axis of the cylinder is a straight line with $\Omega_{\rm pf} = 1$ ($\Sigma_\sigma = 0$) and it is related to the self-similar flat Friedmann-Lemaître (FL) spacetime.

The state space $\mathbf{S}_{\rm pf,\sigma}$ can be analytically extended to include its closure, i.e the invariant boundaries $T = 0$ and $T = 1$ forming a extended space $\bar{\mathbf{S}}_{\rm pf,\sigma}$. The result of Lemma 4.1 is also valid in this case:

Lemma 4.2. *The α-limit set of all interior orbits in $\mathbf{S}_{\rm pf,\sigma}$ is located at $T = 0$, while the ω-limit set of all interior orbits in $\mathbf{S}_{\rm m,\sigma}$ is located at $T = 1$.*

Proof. See lemma 4.1 □

4.2.1 The $T = 0$ Boundary

The flow induced in the $T = 0$ boundary is given by

$$\frac{d\Sigma_\pm}{dN} = -(2-q)\Sigma_\pm, \qquad \frac{dT}{dN} = 0 \tag{4.25}$$

subjected to the constraint $\Omega_{\rm pf} = 1 - \Sigma_+^2 - \Sigma_-^2$. The system (4.23) admits a circular line o fixed points on the invariant shear subset $\Omega_{\rm pf} = 0$ and one at the center with $\Omega_{\rm pf} = 1$.

The isolated fixed point in the pure matter subset is

$$\mathrm{FL}_0 : \quad \Sigma_+ = 0, \quad \Sigma_- = 0, \quad T = 0 \tag{4.26}$$

with $q = \frac{1}{2}(3\gamma_{\rm pf} - 2)$ corresponding to the flat FL self-similar solution. The linearisation around this fixed point yields to the eigenvalues $-\frac{3}{2}(2 - \gamma_{\rm pf})$, $-\frac{3}{2}(2 - \gamma_{\rm pf})$ and $\frac{3\gamma_{\rm pf}}{2}$ where the eigenvectors are the canonical basis of $\mathbb{R}^3$. FL_0 has two negative real eigenvalues and a positive real eigenvalue, being a hyperbolic saddle, and the α-limit set of orbits in $\mathbf{S}$.

On the intersection of the invariant boundary $T = 0$ with the subset $\Omega_{\rm pf}$, the circular line of fixed points

$$\mathbf{L}_{\Sigma,0} : \quad \Sigma_+ = \Sigma_0, \quad \Sigma_- = \pm\sqrt{1 - \Sigma_0^2}, \quad T = 0. \tag{4.27}$$

with $q = 2$ corresponding to the Kasner vacuum solution. The linearisation around this line of fixed points yields to the eigenvalues $3(2 - \gamma_{\rm pf})$, 0, and 3 with the eigenvectors $\left(\frac{\Sigma_0}{\sqrt{1-\Sigma_0^2}}, 1, 0\right)$, $\left(-\frac{\sqrt{1-\Sigma_{0+}^2}}{\Sigma_0}, 1, 0\right)$, and $(0, 0, 1)$. In this case the Kasner circle is semi-hyperbolic. To analyse the center manifold we introduce the adapted variables $\bar{\Sigma}_+ = \frac{1}{\Sigma_0\sqrt{1-\Sigma_0^2}}\Sigma_+ + (1 - \Sigma_0^2)\Sigma_-$ and $\bar{\Sigma}_- = -\Sigma_0\sqrt{1 - \Sigma_0^2}\Sigma_+ + \Sigma_0^2\Sigma_-$. The center manifold reduction theorem yields that the system above is locally topological equivalent to the 1-dimensional decoupled equation on the center manifold, which can be locally represented as the graph $h : E^c \to E^u$, i.e. $\bar{\Sigma}_+ = h(\bar{\Sigma}_-)$ which solves the non-linear ordinary differential equation

$$\frac{dh}{d\bar{\Sigma}_-}\bar{\Sigma}_- = \sqrt{1 - \Sigma_0^2} + h(\bar{\Sigma}_-) \tag{4.28}$$

subjected to the fixed point $h(0) = 0$ and tangency $\frac{dh}{d\bar{\Sigma}_-}{=}0$, conditions. In general is not possible to solve for h explicitly. However we can approximate the solutions by making formal power series for $h(\bar{\Sigma}_-)$ and solving for the coefficients gives as $\bar{\Sigma}_- \to 0$, which yields on the center manifold

$$\frac{d\bar{\Sigma}_-}{dN} = \frac{3(2 - \gamma_{\rm pf})}{\Sigma_0^4}\bar{\Sigma}_-^5 \tag{4.29}$$

and therefore it is a one dimensional unstable center manifold. Therefore in the asymptotic past the Kasner circle is a repeller.

The system (4.25) admit a conserved quantity for $\Omega_{\rm pf} > 0$,

$$\Sigma_+ = C\Sigma_- \tag{4.30}$$

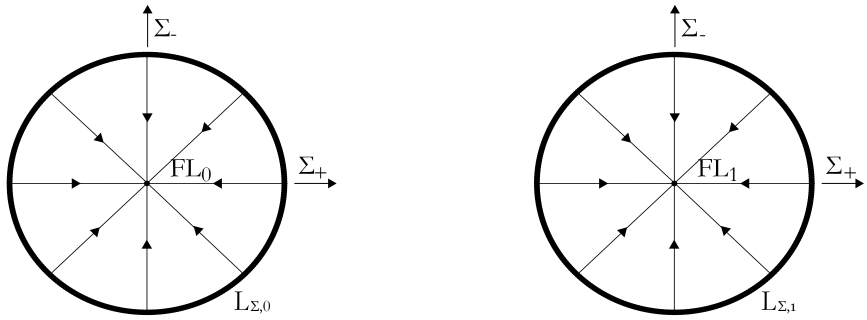

(A) $T = 0$ boundary for $\gamma_{\rm pf} = \frac{4}{3}$.

(B) $T = 1$ boundary for $\gamma_{\rm pf} = \frac{4}{3}$.

Figure 4.1: The $T = 0$ and $T = 1$ invariant boundaries for the anisotropic case in a universe without scalar field.

where C is a real constant that parameterises the solutions. Where the flow in invariant under the transformation $(\Sigma_+, \Sigma_-) \to (-\Sigma_+, -\Sigma_-)$.

A straightforward inspection of the flow shows the line $\mathbf{L}_{\Sigma,0}$ is a source while FL_0 is a saddle, see Fig.4.1a.

Theorem 4.3. *The α-limit set of orbits, consists of fixed points on $T = 0$. In particular as $N \to -\infty$, a 2-parameter set of orbits converge to each point on the line of fixed points with asymptotics*

$$\Sigma_+(N) = \left((1-\Sigma_{0+}^2)C_{\Sigma_+} \mp \Sigma_{0+}\sqrt{1-\Sigma_{0+}^2}C_{\Sigma_-}\right) + \Sigma_{0+}\left(\Sigma_{0+}C_{\Sigma_+} \pm \sqrt{1-\Sigma_{0+}^2}C_{\Sigma_-}\right)e^{3(2-\gamma_{\rm pf})N} \tag{4.31a}$$

$$\Sigma_-(N) = \Sigma_{0+}\left(\Sigma_{0+}C_{\Sigma_-} \mp \sqrt{1-\Sigma_{0+}^2}\right) + \left(\Sigma_{0+}\sqrt{1-\Sigma_{0+}}C_{\Sigma_+} + (1-\Sigma_{0+}^2)C_{\Sigma_-}\right)e^{3(2-\gamma_{\rm pf})N} \tag{4.31b}$$

$$\tilde{T}(N) = C_T e^{3N} \tag{4.31c}$$

with C_{Σ_+}, $C_{\Sigma_-} > 0$, and $C_T > 0$.

4.2.2 The $T = 1$ Boundary

The flow induced in this boundary is given by

$$\frac{d\Sigma_+}{dN} = -(2-q)\Sigma_+ \quad \frac{d\Sigma_-}{dN} = -(2-q)\Sigma_-, \quad \frac{dT}{dN} = 0, \tag{4.32}$$

subjected to the constraint $\Omega_{\rm pf} = 1 - \Sigma_+^2 - \Sigma_-^2$. Since the system is similar to the $T = 0$ boundary we once again have a line of fixed points $(\mathbf{L}_\Sigma, 1)$ in the shear subset $(\Omega_{\rm pf} = 0)$ and one isolated fixed point (FL_1) in the matter subset $(\Omega_{\rm pf} = 1)$. The isolated fixed point in the matter subset is

$$\mathrm{FL}_1 : \quad \Sigma_+ = 0, \quad \Sigma_- = 0, \quad T = 1 \tag{4.33}$$

with $q = \frac{1}{2}(3\gamma_{\rm pf} - 1)$ corresponding once again to the flat FL self-similar solution. The linearisation around this fixed point yields to the eigenvalues $-\frac{3}{2}(2 - \gamma_{\rm pf})$, $-\frac{3}{2}(2 - \gamma_{\rm pf})$ and $-\frac{3\gamma_{\rm pf}}{2}$ where the eigenvectors are the canonical basis of $\mathbb{R}^3$. FL_1 has three negative eigenvalues being a hyperbolic sink.

The circle of fixed points is given by

$$\mathbf{L}_{\Sigma 1} : \quad \Sigma_+ = \Sigma_0, \quad \Sigma_- = \pm\sqrt{1 - \Sigma_0^2}, \quad T = 1. \tag{4.34}$$

with $q = 2$ that is the Kasner vacuum solution. The linearisation around this line of fixed points yields to the eigenvalues $3(2 - \gamma_{\rm pf})$, 0 and -3 were the respective eigenvectors are $\left(\frac{\Sigma_0}{\sqrt{1-\Sigma_0^2}}, 1, 0\right)$, $(-\frac{\sqrt{1-\Sigma_0^2}}{\Sigma_0}, 1, 0)$, and $(0, 0, 1)$. As in the $T = 0$ the Kasner circle as a similar dynamic in the center manifold, i.e. the center manifold is unstable

The system admits a similar conserved quantity as the one described in (4.30).

An inspection of the eigenvalues in this boundary tells us that the circular line of fixed points, $\mathbf{L}_{\Sigma,1}$, is a saddle and FL_1 is a sink, see Fig.4.1b.

Theorem 4.4. *The ω-limit set of orbits, consists of fixed points on $T = 1$. A 1-parameter set converges to FL_1 as $N \to +\infty$ with asymptotics*

$$\Sigma_+(N) = C_{\Sigma_+} e^{-\frac{3}{2}(2-\gamma_{\rm pf})N}, \quad \Sigma_-(N) = C_{\Sigma_-} e^{-\frac{3}{2}(2-\gamma_{\rm pf})N}, \quad \tilde{T}(N) = C_T e^{-\frac{3\gamma_{\rm pf}}{2}N} \tag{4.35}$$

4.2.3 Global Dynamics

We now make use of the previous analysis to prove the following result

Proposition 4.5. *Consider solutions of the system (4.25) with $0 < \Omega_{\rm pf} < 1$: For $\gamma_{\rm pf} \in (0, 2)$, a 1-parameter set of solutions converges, for $\bar{\tau} \to -\infty$, to each point of the circle of fixed points $(\mathrm{L}_{\Sigma,0})$ with $\Omega_{\rm pf} = 0$, while, for $\bar{\tau} \to \infty$, all solutions converge to the fixed point FL_1 with $\Omega_{\rm pf} = 1$.*

This means that the model is past asymptotic dominated by the anisotropy (Kasner vacuum solution) and future asymptotic dominated by the perfect fluid (flat FL solution), see figure 4.2 for the representative solution.

Proof. To prove this we need to use Lemma 4.2 were it says that the α-limit sets are fixed points at $T = 0$ and the ω-limit sets are fixed points at $T = 1$ together with analysis of the fixed points.

In order to study the asymptotic behaviour, we make use of the auxiliary equation (4.24). So for $\Sigma_\sigma \in (0,1)$ and $\gamma_{\text{pf}} \in (2/3, 2)$ we get

$$\left(\frac{1-\Sigma_\sigma}{\Sigma_\sigma^{\frac{\gamma_{\text{pf}}}{2}}}\right)^{\frac{1}{2-\gamma_{\text{pf}}}} = C\frac{T}{1-T},$$

where $C > 0$ is real and parameterize the solution. From the above equation its easy to see that when $T \to 0$ then $\Sigma_\sigma \to 1$ and when $T \to 1$ then $\Sigma_\sigma \to 0$, i.e. all solution with $0 < \Omega_{\text{pf}} < 1$ start in the line of fixed points $\mathrm{L}_{\Sigma,0}$ and end at FL_1.

□

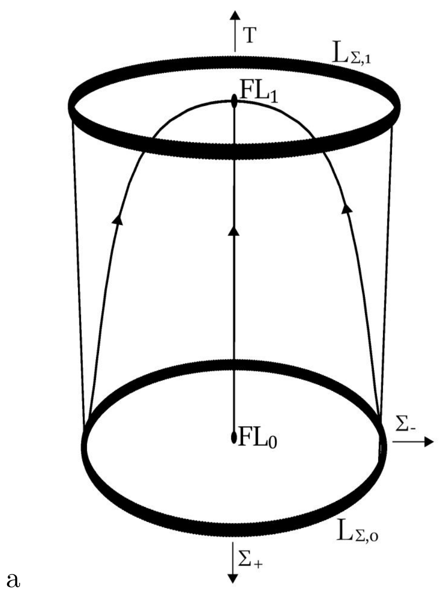

Figure 4.2: Qualitative global evolution for the dynamical system (4.23) in $\bar{\mathbf{S}}_{\mathbf{pf},\sigma}$ for $\gamma_{\text{pf}} = \frac{4}{3}$, illustrating the results of Proposition 4.5.

4.3 Model with a scalar field and Perfect Fluid

Consider now the full 5-dimensional system (4.13) with scalar field and perfect fluid.

4.3.1 The $T = 0$ Boundary

The flow induced in the $T = 0$ boundary is given by

$$\frac{dX}{d\tau} = \frac{1}{n}(1+q)X \tag{4.36a}$$
$$\frac{d\Sigma_\phi}{d\tau} = -(2-q)\Sigma_\phi \tag{4.36b}$$
$$\frac{d\Sigma_+}{d\tau} = -(2-q)\Sigma_+ \tag{4.36c}$$
$$\frac{d\Sigma_-}{d\tau} = -(2-q)\Sigma_-, \tag{4.36d}$$

subjected to the constraint $\Omega_{\rm pf} = 1 - \Omega_\phi - \Sigma_\sigma = 1 - X^{2n} - \Sigma_\phi^2 - \Sigma_+^3 - \Sigma_-^2$. In this case the system (4.36) admits a circle of fixed points in the pure anisotropic subset ($\Sigma_\sigma = 1$), four fixed points in the scalar field subset ($\Omega_\phi = 1$) and one isolated fixed point in the pure matter subset ($\Omega_{\rm pf} = 1$).

The two first equivalent fixed points in the intersection of $T = 0$ with the pure scalar field subset $\Omega_\phi = 1$ are

$$\mathrm{K}^\pm: \quad X = 0, \quad \Sigma_\phi = \pm 1, \quad \Sigma_+ = 0, \quad \Sigma_- = 0, \quad T = 0 \tag{4.37}$$

with $q = 2$ corresponding to the massless scalar field solution. The linearisation around this fixed points yields to the eigenvalues $\frac{3}{n}$, $3(2-\gamma_{\rm pf})$, 0, 0 and $\frac{3}{n}$ where the eigenvectors are $(1,0,0,0,0)$, $(0,1,0,0,0)$, $(0,0,1,0,0)$, $(0,0,0,1,0)$, and $(\mp 1,0,0,0,1)$. In the $\{\Sigma_\sigma = 0\}$ subset $\mathrm{K}^\pm$ is a source. We also have two zero eigenvalues in the Kasner subset corresponding to a center manifold. In order to study what happens in the Kasner circle we will make use of unbounded system (4.7) for the variable $\tilde{T}$. This allow us to introduce the adapted variables

$$\bar{X} = X - \tilde{T}, \quad \bar{\Sigma}_\phi = \Sigma_\phi \pm 1, \quad \bar{\Sigma}_+ = \Sigma_+, \quad \bar{\Sigma}_- = \Sigma_-, \quad \bar{T} = \tilde{T} \tag{4.38}$$

which leads to the adapted system

$$\frac{d\bar{X}}{dN} = \frac{3}{n}\bar{X} + F(\bar{\mathbf{x}}), \quad \frac{d\bar{\Sigma}_\phi}{dN} = 3(2-\gamma_{\rm pf})\bar{\Sigma}_\phi + G(\bar{\mathbf{x}}), \quad \frac{d\bar{\Sigma}_\pm}{dN} = H_\pm(\bar{\mathbf{x}}), \quad \frac{d\bar{T}}{dN} = \frac{3}{n}\bar{T} + N(\bar{\mathbf{x}}) \tag{4.39}$$

where $\bar{\mathbf{x}} = (\bar{X}, \bar{\Sigma}_\phi, \bar{\Sigma}_+, \bar{\Sigma}_-, \bar{T})$ and F, G, $H_\pm$, and N are functions of higher order. With this new adapted variables we relocated the fixed points $K^\pm$ to the origin of coordinates $(\bar{x}) = (0,0,0,0,0)$. The 2-dimensional center manifold can be locally represented by the graph $h : E^c \to E^u$, i.e, $\left(\bar{X}, \bar{\Sigma}_\phi, \bar{T}\right) = \left(h_1\left(\bar{\Sigma}_+, \bar{\Sigma}_-\right), h_2\left(\bar{\Sigma}_+, \bar{\Sigma}_-\right), h_3\left(\bar{\Sigma}_+, \bar{\Sigma}_-\right)\right)$ satisfying the fixed point $h(0,0) = 0$ and the tangency $\nabla h(0,0) = 0$ conditions which solves the following nonlinear partial differential equations

$$H_+(\bar{\mathbf{x}})\partial_{\bar{\Sigma}_+}h_1(\bar{\Sigma}_+,\bar{\Sigma}_-)+H_-(\bar{\mathbf{x}})\partial_{\bar{\Sigma}_-}h_1(\bar{\Sigma}_+,\bar{\Sigma}_-)=\frac{3}{n}h_1(\bar{\Sigma}_+,\bar{\Sigma}_-)+F(\bar{\mathbf{x}}) \tag{4.40a}$$

$$H_+(\bar{\mathbf{x}})\partial_{\bar{\Sigma}_+}h_2(\bar{\Sigma}_+,\bar{\Sigma}_-)+H_-(\bar{\mathbf{x}})\partial_{\bar{\Sigma}_-}h_2(\bar{\Sigma}_+,\bar{\Sigma}_-)=3(2-\gamma_{\rm pf})h_2(\bar{\Sigma}_+,\bar{\Sigma}_-)+G(\bar{\mathbf{x}}) \tag{4.40b}$$

$$H_+(\bar{\mathbf{x}})\partial_{\bar{\Sigma}_+}h_3(\bar{\Sigma}_+,\bar{\Sigma}_-)+H_-(\bar{\mathbf{x}})\partial_{\bar{\Sigma}_-}h_3(\bar{\Sigma}_+,\bar{\Sigma}_-)=\frac{3}{n}h_3(\bar{\Sigma}_+,\bar{\Sigma}_-)+N(\bar{\mathbf{x}}) \tag{4.40c}$$

.

In general is very difficult to solve h explicitly. However we can approximate the solutions by making a formal multi-power expansion series for $h(\bar{\Sigma}_+,\bar{\Sigma}_-)=\sum a_{ij}\bar{\Sigma}_+^i\bar{\Sigma}_-^j$ and solving for the coefficients $(\bar{\Sigma}_+,\bar{\Sigma}_-)\to 0$.

The flow on the center manifold reads

$$\frac{d\bar{\Sigma}_+}{dN}=\frac{3}{8}(2-\gamma_{\rm pf})\bar{\Sigma}_+\left(\bar{\Sigma}_+^2+\bar{\Sigma}_-^2\right)^2,\quad \frac{d\bar{\Sigma}_-}{dN}=\frac{3}{8}(2-\gamma_{\rm pf})\bar{\Sigma}_-\left(\bar{\Sigma}_+^2+\bar{\Sigma}_-^2\right)^2 \tag{4.41}$$

and therefore it is two dimensional unstable center manifold.

The remaining other two equivalent fixed points in the intersection of $T=0$ with a pure scalar field subset are

$$\mathrm{dS}_0^{\pm}:\quad X=\pm 1,\quad \Sigma_\phi=0,\quad \Sigma_+=0,\quad \Sigma_-=0,\quad T=0 \tag{4.42}$$

and corresponds to a quasi-de-Sitter state with $q=-1$. The linearisation around these fixed points yields the eigenvalues $-3\gamma_{\rm pf}$, -3, -3, -3, and 0 with the associated eigenvectors $(1,0,0,0,0)$, $(0,1,0,0,0)$, $(0,0,1,0,0)$, $(0,0,0,1,0)$, and $(0,\mp\frac{n}{3},0,0,1)$. The fixed points $\mathrm{dS}_0^{\pm}$ have four negative eigenvalues (since $\gamma_{\rm pf}>0$) and a zero eigenvalue corresponding to a center manifold. Due to the monotonicity of T it is clear that a single orbit originates from each $\mathrm{dS}_0^{\pm}$ into $\mathbf{S}$ corresponding to the 1-dimensional center manifold (see A.5) of each fixed point. This center manifold is usually called the *inflationary attractor solution*. Again to solve the center manifold problem we will make use of the system (4.7) for the unbounded variable $\tilde{T}$, and introduce the adapted variables

$$\bar{X}=X\mp 1,\quad \bar{\Sigma}_\phi=\Sigma_\phi\mp\frac{n}{3}\tilde{T},\quad \bar{\Sigma}_+=\bar{\Sigma}_+,\quad \bar{\Sigma}_-=\Sigma_-,\quad \bar{T}=\tilde{T} \tag{4.43}$$

which leads to the adapted system

$$\begin{aligned}&\frac{d\bar{X}}{dN}=-3\gamma_{\rm pf}\bar{X}+F(\bar{\mathbf{x}}),\quad \frac{d\bar{\Sigma}_\phi}{dN}=-3\bar{\Sigma}_\phi+G(\bar{\mathbf{x}}),\quad \frac{d\bar{\Sigma}_+}{dN}=-3\bar{\Sigma}_++H_+(\bar{\mathbf{x}})\\ &\frac{d\bar{\Sigma}_-}{dN}=-3\bar{\Sigma}_-+H_-(\bar{\mathbf{x}}),\quad \frac{d\bar{T}}{dN}=N(\bar{\mathbf{x}})\end{aligned} \tag{4.44}$$

here $\bar{\mathbf{x}} = (\bar{X}, \bar{\Sigma}_\phi, \bar{\Sigma}_+, \bar{\Sigma}_-, \bar{T})$ and F, G, $H_\pm$, and N are functions of higher order. With this new adapted variables we relocated the fixed points $K^\pm$ to the origin of coordinates $(\bar{x}) = (0,0,0,0,0)$. The 1-dimensional center manifold can be locally represented by the graph $h : E^c \to E^s$, i.e, $\left(\bar{X}, \bar{\Sigma}_\phi, \bar{\Sigma}_+, \bar{\Sigma}_-\right) = \left(h_1\left(\bar{T}\right), h_2\left(\bar{T}\right), h_3\left(\bar{T}\right), h_4\left(\bar{T}\right)\right)$ satisfying the fixed point $h(0) = 0$ and the tangency $\frac{dh(0)}{d\bar{T}} = 0$ conditions which solves the following nonlinear partial differential equations

$$N(\bar{\mathbf{x}})h_i'(\bar{T}) = \lambda_i h_i(\bar{T}) + \bar{\mathbf{F}}_i(\bar{\mathbf{x}}), \quad i = 1,2,3,4 \tag{4.45}$$

where $h_i'(\tilde{T})$ is the first derivative of h with respect to $\bar{T}$, $\lambda_i = (-3\gamma_{\rm pf}, -3, -3, -3)$ and $\bar{\mathbf{F}}_i(\bar{\mathbf{x}}) = (F(\bar{\mathbf{x}}), G(\bar{\mathbf{x}}), H_+(\bar{\mathbf{x}}), H_-(\bar{\mathbf{x}}))$. In general founding an explicit solution of h can be very challenging and almost impossible, however, we can approximate the solutions using Taylor power series expansion for $h(\tilde{T}) = \sum a_i \tilde{T}i$ so using the expansion $(\bar{X} \pm 1)^{2n} = 1 \pm 2n\bar{X} + \binom{2n}{2n-2}\bar{X}^2 + ...$ and solving the resulting linear system of equations for the coefficients of the expansion as $\tilde{T} \to 0$,

$$X = \pm 1 \mp \frac{n}{18}\tilde{T}^2 \pm \frac{n^2}{648}(5-2n)\tilde{T}^4 + \mathcal{O}(\tilde{T}^6) \tag{4.46a}$$

$$\Sigma_\phi = \mp\frac{n}{3}\tilde{T}\left(1 \mp \frac{n}{18}\tilde{T}^2 \pm \frac{n^2}{648}(17-6n)\tilde{T}^4\right) + \mathcal{O}(\tilde{T}^7) \tag{4.46b}$$

$$\Sigma_\pm = 0 \tag{4.46c}$$

Therefore, it follows that to the leading order on the center manifold

$$\frac{d\tilde{T}}{dN} = \frac{n}{3}\tilde{T}^3 + \mathcal{O}(\tilde{T}^4), \quad \text{as} \quad \tilde{T} \to 0 \tag{4.47}$$

which shows explicitly that $\mathrm{dS}_0^\pm$ are center saddles with unique center manifold orbit originating from each fixed point into the interior orbit of **S**.

The circular line of fixed points that lie in the intersection of $T = 0$ with the pure anisotropic subset $\{\Sigma_\sigma = 1\}$ are

$$\mathrm{L}_\Sigma: \quad X = 0, \quad \Sigma_\phi = 0, \quad \Sigma_+ = \Sigma_0, \quad \Sigma_- = \pm\sqrt{1-\Sigma_0^2}, \quad T = 0 \tag{4.48}$$

which has $q = 2$ and corresponds to the Kasner vacuum solution. The linearisation around these line of fixed points yields the eigenvalues $\frac{3}{n}$, 0, 0, $3(2-\gamma_{\rm pf})$, and $\frac{3}{n}$ with associated eigenvectors $(1,0,0,0,0)$, $(0,1,0,0,0)$, $(0,0,\pm\frac{\Sigma_0}{\sqrt{1-\Sigma_0^2}}1,0)$, $(0,0,\mp\frac{\sqrt{1-\Sigma_0^2}}{\Sigma_0},1,0)$ and $(0,0,0,0,1)$. In the $\{\Omega_\phi = 0\}$ subset, L_Σ is a semi-hyperbolic source and the same can be said for the line of fixed points in the $\{\Sigma_\sigma = 0\}$ subset. We have a center manifold between two subsets. Doing a similar approach as in (4.40) but using (Σ_ϕ, Σ_+) as independent variables we see that

$$\frac{d\Sigma_\phi}{dN} = \frac{3}{8}(2-\gamma_{\rm pf})\Sigma_\phi\left(\Sigma_\phi^2 + \left(\frac{\Sigma_+}{\Sigma_0}\right)^2\right), \qquad \frac{d\Sigma_+}{dN} = \frac{3}{8}(2-\gamma_{\rm pf})\Sigma_+\left(\Sigma_\phi^2 + \left(\frac{\Sigma_+}{\Sigma_0}\right)^2\right) \tag{4.49}$$

and therefore it is a two dimensional unstable center manifold.

The last fixed point, is located at the intersection of $T = 0$ with the pure matter subset $\{\Omega_\phi = 1\}$, as is given by

$$\mathrm{FL}_0: \quad X = 0, \quad \Sigma_\phi = 0, \quad \Sigma_+ = 0, \quad \Sigma_- = 0, \quad T = 0 \tag{4.50}$$

with $q = \frac{1}{2}(3\gamma_{\rm pf} - 2)$ corresponding to the flat FL self-similar solution. The linearisation around this fixed point yields the eigenvalues $\frac{3}{2n}\gamma_{\rm pf}$, $-\frac{3}{2}(2-\gamma_{\rm pf})$, $-\frac{3}{2}(2-\gamma_{\rm pf})$, $-\frac{3}{2}(2-\gamma_{\rm pf})$ and $\frac{3}{2n}\gamma_{\rm pf}$ where the eigenvectors are the canonical basis of $\mathbb{R}^5$. Since $\gamma_{\rm pf} \in (0,2)$, FL_0 has two positive real eigenvalues and three negative real eigenvalues, being a hyperbolic saddle, and the α-limit point of a 1-parameter set of orbits n $\mathbf{S}$.

We can now show that on $T = 0$ the above fixed points are the only possible α-limit sets where the structure on $T = 0$ consists only of heteroclinic orbits that connect these fixed points.

Lemma 4.6. *The $T = 0$ invariant boundary consists only of heteroclinic orbits connecting the fixed points as depicted in Fig.4.3*

Proof. Taking into considerations the monotonic functions, Z_1, Z_2 and Z_3, a straightforward inspection of $\{\Sigma_\sigma = 1\}$ show us that this is a 2-dimensional subset consisting of heteroclinic orbits $\mathrm{L}_\Sigma \to \mathrm{FL}_0$. Moreover it is also easy to check that $\{\Sigma_\phi = 0\}$ and $\{X = 0\}$ are 1-dimensional subsets consisting of heteroclinic orbits $\mathrm{FL}_0 \to \mathrm{dS}_0^\pm$, and $\mathrm{K}^\pm \to FL_0$ respectively. Therefore the two axis will divide the deformed circle $\{X^{2n} + \Sigma_\phi^2 = 1\}$ consisting of heteroclinic orbits $\mathrm{K}^+ \to \mathrm{dS}_0^\pm$ and $\mathrm{K}^- \to \mathrm{dS}_0^\pm$ into 4-invariant quadrants. Since we don't have any fixed points in the interior of each quadrant by the *index theorem* we also don't have closed curves. It follows by the *Poincaré-Bendixson theorem* that each quadrant consists of heteroclinic orbits connecting the fixed points. A similar approach can be taken when looking to the Kasner circle. Since we don't have any fixed point in the interior of Kasner circle other than the FL_0 then by the index theorem (see A.28) we have no closed curves. So by the Poincaré-Bendixson theorem (see A.25) the interior of the Kasner circle consists only of heteroclinic orbits connecting each point of the circle to FL_0. Moreover in this case the $T = 0$ invariant boundary admits the following conserved quantity.

$$\mathbf{S}_{\mathrm{pf},\phi}: \quad \Sigma_\phi{}^{\gamma_{\rm pf}} X^{(2-\gamma_{\rm pf})n}\Omega_\phi = const, \tag{4.51a}$$

$$\mathbf{S}_{\mathrm{pf},\sigma}: \quad \Sigma_+\Sigma_-^{-1} = const \tag{4.51b}$$

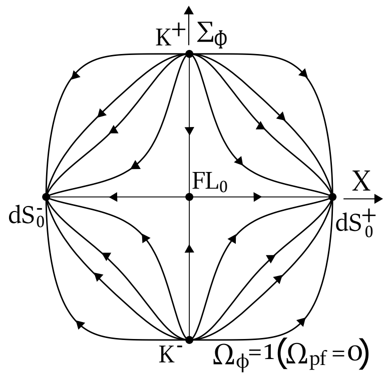

(A) $\Sigma = 0$ plane in the $T = 0$ boundary.

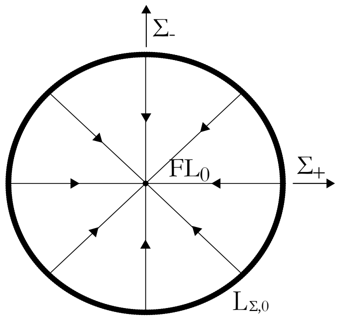

(B) The Kasner circle in the $\Omega_\phi = 0$ plane in the $T = 0$ boundary.

FIGURE 4.3: he invariant $T = 0$ boundary and the invariant subset for a monomial potential $V = \frac{1}{4}(\lambda\phi)^4$.

which determines the solution trajectories on $T = 0$, see Figure 4.3 □

Theorem 4.7. *The α-limit set of orbits consists of fixed points on $T = 0$. In particular as $\tau \to -\infty$ ($N \rightarrowtail -\infty$), a 2-parameter set of orbits converge to each $\mathrm{K}^{\pm}$, with asymptotics*

$$X(N) = (C_X \pm C_T N)\, e^{\frac{3}{n}N}, \quad \Sigma_\phi(N) = \pm 1 + C_\Sigma e^{3(2-\gamma_{\rm pf})N}, \quad \tilde{T}(N) = C_T e^{\frac{3}{n}N} \tag{4.52a}$$

$$\Sigma_+ = \pm\left(\frac{3}{2}(2-\gamma_{\rm pf})(1+C_{\Sigma_+})^2 N + 8C_{\Sigma_-}\right)^{-\frac{1}{4}}, \quad \Sigma_- = \pm C_{\Sigma_+}\left(\frac{3}{2}(2-\gamma_{\rm pf})(1+C_{\Sigma_+})^2 N + 8C_{\Sigma_-}\right)^{-\frac{1}{4}} \tag{4.52b}$$

with C_X, C_Σ, C_{Σ_+}, $C_{\Sigma_-} > 0$ and $C_T > 0$. A unique center manifold converge to each $\mathrm{dS}_0^{\pm}$, with asymptotics

$$X(N) = \pm 1 \mp \frac{n}{18}\left(1 - \frac{2n}{N}\right)^{-1}, \quad \Sigma_\phi(N) = \mp\frac{n}{3}\left(1-\frac{2n}{N}\right)^{-1/2} \quad \tilde{T}(N) = \left(1 - \frac{2n}{N}\right)^{-1/2} \tag{4.53a}$$

$$\Sigma_+(N) = 0, \quad \Sigma_-(N) = 0. \tag{4.53b}$$

A 2-parameter set converges to each point on the line of fixed points, $\mathbf{L}_\Sigma$, with asymptotics

$$X(N) = C_X e^{\frac{3}{n}N}, \quad \Sigma_\phi(N) = -\frac{nC_T}{6C_X}\left(C_X e^{\frac{3}{n}N}\right)^{2n}, \quad \tilde{T} = C_T e^{\frac{3}{n}N} \tag{4.54a}$$

$$\Sigma_+(N) = \mp\Sigma_{0+}\sqrt{1-\Sigma_0^2}\left(1 - e^{3(2-\gamma_{\rm pf})N}\right) C_{\Sigma_-} + C_{\Sigma_+}\left(1 - \Sigma_0^2\left(1 - e^{3(2-\gamma_{\rm pf})N}\right)\right) \tag{4.54b}$$

$$\Sigma_-(N) = \pm\Sigma_0\sqrt{1-\Sigma_{0+}^2}\left(1 - e^{3(2-\gamma_{\rm pf})N}\right) C_{\Sigma_+} + C_{\Sigma_-}\left(1 - \Sigma_0^2\left(1 - e^{3(2-\gamma_{\rm pf})N}\right)\right). \tag{4.54c}$$

with C_X*,* C_{Σ_+}*,* C_{Σ_-} *and* $C_T > 0$*. A* 1*-parameter set converges to* FL_0 *with asymptotics*

$$X(N) = C_X e^{\frac{3\gamma_{\rm pf}}{2n}N}, \quad \Sigma_\phi(N) = 0, \quad \Sigma_+(N) = 0, \quad \Sigma_-(N) = 0, \quad \tilde{T} = C_T e^{\frac{3\gamma_{\rm pf}}{2n}N} \tag{4.55}$$

with C_X*, and* $C_T > 0$*.*

Proof. The proof follows by Lemmas 4.1, and 4.6, and the local analysis of fixed points. □

Remark 4.8. *The orbit solutions which approach* $K^{\pm}$ *behaves as the self-similar massless scalar field or kinaton solution, the ones approaching* $\mathbf{L}_\Sigma$ *behaves as the self-similar Kasner vacuum solution, and the orbits approaching* FL_0 *as the self-similar Friedmann-Lemaître solution whose asymptotics towards the past exhibit well-known Big-Bang singularities. In context of cosmological inflation, the physical interesting solution is the inflationary attractor solution, i.e. the center manifold originating from* $\mathrm{dS}_0^{\pm}$ *whose asymptotics are given by*

$$n=1: \quad H \sim -t, \quad \phi \sim -t, \quad \sigma \sim 0, \quad \rho_{\rm pf} \sim (-t)^{-2}, \quad as \quad t \to -\infty \tag{4.56a}$$
$$n=2: \quad H \sim e^{-\frac{2}{3}t}, \quad \phi \sim e^{-\frac{t}{3}}, \quad \sigma \sim 0, \quad \rho_{\rm pf} \sim e^{\frac{-4}{3}t}, \quad as \quad t \to -\infty \tag{4.56b}$$
$$n\geq 3: \quad H \sim (-t)^{\frac{n}{n-2}}, \quad \phi \sim (-t)^{\frac{2}{n-2}}, \quad \sigma \sim 0, \quad \rho_{\rm pf} \sim (-t)^{-\frac{2n}{n-2}}, \quad as \quad t \to -\infty \tag{4.56c}$$

4.3.2 The $T = 1$ Boundary

On the $T = 1$ boundary, the system (4.13) reduces to

$$\frac{dX}{d\tau} = \Sigma_\phi, \quad \frac{d\Sigma_\phi}{d\tau} = -nX^{2n-1}, \quad \frac{d\Sigma_+}{d\tau} = 0, \quad \frac{d\Sigma_-}{d\tau} = 0, \quad \frac{dT}{d\tau} = 0. \tag{4.57}$$

System (4.57) presents one fixed point in the $\{\Sigma_\sigma = 0\}$ subset and an infinite amount of fixed points displayed on the disk $\{\Sigma_+^2 + \Sigma_-^2 \leq 1\}$ in the pure anisotropic subset. The fixed points are

$$\mathrm{FL}_1: \quad X = 0, \quad \Sigma_\phi, \quad \Sigma_+ = c_1, \quad \Sigma_- = c_2, \quad T = 1, \tag{4.58}$$

where $c_1, c_2 \in [-1, 1]$ and $\Omega_{\rm pf} = 1 - c_1^2 - c_2^2$. Notice that when $c_1 = c_2 = 0$ we only have one fixed point that corresponds to the flat FL solution similar to the one found in [68]. This fixed points have null eigenvalues however FL_1 resides in the intersection between two invariant subsets: the $T = 1$ invariant subset and the $\Omega_\phi = 0$ subset. The infinite disk of fixed points is located in (Σ_+, Σ_-)-plane and can be seen in Fig. 4.4a.

On $T = 1$ we see that

$$\Omega_\phi = X^{2n} + \Sigma_\phi^2 = const, \quad \Sigma_\sigma = \Sigma_+^2 + \Sigma_-^2 \tag{4.59}$$

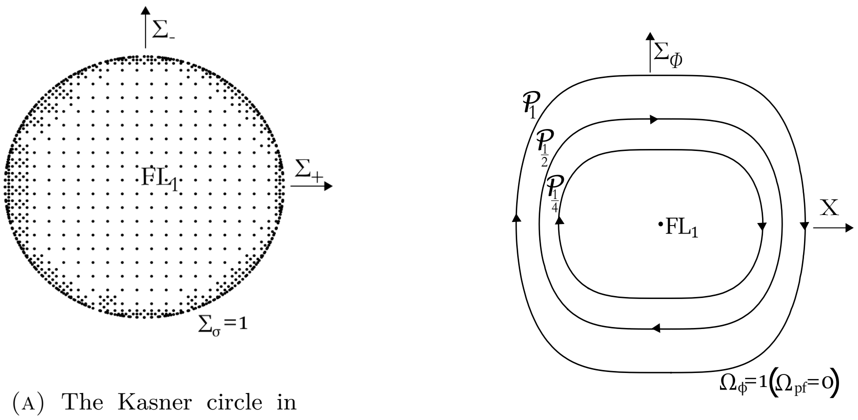

(A) The Kasner circle in the $\Omega_\phi = 0$ plane in the $T = 1$ boundary.

(B) $\Sigma = 0$ plane in the $T = 1$ boundary..

FIGURE 4.4: he invariant $T = 0$ boundary and the invariant subset for a monomial potential $V = \frac{1}{4}(\lambda\phi)^4$.

so the subset $T = 1$ is foliated by periodic orbits in the neighbourhood of fixed points FL_1 in the (X, Σ_ϕ)-plane, see Fig. 4.4b. Instead of studying this infinite amount of fixed points we will use averaging theory alongside the auxiliary functions (4.14) to see the behaviour of the internal orbits in the $T = 1$ boundary and reduce a disk of infinite fixed points into a line of infinite fixed points.

Theorem 4.9. *Consider the system (4.13) with* $0 < \Omega_{\mathrm{pf}} < 1$ *and* $\gamma_{\mathrm{pf}} \in (0, 2)$*:*

(i) If $\gamma_{\mathrm{pf}} > \langle\gamma_\phi\rangle$*, then all solutions will converge to the outer periodic orbit* $\mathcal{P}_1$ *with* $\Omega_{\mathrm{pf}} = 0$ *and* $\Sigma_\sigma = 0$*.*

(ii) If $\gamma_{\mathrm{pf}} < \langle\gamma_\phi\rangle$ *then all solutions will converge to the fixed point* FL_1 *with* $\Omega_{\mathrm{pf}} = 1$*.*

(iii) If $\gamma_{\mathrm{pf}} = \langle\gamma_\phi\rangle$*, then a* 1*-parameter set of solutions converge to each inner periodic orbit* $\mathcal{P}_{\Omega_\phi}$*.*

Proof. To prove this theorem we need to use Lemma 4.1 alongside with generalized averaging techniques based on the methods used in [50, 68, 80]. We make the same approach regarding ϵ as previous seen in Chapters 2-3. So given real function f, its average over a time period associated to Ω_ϕ is given by

$$\langle f\rangle = \frac{1}{P(\Omega_\phi)}\int_{\tau_0}^{\tau_0+P(\Omega_\phi)} f(\tau)d\tau. \tag{4.60}$$

Taking the time averaging for $\frac{dX}{d\tau}$ in (4.57) and using the equation for Σ_ϕ it gives

$$\frac{d}{d\tau}\left(X\frac{dX}{d\tau}\right) - \left(\frac{dX}{d\tau}\right)^2 + nX^{2n} = 0. \tag{4.61}$$

Taking the time averaging for the orbit we get

$$\left\langle \left(\frac{dX}{d\tau}\right)^2 \right\rangle = \langle \Sigma_\phi^2 \rangle = n\langle X^{2n}\rangle. \tag{4.62}$$

Thus, using this result for a periodic orbit on $T = 1$ in (4.10) we get

$$\langle \gamma_\phi \rangle = \frac{2n}{n+1}. \tag{4.63}$$

We now set $\epsilon(\tau) = 1 - T(\tau)$ and consider the system

$$\frac{d\Omega_\phi}{d\tau} = 3\epsilon \left[(\gamma_{\rm pf} - \gamma_\phi)(1-\Omega_\phi) + (2-\gamma_{\rm pf})\Sigma_\sigma^2 \right] \Omega_\phi \tag{4.64a}$$

$$\frac{d\Sigma_\sigma}{d\tau} = -\frac{3}{2}\epsilon \left[(2-\gamma_{\rm pf})(1-\Sigma_\sigma^2) + (\gamma_{\rm pf} - \gamma_\phi)\Omega_\phi \right] \Sigma_\sigma \tag{4.64b}$$

$$\frac{d\epsilon}{d\tau} = -\frac{1}{n}\epsilon^2(1-\epsilon)(1+q) \tag{4.64c}$$

where $(X, \Sigma_\phi, \Sigma_+, \Sigma_-)$ solves (4.13) and

$$q + 1 = \frac{3}{2}(2\Sigma_\phi^2 + 2\Sigma_+^2 + 2\Sigma_-^2 + \gamma_{\rm pf}(1 - \Omega_\phi - \Sigma_\sigma^2)). \tag{4.65}$$

The general idea of this averaging method is based on making the near identity transformation

$$\Omega_\phi(\tau) = y(\tau) + \epsilon(\tau) w(y, z, \tau, \epsilon) \tag{4.66a}$$

$$\Sigma_\sigma(\tau) = z(\tau) + \epsilon(\tau) g(y, z, \tau, \epsilon), \tag{4.66b}$$

and then prove that the evolution of the variables y and z are approximated, at first order, by the solution of $\bar{y}$ and $\bar{z}$ respectively of the averaged equation.

So starting with y the evolution equation for this new variable can be obtained using equations (4.64a) and (4.64c) together with the evolution equation for Ω_ϕ. This then gives

$$\begin{aligned}
\frac{dy}{d\tau} &= \left(1 + \epsilon\frac{\partial w}{\partial y}\right)^{-1} \left[\frac{d\Omega_\phi}{d\tau} - \left(w + \epsilon\frac{\partial w}{\partial \epsilon}\right)\frac{d\epsilon}{d\tau} - \epsilon\frac{\partial w}{\partial \tau} - \epsilon\frac{\partial w}{\partial z}\frac{dz}{d\tau} \right] \\
&= \left(1 + \epsilon\frac{\partial w}{\partial y}\right)^{-1} \Bigg[3\epsilon \left((\gamma_{\rm pf} - \langle\gamma_\phi\rangle)\, y\,(1-y) + (\langle\gamma_\phi\rangle - \gamma_\phi)\, y(1-y) + (2-\gamma_{\rm pf}) y z^2 \right) \\
&- 3\epsilon^2 \left((\gamma_{\rm pf} - \gamma_\phi)(1-2y)\, w + w\,(2-\gamma_{\rm pf})\, z^2 + g(2-\gamma_{\rm pf}) y \right) \\
&+ 3\epsilon^3 \left((2-\gamma_{\rm pf})\, g w - (\gamma_{\rm pf} - \gamma_\phi)\, w^2 + (2-\gamma_{\rm pf}) g^2 y \right) - \left(w + \epsilon\frac{\partial w}{\partial \epsilon}\right)\frac{d\epsilon}{d\tau} - \epsilon\frac{\partial w}{\partial \tau} - \epsilon\frac{\partial w}{\partial z}\frac{dz}{d\tau} \Bigg].
\end{aligned} \tag{4.67}$$

For z we made a similar thing using the equations (4.64b) and (4.64c) and we get

$$
\begin{aligned}
\frac{dz}{d\tau} &= \left(1+\epsilon\frac{\partial g}{\partial z}\right)^{-1}\left[\frac{d\Sigma_\sigma}{d\tau}-\left(g+\epsilon\frac{\partial g}{\partial \epsilon}\right)\frac{d\epsilon}{d\tau}-\epsilon\frac{\partial w}{\partial \tau}-\epsilon\frac{\partial g}{\partial y}\frac{dy}{d\tau}\right]\\
&= \left(1+\epsilon\frac{\partial g}{\partial z}\right)^{-1}\Bigg[-\frac{3}{2}\epsilon\Big((2-\gamma_{\rm pf})z(1-z^2)+(\gamma_{\rm pf}-\langle\gamma_\phi\rangle)yz+(\langle\gamma_\phi\rangle-\gamma_\phi)yz\Big)\\
&- \frac{3}{2}\epsilon^2\left((2-\gamma_{\rm pf})g\left((1-z)^2-2\right)+(\gamma_{\rm pf}-\gamma_\phi)wz+(\gamma_{\rm pf}-\gamma_\phi)gy\right) \qquad (4.68)\\
&+ \frac{3}{2}\epsilon^3\left((2-\gamma_{\rm pf})zg^2+(2-\gamma_{\rm pf})g^3-(\gamma_{\rm pf}-\gamma_\phi)gw\right)-\left(g+\epsilon\frac{\partial g}{\partial \epsilon}\right)\frac{d\epsilon}{d\tau}-\epsilon\frac{\partial g}{\partial \tau}-\epsilon\frac{\partial g}{\partial y}\frac{dy}{d\tau}\Bigg].
\end{aligned}
$$

Setting

$$
\frac{\partial w}{\partial \tau} = f_1(y,z,\tau,\epsilon)-\langle f_1(y,z,.,0)\rangle = 3\left(\langle\gamma_\phi\rangle y-2\Sigma_\phi^2\right)y\,(1-y) \qquad (4.69a)
$$

$$
\frac{\partial g}{\partial \tau} = f_2(y,z,\tau,\epsilon)-\langle f_2(y,z,.,0)\rangle = 3\,(\gamma_\phi-\langle\gamma_\phi\rangle)\,yz \qquad (4.69b)
$$

and expanding (4.67) and (4.68) in powers of ϵ small enough, we get

$$
\frac{dy}{d\tau} = \epsilon\langle f_1\rangle(y,z)+\epsilon^2 h_1(y,z,w,g,\tau,\epsilon)+\mathcal{O}(\epsilon^3) \qquad (4.70a)
$$

$$
\frac{dz}{d\tau} = \epsilon\langle f_2\rangle(y,z)+\epsilon^2 h_2(y,z,w,g,\tau,\epsilon)+\mathcal{O}(\epsilon^3) \qquad (4.70b)
$$

where

$$
\langle f_1\rangle(y,z) = \langle f_1(y,z,.,0)\rangle = 3(\gamma_{\rm pf}-\langle\gamma_\phi\rangle)y(1-y)+3(2-\gamma_{\rm pf})yz^2 \qquad (4.71a)
$$

$$
\langle f_2\rangle(y,z) = \langle f_2(y,z,.,0)\rangle = -\frac{3}{2}(2-\gamma_{\rm pf})z(1-z^2)-\frac{3}{2}(\gamma_{\rm pf}-\langle\gamma_\phi\rangle)yz \qquad (4.71b)
$$

$$
\begin{aligned}
h_1(.) =& 3\left((\gamma_{\rm pf}-\gamma_\phi)(1-2y)w+w(2-\gamma_{\rm pf})(wz^2+gy)\right)+\frac{1}{n}(1+q)(1-\epsilon)w \qquad (4.71c)\\
&\frac{3}{2}\frac{\partial w}{\partial z}\left((2-\gamma_{\rm pf})z(1-z^2)+(\gamma_{\rm pf}-\langle\gamma_\phi\rangle)yz\right)-3\frac{\partial w}{\partial y}\left((\gamma_{\rm pf}-\langle\gamma_\phi\rangle)y(1-y)+(2-\gamma_{\rm pf})yz^2\right)
\end{aligned}
$$

$$
\begin{aligned}
h_2(.) =& -\frac{3}{2}\left((2-\gamma_{\rm pf})g\left((1-z)^2-2\right)+(\gamma_{\rm pf}-\gamma_\phi)(wz-gy)\right)+\frac{1}{n}(1+q)(1-\epsilon)w \qquad (4.71d)\\
&-3\frac{\partial g}{\partial y}\left((\gamma_{\rm pf}-\langle\gamma_\phi\rangle)y(1-y)+(2-\gamma_{\rm pf})yz^2\right)+\frac{3}{2}\frac{\partial g}{\partial z}\left((2-\gamma_{\rm pf})z(1-z^2)+(\gamma_{\rm pf}-\langle\gamma_\phi\rangle)yz\right).
\end{aligned}
$$

Notice that for large times, $T\approx 1$, $\epsilon\approx 0$, the right-hand side of (4.70a) and (4.70b) is almost periodic meaning that $\langle\gamma_\phi\rangle-\gamma_\phi\approx 0$ which implies that w and g are bounded. So it follows from (4.66) that y and z are also bounded. We can now drop the high order terms in ϵ in (4.70) and study the truncated averaged equation, which leads to then system

$$\frac{d\bar{y}}{d\tau} = 3\epsilon\left(\gamma_{\mathrm{pf}} - \langle\gamma_\phi\rangle\right)\bar{y}\left(1-\bar{y}\right) + 3\epsilon\left(2-\gamma_{\mathrm{pf}}\right)\bar{y}\bar{z}^2 \tag{4.72a}$$

$$\frac{d\bar{z}}{d\tau} = -\frac{3}{2}\epsilon\left(2-\gamma_{\mathrm{pf}}\right)\bar{z}\left(1-\bar{z}^2\right) - \frac{3}{2}\epsilon\left(\gamma_{\mathrm{pf}} - \langle\gamma_\phi\rangle\right)\bar{y}\bar{z} \tag{4.72b}$$

$$\frac{d\epsilon}{d\tau} = -\frac{1}{n}\epsilon^2(1-\epsilon)(1+q). \tag{4.72c}$$

Without loss of generality we can introduce a new time variable

$$\frac{1}{\epsilon}\frac{d}{d\tau} = \frac{d}{d\bar{\tau}}, \tag{4.73}$$

that will reduce the system. The new system reads

$$\frac{d\bar{y}}{d\tau} = 3\left(\gamma_{\mathrm{pf}} - \langle\gamma_\phi\rangle\right)\bar{y}\left(1-\bar{y}\right) + 3\left(2-\gamma_{\mathrm{pf}}\right)\bar{y}\bar{z}^2 \tag{4.74a}$$

$$\frac{d\bar{z}}{d\tau} = -\frac{3}{2}\left(2-\gamma_{\mathrm{pf}}\right)\bar{z}\left(1-\bar{z}^2\right) - \frac{3}{2}\left(\gamma_{\mathrm{pf}} - \langle\gamma_\phi\rangle\right)\bar{y}\bar{z} \tag{4.74b}$$

$$\frac{d\epsilon}{d\tau} = -\frac{1}{n}\epsilon(1-\epsilon)(1+q). \tag{4.74c}$$

Fixed points and stability in the case $\gamma_{\mathrm{pf}} \neq \langle\gamma_\phi\rangle$

For $\gamma_{\mathrm{pf}} \neq \langle\gamma_\phi\rangle$ the dynamical system admits four fixed points. One in scalar field subset ($\Omega_\phi = 1$), two equivalent fixed points in the pure anisotropic subset ($\Sigma_\sigma = 1$) and one isolated fixed point in the pure matter subset ($\Omega_{\mathrm{pf}} = 1$). The first fixed point is located on the intersection of $\epsilon = 0$ ($T = 1$) with the pure scalar field subset and is

$$F_1: \quad \bar{y} = 1, \quad \bar{z} = 0, \quad \epsilon = 0. \tag{4.75}$$

The linearisation around this fixed point yields to the eigenvalues $-3(\gamma_{\mathrm{pf}} - \langle\gamma_\phi\rangle)$, $-\frac{3}{2}(2-\langle\gamma_\phi\rangle)$, and $-\frac{3\langle\gamma_\phi\rangle}{2n}$ were the associated eigenvectors are the canonical basis of $\mathbb{R}^3$.

The two equivalent fixed points located in the intersection of $\epsilon = 0$ with the pure anisotropic subset are

$$F_2^{\pm}: \quad \bar{y} = 0, \quad \bar{z} = \pm 1, \quad \epsilon = 0. \tag{4.76}$$

The linearisation around this fixed points yields to the eigenvalues $3(2-\langle\gamma_\phi\rangle)$, $3(2-\gamma_{\mathrm{pf}})$ and $-\frac{3}{n}$ whose eigenvectors are $(\mp 2, 1, 0)$, $(0, 1, 0)$ and $(0, 0, 1)$.

The isolated fixed point is

$$F_3: \quad \bar{y} = 0, \quad \bar{z} = 0, \quad \epsilon = 0, \tag{4.77}$$

the linearisation around this fixed points yields to the eigenvalues $3(\gamma_{\mathrm{pf}} - \langle\gamma_\phi\rangle)$, $-\frac{3}{2}(2-\gamma_{\mathrm{pf}})$, and $-\frac{3\gamma_{\mathrm{pf}}}{2n}$ whose eigenvectors are the canonical basis of $\mathbb{R}^3$.

Regarding the eigenvalues of each fixed point we need to split the analysis depending on the sign of $\gamma_{\rm pf} - \langle \gamma_{\rm pf} \rangle$.

- If $\gamma_{\rm pf} > \langle \gamma_\phi \rangle$, F_1 has three negative eigenvalues since $\langle \gamma_\phi \rangle \in (0,2)$ so it is a hyperbolic sink. For $F_2^{\pm}$ since $\gamma_{\rm pf} \in (0,2)$ we see that two eigenvalues are positive and the one in the ϵ-direction is negative, so $F_2^{\pm}$ is an hyperbolic saddle, being a source in the $\{\epsilon = 0\}$-subset. Lastly F_3 as two negative eigenvalues and one positive eigenvalue being a hyperbolic saddle. So in this case F_1 is the future attractor, so the universe will asymptotically approach the pure scalar field solution when $\bar{\tau} \to +\infty$.
- If $\gamma_{\rm pf} < \langle \gamma_\phi \rangle$, F_1 has two negative eigenvalues an one positive eigenvalue so it is a hyperbolic saddle. Regarding $F_2^{\pm}$ we have two positive eigenvalues and one negative eigenvalue, moreover in the $\{\epsilon = 0\}$ subset $F_2^{\pm}$ is a hyperbolic source. Lastly, F_3 has three negative eigenvalues being a hyperbolic sink. In this case F_3 is the future attractor, so the universe will asymptotically approach the the flat FL solution when $\bar{\tau} \to +\infty$.

Convergence of the solutions in the case $\gamma_{\rm pf} - \langle \gamma_\phi \rangle$

Now we need to prove that the variables y and Ω_ϕ follows this evolution and the same need to be done for z and Σ_σ.

We start by introducing two new variables

$$|\eta(\tau)| := |y(\tau) - \bar{y}(\tau)|, \quad |\zeta(\tau)| := |z(\tau) - \bar{z}(\tau)| \tag{4.78}$$

that we need to estimate. In order to do so we define the sequences $\{\tau_n\}$ and $\{\epsilon_n\}$ such that $\epsilon_n = \epsilon(\tau_n)$, with $n \in \mathbb{N}$ and

$$\tau_{\rm n+1} - \tau_n = \frac{1}{\epsilon_n}, \quad \tau_0 = 0, \quad \epsilon_0 > 0 \tag{4.79}$$

where $\lim \tau_n = +\infty$ and $\lim \epsilon_n = 0$. So starting with the estimation of $|\eta(\tau)|$ we get

$$
\begin{aligned}
|\eta(\tau)| &= \Big| \int_{\tau_n}^{\tau} 3\epsilon(\gamma_{\mathrm{pf}} - \langle\gamma_\phi\rangle)y(1-y) + 3\epsilon(2-\gamma_{\mathrm{pf}})yz^2 + \epsilon^2 h_1(y,z,w,g,s,\epsilon)ds \\
&- \int_{\tau_n}^{\tau} \left(3\epsilon(\gamma_{\mathrm{pf}} - \langle\gamma_\phi\rangle)\right) \bar{y}(1-\bar{y}) + 3\epsilon(2-\gamma_{\mathrm{pf}})\bar{y}\bar{z}^2 \Big| \\
&\leq 3\epsilon_n \int_{\tau_n}^{\tau} \underbrace{|\gamma_{\mathrm{pf}} - \langle\gamma_\phi\rangle|}_{|.|\leq C_1} |(y-\bar{y})| \underbrace{|1-(y+\bar{y})|}_{|.|\leq 1} ds + 3\epsilon_n \int_{\tau_n}^{\tau} \underbrace{|2-\gamma_{\mathrm{pf}}|}_{C_2} \underbrace{|yz^2 - \bar{y}\bar{z}^2|}_{|.|\leq|y-\bar{y}|+|z^2-\bar{z}^2|} ds \\
&+ \epsilon_n^2 \int_{\tau_n}^{\tau} \underbrace{|h_1(y,z,w,g,s,\epsilon)|}_{|.|M_1} ds + \mathcal{O}(\epsilon_n^3) \\
&\leq 3\epsilon_n (C_1 + C_2) \int_{\tau_n}^{\tau} |\eta(s)|ds + 3\epsilon_n \int_{\tau_n}^{\tau} \underbrace{|z^2 - \bar{z}^2|}_{|.|\leq|z-\bar{z}||z+\bar{z}|\leq 2|z-\bar{z}|} + \epsilon_n^2 M_1(\tau - \tau_n) + \mathcal{O}(\epsilon_n^3) \\
&\leq 3\epsilon_n (C_1 + C_2) \int_{\tau_n}^{\tau} |\eta(s)|ds + 6C_2\epsilon_n \int_{\tau_n}^{\tau} |\zeta(s)|ds + \epsilon_n^2 M_1(\tau - \tau_n) + \mathcal{O}(\epsilon_n^3). \qquad (4.80)
\end{aligned}
$$

For $|\zeta(\tau)| = |z(\tau) - \bar{z}(\tau)|$, in this case we get

$$
\begin{aligned}
|\zeta(\tau)| &= \Big| \int_{\tau_n}^{\tau} -\frac{3}{2}\epsilon\,(2-\gamma_{\mathrm{pf}})\,z(1-z^2) - \frac{3}{2}\epsilon\,(\gamma_{\mathrm{pf}} - \langle\gamma_\phi\rangle)\,yz + \epsilon^2 h_2(y,z,w,g,s,\epsilon)ds \\
&- \int_{\tau_n}^{\tau} \left(-\frac{3}{2}\epsilon\,(2-\gamma_{\mathrm{pf}})\,\bar{z}(1-\bar{z}^2) - \frac{3}{2}\epsilon\,(\gamma_{\mathrm{pf}} - \langle\gamma_\phi\rangle)\,\bar{y}\bar{z}\right) \Big| \\
&\leq \frac{3}{2}\epsilon_n \int_{\tau_n}^{\tau} \underbrace{|2-\gamma_{\mathrm{pf}}|}_{|.|\leq C_2} |z-\bar{z}| \underbrace{|1 - z\bar{z} - z^2 - \bar{z}^2|}_{|.|\leq 2} ds + \frac{3}{2}\epsilon_n \int_{\tau_n}^{\tau} \underbrace{|\gamma_{\mathrm{pf}} - \langle\gamma_\phi\rangle|}_{|.|\leq C_1} \underbrace{|yz - \bar{y}\bar{z}|}_{|.|\leq|y-\bar{y}|+2|z-\bar{z}|} ds \\
&+ \epsilon_n^2 \int_{\tau_n}^{\tau} \underbrace{|h_2(y,z,w,g,s,\epsilon)|}_{|.|\leq M_2} ds + \mathcal{O}(\epsilon_n^3) \\
&\leq 3\epsilon_n (C_1 + C_2) \int_{\tau_n}^{\tau} |\zeta(s)|ds + \frac{3}{2}\epsilon_n C_1 \int_{\tau_n}^{\tau} |\eta(s)|ds + \epsilon_n^2 M_2(\tau - \tau_n) + \mathcal{O}(\epsilon_n^3). \qquad (4.81)
\end{aligned}
$$

where C_1, C_2, M_1, and M_2 are positive constants.

Let's introduce a new function $|\psi(\tau)| = |\eta(\tau)| + |\zeta(\tau)|$ so adding the two above equations to each other we get

$$
\begin{aligned}
|\psi(\tau)| &= 3\epsilon_n (C_1 + C_2) \int_{\tau_n}^{\tau} |\eta(s)|ds + 6C_2\epsilon_n \int_{\tau_n}^{\tau} |\zeta(s)|ds + \epsilon_n^2 M_1(\tau - \tau_n) \\
&+ 3\epsilon_n (C_1 + C_2) \int_{\tau_n}^{\tau} |\zeta(s)|ds + \frac{3}{2}\epsilon_n C_1 \int_{\tau_n}^{\tau} |\eta(s)|ds + \epsilon_n^2 M_2(\tau - \tau_n) + \mathcal{O}(\epsilon_n^3) \\
&= 3\epsilon_n(C_1 + C_2) \int_{\tau_n}^{\tau} (|\eta(s)| + |\zeta(s)|)\,ds + 6C_2\epsilon_n \int_{\tau_n}^{\tau} |\zeta(s)|ds + \frac{3}{2}\epsilon_n C_1 \int_{\tau_n}^{\tau} |\eta(s)|ds \\
&+ \epsilon_n^2(M_1 + M_2)(\tau - \tau_n) + \mathcal{O}(\epsilon_n^3)
\end{aligned}
$$

Using the fact that

$$
6C_2 \int_{\tau_n}^{\tau} |\zeta(s)|ds + \frac{3}{2}C_1 \int_{\tau_n}^{\tau} |\eta(s)|ds \leq 2\max\{6C_2, \frac{3}{2}C_1\} \left(\int_{\tau_n}^{\tau} |\zeta(s)|ds + \int_{\tau_n}^{\tau} |\eta(s)|ds \right)
$$

we get

$$|\eta(\tau)| \leq \epsilon_n C_* \int_{\tau_n}^{\tau} |\psi(s)| ds + \epsilon_n^2 M_*(\tau - \tau_n) \tag{4.82}$$

$$\leq \epsilon_n \frac{M_*}{C_*} \left(e^{C_* \epsilon_n (\tau - \tau_n)} - 1 \right) + \mathcal{O}(\epsilon_n^2) \tag{4.83}$$

where $C_* = 3\,(C_1 + C_2) + 2\max\{6C_2, \frac{3}{2}C_1\}$ and $M_* = M_1 + M_2$ are positive constants .

So for $\tau - \tau_n \in [0, 1/\epsilon_n]$ the above inequality becomes

$$|\psi(\tau)| \leq \epsilon_n K \tag{4.84}$$

where $K > 0$. Since $|\psi(\tau)| = |\eta(\tau)| + |\zeta(\tau)| \to 0$ as $\epsilon_n \to 0$ it follows that $|\eta(\tau)| \to 0$ and $|\zeta(\tau)| \to 0$ as $\epsilon_n \to 0$. It follows than from (4.66a) , the triangle inequality, and the fact that $\epsilon \to 0$ as $\tau \to +\infty$, it follows from that Ω_ϕ has the same limit as $\bar{y}$ and, therefore converges for 0 or 1 depending on the sign of $\gamma_{\rm pf} - \langle\gamma_\phi\rangle$. Regarding Σ_σ using (4.66b), the triangle inequality and $\epsilon \to 0$ as $\tau \to +\infty$, it follow that Σ_σ goes to zero since the system will converge to the point $(\Omega_\phi, \Sigma_\sigma, \epsilon) = (1, 0, 0)$ if $\gamma_{\rm pf} > \langle\gamma_\phi\rangle$ and will converge to the point $(\Omega_\phi, \Sigma_\sigma, \epsilon) = (0, 0, 0)$ if $\gamma_{\rm pf} < \langle\gamma_\phi\rangle$. This completes the proof for the cases (i) and (ii) of the theorem.

Fixed points and stability in the case $\gamma_{\rm pf} = \langle\gamma_\phi\rangle$

Now we analyse the case $\gamma_{\rm pf} = \langle\gamma_\phi\rangle$. In this case our averaged system (4.74) reads

$$\frac{d\bar{y}}{d\tau} = 3(2 - \gamma_{\rm pf})\bar{y}\bar{z}^2 \tag{4.85a}$$

$$\frac{d\bar{z}}{d\tau} = -\frac{3}{2}(2 - \gamma_{\rm pf})\bar{z}(1 - \bar{z}^2) \tag{4.85b}$$

$$\frac{d\epsilon}{d\tau} = -\frac{1}{n}\epsilon(1 - \epsilon)(1 + q). \tag{4.85c}$$

The system admits a line of fixed points in the intersection of the scalar field subset with $\epsilon = 1$ that is given by

$$L_y: \quad \bar{y} = y_0, \quad \bar{z} = 0, \quad \epsilon = 0 \tag{4.86}$$

the linearisation around this line of fixed points yields to the eigenvalues 0, $-\frac{3}{n+1}$, and $-\frac{3}{n+1}$ whose eigenvectors are the canonical basis of $\mathbb{R}^3$. In this case we have two negative eigenvalues (since $\gamma_{\rm pf} \in (0, 2)$) and a zero eigenvalue corresponding to a center manifold. To solve this we will introduce adapted variables

$$\tilde{y} = \bar{y} - \bar{y}_0, \quad \tilde{z} = \bar{z}, \quad \tilde{\epsilon} = \epsilon \tag{4.87}$$

which leads to the adapted system

$$\frac{d\tilde{y}}{d\tau} = F(\tilde{y}, \bar{z}, \epsilon), \quad \frac{d\bar{z}}{d\tau} = -\frac{3}{2}(2-\gamma_{\rm pf})\bar{z} + G(\tilde{y}, \bar{z}, \epsilon), \quad \frac{d\epsilon}{d\tau} = -\frac{3\gamma_{\rm pf}}{2n}\epsilon + N(\tilde{y}, \bar{z}, \epsilon) \tag{4.88}$$

where F, G and N are high order functions. With this new adapted variables we relocated the fixed points on the line L_y to the origin. The 1-dimensional center manifold can be locally represented by the graph $h : E^c \to E^s$, i.e., $(\bar{z}, \epsilon) = (h_1(\tilde{y}), h_2(\tilde{y}))$ satisfying the fixed point, $h(0) = 0$ and the tangency, $\frac{dh(0)}{d\tilde{y}} = 0$ conditions which solves the following equations

$$F(\tilde{y}, h_1(\tilde{y}), h_2(\tilde{y}))h_1'(\tilde{y}) = -\frac{3}{2}(2-\gamma_{\rm pf})h_1(\tilde{y}) + G(\tilde{y}, h_1(\tilde{y}), h_2(\tilde{y})) \tag{4.89a}$$

$$F(\tilde{y}, h_2(\tilde{y}), h_2(\tilde{y}))h_1'(\tilde{y}) = -\frac{3\gamma_{\rm pf}}{2n}h_2(\tilde{y}) + N(\tilde{y}, h_1(\tilde{y}), h_2(\tilde{y})) \tag{4.89b}$$

In general is not possible to find the exact solution for h_i and Taylor expansion are used, however in this particular case the can find an exact solution for h_1 and h_2 so we get

$$h_1(\tilde{y}) = \pm\sqrt{1 + e^{2C_z}(\tilde{y} + y_0)}, \quad h_2(\tilde{y}) = \frac{1}{1 + \left(\frac{\tilde{y}+y_0}{1+C_\epsilon e^{2C_z(\tilde{y}+y_0)}}\right)^{\frac{\gamma_{\rm pf}}{2n(2-\gamma_{\rm pf})}}} \tag{4.90}$$

Therefore, it follows that the center manifold reads

$$\frac{d\tilde{y}}{d\tau} = 3y(1 + e^{2C_z}(y + y_0))(2-\gamma_{\rm pf}) \tag{4.91}$$

which shows explicitly that each point on the line L_y are center saddles.

The system also admits two more fixed points in the intersection of the subset $\{z = 1\}$ and $\{\epsilon = 0\}$ given by

$$F_2^{\pm} : \quad y = 0, \quad z = \pm 1, \quad \epsilon = 0. \tag{4.92}$$

The linearisation around this fixed points yields to the eigenvalues $\frac{3}{n+1}$, $\frac{3}{n+1}$, and $-\frac{3}{n}$ were the associated eigenvectors are the canonical basis of $\mathbb{R}^3$. In this case we have two positive eigenvalues and a negative eigenvalue, so we are in a presence of a saddle. Moreover in the $\{\epsilon = 0\}$ subset we see that $F_2^{\pm}$ are sources.

Therefore the line of fixed is normally hyperbolic and each point on the line is the ω-limit point of a unique interior orbit. So there exists an orbit of the dynamical system (4.85) with $\epsilon > 0$ initially that converges to $(y_0, 0, 0)$ for each y_0 as $\tau \to +\infty$.

Convergence of solutions in the case $\gamma_{\rm pf} = \langle\gamma_\phi\rangle$

Just as in the proof of the cases (i) and (ii), we can again estimate $|\eta(\tau)|$ and $|\zeta(\tau)|$ however the estimation is very similar to the ones introduced in (4.80) and (4.81) since the only difference is that $\gamma_{\rm pf} - \langle\gamma_\phi\rangle = 0$. As $\epsilon_n \to 0$ then $|\eta(\tau)| \to 0$ and so y and $\bar{y}$ have the same limit and the same can be said regarding z and $\bar{z}$. Finally, from equation (4.66a), the triangle inequality, and the fact that $\epsilon \to 0$ as $\tau \to +\infty$, it follows from that Ω_ϕ has the same limit as $\bar{y}$ and therefore will converge to a point between $(0,1)$. In the case of Σ_σ using (4.66b), the triangle inequality and $\epsilon \to 0$ as $\tau \to +\infty$, it follow that Σ_σ goes to zero. This concludes the proof of the case (iii).

□

The global profile for our solutions in the (X, Σ_ϕ, T)-plane can be seen in Fig. 4.5. While the qualitative solutions for the (Σ_+, Σ_-, T)-plane can be found in Fig.4.6

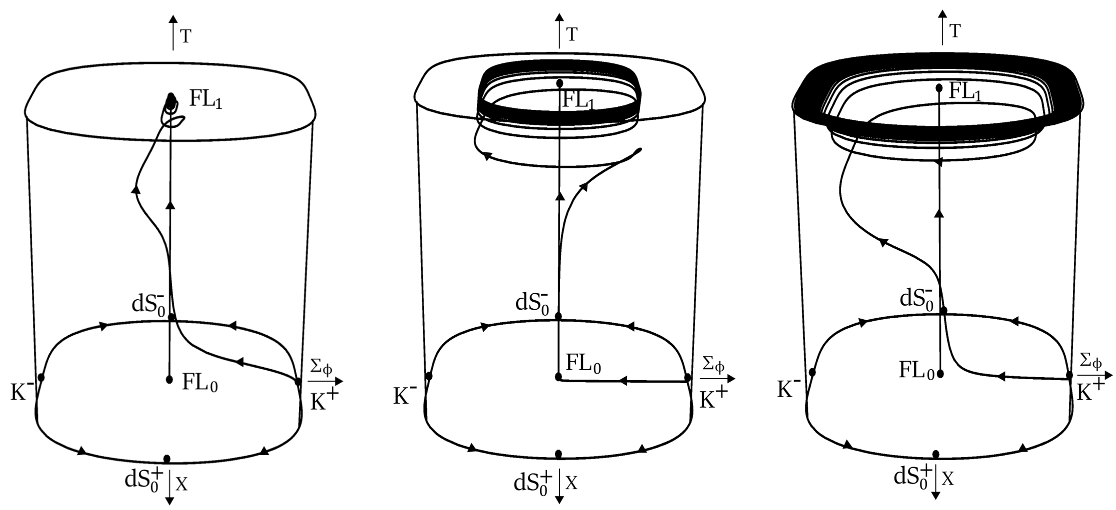

(A) Global picture for $\gamma_{\rm pf} = 1$.

(B) Global picture for $\gamma_{\rm pf} = \frac{4}{3}$.

(C) Global picture for $\gamma_{\rm pf} = \frac{3}{2}$.

Figure 4.5: Qualitative solutions for the scalar field potential $V(\phi) = \frac{1}{4}(\lambda\phi)^4$ in the (X, Σ_ϕ, T)-plane for various matter of state.

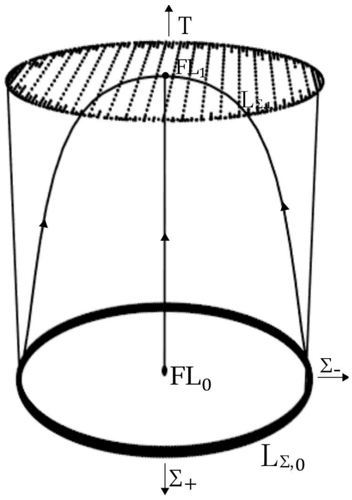

Figure 4.6: Qualitative solutions for the scalar field potential $V(\phi) = \frac{1}{4}(\lambda\phi)^4$ in the (Σ_+, Σ_-, T)-plane for $\gamma_{\rm pf} = \frac{4}{3}$.

4.4 Concluding Remarks

We used a dynamical system's approach to study spatially homogeneous but anisotropic cosmologies of Bianchi type I with a scalar field co-evolving with a perfect fluid. We have built a new regular 5-dimensional dynamical system on a compact phase-space by finding appropriate variables. We have analysed the geometry of the invariant boundaries including a thorough characterization of the past and future asymptotic boundaries regarding the existence and stability of fixed points and limit cycles.

In comparison to the FLRW case the Bianchi I model, the past asymptotic dynamics is dominated by the Kasner vacuum solution, due to the presence of shear. Crucial to the proof of this result are some monotonic functions which exclude the existence of periodic and recurrent orbits and ensure the existence of a circle of fixed points, the Kasner cycle. This allows the existence of an anisotropies which can will play a role of the physical processes of the early universe such as nucleosynthesis and structure formation [117, 118].

We also found the existence of a quasi-de Sitter solution that is commonly known as the inflationary attractor solution. This solution corresponds to a 1-dimensional center manifold on the 4-dimensional past boundary. Central manifold analysis showed that those fixed point solutions are center saddles.Lastly, we have derived precise asymptotic estimates for the dynamics towards the past and our main results for this part are in Lemma 4.2 and Theorem 4.7.

Regarding the late time dynamics we conclude that the shear terms are diluted and the dynamics is similar to the late flat FLRW case. However, the proofs in this case are more elaborate since we needed to use averaging methods for a 3-dimensional non-linearly coupled system. So we found that the quantities that will dominate the universe at late times will depend on the values of $\gamma_{\rm pf}$.

In the case where $\gamma_{\rm pf}$ is large enough, the future behaviour is dominated by the scalar field and described by a limit cycle where the deceleration parameter oscillates toward the future. A consequence of this is that this type of models exhibit a future asymptotic manifest self-similarity breaking. For $\gamma_{\rm pf}$ small enough the future state will be dominated by the perfect fluid solution which is self-similar. Finally, for the critical value $\gamma_{\rm pf} = \langle\gamma_\phi\rangle$ all solution oscillate towards the future so there is also a self-similarity breaking as neither the scalar field or perfect fluid will dominate the dynamics. In the case where we only have the perfect fluid in an anisotropic universe we recover the well-known results that towards the future the universe will simply isotropize.

Appendix A

Theory of Dynamical Systems

The results presented in this appendix are a collection of useful results taken well-known textbooks in dynamical systems including Hirsch & Smale (1974) [119]; Wiggins (1990) [120] ;Guckenheimer & Holmes (1990) [111]; Arrowsmith & Place (1990) [121]; Verhulst (1996) [122]; Perko (2001) [102]. For an approach more related to the cosmological point of view see Wainwright & Ellis (1997) [8], A. A Coley (2003) [66] and S. Bahamonde et al (2018) [67].

A.1 Principles of Dynamical Systems

A dynamical system describes the evolution of a given system in a geometrical space called *phase or state space*. Here we consider continuous dynamical systems.

Introduce $\mathbf{x} = (x_1, x_2, ..., x_{\rm n}) \in \boldsymbol{X}$ as an element of the state space $\boldsymbol{X} \subseteq \mathbb{R}^n$. A system of ordinary differential equations (ODEs) can be written as

$$\dot{\mathbf{x}} = \mathbf{f}(\mathbf{x}), \tag{A.1}$$

where $\mathbf{f} : \boldsymbol{X} \to \boldsymbol{X}$, $\mathbf{f}(\mathbf{x}) = (f_1(\mathbf{x}), \ldots, f_n(\mathbf{x}))$ is viewed as a vector field and the dot represents the differentiation with respect to some parameter $t \in \mathbb{R}$ that we are going to refer to as time although in general, this t does not need to refer to any physical quantity. In this work, we only consider the dynamical systems that are *autonomous* , i.e. where $\mathbf{f}$ does not depend explicitly on t as opposed to *nonautonomous* systems where $\mathbf{f}$ can depend on t, i.e. $\dot{\mathbf{x}} = \mathbf{f}(\mathbf{x}, t)$.

The solution of (A.1) is normally referred to as *orbit* or *trajectory* of the phase space. Since in cosmology most of the dynamical systems are finite and continuous, we restrict our work to those systems. However, it is possible in more complex cases to have a function $\mathbf{f}$ that presents some singularities. Also, it is important to note that since the function $\mathbf{f}$ is smooth, it is possible to prove the local existence and uniqueness of a solution for given initial conditions (see [119]).

Definition A.1. (*Flow*)

Let $\phi : \boldsymbol{X} \to \boldsymbol{X}$ be the flow of (A.1) so that the orbit is given by

$$\phi_t(\mathbf{x}_0) = \mathbf{x}_s(t, \mathbf{x}_0) \tag{A.2}$$

where $\mathbf{x}_s(t, x_0)$ is the solution of (A.1) for a given initial condition $\mathbf{x}_0$ at some time $t = t_0$. At any time t, the flow ϕ_t gives the state of the system $\mathbf{x} = \phi_t(\mathbf{x}_0)$ for all initial states $\mathbf{x}_0$.

The flow obeys the following properties

- Identity
$$\phi_0(\mathbf{x}) = \mathbf{x}$$
- Differentiability
$$\frac{d}{dt}\phi_t(\mathbf{x})|_{t=0} = \mathbf{f}(\mathbf{x})$$
- Group
$$\phi_{t+s}(\mathbf{x}) = \phi_t(\phi_s(\mathbf{x}))$$

The group property is related to the fact that the orbits of the flow are solutions of the ODE system.

The flow of a dynamical system is important regarding to the following concept.

Definition A.2. (*Invariant set*)

A subset $S \subset \mathbf{X}$ is an *invariant set* of the flow ϕ_t if for all $\mathbf{x} \in S$ and all $t \in \mathbb{R}$ then $\phi_t(\mathbf{x}) \in S$. Moreover, if $\phi_t \in S$ only for $t < 0$ ($t > 0$) then S is called a *negatively* (*positively*) invariant set.

Also related to flow is the concept of a periodic orbit.

The main goal of the theory of dynamical systems is not to solve analytically the ODEs, instead, one tries to understand and characterize the geometry inherent to the phase space (its parameters dependence and how the orbits evolve with the time under the variation of such parameters).

A.2 Fixed Points

One of the most important concepts in dynamical system theory is the concept of a fixed point.

Definition A.3. (*Fixed, critical or equilibrium point*)

Equation (A.1) is said to have a fixed (critical / equilibrium) point at $\mathbf{x} = \mathbf{x}_0$ if and only if $\mathbf{f}(\mathbf{x}_0) = 0$.

Definition A.4. (*Heteroclinic and Homoclinic orbit*)

An orbit connecting two different fixed points is said to be *heteroclinic* while an orbit connecting a fixed point to itself is said to be *homoclinic*.

An important note is the fact that the fixed points are not part of a heteroclinic or homoclinic orbit; instead, they are approached by the orbit as $t \to \pm\infty$.

So, finding the fixed points of a system is the first step when analyzing a dynamical system. The next step is to linearise the system around the fixed points, this will allow us to understand the stability properties of each fixed point. This leads to the following definitions.

Definition A.5. (*Stable fixed point*)

Let $\mathbf{x}_0$ be a fixed point of the system (A.1). This fixed point is called *stable* if and only if for every $\epsilon > 0$ there exists a δ such that if $\phi(t)$ is a solution of (A.1) satisfying $||\phi(t_0) - \mathbf{x}_0|| < \delta$, then the solution $\phi(t)$ exists for every $t \geq t_0$ and the solution remains in a distance of ϵ, i.e $||\phi(t) - \mathbf{x}_0|| < \epsilon$ for all $t \geq t_0$.

Definition A.6. (*Asymptotically stable fixed points*)

A fixed point is asymptotically stable if it is stable and if exists a δ such that if $\phi(t)$ is a solution of (A.1) satisfying $||\phi(t_0) - \mathbf{x}_0|| < \delta$, then $\lim_{t\to\infty} \phi(t) = \mathbf{x}_0$.

As one can see from definition A.6 all the trajectories near an asymptotically stable fixed point eventually will reach the fixed point, while taking into consideration definition A.5 the solution can, for example, circle around the stable fixed point. If we take these concepts to the theory of dynamical systems in cosmology, we see that almost every stable point in cosmology is also asymptotically stable [67]. A fixed point is called unstable if it is not stable.

After introducing the concepts of fixed points and the stability of fixed points, we can now introduce how we study this stability. The most common method to study such stability is to use linear stability techniques that often are sufficient to understand the flow in the neighborhood of such points; however, we also introduce Lyapunov stability alongside the center manifold theory.

A.3 Linear Stability Theory

So let $\mathbf{x}_0$ be a fixed point of the system (A.1). Assuming the regularity of $\mathbf{f}$ we can linearise the system around this fixed point. So considering the Taylor expansion,

$$\mathbf{f} = \mathbf{f}(\mathbf{x}_0) + \mathbf{Df}(\mathbf{x}_0)(\mathbf{x} - \mathbf{x}_0) + \mathcal{O}(||\mathbf{x} - \mathbf{x}_0||^2), \tag{A.3}$$

where $\mathbf{Df}(\mathbf{x}_0)$ is the *Jacobian matrix* of the function $\mathbf{f}$ at $\mathbf{x}_0$.

The information about the stability of the fixed points $\mathbf{x}_0$ is related to the eigenvalues of the Jacobian matrix evaluated in such fixed points. This matrix is a $n \times n$ matrix where n is the dimension of the dynamical system. The most important concept related to linear stability is the concept of the *hyperbolic* fixed point.

Definition A.7. (*Hyperbolic fixed point*)

Let $\mathbf{x}_0$ be a fixed point of a give ODE system. $\mathbf{x}_0$ is said to be hyperbolic if none of the eigenvalues of the Jacobian matrix has a zero real part. Otherwise, the point is called non-hyperbolic.

This leads to the following theorem:

Theorem A.8. *(Hartman-Grobman theorem)*

Let S be a open subset of $\mathbb{R}^n$ containing the origin and let $f \in C^1(S)$ such that $\boldsymbol{f}(\boldsymbol{x}_0) = 0$ and the matrix $A = D\boldsymbol{x}(\boldsymbol{x}_0)$ has no eigenvalues with zero real part. Then there exists a homeomorphism H of an open set U containing the origin onto a open set V containing the origin such that for each $\boldsymbol{x}_0 \in U$, there exists an open interval $I_0 \subset \mathbb{R}$ containing zero such that for all $\boldsymbol{x}_0 \in U$ and $t \in I_0$

$$H(\phi(t, \boldsymbol{x})) = e^{tA} H(\boldsymbol{x})$$

for all $\boldsymbol{x} \in U$ and $|t| \leq 1$.

Proof. See [102]. □

The Hartman-Grobman Theorem basically tells us that the stability of a fixed point concerning the linearised ODE corresponds to the stability of the full non-linear ODE. This theorem fails when the fixed point is non-hyperbolic. In this case further studies need to be made to understand what happens in the neighborhood of these fixed points.

Definition A.9. (*Stable, unstable and center subspaces*)

Let λ_i be the eigenvalues with corresponding eigenvectors $\mathbf{e}_i$ $(i = 1, 2, \ldots, n)$ of the Jacobian matrix in some fixed point $\mathbf{x}_0$. Which can generate the following subspaces of $\boldsymbol{X}$:

$$\textit{Stable subspace} \qquad E^s = span(\mathbf{e}_1, \ldots, \mathbf{e}_s) \tag{A.4a}$$

$$\textit{Unstable subspace} \qquad E^u = span(\mathbf{e}_{s+1}, \ldots, \mathbf{e}_{s+u}) \tag{A.4b}$$

$$\textit{Center subspace} \qquad E^c = span(\mathbf{e}_{s+u+1}, \ldots, \mathbf{e}_{s+u+c}) \tag{A.4c}$$

where $\{\mathbf{e}_1, \ldots, \mathbf{e}_s\}$ are all the eigenvectors for the eigenvalues with *negative real part*, $\{\mathbf{e}_{s+1}, \ldots, \mathbf{e}_{s+u}\}$ are all the eigenvectors for the eigenvalues with *positive real part* and $\{\mathbf{e}_{s+u1}, \ldots, \mathbf{e}_{s+u+c}\}$ are all the eigenvectors for the eigenvalues with *null real part* . This leads to the following result (see Perko, 2001, p.55)

$$E^s \oplus E^u \oplus E^c = \boldsymbol{X} \subseteq \mathbb{R}^n, \quad i.e \quad s + u + c \leq n \tag{A.5}$$

It is now possible to classify a specific fixed point $\mathbf{x}_0$ to better understand the orbits in its neighborhood,

Definition A.10. (*Sink, source, saddle*)

Let $\mathbf{x}_0$ be the fixed point of a dynamical system. Considering $Df(\mathbf{x}_0)$, the fixed point is

- *a sink* if all eigenvalues have negative real part;
- *a source* if all eigenvalues have positive real part;
- *a saddle point* if the eigenvalues have positive and negative real part.

The *stable point* is regarded as an *attractor* and the *unstable point* is often called *repeller*.

Although the Hartman–Grobman theorem tells us that it is possible to study the stability of the system (A.1) using only a linear system (if the fixed points are hyperbolic) it is important to notice that the subspaces E^s, E^u, and E^c are only invariant sets of such system. For the non-linear ODE (A.1) we need to introduce the following invariant sets.

Definition A.11. (*Stable, unstable and center manifold*)

Let $\mathbf{x}_0$ be a fixed point of the ODE (A.1). The *stable (unstable) manifold* W^s of this fixed point is the differential manifold that has tangent space in $\mathbf{x}_0$ that coincides with asymptotically with E^s (E^u) as $t \to +\infty$ $(t \to -\infty)$. The *center manifold* W^c of this fixed point is the differential manifold that has tangent space in $\mathbf{x}_0$ that coincides asymptotically with E^c.

A.3.1 Example 1: Generic 2D Dynamical System

Let us use the example from [119] (p. 62) with a 2D dynamical system that is given by

$$\dot{x} = f(x, y), \qquad \dot{y} = g(x, y), \tag{A.6}$$

where we assume that $f(x, y)$ and $g(x, y)$ are smooth functions in x and y. Let us assume that the dynamical system presents a fixed point (x_0, y_0) such that $f(x_0, y_0) = 0$ and $g(x_0, y_0) = 0$. The jacobian matrix of this system reads

$$J = \begin{pmatrix} \left.\frac{\partial f(x,y)}{\partial x}\right|_{x_0,y_0} & \left.\frac{\partial f(x,y)}{\partial y}\right|_{x_0,y_0} \\ \left.\frac{\partial g(x,y)}{\partial x}\right|_{x_0,y_0} & \left.\frac{\partial g(x,y)}{\partial y}\right|_{x_0,y_0} \end{pmatrix} = \begin{pmatrix} f_x & f_y \\ g_x & g_y \end{pmatrix} \tag{A.7}$$

The system presents two eigenvalues

$$\lambda_{1,2} = \frac{1}{2}(f_x + g_y) \pm \frac{1}{2}\sqrt{(f_x + g_y)^2 - 4(f_x g_y - f_y g_x)}. \tag{A.8}$$

So using the fact that $T = \operatorname{Tr} J = f_x + g_y$ and $D = \det J = f_x g_y - f_y g_x$, the eigenvalues can be written as

$$\lambda_{1,2} = \frac{1}{2}\Big(T \pm \sqrt{T^2 - 4D}\Big). \tag{A.9}$$

We can now display these results in a *trace-determinant plane*. The geometry of each phase portrait will depend on the location in the TD-plane. The possible outcomes of the eigenvalue analysis are the following:

1. If $T^2 - 4D < 0$ the eigenvalues have non-zero imaginary part and are a
   (a) Spiral sink if $T < 0$
   (b) Spiral source if $T > 0$
   (c) Center if $T = 0$
2. If $T^2 - 4D > 0$ (for $T \neq 0$ and $D \neq 0$) the eigenvalues are real and distinct and are a
   (a) Sink if $T < 0$ and $D > 0$
   (b) Source if $T > 0$ and $D > 0$
   (c) Saddle if $T > 0$ and $D < 0$
3. If $T^2 - 4D > 0$ and $D = 0$ we have
   (a) a zero and non-zero eigenvalues if $T \neq 0$

   (b) two zero eigenvalues if $T = 0$

4. If $T^2 - 4D = 0$ the eigenvalues are real and equal to each other ($T \neq 0$) and are a
   (a) Sink if $T < 0$
   (b) Saddle if $T > 0$

5. If $T^2 - 4D = 0$ the eigenvalue are both zero if $T = 0$.

More examples can be found in [123].

A.4 Lyapunov Stability Theory

As mentioned in Sec. A.3 when a fixed point is hyperbolic the linear stability theory alongside the Hartman-Grobman theory is enough to obtain the dynamics in the neighborhood of such point. However, many dynamical systems, in cosmology, for example, present non-hyperbolic fixed points. So for a complete description of the local and global stability of such points, we need more powerful tools. One of these tools is *Lyapunov's method* which can be used for both hyperbolic and non-hyperbolic points. This method does not rely on linear stability, however we need to find the so-called *Lyapunov function* without having a method to do so.

So let's introduce the following theorem (see [102], p. 132)

Theorem A.12. *(Lyapunov Stability)*

Let $\boldsymbol{x}_0$ be a fixed point of the dynamical system (A.1). Let us assume that there exists a C^1 function $V : \mathbb{R}^n \to \mathbb{R}$ in the neighborhood U of $\boldsymbol{x}_0$ such that $V(\boldsymbol{x}_0) < V(x)$ for all $\boldsymbol{x} \in U \setminus \{\boldsymbol{x}_0\}$. Then

1. *$\dot{V} \leq 0 \;\; \forall \boldsymbol{x} \in U$, $\boldsymbol{x}_0$ is stable;*
2. *$\dot{V} < 0 \;\; \forall \boldsymbol{x} \in U \setminus \{\boldsymbol{x}_0\}$, $\boldsymbol{x}_0$ is asymptotically stable;*
3. *$\dot{V} > 0 \;\; \forall \boldsymbol{x} \in U \setminus \{\boldsymbol{x}_0\}$, x_0 is unstable;*

which leads to the following definition:

Definition A.13. (*Lyapunov function*)

Let V the function that satisfies the conditions of the theorem A.12. If

1. $\dot{V}(\mathbf{x}) = \frac{dV(\mathbf{x})}{dt} = \nabla V \cdot \mathbf{f}(\mathbf{x}) \leq 0$ then V is a *Lyapunov function*;
2. $\dot{V}(\mathbf{x}) = \frac{dV(\mathbf{x})}{dt} = \nabla V \cdot \mathbf{f}(\mathbf{x}) < 0$ then V is a *strict Lyapunov function*.

Some applications of the Lyapunov function in cosmology can be found in [124, 125] where the authors used the Lyapunov function in form of a first integral. Also notice that, in physics a viable Lyapunov function candidate is the total energy stored in the system.

Some useful examples using this technique can be found in [123] (p.127).

Although Lyapunov stability is a fair method for studying the stability of an equilibrium solution it is possible to be more general. The LaSalle invariance principle gives us conditions to describe the behavior of all solutions as $t \to \infty$. So consider an autonomous ODE system like (A.1) and let $\phi_t(.)$ denote the flow generated by (A.1) and let $\mathbf{M} \subset \mathbb{R}^n$ be a positive invariant set that is compact. Suppose that we have a scalar valued function

$$V : \mathbb{R}^n \to \mathbb{R}, \quad \dot{V}(x) \leq 0 \ in \ \mathbf{M} \tag{A.10}$$

Let $E = \{x \in \mathbf{M} | \dot{V}(x) = 0\}$ and M ={the union of all trajectories that start in E and remain in E for all $t \geq 0$}, then the LaSalle's invariance principle states that for all $x \in \mathbf{M}$, $\phi_t(x) \to M$ as $t \to \infty$.

A.5 Center Manifold Theory

As already mentioned, linear stability theory and the Hartman-Grobman theorems fails when one of the eigenvalues has a null real part. We saw in Sec A.4 that it is possible to study non-hyperbolic fixed points using the Lyapunov function, however, in a variety of cases such function is not possible to find or even guess. So in this particular situation we can use *center manifold theory* that reduces the dimension of a dynamical system. So let us consider the ODE (A.1) where $\mathbf{x}_0$ is a fixed point of the system. To better study the center manifold let us move the fixed point to the origin. To do this we use the transformation

$$\bar{\mathbf{x}} = P^{-1}(\mathbf{x} - \mathbf{x}_0) \tag{A.11}$$

where P is the matrix that has the eigenvectors of the jacobian matrix as columns. This transformation allows us to write the dynamical system as

$$\dot{\bar{\mathbf{x}}} = A\bar{\mathbf{x}} + f(\bar{\mathbf{x}}, \bar{\mathbf{y}}) \tag{A.12a}$$

$$\dot{\bar{\mathbf{y}}} = B\bar{\mathbf{y}} + g(\bar{\mathbf{x}}, \bar{\mathbf{y}}) \tag{A.12b}$$

where $(\bar{\mathbf{x}}, \bar{\mathbf{y}}) \in \mathbb{R}^c \times \mathbb{R}^s$ where c and s are the dimension of the center (E^c) and the stable (E^s) manifold. The functions f and g satisfy

$$f(0,0) = 0, \qquad \nabla f(0,0) = 0 \tag{A.13a}$$

$$g(0,0) = 0, \qquad \nabla g(0,0) = 0 \tag{A.13b}$$

that are the fixed point and tangency conditions. In (A.12) A is a $c \times c$ matrix where the eigenvalues have vanishing real part, B is a $s \times s$ matrix with all eigenvalues having negative real part and f and g are at least C^1 functions.

Definition A.14. (*Center manifold*) A geometrical space is a center manifold of (A.12) if it can be locally represented as

$$W^c(0) = \{(\bar{\mathbf{x}}, \bar{\mathbf{y}}) \in \mathbb{R}^c \times \mathbb{R}^s | \bar{\mathbf{y}} = h(\bar{\mathbf{x}}), |\bar{\mathbf{x}}| < \delta, h(0) = 0, \nabla h(0) = 0\} \tag{A.14}$$

for δ sufficiently small and for some h that is a function of $\mathbb{R}^s$.

The center manifold theory, is based on three theorems (whose the proofs can be found in [5]):

Theorem A.15. *(Existence)*

If there exists a center manifold for (A.12), then the dynamics of the system (A.12) restricted to the center manifold is given by

$$\dot{\boldsymbol{u}} = A\boldsymbol{u} + f(\boldsymbol{u}, h(\boldsymbol{u})) \tag{A.15}$$

for a sufficiently small $u \in \mathbb{R}^c$.

Theorem A.16. *(Stability)*

Let the zero solution be a stable (asymptotic stable or unstable) solution of (A.15). Then the zero solution of (A.12) is also stable (asymptotic stable or unstable) . Furthermore, if $(\bar{\boldsymbol{x}}(t), \bar{\boldsymbol{y}}(t))$ is also a solution of (A.12) with a $(\bar{\boldsymbol{x}}(0), \bar{\boldsymbol{y}}(0))$ sufficient small, then there exists a solution $\boldsymbol{u}(t)$ of (A.15) such that

$$\bar{\boldsymbol{x}}(t) = \boldsymbol{u}(t) + \mathcal{O}\left(e^{-\gamma t}\right) \tag{A.16a}$$

$$\bar{\boldsymbol{y}}(t) = h(\boldsymbol{u}(t)) + \mathcal{O}\left(e^{-\gamma t}\right) \tag{A.16b}$$

as $t \to \infty$, where $\gamma > 0$ is a constant.

From the previous two theorems we see that if we are able to find the function $h(\mathbf{x})$, then the stability restricted to the center manifold is given by (A.15). Moreover when $t \to +\infty$ the orbits passing close to the origin will approximate the orbits in the center manifold, W^c. So we are going now to provide the tools to find $h(\bar{\mathbf{x}})$. Accordingly to definition A.14 we have $\bar{\mathbf{y}} = h(\bar{\mathbf{x}})$, applying the time derivative alongside the chain rule we get

$$\dot{\bar{\mathbf{y}}} = \nabla h(\bar{\mathbf{x}}) \cdot \dot{\bar{\mathbf{x}}} \tag{A.17}$$

From theorem A.15 we know that the stability of $W^c(0)$ is given by (A.12) so taking this into consideration we get

$$Bh(\bar{\mathbf{x}}) + g(\bar{\mathbf{x}}, h(\bar{\mathbf{x}})) = \nabla h(\bar{\mathbf{x}}) \cdot [A\bar{\mathbf{x}} + f(\bar{\mathbf{x}}, h(\bar{\mathbf{x}}))] \,. \tag{A.18}$$

where we used the fact that $\bar{\mathbf{y}} = h(\bar{\mathbf{x}})$

Re-arranging the previous equation we get

$$\mathcal{N}(h(\bar{\mathbf{x}})) := Dh(\bar{\mathbf{x}}) \, [A\bar{\mathbf{x}} + f(\bar{\mathbf{x}}, h(\bar{\mathbf{x}}))] - Bh(\bar{\mathbf{x}}) - g(\bar{\mathbf{x}}, h(\bar{\mathbf{x}})) = 0, \tag{A.19}$$

which is a quasilinear partial differential equation satisfied by $h(\bar{\mathbf{x}})$ to characterize the center manifold.

Generally, it is not possible to solve (A.19) and find $h(\bar{\mathbf{x}})$ explicitly, however, this next theorem tells us that we do not need to know the entire function and provides us with a method to find the approximated solution with a given degree of accuracy.

Theorem A.17. *(Approximated solution)*

Let $\psi : \mathbb{R}^c \to \mathbb{R}^s$ be a C^1 map that obeys the fixed point and tangency conditions ($\psi(0) = 0, \nabla\psi(0) = 0$) such that $\mathcal{N}(\psi(\bar{\boldsymbol{x}})) = \mathcal{O}\left(||\bar{\boldsymbol{x}}||^p\right)$ as $\bar{\boldsymbol{x}} \to 0$ for some $p > 1$. Then

$$|h(\bar{\boldsymbol{x}}) - \psi(\bar{\boldsymbol{x}})| = \mathcal{O}\left(||\bar{\boldsymbol{x}}||^p\right) \quad as \quad \bar{\boldsymbol{x}} \to 0 \tag{A.20}$$

So the collection of these three theorems (Carr(1981)) tells us that the approximated solution of the center manifold expansion will return the same qualitative information as the exact solution of (A.18) with a great degree of accuracy. Moreover, the approximated solution for the center manifold can be often found assuming a *Taylor expansion* in h and finding the coefficients that satisfy (A.18).

We refer the reader to [102] (p.156 and 158) for some useful examples when dealing with the center manifold in one and two dimensions.

A.6 Limit sets and Attractors

In the previous section, we focused on the study of the local stability of fixed points. However, in some cases, we are also interested in studying how the orbits will evolve when $t \to \pm\infty$. To achieve this we require advanced methods of dynamical systems theory, such as bifurcation theory. Here we will only introduce concepts that are important in this thesis. For a more advanced study see [102, 119, 120]

Definition A.18. (*Limit point*)

Let $\mathbf{x}$ be a point on the phase space $\boldsymbol{X} \subseteq \mathbb{R}^n$ and ϕ_t the flow of a given dynamical system. $\mathbf{x}$ is an α-limit (ω-limit) point of $\mathbf{x}_i \in \mathbb{R}^n$ if there exist a sequence $t_N \to -\infty(+\infty)$ such that

$$\lim_{N \to -\infty(+\infty)} \psi_{t_N}(\mathbf{x}_i) = \mathbf{x}. \tag{A.21}$$

Definition A.19. (*Limit sets*)

The set of all α-limit (ω-limit) points of $\mathbf{x_i}$ is called the α-limit (ω-limit) set of $\mathbf{x_i}$ and is denoted by $\alpha(\mathbf{x_i})(\omega(\mathbf{x_i}))$

Theorem A.20. *The $\alpha(\mathbf{x}_i)$-limit ($\omega(\mathbf{x_i})$)-limit sets are closed subsets of $\boldsymbol{X} \subseteq \mathbb{R}^n$ and if the negative (positive) orbits passing through $\mathbf{x_i}$ are bounded, then $\alpha(\mathbf{x}_i)(\omega(\mathbf{x_i}))$ is bounded, non-empty and connected.*

Proof. See [102] (p. 175). □

There are many examples of an α-limit (ω-limit) set such as: periodic orbits; homoclinic orbits; heteroclinic cycle (a sequence of critical points that are joined by heteroclinic orbits).

One goal of the dynamical system theory is to obtain the asymptotic behaviour of a given system and to do so we need to consider the α-limit and ω-limit sets for all points in the state space. This leads to the introduction of *past* and *future* attractors.

Definition A.21. (*Past and Future Attractors*)

The *future (past attractor)* $\{A^{\pm}\}$ is the smallest closed invariant set such that $\omega(\mathbf{x}_i)(\alpha(\mathbf{x}_i)) \subset A^{\pm}$ for all $\mathbf{x}_i \in \boldsymbol{X} \subseteq \mathbb{R}^n$ a part from a set of measure zero. If the subset $\boldsymbol{X}$ is compact, then each point $\mathbf{x} \in \boldsymbol{X}$ has a non-empty α and ω-limit sets and then $A^{\pm} \neq \emptyset$.

A.7 Special Theorems in Dynamical System Theory

In this section we will turn our attention to advanced methods and special theorems to analyse dynamical systems in $\mathbb{R}^2$. It's important to notice that several results that arise from the study of a 2-dimensional dynamical system cannot be applied in higher dimensions.

A.7.1 Global Behaviour Of The State Space: Special Theorems

We will introduce some important results that help to determine the absence of periodic orbits and fixed points.

Definition A.22. *Monotone functions*

Let ϕ_t be the flow on $\boldsymbol{X} \subseteq \mathbb{R}^n$, let S be an invariant set of ϕ_t, and let $Z : S \to \mathbb{R}$ be a continuous function. Z is a *monotone decreasing (increasing) function for the flow* on S if for all $\mathbf{x} \in S$, $Z(\phi_t(\mathbf{x}))$ is a monotone decreasing (increasing) function of t.

Consider the ODE (A.1) and the corresponding flow ϕ_t and suppose that Z is C^1. If

$$Z' := \nabla Z.\mathbf{f} < 0, \quad on \quad S \tag{A.22}$$

then Z is a monotone decreasing on S.

The following proposition shows that the existence of a monotone function on an invariant set S simplifies the orbits in S significantly.

Proposition A.23. *Monotonicity principle*

Let $S \subset \mathbb{R}$ be an invariant set of a flow ϕ_t. If there exists a monotone function $Z : S \to \mathbb{R}$ on S, then S contains no equilibrium points, periodic orbits, recurrent orbits or homoclinic orbits.

Proof. See [114] (p. 1418). □

Another important result is the *Bendixson-Dulac theorem* (see [102], p.246) which is useful to exclude the presence of periodic orbits in the state-space.

Theorem A.24. *(Bendixson-Dulac)*

Let $\dot{\boldsymbol{x}} = \boldsymbol{f}(x)$ be a ODE on $\boldsymbol{X} \subseteq \mathbb{R}^2$ where $\boldsymbol{x} = (x, y)$ and $\boldsymbol{f} = (f_1, f_2)$. Let us assume that exists a scalar function Φ in a simply connected domain such that

$$\nabla \cdot (\Phi \boldsymbol{f}) = \frac{\partial}{\partial x}(\Phi f_1) + \frac{\partial}{\partial y}(\Phi f_2) > 0 \quad or \quad < 0. \tag{A.23}$$

Then the phase space does not contain periodic-orbits.

Note that this criterion is only valid to infer the non-existence of periodic orbits.

The next result characterizes all the possible asymptotic behaviors in the 2-dimensional phase space and is called *Poincaré-Bendixson theorem* (see Wiggins, 1990, p. 46).

Theorem A.25. *(Poincaré-Bendixson)*

Let S be a negative (positive) invariant set of $\dot{\boldsymbol{x}} = \boldsymbol{f}(x)$ on $\boldsymbol{X} \subseteq \mathbb{R}^2$ that contains a finite number of fixed points. Let $\boldsymbol{x}_i \in S$ and consider the α-limit (ω-limit) set $\alpha(\boldsymbol{x}_i)(\omega(\boldsymbol{x}_i))$. Then if $\alpha(\boldsymbol{x}_i)(\omega(\boldsymbol{x}_i)) \neq \emptyset$, one of the following possibilities must hold:

i. $\alpha(\boldsymbol{x}_i)(\omega(\boldsymbol{x}_i))$ *is a critical point;*

ii. $\alpha(\boldsymbol{x}_i)(\omega(\boldsymbol{x}_i))$ *is a periodic orbit;*

iii. $\alpha(\boldsymbol{x}_i)(\omega(\boldsymbol{x}_i))$ *is a finite heteroclinic sequence;*

When S is compact then $\alpha(\mathbf{x}_i)(\omega(\mathbf{x}_i)) \neq \emptyset$.

Corollary A.26. *Let S be a bounded close set containing no fixed points and suppose that S is positively invariant. Then there exists a limit cycle contained in S.*

For some useful examples we refer the reader to [123] (p. 96-98).

Another important theorem that will be useful later on is the *index theorem.* Before we present this theorem we need to introduce the definition of index of a curve.

Definition A.27. (*Index of a curve*)

For a vector field on the plane given by

$$\dot{x} = f(x, y), \quad \dot{y} = g(x, y)$$

the index, k, of the curve C is given by

$$k = \frac{1}{2\pi} \oint_C d\phi = \frac{1}{2\pi} \oint_C d\left(\tan^{-1} \frac{g(x,y)}{f(x,y)}\right) = \frac{1}{2} \oint_C \frac{f dg - g df}{f^2 + g^2} \tag{A.24}$$

Theorem A.28. *(Index Theorem)*

- *The index of a sink, a source, or a center is $+1$.*
- *The index of a hyperbolic saddle is -1.*
- *The index of a closed orbit is $+1$.*
- *The index of a closed curve not containing any fixed point is 0.*
- *The index of a closed curve is equal to the sum of the indices of the fixed points within it.*

Corollary A.29. *Inside any closed orbit γ there must be at least one fixed point. If there is only one fixed point, then it must be a sink, source or center. If all the fixed points within γ are hyperbolic, then there must be an odd number, $2n + 1$, of which n are saddles and $n + 1$ are either sinks, sources, or centers.*

A.7.2 Liénard Systems

In the previous section we revised the Poincaré-Bendixson theorem that allows us to infer the existence of limit cycles for a given planar system and although this is a powerful tool when analysing a dynamical system this does not tell us how many limit cycles are present in a dynamical system. However there are classic result about the uniqueness of limit cycles for the giving equation

$$\ddot{x} + f(x)\dot{x} + g(x) = 0 \tag{A.25}$$

that can be converted into a non-standard autonomous system

$$\dot{x} = y - F(x) \qquad \dot{y} = -g(x) \tag{A.26}$$

where $F(x) = \int_0^x f(u)du$. This result was introduced by Liénard in 1928 and the equation above is referred as Liénard equation. This second-order differential equation includes a special case, the famous Van der Pol equation

$$\ddot{x} + \mu(x^2 - 1)\dot{x} + x = 0. \tag{A.27}$$

One of the most important results of for the Liénard system is the following theorem

Theorem A.30. *(Liénard's Theorem)*

Suppose that:

- *F and g are continuous differentiable*
- *F and g are odd functions of x*
- *$xg(x) > 0$ for $x \neq 0$.*
- *$F(0) = 0$ and $F'(0) < 0$*
- *$F(x) > 0$ and increasing for $x > a$ and has a single positive zero at $x = a$.*

Then it follows that the Liénard system (A.26) has exactly one limit cycle and it is stable.

Proof. See [102] p. 254. □

A.7.3 Poincaré Compactification

The Poincaré compactification allows us to map the phase plane onto the so-called *Poincaré sphere*. This allows to study the flow at the infinity by mapping points (at the infinity) onto the sphere equator.

Definition A.31. (*Poincaré sphere*)

Let the unit sphere

$$S^3 = \{(X, Y, Z, U) \in \mathbb{R}^3 | X^2 + Y^2 + Z^2 + U^2 = 1\}, \tag{A.28}$$

be the Poincaré sphere such that its north (or south) pole is tangent to the (x, y)-plane in the origin. In order to map points of the (x, y)-plane on the upper hemisphere (note that is also possible to map in the lower hemisphere) we need to make the variable transformation

$$X = xU, \quad Y = yU, \quad Z = zU, \quad U = \frac{1}{\sqrt{1 + x^2 + y^2 + z^2}} \tag{A.29}$$

We will now introduce two theorems that have great importance to determine the flow at infinity. Specific details and proofs of such theorems will not be given instead we refer the readers to [102].

Consider the flow defined by a dynamical system in $\mathbb{R}^3$

$$\dot{x} = P(x, y, z) \tag{A.30a}$$

$$\dot{y} = Q(x, y, z) \tag{A.30b}$$

$$\dot{z} = R(x, y, z) \tag{A.30c}$$

where P, Q, and R are polynomial functions of x, y, and z. Let m denote the maximum degree of the terms in P, Q, and R and let P_j, Q_j, and R_j be the jth degree polynomials in x, y, and z.

Theorem A.32. *(Fixed Points at infinity)*

The fixed points at infinity for the mth degree polynomial of the system (A.30) arise at $(X, Y, Z, 0)$ of the equator of the Poincaré sphere where $X^2 + Y^2 + Z^2 = 1$ and

$$XQ_m(X, Y, Z) - YP_m(X, Y, Z) = 0 \tag{A.31a}$$

$$XR_m(X, Y, Z) - ZP_m(X, Y, Z) = 0 \tag{A.31b}$$

$$YR_m(X, Y, Z) - ZQ_m(X, Y, Z) = 0 \tag{A.31c}$$

The stability of the fixed points at infinity can be described by projecting the flow onto three planes (y, z, u), (x, z, u) and (x, y, u), tangent to the equator points $X = 1$, $Y = 1$ and $Z = 1$ respectively. This can be seen as follows:

Theorem A.33. *(Stability at infinity)*

The flow defined on (A.30) in a neighbourhood *(a) of* $(\pm 1, 0, 0, 0) \in S^3$ *is topologically equivalent to the flow defined by the system*

$$\pm\dot{y} = yu^m P\left(\frac{1}{u}, \frac{y}{u}, \frac{z}{u}\right) - u^m Q\left(\frac{1}{u}, \frac{y}{u}, \frac{z}{u}\right) \tag{A.32a}$$

$$\pm\dot{z} = zu^m P\left(\frac{1}{u}, \frac{y}{u}, \frac{z}{u}\right) - u^m R\left(\frac{1}{u}, \frac{y}{u}, \frac{z}{u}\right) \tag{A.32b}$$

$$\pm\dot{u} = u^{m+1} P\left(\frac{1}{u}, \frac{y}{u}, \frac{z}{u}\right) \tag{A.32c}$$

(b) of $(0, \pm 1, 0, 0) \in S^3$ *is topologically equivalent to the flow defined by the system*

$$\pm\dot{x} = xu^m Q\left(\frac{x}{u}, \frac{1}{u}, \frac{z}{u}\right) - u^m P\left(\frac{x}{u}, \frac{1}{u}, \frac{z}{u}\right) \tag{A.33a}$$

$$\pm\dot{z} = zu^m Q\left(\frac{x}{u}, \frac{1}{u}, \frac{z}{u}\right) - u^m R\left(\frac{x}{u}, \frac{1}{u}, \frac{z}{u}\right) \tag{A.33b}$$

$$\pm\dot{u} = u^{m+1} Q\left(\frac{x}{u}, \frac{1}{u}, \frac{z}{u}\right) \tag{A.33c}$$

and

(c) of $(0, 0, \pm 1, 0) \in S^3$ *is topologically equivalent to the flow defined by the system*

$$\pm\dot{x} = xu^m R\left(\frac{x}{u}, \frac{y}{u}, \frac{1}{u}\right) - u^m P\left(\frac{x}{u}, \frac{y}{u}, \frac{1}{u}\right) \tag{A.34a}$$

$$\pm\dot{y} = yu^m R\left(\frac{x}{u}, \frac{y}{u}, \frac{1}{u}\right) - u^m Q\left(\frac{x}{u}, \frac{y}{u}, \frac{1}{u}\right) \tag{A.34b}$$

$$\pm\dot{u} = u^{m+1} R\left(\frac{x}{u}, \frac{y}{u}, \frac{1}{u}\right) \tag{A.34c}$$

The direction of the flow is not determined by Theorem A.33, instead it is determined by the original system (A.30).

A.8 Averaging

The averaging method is a powerful tool when analyzing nonlinear dynamical systems that allow us to sort out fast oscillations and observe the qualitative behaviour of the resulting dynamics. The use of this method can be traced back to 1788 when Lagrange try to formulate the gravitational three-body problem as a perturbation of a two-body problem. However only in 1920 Fatou was able to prove some asymptotic results which lead to more important results in the $1930's$ making the averaging method an important tool when analyzing nonlinear oscillations.

The averaging method is applicable to system of the form

$$\dot{\mathbf{x}} = \epsilon f(\mathbf{x}, t, \epsilon), \qquad x \in U \subseteq \mathbb{R}^n, \quad \epsilon \ll 1, \tag{A.35}$$

where $f : \mathbb{R}^n \times \mathbb{R} \times \mathbb{R}^+$ is C^r, $r \geq 1$ bounded on bounded sets, and of period $P > 0$ in t; U is bounded and open. The associated autonumous averaged system is defined as

$$\dot{\mathbf{y}} = \frac{1}{P}\epsilon \int_0^P f(\mathbf{y}, t, 0)dt \equiv \epsilon \bar{f}(y). \tag{A.36}$$

The averaging method approximates the original system in $\mathbf{x}$ by the averaged system $\mathbf{y}$, which in general it is easier to study.

However in general weakly nonlinear system is usually given $\dot{\mathbf{x}} = A\mathbf{x} + \epsilon f(\mathbf{x}, t, \epsilon)$ it is possible to apply the Lagrange Standard Form that use the comoving coordinates as $\mathbf{x} = \Phi(t)y$ where $\Phi(t)$ is the fundamental matrix of the unperturbed system ($\epsilon = 0$) which allows, without loss of generality, to write the system as

$$\dot{\mathbf{y}} = \epsilon f(\mathbf{y}, t). \tag{A.37}$$

The important question that comes into mind is: how the qualitative properties of the solutions of the averaged system corresponds to those of original system? To answer this we use *The Averaging Theorem*

Theorem A.34. *(The Averaging Theorem)*

There exists a C^r change of coordinates $\boldsymbol{x} = \boldsymbol{y} + \epsilon g(\boldsymbol{y}, t, \epsilon)$ under which (A.35) becomes

$$\dot{\boldsymbol{y}} = \epsilon \bar{f}(\boldsymbol{y}) + \epsilon^2 f_1(\boldsymbol{y}, t, \epsilon) \tag{A.38}$$

where f_1 is of period P in t. Moreover

(i) If $\boldsymbol{x}(t)$ and $\boldsymbol{y}(t)$ are solutions of (A.35) and (A.36) based at $\boldsymbol{x}_0$, $\boldsymbol{y}_0$, respectively, at $t = 0$, and $|\boldsymbol{x}_0 - \boldsymbol{y}_0|$, then $|\boldsymbol{x}(t) - \boldsymbol{y}(t)| = \mathcal{O}(\epsilon)$ on a time scale $t \sim \epsilon^{-1}$.

(ii) If p_0 is a hyperbolic fixed point of (A.36) then there exists $\epsilon_0 > 0$ such that, for all $0 < \epsilon \leq \epsilon_0$, (A.35) possesses a unique hyperbolic periodic orbit $\gamma_\epsilon = p_0 + \mathcal{O}(\epsilon)$ of the same stability type as p_0.

(iii) If $\boldsymbol{x}^s(t) \in W^s(\gamma_\epsilon)$ is a solution of (A.35) lying in the stable manifold of the hyperbolic periodic orbit $\gamma_\epsilon = p_0 + \mathcal{O}(\epsilon)$, $\boldsymbol{y}^s \in W^s(p_0)$ is a solution of (A.36) lying in the stable manifold of the hyperbolic fixed point p_0 and $|\boldsymbol{x}^s(0) - \boldsymbol{y}^s(0)| = \mathcal{O}(\epsilon)$, then $|\boldsymbol{x}^s(t) - \boldsymbol{y}^s(t)| = \mathcal{O}(\epsilon)$ for $t \in [0, \infty)$. Similar results apply to solutions lying in the unstable manifolds on the time interval $t \in (-\infty, 0]$.

Proof. See [111, 120, 122]. □

In general the standard averaging theory uses ϵ as a parameter however in Chapters 3,2 and 4, ϵ is not treated as a parameter but as a variable that slowly goes to zero.

Bibliography

[1] A. Berera, *The warm inflationary universe*, Contemp. Phys. **47** (2006), 10.1080/00107510500392030, arXiv:0809.4198 [hep-ph] .

[2] R. M. Wald, *General Relativity* (Chicago University Press, 1984).

[3] S. Weinberg, *Gravitation and Cosmology: Principles and Applications of the General Theory of Relativity* (John Wiley and Sons, 1972).

[4] C. W. Misner, K. S. Thorne and J. A. Wheeler, *Gravitation* (W. H. Freeman, 1973).

[5] J. Carr, *Applications of Centre Manifold Theory* (Springer, 1981).

[6] S. Carroll, *Spacetime and Geometry: An Introduction to General Relativity* (Pearson Higher Education & Professional Group, 2013).

[7] R. D'Inverno, *Introducing Einstein's Relativity* (Clarendon Press, 1992).

[8] J. Wainwright and G. F. R. Ellis, *Dynamical Systems in Cosmology* (Cambridge University Press, 1997).

[9] R. Durrer and R. Maartens, *Dark Energy and Modified Gravity*, (2008), https://doi.org/10.48550/arXiv.0807.1640.

[10] F. S. N. Lobo, *The Dark side of gravity: Modified theories of gravity*, (2008), arXiv:0807.1640 [gr-qc] .

[11] S. Capozziello and M. De Laurentis, *Extended Theories of Gravity*, Phys. Rept. **509** (2011), 10.1016/j.physrep.2011.09.003, arXiv:1108.6266 [gr-qc] .

[12] H. A. Buchdahl, *Non-Linear Lagrangians and Cosmological Theory*, Monthly Notices of the Royal Astronomical Society **150** (1970), 10.1093/mnras/150.1.1.

[13] T. P. Sotiriou and V. Faraoni, *$f(R)$ theories of gravity*, Rev. Mod. Phys. **82** (2010), 10.1103/RevModPhys.82.451.

[14] A. De Felice and S. Tsujikawa, *f(R) theories*, Living Rev. Rel. **13** (2010), 10.12942/lrr-2010-3, arXiv:1002.4928 [gr-qc] .

[15] A. Alho, S. Carloni and C. Uggla, *On dynamical systems approaches and methods in $f(R)$ cosmology*, JCAP **08**, 064 (2016), arXiv:1607.05715 [gr-qc] .

[16] Y. Fujii and K. Maeda, *The scalar-tensor theory of gravitation* (Cambridge University Press, 2007).

[17] R. V. Wagoner, *Scalar-Tensor Theory and Gravitational Waves*, Phys. Rev. D **1** (1970), 10.1103/PhysRevD.1.3209.

[18] E. E. Flanagan, *Higher order gravity theories and scalar tensor theories*, Class. Quant. Grav. **21** (2003), 10.1088/0264-9381/21/2/006, arXiv:gr-qc/0309015 .

[19] A. Friedmann, *Über die Krümmung des Raumes*, Zeitschrift für Physik **10** (1922), 10.1007/BF01332580.

[20] A. Friedmann, *Über die Möglichkeit einer Welt mit konstanter negativer Krümmung des Raumes*, Zeitschrift für Physik **21** (1924), 10.1007/BF01328280.

[21] A. Raychaudhuri, *Relativistic cosmology. 1.*, Phys. Rev. **98** (1955), 10.1103/PhysRev.98.1123.

[22] S. Weinberg, *Cosmology* (Oxford University Press, 2008).

[23] D. N. Spergel, R. Bean, O. Dore, M. R. Nolta, *et al.*, *Wilkinson Microwave Anisotropy Probe (WMAP) Three Year Results: Implications for Cosmology*, The Astrophysical Journal Supplement Series **170** (2007), 10.1086/513700.

[24] P. A. R. Ade, *et al.* (Planck), *Planck 2013 results. XVI. Cosmological parameters*, Astron. Astrophys. **571** (2014), 10.1051/0004-6361/201321591, arXiv:1303.5076 [astro-ph.CO] .

[25] A. Linde, *A new inflationary universe scenario: A possible solution of the horizon, flatness, homogeneity, isotropy and primordial monopole problems*, Physics Letters B **108** (1982), https://doi.org/10.1016/0370-2693(82)91219-9.

[26] A. H. Guth, *The inflationary universethe quest for a new theory of cosmic origins* (Vintage, 1997).

[27] A. H. Guth, *Inflationary universe: A possible solution to the horizon and flatness problems*, Phys. Rev. D **23** (1981), 10.1103/PhysRevD.23.347.

[28] A. Starobinsky, *A New Type of Isotropic Cosmological Models Without Singularity*, Physics Letters B **91** (1980), 10.1016/0370-2693(80)90670-X.

[29] A. Linde, *Chaotic inflation*, Physics Letters B **129** (1983), https://doi.org/10.1016/0370-2693(83)90837-7.

[30] A. Albrecht and P. J. Steinhardt, *Cosmology for Grand Unified Theories with Radiatively Induced Symmetry Breaking*, Phys. Rev. Lett. **48** (1982), 10.1103/PhysRevLett.48.1220.

[31] D. D. Baumann, *Cosmology: Part III Mathematical Tripos*, (2005).

[32] A. H. Guth, *Phase transitions in the very early universe*, *Very Early Universe*, (1983).

[33] A. Berera and L.-Z. Fang, *Thermally induced density perturbations in the inflation era*, Phys. Rev. Lett. **74** (1995), 10.1103/PhysRevLett.74.1912, arXiv:astro-ph/9501024 .

[34] A. Berera, *Warm inflation*, Phys. Rev. Lett. **75** (1995), 10.1103/PhysRevLett.75.3218, arXiv:astro-ph/9509049 .

[35] A. Berera, *Thermal properties of an inflationary universe*, Phys. Rev. D **54** (1996), 10.1103/PhysRevD.54.2519, arXiv:hep-th/9601134 .

[36] M. Gleiser and R. O. Ramos, *Microphysical approach to nonequilibrium dynamics of quantum fields*, Phys. Rev. D **50**, 2441 (1994), arXiv:hep-ph/9311278 .

[37] H. P. de Oliveira and R. O. Ramos, *Dynamical system analysis for inflation with dissipation*, Phys. Rev. D **57** (1998), 10.1103/PhysRevD.57.741, arXiv:gr-qc/9710093 .

[38] M. Bastero-Gil, A. Berera, R. O. Ramos and J. G. Rosa, *Warm Little Inflaton*, Phys. Rev. Lett. **117**, 151301 (2016), arXiv:1604.08838 [hep-ph] .

[39] M. Benetti and R. O. Ramos, *Warm inflation dissipative effects: predictions and constraints from the Planck data*, Phys. Rev. D **95**, 023517 (2017), arXiv:1610.08758 [astro-ph.CO] .

[40] L. Visinelli, *Observational Constraints on Monomial Warm Inflation*, JCAP **07** (2016), 10.1088/1475-7516/2016/07/054, arXiv:1605.06449 [astro-ph.CO] .

[41] L. Abbott, E. Farhi and M. B. Wise, *Particle production in the new inflationary cosmology*, Physics Letters B **117** (1982), https://doi.org/10.1016/0370-2693(82)90867-X.

[42] M. Morikawa and M. Sasaki, *Entropy Production in the Inflationary Universe*, Progress of Theoretical Physics **72** (1984), 10.1143/PTP.72.782, https://academic.oup.com/ptp/article-pdf/72/4/782/5242079/72-4-782.pdf .

[43] A. Hosoya and M.-a. Sakagami, *Time development of Higgs field at finite temperature*, Phys. Rev. D **29** (1984), 10.1103/PhysRevD.29.2228.

[44] A. Berera, *Warm inflation in the adiabatic regime — a model, an existence proof for inflationary dynamics in quantum field theory*, Nuclear Physics B **585** (2000), https://doi.org/10.1016/S0550-3213(00)00411-9.

[45] A. Berera, M. Gleiser and R. O. Ramos, *Strong dissipative behavior in quantum field theory*, Phys. Rev. D **58**, 10.1103/PhysRevD.58.123508.

[46] A. Berera and R. O. Ramos, *Construction of a robust warm inflation mechanism*, Phys. Lett. B **567** (2003), 10.1016/j.physletb.2003.06.028, arXiv:hep-ph/0210301 .

[47] I. G. Moss and C. Xiong, *Dissipation coefficients for supersymmetric inflatonary models*, (2006), arXiv:hep-ph/0603266 .

[48] A. Golovnev, V. Mukhanov and V. Vanchurin, *Vector Inflation*, JCAP **06** (2008), 10.1088/1475-7516/2008/06/009.

[49] A. Tartaglia and N. Radicella, *Vector field theories in cosmology*, Phys. Rev. D **76** (2007), 10.1103/PhysRevD.76.083501.

[50] O. Bertolami, V. Bessa and J. Páramos, *Inflation with a massive vector field nonminimally coupled to gravity*, Phys. Rev. D **93** (2016), 10.1103/PhysRevD.93.064002.

[51] Y. Nambu, *Quasi-Particles and Gauge Invariance in the Theory of Superconductivity*, Phys. Rev. **117** (1960), 10.1103/PhysRev.117.648.

[52] J. Goldstone, *Field Theories with Superconductor Solutions*, Nuovo Cim. **19**, 154 (1961).

[53] J. Goldstone, A. Salam and S. Weinberg, *Broken Symmetries*, Phys. Rev. **127** (1962), 10.1103/PhysRev.127.965.

[54] D. Capelo and J. Páramos, *Cosmological implications of Bumblebee vector models*, Phys. Rev. D **91** (2015), 10.1103/PhysRevD.91.104007, arXiv:1501.07685 [gr-qc] .

[55] M. Henneaux, *Remarks on spacetime symmetries and nonabelian gauge fields*, Journal of Mathematical Physics (1982).

[56] D. V. Galtsov and M. S. Volkov, *-Mills cosmology: Cold matter for a hot universe*, Phys. Lett. B **256** (1991), 10.1016/0370-2693(91)90211-8.

[57] P. V. Moniz and J. M. Mourao, *Homogeneous and isotropic closed cosmologies with a gauge sector*, Classical and Quantum Gravity **8** (1991), 10.1088/0264-9381/8/10/008.

[58] G. 't Hooft, ed., *50 years of Yang-Mills theory* (2005).

[59] M. C. Bento, O. Bertolami, P. V. Moniz, J. M. Mourao and P. M. Sa, *On the cosmology of massive vector fields with SO(3) global symmetry*, Class. Quant. Grav. (1993), 10.1088/0264-9381/10/2/010, arXiv:gr-qc/9302034 .

[60] D. V. Galt'sov and M. S. Volkov, (1971).

[61] A. H. Taub, *Empty Space-Times Admitting a Three Parameter Group of Motions*, Annals of Mathematics **53** (1951), https://doi.org/10.2307/1969567.

[62] G. F. R. Ellis and M. A. H. MacCallum, *A class of homogeneous cosmological models*, Communications in Mathematical Physics **12**.

[63] C. B. Collins and S. Hawking, *Why is the Universe isotropic?*, The Astrophysical Journal **180** (1973), 10.1086/151965.

[64] B. Brehm, *Bianchi VIII and IX vacuum cosmologies: Almost every solution forms particle horizons and converges to the Mixmaster attractor*, (2016), arXiv:1606.08058 [gr-qc] .

[65] J. Hell, P. Lappicy and C. Uggla, *Bifurcations and Chaos in Hořava-Lifshitz Cosmology*, (2020), arXiv:2012.07614 [gr-qc] .

[66] A. A. Coley, *Dynamical Systems and Cosmology* (Springer Dordrecht, 2003).

[67] S. Bahamonde, C. G. Böhmer, S. Carloni, E. J. Copeland, *et al.*, *Dynamical systems applied to cosmology: dark energy and modified gravity*, Phys. Rept. **775-777** (2018), 10.1016/j.physrep.2018.09.001.

[68] A. Alho, J. Hell and C. Uggla, *Global dynamics and asymptotics for monomial scalar field potentials and perfect fluids*, Class. Quant. Grav. **32** (2015), 10.1088/0264-9381/32/14/145005, arXiv:1503.06994 [gr-qc] .

[69] D. Escobar, C. R. Fadragas, G. Leon and Y. Leyva, *Phase space analysis of quintessence fields trapped in a Randall-Sundrum Braneworld: a refined study*, Class. Quant. Grav. **29** (2012), 10.1088/0264-9381/29/17/175005.

[70] C. G. Boehmer, N. Chan and R. Lazkoz, *Dynamics of dark energy models and centre manifolds*, Phys. Lett. B **714** (2012), 10.1016/j.physletb.2012.06.064.

[71] A. Cid, G. Leon and Y. Leyva, *Intermediate accelerated solutions as generic late-time attractors in a modified Jordan-Brans-Dicke theory*, JCAP **02** (2016), 10.1088/1475-7516/2016/02/027, arXiv:1506.00186 [gr-qc] .

[72] J. Miritzis, *Dynamical system approach to FRW models in higher order gravity theories*, J. Math. Phys. **44** (2003), 10.1063/1.1602161, arXiv:gr-qc/0305062 .

[73] J. Miritzis, *Scalar field cosmologies with an arbitrary potential*, Class. Quant. Grav. **20** (2003), 10.1088/0264-9381/20/14/301, arXiv:gr-qc/0303014 .

[74] J. M. Heinzle and C. Uggla, *Monotonic functions: Why they exist and how to find them*, Class. Quant. Grav. **27** (2010), 10.1088/0264-9381/27/1/015009.

[75] J. M. Heinzle and C. Uggla, *Dynamics of the spatially homogeneous Bianchi type I Einstein-Vlasov equations*, Class. Quant. Grav. **23** (2006), 10.1088/0264-9381/23/10/016, arXiv:gr-qc/0512031 .

[76] B. D. Normann, S. Hervik, A. Ricciardone and M. Thorsrud, *Bianchi cosmologies with p-form gauge fields*, Class. Quant. Grav. **35** (2018), 10.1088/1361-6382/aab3a7.

[77] P. Sandin and C. Uggla, *Bianchi type I models with two tilted fluids*, Class. Quant. Grav. **25** (2008), 10.1088/0264-9381/25/22/225013, arXiv:0806.0759 [gr-qc] .

[78] S. Calogero and J. M. Heinzle, *Dynamics of Bianchi type I solutions of the Einstein equations with anisotropic matter*, Annales Henri Poincare **10** (2009), 10.1007/s00023-009-0407-y.

[79] A. D. Rendall and C. Uggla, *Dynamics of spatially homogeneous locally rotationally symmetric solutions of the Einstein-Vlasov equations*, Class. Quant. Grav. **17** (2000), 10.1088/0264-9381/17/22/310, arXiv:gr-qc/0005116 .

[80] A. Alho and C. Uggla, *Global dynamics and inflationary center manifold and slow-roll approximants*, J. Math. Phys. **56** (2015), 10.1063/1.4906081, arXiv:1406.0438 [gr-qc] .

[81] G. Leon, E. González, S. Lepe, C. Michea and A. D. Millano, *Averaging generalized scalar field cosmologies I: locally rotationally symmetric Bianchi III and open Friedmann–Lemaître–Robertson–Walker models*, Eur. Phys. J. C **81** (2021), 10.1140/epjc/s10052-021-09185-7, arXiv:2102.05465 [gr-qc] .

[82] G. Leon, E. González, S. Lepe, C. Michea and A. D. Millano, *Averaging generalized scalar-field cosmologies III: Kantowski–Sachs and closed Friedmann–Lemaître–Robertson–Walker models*, Eur. Phys. J. C **81** (2021), 10.1140/epjc/s10052-021-09580-0, arXiv:2102.05551 [gr-qc] .

[83] G. Leon, S. Cuellar, E. Gonzalez, S. Lepe, *et al.*, *Averaging generalized scalar field cosmologies II: locally rotationally symmetric Bianchi I and flat Friedmann–Lemaître–Robertson–Walker models*, Eur. Phys. J. C **81** (2021), 10.1140/epjc/s10052-021-09230-5, arXiv:2102.05495 [gr-qc] .

[84] D. Fajman, G. Heißel and J. W. Jang, *Averaging with a time-dependent perturbation parameter*, Classical and Quantum Gravity **38** (2021), 10.1088/1361-6382/abe883.

[85] A. Alho, V. Bessa and F. C. Mena, *Global dynamics of Yang–Mills field and perfect-fluid Robertson–Walker cosmologies*, J. Math. Phys. **61** (2020), 10.1063/1.5139879, arXiv:1910.04678 [gr-qc] .

[86] J. Beltran Jimenez, L. Heisenberg, R. Kase, R. Namba and S. Tsujikawa, *Instabilities in Horndeski Yang-Mills inflation*, Phys. Rev. D **95** (2017), 10.1103/PhysRevD.95.063533, arXiv:1702.01193 [hep-th] .

[87] C. G. Hewitt and J. Wainwright, *Dynamical systems approach to titled Bianchi cosmologies: Irrotational models of type V*, Phys. Rev. D **46** (1992), 10.1103/PhysRevD.46.4242.

[88] J. D. Barrow, Y. Jin and K.-i. Maeda, *Cosmological coevolution of Yang-Mills fields and perfect fluids*, Phys. Rev. D **72** (2005), 10.1103/PhysRevD.72.103512.

[89] A. Alho and C. Uggla, *Inflationary α-attractor cosmology: A global dynamical systems perspective*, Phys. Rev. D **95** (2017), 10.1103/PhysRevD.95.083517, arXiv:1702.00306 [gr-qc] .

[90] F. V. J. A. Sanders and J. Murdock, *Averaging Methods in Nonlinear Dynamical Systems* (Springer New York, NY, 2007).

[91] B. K. Darian and H. P. Kunzle, *Axially symmetric Bianchi I Yang-Mills cosmology as a dynamical system*, Class. Quant. Grav. **13** (1996), 10.1088/0264-9381/13/10/005, arXiv:gr-qc/9608024 .

[92] B. K. Darian and H. P. Kunzle, *Cosmological Einstein Yang-Mills equations*, J. Math. Phys. **38** (1997), 10.1063/1.532116, arXiv:gr-qc/9610026 .

[93] J. D. Barrow and J. J. Levin, *Chaos in the Einstein Yang-Mills equations*, Phys. Rev. Lett. **80** (1998), 10.1103/PhysRevLett.80.656, arXiv:gr-qc/9706065 .

[94] Y. Jin and K.-i. Maeda, *Chaos of Yang-Mills field in class a Bianchi spacetimes*, Phys. Rev. D **71** (2005), 10.1103/PhysRevD.71.064007, arXiv:gr-qc/0412060 .

[95] I. G. Moss and C. Xiong, *On the consistency of warm inflation*, JCAP **11** (2008), 10.1088/1475-7516/2008/11/023.

[96] A. P. Billyard and A. A. Coley, *Interactions in scalar field cosmology*, Phys. Rev. D **61** (2000), 10.1103/PhysRevD.61.083503.

[97] K. V. Berghaus, P. W. Graham and D. E. Kaplan, *Minimal Warm Inflation*, JCAP **03** (2020), 10.1088/1475-7516/2020/03/034, arXiv:1910.07525 .

[98] M. R. Setare, A. Sepehri and V. Kamali, *Constructing warm inflationary model in brane-antibrane system*, Phys. Lett. B **735** (2014), 10.1016/j.physletb.2014.05.081, arXiv:1405.7949 [gr-qc] .

[99] X.-B. Li, Y.-Y. Wang, H. Wang and J.-Y. Zhu, *Dynamic analysis of noncanonical warm inflation*, Phys. Rev. D **98** (2018), 10.1103/PhysRevD.98.043510, arXiv:1804.05360 [gr-qc] .

[100] M. Bastero-Gil, A. Berera, R. O. Ramos and J. G. Rosa, *General dissipation coefficient in low-temperature warm inflation*, JCAP **01** (2013), 10.1088/1475-7516/2013/01/016.

[101] B. Aulbach, *Continuous and Discrete Dynamics near Manifolds of Equilibria* (Springer Berlin, 1984).

[102] L. Perko, *Differential Equations and Dynamical Systems* (Springer, 2001).

[103] F. Dumortier, *Techniques in the Theory of Local Bifurcations: Blow-Up, Normal Forms, Nilpotent Bifurcations, Singular Perturbations* (Springer Netherlands, 1993).

[104] F. Dumortier, J. Llibre and J. C. Artes, *Qualitative theory of planar differential systems* (Springer Netherlands, 2006).

[105] M. Brunella and M. Miari, *Topological equivalence of a plane vector field with its principal part defined through Newton Polyhedra*, Journal of Differential Equations **85** (1990), https://doi.org/10.1016/0022-0396(90)90120-E.

[106] A. M. Liapunov, *Stability of Motion*, Math. Sci. Eng. 3 **3** (1966).

[107] A. Lins, W. de Melo and C. C. Pugh, *On Liénard's equation in Lecture Notes in Math* (Springer Berlin Heidelberg, 1977).

[108] F. Dumortier and C. Herssens, *Polynomial Liénard Equations near Infinity*, Journal of Differential Equations **153** (1999), https://doi.org/10.1006/jdeq.1998.3543.

[109] M. Sabatini and G. Villari, "On the uniqueness of limit cycles for liénard equation: the legacy of g. sansone," (2011).

[110] A. Gasull and H. Giacomini, *Effectiveness of the Bendixson–Dulac theorem*, Journal of Differential Equations **305** (2021), https://doi.org/10.1016/j.jde.2021.10.011.

[111] J. Guckenheimer and P. Holmes, *Nonlinear oscillations, dynamical systems, and bifurcations of vector fields*, Applied mathematical sciences (Springer New York, NY, 1990).

[112] J. Wainwright, M. J. Hancock and C. Uggla, *Asymptotic selfsimilarity breaking at late times in cosmology*, Class. Quant. Grav. **16** (1999), 10.1088/0264-9381/16/8/302, arXiv:gr-qc/9812010 .

[113] C. B. Collins and J. M. Stewart, *Qualitative Cosmology*, Monthly Notices of the Royal Astronomical Society **153** (1971), 10.1093/mnras/153.4.419.

[114] J. Wainwright and L. Hsu, *A dynamical systems approach to Bianchi cosmologies: Orthogonal models of class A*, Class. Quant. Grav. **6** (1989), 10.1088/0264-9381/6/10/011.

[115] I. S. Kohli and M. C. Haslam, *Dynamical systems approach to a Bianchi type I viscous magnetohydrodynamic model*, Phys. Rev. D **88** (2013), 10.1103/PhysRevD.88.063518, arXiv:1304.8042 [gr-qc] .

[116] A. P. Billyard, A. A. Coley, R. J. van den Hoogen, J. Ibanez and I. Olasagasti, *Scalar field cosmologies with barotropic matter: Models of Bianchi class B*, Class. Quant. Grav. **16** (1999), 10.1088/0264-9381/16/12/320.

[117] K. S. Thorne, *Primordial Element Formation, Primordial Magnetic Fields, and the Isotropy of the Universe*, Astrophys. J. **148** (1967), 10.1086/149127.

[118] S. W. Hawking and R. J. Tayler, *Helium Production in an Anisotropic Big-Bang Cosmology*, Nature **209** (1966), 10.1038/2091278a0.

[119] M. Hirsch and S. Smale, *Differential equations, dynamical systems, and linear algebra* (Academic Press, 1974).

[120] S. Wiggins, *Introduction to Applied No nlinear Dynamical Systems and Chaos* (Springer, 1990).

[121] D. K. Arrowsmith and C. M. Place, *An Introduction to Dynamical Systems.* (Cambridge University Press, 1990).

[122] F. Verhulst, *Nonlinear Differential Equations and Dynamical Systems* (Springer Berlin Heidelberg, 2006).

[123] S. Lynch, *Dynamical Systems with Applications using Mathematica* (Birkhäuse, 2007).

[124] M. Szydlowski and A. Krawiec, *Lyapunov function for cosmological dynamical system*, Demonstratio Mathematica **50** (2017), doi:10.1515/dema-2017-0005.

[125] T. C. Charters, A. Nunes and J. P. Mimoso, *Stability analysis of cosmological models through Lyapunov's method*, Classical and Quantum Gravity **18** (2001), 10.1088/0264-9381/18/9/307.